Ottorino Veneri *Editor*

Technologies and Applications for Smart Charging of Electric and Plug-in Hybrid Vehicles

Springer

Technologies and Applications for Smart Charging of Electric and Plug-in Hybrid Vehicles

Ottorino Veneri
Editor

Technologies and Applications for Smart Charging of Electric and Plug-in Hybrid Vehicles

Springer

Editor
Ottorino Veneri
CNR-National Research Council of Italy
Istituto Motori
Naples, Italy

Acknowledgments

Contents

Part III   Adoption and Market Diffusion

About the Authors

Javier Campillo received his Ph.D. in energy engineering from Mälardalen University in Västerås, Sweden, in 2016. He holds an M.Sc. in energy engineering from Mälardalen University in 2007 and an electronic engineering degree from Tecnológica de Bolívar University in Cartagena, Colombia, in 2003. He has carried out his research focused on developing computational models for simulating future active electric distribution networks with high penetration of distributed generation, demand side management, and electric vehicles.

Giampaolo Carli is a power electronics specialist presently working in the domain of high-voltage generation for X-ray systems at EMD Technologies in Saint-Eustache, Canada. After receiving a bachelor's degree in electrical engineering at McGill University in 1984, he devoted many years to the power electronics industry in various fields ranging from industrial and commercial computer systems, telecom, and LED lighting. In 2009 he obtained an M.S. in electrical engineering from Concordia University in Montreal with specialization in electric vehicle charging technology and infrastructure. Besides his technical pursuits, he also enjoys playing and composing music as well as the study of physics, metaphysics, and philosophy.

Dong Chen received his B.Eng. from Southeast University, Nanjing, China, in 2006; M.Sc. from Zhejiang University, Hangzhou, China, in 2008; and Ph.D. from the Queen's University of Belfast, Belfast, UK, in 2012.

He is currently a lecturer with the School of Engineering and Built Environment, Glasgow Caledonian University. He was previously with Strathclyde University, Glasgow, UK, and Guodian Nanjing Automation, Co. Ltd., Nanjing, China. His research interest includes DC microgrid, power electronics applications to power systems, active distribution power system, and motion control.

Erik Dahlquist received his Ph.D. in chemical engineering at Royal Institute of Technology (KTH) in 1991. From 1997 to 2000 he was Associate Professor at KTM and from May 2000 he is Full Professor at Malardalen University, Vasteras. He started working at ASEA Research from September 1975. He worked as engineer on nuclear power, troubleshooting of electrical equipments and manufacturing processes until 1980. From 1980 to 1992 he worked with Novatune on a self-tuning adaptive controller for waste water treatment. He has also worked as engineer engineering with ASEA Oil and Gas since this company was formed. He was technical project manager for the development of a Cross Flow Membrane filter. From 1989 to 1992 he worked as project leader for the ABBs Black Liquor Gasification project. From 1992 to 1995 he worked as manager of the Combustion and Process Technology Department at ABB Corporate Research Centre. He also joined member of the Director Board of the ABB Corporate Research Centre in Vasteras. From January 1996 to April 2000 he worked as General Manger with ABB Automation Systems. Here he was in charge of the Product Unit, called "Pulp Applications". Since 2000 he has worked as Research Director of the Future Energy Centre, which employs 27 researchers and 45 Ph.D. students of the Royal Academy of Engineering. He holds 25 patents. He is co-author of about 260 scientific papers, refereed journals and conference proceedings with referee procedure. He is co-author of book chapters and editor/coeditor of ten books.

David Dallinger completed a degree in business engineering at Jena University of Applied Sciences in 2006, and an M.Sc. in mechanical engineering and a Ph.D. in electrical engineering at Kassel University in 2008 and 2012, respectively. He has been employed at ABB High Voltage in Switzerland and in China from 2005 to 2006 and joined the Fraunhofer Institute for Systems and Innovation Research ISI in Karlsruhe from 2008 until 2014. He was a visiting scientist at the Energy Analysis Department of the Lawrence Berkeley National Laboratory in California and served as a member of the International Energy Agency Task Force: Plug-in Hybrid Electric Vehicles. He is currently working with Volkswagen in the technical development department for electric vehicles.

Dmitri L. Danilov has a background in physics and mathematics and obtained his M Sc. from Saint-Petersburg University in 1993. In 1997 he started his Ph.D. at the University of Tilburg, studying model selection procedures and pretesting. He obtained his Ph.D. in 2003. At the end of 2002, he joined Eurandom at the TUE campus, first being involved in research activities on "Battery Management and Battery Modelling" EET project, then continued his work on "3D Integrated Batteries" SenterNovem project, FP7 SUPERLION, and Eniac BATTMAN projects. He conducted research on aging and state-of-charge indication for Li-ion rechargeable batteries and various aspects of hydrogen storage. His current research interests include mathematical modeling for complex electrochemical systems, including Li-ion and NiMH batteries, in particular thermal behavior, aging, and degradation processes. He has published as author and coauthor more than 50 papers and book contributions.

Nima Ghaviha received his B.S. in industrial engineering from Sharif University of Technology, Iran, and his M.S. in product and process development from Mälardalen University, Sweden. He recently got his licentiate degree in energy and environmental engineering from Mälardalen University and is currently working toward getting his Ph.D. at Future Energy Center at the same university, developing his research work in energy optimization of train transportation. The focus of his research is on energy efficient train operation for electric multiple units and battery-driven electric multiple units, in cooperation with SICS Swedish ICT and Bombardier Transportation, Sweden.

Robert Kohrs is head of the research group Smart Grid Technology at the Fraunhofer Institute for Solar Energy Systems ISE in Freiburg. He studied physics at the University of Bonn, where he also received his Ph. D. for his work on semiconductor detectors. He joined Fraunhofer ISE in 2009, where he started as project manager with a focus on Energy Management Systems, Smart Metering, and Electric Mobility. Since 2010 he is responsible for the technological integration of smart appliances in the future energy system.

Samir Kouro received his M.Sc. and Ph.D. in electronics engineering from the Universidad Tecnica Federico Santa Maria (UTFSM), Valparaíso, Chile, in 2004 and 2008, respectively. Since 2007, he has been with the Department of Electronic Engineering, where he currently serves as Associate Professor. From 2009 to 2011, he was a Postdoctoral Fellow in the Department of Electrical and Computer Engineering, Ryerson University, Toronto, Canada. His research interests include power electronics, renewable energy conversion systems, and electro-mobility applications.

Dr. Kouro is founding member and Principal Investigator of the Advanced Center of Electrical and Electronics Engineering (AC3E) and of the Solar Energy Research Center (SERC-Chile), both recognized as research centers of excellence in Chile. He has coauthored one book, five book chapters, and over 100 refereed journal and conference papers. He has served as Guest Editor of Special Sections in the IEEE Transactions on Industrial Electronics and IEEE Transactions on Power Electronics. Dr. Kouro is associate editor of the *International Journal of Electrical Power and Energy Systems.*

Dr. Kouro received the 2016 IEEE Industrial Electronics Bimal K. Bose Award for Industrial Electronics Applications in Energy Systems, the 2015 IEEE Industrial Electronics Society J. David Irwin Early Career Award, the 2012 IEEE Power Electronics Society Richard M. Bass Outstanding Young Power Electronics Engineer Award, the 2012 IEEE Industry Applications Magazine first prize paper award, the 2011 IEEE Transactions on Industrial Electronics Best Paper Award, and the 2008 IEEE Industrial Electronics Magazine Best Paper Award.

Reinhard Madlener is a full professor of energy economics and management at the School of Business and Economics, RWTH Aachen University, Germany. His main research interests, on which he has published extensively over the last 20 years, are in the fields of energy economics and policy, sustainable energy systems, and the adoption, temporal and spatial diffusion, and financing of innovative energy technologies under uncertainty. The teaching activities of Professor Madlener are mainly in energy economics, environmental economics, economics of technological diffusion, economics of technical change, and public choice. He is presently associate editor of *Energy Policy* and serves on the editorial boards of a number of international scientific journals, including *Applied Economics Quarterly*; *Applied Energy*; *Energy Efficiency*; *Energy Systems*; *Energy, Sustainability and Society*; *International Journal of Energy Sector Management*; *International Journal of Future Cities and Environment*; *Journal of Energy Storage*; and *Sustainable Cities and Society*. Professor Madlener has been President of the Swiss Association for Energy Economics (SAEE) for several years. He is the founding and current director of the Institute for Future Energy Consumer Needs and Behavior (FCN), which is an integral part of the interdisciplinary and integrated E.ON Energy Research Center established at RWTH Aachen University in 2006.

Vincenzo Marano is System Architecture Engineer at Magneti Marelli (FCA group)—Technology Innovation, Italy. Currently, he manages and conducts projects related to advanced driver assistance systems (ADAS) and to the broad area of CO_2 reduction with specific focus on automotive eco-innovation technologies. In 2012–2015, he has been Research Fellow at the University of Salerno (UNISA), Italy, with the main focus on technologies toward CO_2 reduction, hybrid and plug-in hybrid electric vehicles energy management, and interactions between vehicles, renewable energy, and the grid (V2X). At UNISA he also served as Local Coordinator of CO_2RE-Lab, a joint R&D lab of Magneti Marelli–UNISA (since June 2014).

In 2008–2012, Dr. Marano has served as program manager of the SMART@CAR consortium, an international collaborative research and development program of the Ohio State University—Center for Automotive Research (USA)—focused on plug-in electric vehicles (PEVs) and intelligent charging, and sponsored by major automotive OEMs and electric utilities. He managed research development efforts and was responsible for establishing/developing working relationships with potential and existing sponsors. His research interests were in the broad areas of energy systems and alternative vehicles, with focus on plug-in

electric vehicles, energy storage, energy management, control strategies for plug-in hybrid electric vehicles, their interaction with renewable energy sources and the grid, macroeconomics, and energy policy.

He received his B.S./M.S. "cum laude" in mechanical engineering in 2003 and his Ph.D. in mechanical engineering in 2007, all from the University of Salerno (Italy).

As member of ASME and SAE, he has authored about 60 scientific papers. He regularly serves as reviewer for ISI journals and international conferences, organized by SAE, ASME, and IEEE. He has been invited as member of the international panels on sustainable transportation and renewable energy.

Simon Marwitz trained and worked as a power electronics engineer at K+S KALI GmbH and studied electrical engineering at the University of Kassel and the Karlsruhe Institute of Technology. His master's degree at the Karlsruhe Institute of Technology focused on energy systems and energy technologies. His master's thesis was on the "Simulation of the driving and charging behaviour of electric vehicles." Since October 2012, he has been working as a researcher at the Fraunhofer Institute for Systems and Innovation Research ISI in the Competence Center Energy Technology and Energy Systems, where he is primarily concerned with the integration of renewable energies and electric vehicles on distribution grid level.

Michael Mierau studied mechatronics at Dresden University of Technology. In 2010 he completed his diploma thesis on the implementation of an intelligent charging infrastructure for EVs at the Fraunhofer Institute for Solar Energy Systems ISE. From 2010 to 2015, he has been working as a project manager in the division of Electrical Energy Systems at the Fraunhofer ISE, where he was in charge of various electric mobility projects focusing on the intelligent integration of electric vehicles into the grid. He is currently working at the Fraunhofer ISE Spin-off ENIT Energy IT Systems GmbH, which is focused on the development of energy management solutions for industrial applications.

Peter H.L. Notten was born in the Netherlands in 1952, was educated in analytical chemistry, and joined Philips Research in 1975. While working at these laboratories on the electrochemistry of etching of III–V semiconductors, he received his Ph.D. from the Eindhoven University of Technology in 1989. Since then his activities have been focused on the research of hydride-forming (electrode) materials for application in rechargeable NiMH batteries, switchable optical mirrors and gas phase storage, and Lithium-based rechargeable battery systems. Since 2000 he has been appointed as professor at the Eindhoven University of Technology where he is heading the group Energy Materials and Devices. In 2014 he has been appointed as International Adjunct Faculty (visiting professor) at Amrita University, Coimbatore, India, and at Forschungszentrum Jűlich, Germany. His main interest includes the development of (a) advanced battery and hydrogen storage materials, (b) new battery technologies, (c) modeling of energy storage materials and complete rechargeable battery (NiMH and Li-ion) systems, and (d) the development of sophisticated battery management systems (BMS). He is member of the editorial board of *Advanced Energy Materials* and *International Journal of Electrochemical Science*. He has published as (co)author about 250 scientific papers and contributions to scientific books and owns about 30 patents.

Cagil Ozansoy received his B.Eng. and Ph.D. from Victoria University in 2002 and 2006. He joined Victoria University as a lecturer in 2007 and was promoted to senior lecturer in 2013. Since 2013, he has been undertaking the first year champion role, where he has been implementing effective strategies for improving student retention, teaching and curriculum quality, and engagement in the common first year. His main research strength is in the design and development of power systems protection, automation, and control applications. He is well known internationally for his investigations in the novel use of international standards in various fields including substations, microgrids, and industrial plants. He is a member of the Standards Australia (SA) Technical Committee EL-050 on Power System Control and Communication. He has published over 50 papers on many journals and conference proceedings, related to his research fields. He has undertaken many industry/community engagement projects and consultancies. His research interests cover power system protection, distributed generation, microgrids, smart grids and energy from waste.

Vamsi Krishna Pathipati received his Bachelor of Technology (B.Tech.) degree in electrical and electronics engineering from Jawaharlal Nehru Technological University (JNTU), Anantapur, Andhra Pradesh, India, in 2011. He received the Master of Applied Science (M. A.Sc.) degree in electrical and computer engineering from the University of Ontario Institute of Technology (UOIT), Oshawa, ON, Canada, in 2016 specializing in automotive power electronics and advanced battery charging from Advanced Storage Systems for Electric Transportation (ASSET) lab within the Smart Transportation Electrification and Energy Research (STEER) group at UOIT. Currently, Mr. Pathipati is working as a Systems Engineer, Charging, R&D at Tesla Motors Inc., Palo Alto, CA, USA. From 2011 to 2014, Mr. Pathipati worked at Mahindra Reva Electric Vehicles Pvt. Ltd., Bangalore, KA, India, as Member—R&D. He was one of the design engineers for the Mahindra Reva's Future of Mobility projects SUN2CAR™ and CAR2HOME™. At Mahindra Reva, he has also worked on designing charging systems for electric vehicles with compliance to various global standards.

Sebastian Rivera was born in Valparaiso, Chile, in 1986. He received his B.Sc. and M.Sc. in electronics engineering from Universidad Tecnica Federico Santa Maria (UTFSM), Chile, in 2007 and 2011, respectively, and his Ph.D. in electrical and computer engineering from Ryerson University, Toronto, ON, Canada, in 2015. He recently joined the University of Toronto as a Postdoctoral Fellow at the Laboratory for Advanced Power Conversion and Systems Analysis. His research interests include high-power multilevel converters, renewable energy conversion systems, and electric vehicles.

Dr. Rivera received the Emerging Leaders in the Americas Program Scholarship from the Canadian Bureau for International Education in 2010, the Ph.D. Scholarship from the Chilean National Commission for Scientific and Technological Research (CONICYT) in 2011, and the 2016 Academic Gold Medal from Governor General of Canada.

Arash Shafiei Arash Shafiei received his bachelor's degree in electrical and computer engineering specializing in power systems and networks from Shiraz University, Iran, in 2008. He obtained a Master of Applied Science (M.A.Sc.) degree in electrical and computer engineering specializing in power electronics, electric vehicles, and renewable energies in Power Electronics and Energy Research (PEER) group at Concordia University in 2013. He has published peer-reviewed papers on the subjects of electric vehicle battery charging and solar energy harvesting for charging purposes. He has also coauthored books on the topics of power electronics applications in automotive, renewable energies and distributed energy systems. His main areas of interest and research are highly efficient and reliable power generation and power distribution systems in automotive and aerospace applications.

Previously, he has been working with leading companies such as Bombardier Aerospace and Honeywell Aerospace as electrical design engineer, designing power generation and distribution systems in aircrafts and employing renewable energies in more electric aircrafts. Currently, he is with Mobile Climate Control (MCC) designing HVAC systems for electric vehicles and electric buses.

Taha Selim Ustun received his Ph.D. in electrical engineering from Victoria University, Melbourne, VIC, Australia. He is an Assistant Professor of Electrical Engineering with the School of Electrical and Computer Engineering, Carnegie-Mellon University, Pittsburgh, PA, USA. He has taught courses such as Fundamentals in Power Systems, Renewable Energy, Microgrids and New Age Power Networks, Power Electronics, and Embedded Systems. His research interests include power systems protection, communication in power networks, distributed generation, microgrids, and smart grids. Recently, he started working on novel technologies and business policy models to increase electricity penetration in underserved communities. This versatile field spans a wide area from battery management systems for PV battery solutions to microgrid sizing, renewable energy intermittency mitigation, and business policy directions for sustainable development. These novel ideas can be exported back to the developed world where the energy paradigm is drastically changing. Novel microgrid topologies may help accommodate more electric vehicles or some tariff structures used in an underdeveloped community may be implemented as a demand side management strategy in the developed world. He has over 40 publications that appeared in international peer-reviewed journals and conferences. He is a reviewer in reputable journals such as *IEEE Transactions on Power Systems* and *IEEE Transactions on Power Delivery*.

He has taken active role in organizing international conferences and chairing sessions such as in IEEE Latincom, IEEE SmartgridComm, IEEE IRSEC, IEEE PowerAfrica as well as IEEE Tencon. He delivered talks for World Economic Council, Waterloo Global Science Initiative, European Union Energy Initiative (EUEI), and Qatar Foundation. He has also been invited to run short courses in Africa, India, and China.

Iana Vassileva holds a Ph.D. in energy and environmental engineering (2012, Mälardalen University, Sweden). In 2012 she was granted a Postdoctoral Fellowship at Mälardalen University, Sweden. She has participated in and led numerous Swedish and European research projects with focus on technology adoption, energy consumption feedback and visualization, energy efficiency, electric vehicles, and smart cities. She has been part of the Organizing Committees of international conferences (International Green Energy Conference; International Conferences on Applied Energy; and Applied Energy Symposium and Summit: Low-Carbon Cities and Urban Energy); a panel speaker at the World Renewable Energy Congress, London 2014; and an invited speaker at the Smart Cities and Energy Efficiency event, Santiago de Compostela, Spain, 2015. She has been appointed as an expert evaluator for the Intelligent Energy—Europe Programme and Horizon 2020 on several occasions, where she evaluated project proposals focusing on consumer behavior and awareness, energy efficiency, and smart cities. Currently, she works as a Technology Research Analyst for the Accenture Centre for Innovation in Dublin.

Ottorino Veneri graduated in electrical engineering from the University of Naples Federico II in 1996. In March 2000, he was awarded his Ph.D. in electrical engineering by the same University. From 1999 to 2001, he had a research grant provided by the Department of Electrical Engineering of the University of Naples Federico II. Since 2002, he works as researcher with the Istituto Motori of the National Research Council (CNR) of Italy in Naples. In recent years, he has also become Full Professor at the International Telematic University UNINETTUNO. His main research fields are the electric drives for transportation systems, electric energy converters, electric energy storage systems, power sources with hydrogen fuel cells, and hybrid propulsion architecture.

He is co-author of a book, published by Springer, two chapters in contributed volumes and about 100 scientific papers, published in international journals and in conference proceedings. He is member of editorial board, subject editor and reviewer of international journals that publish material in the area of energy and

power conversion. He is technical reviewer of Research and Development Projects, granted by the Italian Ministri of Economic Development. He is director of operative units at Istituto Motori CNR, working on more than 10 national and international research projects.

Julius Wesche studied economics and management at the Hamburg School of Business Administration, 2006–2009, and gained work experience as a trainee at the German mail order company Otto GmbH & Co. KG. Following his bachelor's thesis he completed internships at the German Bundestag, among others, and started his M.A. degree in sustainability economics with a concentration on the energy sector at the University of Kassel in 2010. Study visit at the University of Wisconsin, Madison, USA. In his master's thesis, he analyzed the acceptance of battery charging tariffs in the e-mobility. He joined the Competence Center Energy Policy and Energy Markets at Fraunhofer ISI as a research fellow in March 2014.

Sheldon S. Williamson (S'01–M'06–SM'13) received his Bachelor of Engineering (B.E.) degree in electrical engineering with high distinction from the University of Mumbai, India, in 1999. He received the Master of Science (M.S.) degree in 2002 and the Doctor of Philosophy (Ph.D.) degree (with Honors) in 2006, both in electrical engineering, from the Illinois Institute of Technology, Chicago, IL. From June 2006 to June 2014, Dr. Williamson held a tenure-track Assistant Professor position, followed by a tenured Associate Professor position in the Department of Electrical and Computer Engineering, at Concordia University, in Montreal, Canada. Dr. Williamson currently holds an Associate Professor position in the Department of Electrical, Computer, and Software Engineering at the University of Ontario-Institute of Technology (UOIT), in Oshawa, Ontario, Canada. Since July 2015, Dr. Williamson also holds the prestigious title of NSERC Canada Research Chair in Electric Energy Storage Systems for Transportation Electrification. Dr. Williamson's research interests include transportation electrification, electric energy storage systems, automotive power electronics, and motor drives. Dr. Williamson is a Senior Member of the IEEE and a Distinguished Lecturer of the IEEE Vehicular Technology Society.

Bin Wu graduated from Donghua University, Shanghai, China, in 1978 and received his M.A.Sc. and Ph.D. in electrical and computer engineering from the University of Toronto, Canada, in 1989 and 1993, respectively. After being with Rockwell Automation Canada from 1992 to 1993, he joined Ryerson University, where he is currently a Professor in the Department of Electrical and Computer Engineering and a Senior NSERC/Rockwell Industrial Research Chair (IRC) in Power Electronics and Electric Drives. Dr. Wu has published more than 350 peer-reviewed technical papers, two Wiley-IEEE Press books, and holds more than 30 issued and pending patents in power electronics, adjustable-speed drives, and renewable energy systems. Dr. Wu is the founder of the Laboratory for Electric Drive Applications and Research (LEDAR), which has been recognized as the most advanced research facility of its kind in a Canadian university.

Dr. Wu has worked closely with Canadian companies and assisted them in achieving technical and commercial success through research and innovation. He has authored/coauthored more than 200 technical reports. Some of his inventions and patents have been adopted by industry and implemented in the production line, resulting in significant economic benefits.

Dr. Wu received the Gold Medal of the Governor General of Canada in 1993, Premier's Research Excellence Award in 2001, NSERC Synergy Award for Innovation in 2002, Ryerson Distinguished Scholar Award in 2003, Ryerson FEAS Research Excellence Award in 2007, Ryerson YSGS Outstanding Contribution to Graduate Education Award and Professional Engineers Ontario (PEO) Engineering Excellence Medal in 2014. He is a fellow of the Institute of Electrical and Electronics Engineers (IEEE), Engineering Institute of Canada (EIC), and Canadian Academy of Engineering (CAE). Dr. Wu is a Registered Professional Engineer in the Province of Ontario, Canada.

Lie Xu (M'03–SM'06) is currently Professor of electrical power engineering at the University of Strathclyde, UK. He graduated from Zhejiang University, China, and received his Ph.D. in electrical engineering from the University of Sheffield, UK, in 2000. He started his career with ALSTOM T&D in the UK working on the development of VSC-based HVDC systems and was a Lecture/Senior Lecturer in Queen's University of Belfast, UK, from 2004 to 2012.

His main areas of research are power electronics application for power transmission and distribution, wind generator control and operation, wind farm integration using HVDC transmission, DC microgrid, etc. He has authored/coauthored over 60 journal publications in IEEE/IET journals and received the 2013 Premium Award from IET Renewable Power Generation.

Aladin Zayegh received his BE in electrical engineering from Aleppo University in 1970 and Ph.D. from Claude Bernard University, Lyon, France, in 1979. He has held lecturing position at several universities and since 1991 he has been at Victoria University, Melbourne, Australia. He has been head of the School of Electrical and Electronic Engineering for several years and research director where he has conducted research, supervised several Ph.D. and master's degree students, and published more than 300 papers, books chapters, in peer-reviewed international conferences and journals. He has been the deputy leader of Smart Energy Research group at Victoria University and through his research leadership he has delivered successful R&D projects that led to industry uptake of project outcomes. He organized and run several continuing education programs for practicing engineers and provided consultancy for industries. He is currently Adjunct Professor at the College of Engineering and Science, Victoria University, Melbourne, Australia. His research interests include renewable energy, instrumentation, data acquisition/interfacing, sensors and microelectronics for biomedical applications.

Nathan Zimmerman holds a B.Sc. in chemical engineering from the University of Tennessee, Knoxville, in 2007 and an M.Sc. in energy engineering from Mälardalen University in 2012 where he carried out research in the emerging area of vanadium redox flow batteries. He's currently a doctoral candidate at the same university working in modeling, optimization, and control of waste fired fluidized bed boilers. He is also a member of the Future Energy Center at MDH.

Introduction

Electric vehicles and renewable energy sources are expected to play a fundamental role in reducing huge amount of carbon emissions caused by both the transportation and power generation sectors. Consequently a transition toward sustainable transport systems is becoming a crucial issue to be faced by the different players involved in these sectors. In this context, road vehicles, based on full electric or hybrid drives, represent a very interesting opportunity to solve various problems concerning liquid fossil fuel dependence. In addition, the electrochemical energy storage systems, utilized in their common use to power the electric and plug-in hybrid vehicles may, when connected to recharging stations, represent an additional great advantage for the main grid in terms of integration/interaction with the renewable energy generation sources, such as wind and solar energy, characterized by their natural power fluctuations. From this point of view, academia and the electric power systems industry are about to face technical and economic issues related to the massive integration of electric and plug-in hybrid electric vehicles in the electric grid, as electricity is becoming the preferred energy vector for the next new generation of road vehicles. Starting from a deep analysis of the above main issues, based on the status of the literature and ongoing research projects, this book presents a wide review of the new power technologies that allow the design of innovative solutions of charging architectures supporting, for example, DC fast charging operations for electric and plug-in hybrid vehicles. In particular, the grid-connected power converters and different typologies of energy storage systems are analyzed as key components to implement the new concepts of "distributed generation" and "storage system integration" into Smart Grids. In fact, these technologies represent the effective interfaces for the control and management of renewable and sustainable distributed energy resources. In addition, different standards and various applications of the main results of microgrid pilot projects, in various contexts and areas around the world, are reported in this book, as example case studies showing the convenience and feasibility of going toward a new smart concept of distributed energy management. As clearly demonstrated by the authors of this book in each respective chapter, the concept of smart energy management will

represent potential avenues for further research, in achieving a more reliable, secure, and cleaner energy availability.

The book is divided into three main parts: the first part devoted to charging technologies, the second one presenting significant charging applications, and the third analyzing EVs adoption and market diffusion. These parts, from different perspectives, are aimed to support a sustainable smart mobility, based on electric and plug-in hybrid vehicles. In fact, each one of the parts integrates various research projects, carried out by authors from different continents, on specific aspects concerning the new smart charging infrastructures. In detail, the analysis ranges over many topics: from the main issues and potential impacts of the vehicle electrification on the electric grid infrastructure (Chap. 1) to the different barriers explaining the slow market penetration of EVs and the lessons learned by policy-makers (Chap. 8); from the analysis of the huge potentialities offered by traditional and innovative battery technologies for transportation applications (Chap. 5) to the practical results of a German research project iZEUS, which has involved well-known car manufacturers and investigated how electric and plug-in hybrid vehicles can benefit from renewable energy sources, avoiding the negative effects on the electric grid of a unpredictable load peak associated for example with a simultaneous charging of many vehicles (Chap. 8); from the basic issues of control, operations, and protections of DC microgrids integrated with distributed energy sources (Chaps. 2 and 3) to worldwide experiences and applications of electric and hybrid vehicles in power system networks (Chap. 7).

Part I
Overview of Technologies

Chapter 1
Vehicle Electrification: Main Concepts, Energy Management, and Impact of Charging Strategies

Reinhard Madlener, Vincenzo Marano, and Ottorino Veneri

Abstract In this chapter the main issues related to the displacement of conventional vehicles in favor of electric vehicles, which is needed for the eventual decarbonization of the transportation sector, are discussed. First, an introduction to the various vehicle propulsion concepts and their pros and cons is provided, followed by smart energy management considerations for plug-in electric vehicles. Then, energy systems, economic and environmental considerations, as well as the impacts of charging strategies on the electric grid are discussed. Finally, some further issues which are important for the acceptance of electric vehicles—including safety, battery lifetime and optimal sizing, charging infrastructure, and business models—are analyzed.

1.1 Introduction

There is perhaps no apter symbol of the twenty-first century than the automobile—the dominant means of transport aspired to throughout the world. Today, the energy for personal transportation comes predominantly from petroleum, which is used in the form of either gasoline or diesel in conventional vehicles powered by internal combustion engines. Displacing petroleum without penalizing personal and commercial mobility has therefore become a major objective for the automotive industry and for government agencies worldwide. Today, the most viable options

R. Madlener (✉)
Institute for Future Energy Consumer Needs and Behavior (FCN), School of Business and Economics / E.ON Energy Research Center, RWTH Aachen University, Aachen, Germany
e-mail: RMadlener@eonerc.rwth-aachen.de

V. Marano
Center for Automotive Research, The Ohio State University, Columbus, OH, USA

O. Veneri
National Research Council, Istituto Motori, Naples, Italy
e-mail: o.veneri@im.cnr.it
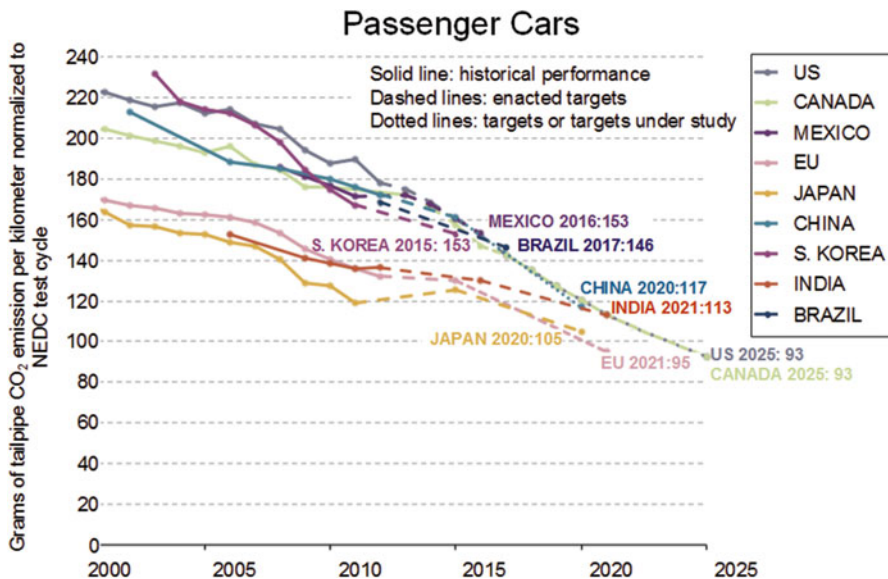
Fig. 1.1 CO_2 g/km efficiency standards, normalized to the New European Driving Cycle (*source*: ICCT [4])

include fuel economy improvements in conventional vehicles, vehicle hybridization/electrification, and recourse to alternative fuels (natural gas, LPG, biodiesel, etc.) (cf. [1–3]).

Passenger cars are required by law to become more fuel-efficient and environmentally friendly. In the USA, the National Highway Traffic Safety Administration (NHTSA) has recently set standards to rapidly increase Corporate Average Fuel Economy (CAFE) levels over the next several years, while in other countries fuel efficiency standards are regulated by way of CO_2 emission mandates, and are well above those of the USA (Fig. 1.1).

Regardless of technology improvements and legislative requirements, consumers will be the key drivers in the development of alternative-fuel vehicles. Higher cost, limited range, and long recharging time represent serious drawbacks that limit market penetration of virtually all alternative-fuel vehicles in the personal transportation sector. The choice of one particular vehicle option over other options is complex, and involves a variety of subjective factors regarding income, attitude towards cleaner technologies, practical needs, and others (see Chap. 8). As discussed in [1–3], the automotive industry is focusing on alternative-fuel vehicles and a variety of specific technologies and strategies, including engine downsizing and boosting, direct injection and variable valve actuation, weight reduction, and mild hybridization (including engine start-stop technologies) to achieve greater fuel economy in conventional vehicles.

Clearly, as demand for mobility continues to rise around the world, environmental and energy problems are rapidly making automobile transportation, as we know it, unsustainable for our society. Thus, the role of the automobile in the future needs to be rigorously reexamined. Vehicles are becoming part of a much bigger "energy network," wherein information, communication, and optimization play a key role. As a consequence, research is moving quickly towards vehicle electrification that helps to enhance both the transportation and the electricity sector. Electricity is the only potential energy source for transportation that addresses the simultaneous need for fuel diversity, energy supply security, reductions in greenhouse gas emissions, and improvements in air quality, and that is widely available and produced domestically. However, the impact of charging millions of vehicles from the power grid could be significant, e.g., in the form of increased loading of power plants, transmission and distribution lines, emissions, and economics. Therefore, this effect should be considered in an intelligent way by controlling and scheduling the charging through a communication-based distributed control system.

This introductory chapter focuses in particular on the use of electricity as a transportation energy source, and outlines how new and existing technologies could spur a different mix of vehicles and an improved energy infrastructure, serving as the backbone of the interaction between vehicles and the utility grid.

1.2   Vehicle Electrification: Introduction and Definitions

The current energy situation leads to social, environmental, political, and economic problems that have huge and critical impacts on everyday's life. The scientific community is putting great effort into curbing and rationalizing energy consumption in order to mitigate oil dependency and environmental issues. Over the past decade, the desire to reduce carbon emissions stemming from transportation sources has led to the development of new propulsion technologies, a number of which are focused on vehicle electrification. Plug-in electric vehicles (PEVs) are receiving a great deal of interest due to their energy efficiency, convenient and low-cost recharging capabilities, and reduced use of petroleum. The term PEV includes all motor vehicles that can be recharged from any external source of electricity, such as wall sockets, and where the electricity stored in the rechargeable battery packs either drives or contributes to driving the wheels. PEV is a superset of electric vehicles that includes all-electric or battery electric vehicles (BEVs), fuel-cell vehicles (FCVs), and plug-in hybrid vehicles (PHEVs).

1.2.1   From HEVs to Plug-In Hybrid Electric Vehicles

Hybrid electric vehicles (HEVs) benefit from an efficient combination of at least two power sources to propel the vehicle. Generally, one or more electric motors

alongside an internal combustion engine (ICE) or a fuel cell as a primary energy source, operate the propulsion system. A battery or a super-capacitor as a bidirectional energy source provides power to the drivetrain, and also recuperates part of the braking energy dissipated in conventional ICE vehicles. Generally speaking, the term HEV is used for a vehicle combining an engine with an electric motor. The main advantages of the HEV drivetrain can be summarized as follows:

- ICE downsizing: Since the peak power demand can be provided by a combination of the ICE and the battery, the ICE could be sized for the average power demand of the vehicle. This reduces the weight and improves the efficiency of the ICE when operating at the same load of a larger engine.
- Regenerative braking: The on-board battery or super-capacitor of an HEV can be recharged while the electric motor operates in generator mode, providing braking force instead of friction brake.
- Engine on/off functionality: The engine can be turned off when the vehicle is at standstill or the vehicle power demand is low. This prevents unnecessary engine idling or its operation at low power, which is generally inefficient.
- Control flexibility: The additional degree of freedom to provide the vehicle power demand from either one of the power sources gives the flexibility to operate the powertrain components in a more energy-efficient manner.

Plug-in hybrid electric vehicles (PHEVs) benefit from the features of both conventional HEVs and electric vehicles (EVs) by having a large battery which can be recharged when plugged into an electric power source. A PHEV is a viable solution to replace some part of the energy used in vehicular transportation with electricity, until full electrification of vehicles becomes mature. Moreover, PHEVs can eliminate concerns about EVs' recharging time and range anxiety. PHEVs can exceed the limited 100 mile (160 km) range per charge of most electric vehicles and have the potential to limit air pollutant emissions to near zero. A PHEV can achieve the cruising range and performance advantages of conventional vehicles with the low noise, low exhaust emissions, and energy independence benefits of electric vehicles. Also, PHEVs have considerable influence on propelling the shift from fossil fuels to electric energy sources for a significant part of the daily commutes. According to an investigation conducted by Toyota, the accumulative daily travel of around 75 %, 80 %, and 95 % of vehicles in North America, Europe, and Japan, respectively, is lower than 60 km [5].

Extended-range electric vehicles (EREVs) are PHEVs that can operate in pure electric vehicle mode. Both the battery and the tractive motor of PHEVs are capable of providing maximum tractive and auxiliary power demand for the powertrain. The maximum range that can be covered in the EV mode for a standard power cycle is called "all-electric range" (AER) for the specific cycle. The market of EREVs is focused on daily commuters who prefer the benefits of driving in the EV mode for daily routine travels while at the same time enjoying driving without the range anxiety for longer journeys that is still commonplace with all-electric cars [63].

The auxiliary power unit (APU) of a PHEV supplies the required baseline power to the vehicle, recharges the batteries, and powers accessories such as the air
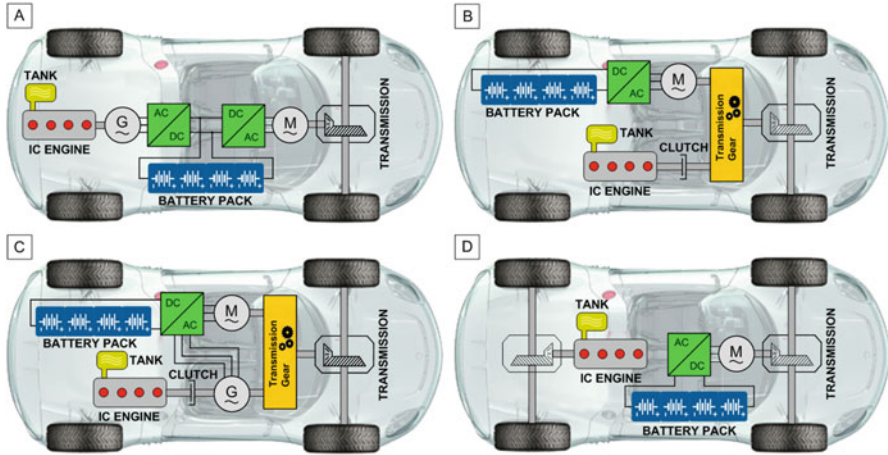
Fig. 1.2 Hybrid thermal-electric architectures: serial configuration (**A**), parallel configuration (**B**), power-split configuration (**C**), serial–parallel configuration (**D**)

conditioner and heater. Typically, the APU consists of a conventional combustion engine, but can be any kind of mechanical-type engine or a fuel cell, and several alternative fluids could be employed.

The combinations of connections between components of the propulsion system define the architecture of PHEVs or HEVs in general. Conventionally, HEVs are categorized into four basic drivetrain architectures: serial, parallel, power-split, and serial–parallel. A schematic representation of these four basic architectures is given in Fig. 1.2. A detailed description of the different architectures is beyond the scope of this section, but can be found in the specific literature (e.g., [6, 34, 62]); here, we restrict ourselves to a brief overview, specifically for PHEV applications.

The serial configuration is commonly recognized as an electric vehicle that has an engine and a generator to recharge the battery, so that it is easier to upgrade it to a PHEV. The serial architecture drivetrain has an electric motor sized to satisfy the designed vehicle maximum traction power. The increase in power capacity of the battery enables the AER and the zero-emission operation of the serial architecture. Since there is no mechanical coupling between the wheels and the engine in this architecture, the engine can operate independently around its most efficient torque-speed region. However, the well-known drawback of the serial drivetrain is the conversion of the engine mechanical power into electrical and then back into mechanical energy in the electric motor. This efficiency chain reduces the overall efficiency of the drivetrain. For example, the GM Volt is a 64 km EREV with a base platform of a serial drivetrain. The Volt benefits from a mode-changing architecture by employing a planetary gear set and two brakes. The mechanism enables the vehicle to shift from the serial to the serial–parallel architecture and thus solves the above-mentioned drawback. In this mode, the engine can mechanically transfer power to the final drive in times of higher vehicle speeds and power demands. Also,

it has two different EV modes in which the EV mode is shifted from one to two electric motor drives in order to reduce the losses associated with high-speed operation of the electric motors, particularly during cruise operation [7].

In the parallel drivetrain, both the engine and the electric motor can propel the wheels directly. A properly sized electric motor and battery are necessary to upgrade a parallel drivetrain to an EREV. In the pre-transmission parallel architecture similar to that of the Honda Insight, Civic, and Accord HEVs, a small electric motor is located between the engine and the transmission, replacing the flywheel. It is also possible for a parallel HEV to use its engine to drive one of the vehicle's axles, while its electric motor drives the other axle. Daimler Chrysler PHEV Sprinter has this powertrain configuration. On the one hand, a direct mechanical connection between the wheels and the engine eliminates the conversion losses from which the serial architecture suffers. On the other hand, it reduces the degree of freedom of the engine speed control to the transmission ratio selection.

The serial–parallel or power-split architecture is the most commonly used drivetrain for HEVs. Toyota Prius, the most often sold HEV, the Toyota Camry and Highlander hybrids, the Lexus RX 400 h, and the Ford Escape and Mariner hybrids all benefit from the features of this architecture. The serial–parallel hybrid powertrain combines the serial with the parallel hybrid architecture to achieve the maximum advantage of both systems. In this powertrain, the mechanical energy passes through the power split in serial and parallel paths. In the serial path, the engine power output is converted into electrical energy by means of a generator. In the parallel path, in contrast, there is no energy conversion, and the mechanical energy of the engine is directly transferred to the final drive through the power split, which is a planetary gear system. Generally, similarly to the parallel drivetrain, the serial–parallel architecture does not have an electric motor designed for the maximum traction power demand of the vehicle. The pure EV mode is possible for the serial–parallel drivetrain; however, in addition to the electric motor power capability, there is a mechanical constraint that arises from the planetary gear set dynamics. There is no clutch to release the electric motor from the planetary gear set in the serial–parallel architecture. Therefore, during the EV mode, the generator speed increases sharply, and proportional to the motor speed, with a ring-to-sun gear teeth number ratio.

Another design for the power-split HEV is the Allison Hybrid System, also known as AHSII [8]. This system is a dual-mode system with two planetary gear sets, designed by GM and currently employed for several mid-sized SUVs and pick-up trucks, respectively.

1.2.2   PHEV Energy Management

It is worth pointing out that energy management algorithms are an integral part of electric mobility and are very important for achieving performance benefits. In fact, improving the energy management in electrified vehicles can result in important

benefits, such as the achievement of a minimum amount of fuel consumed and air pollutant emissions released, giving support to today's quest for sustainable (individual) mobility. Nonetheless, the achievable improvements deeply depend on the vehicle typology and components and on the driving mission, and can only be reached by implementing an on-board sophisticated control strategy that is able to optimize the energy flows within the vehicle powertrain. Energy management algorithms for PHEVs are crucial for vehicle performance. Energy management strategies in a PHEV are similar to those employed in HEVs, with the additional degree of freedom corresponding to the ability to deplete the battery pack in order to obtain electric tractive power in significant quantities, coupled with the possibility of recharging the pack [9]. Given the complexity of the PHEV architecture, the control strategy algorithm is required to perform multi-objective optimization of fuel economy, AER, total emissions, battery life, and ease of implementation, along with the constraints related to charging issues and availability, battery aging, and expected performance. Energy management algorithms can be broadly divided into analytical ones (e.g., dynamic programming, Pontryagin principle, equivalent consumption minimization strategy (ECMS)) and empirical ones (rule-based, fuzzy logic, artificial neural networks) [10].

Control strategies can be categorized into two groups: EV mode control and blended mode control. The EV mode control is a simple method with two stages—charge-depleting (all-electric) and charge-sustaining. The control algorithm selects only the electric motor as long as the battery state of charge (SOC) is greater than a threshold value. Once the SOC reduces below this value, the control algorithm switches to charge-sustaining (PHEV behaving like an HEV). In blended mode control, the objective is to achieve the lower limit of the SOC only at the end of the trip. The battery SOC is reduced slowly throughout the trip, and the SOC profile followed in this control mode can be optimally selected by principles from optimization theory like dynamic programming. This method can provide better fuel economy, but at the cost of higher information requirements. The comparison of battery SOC profile for blended versus EV mode control is shown in Fig. 1.3.

The blended mode control requires sophisticated algorithms in order to achieve better fuel economy with reduced information requirements. ECMS is one such algorithm that is widely used for hybrid vehicles and that can be applied to PHEVs. It is based on the fact that in a hybrid vehicle, in general, the energy consumption from the battery is replenished by running the engine [12]. Therefore, battery discharging at any time is equivalent to some fuel consumption in the future. For PHEV applications, the ECMS also needs to consider the energy coming from the grid: this effective fuel consumption is used as the objective function for control optimization, while the input to the ECMS algorithm is total power demand. The ECMS searches the best combination between the engine and motor power that minimizes the effective fuel consumption. The ECMS algorithm is applied to PHEVs in tracking mode, where the algorithm tracks an optimal reference state of charge profile. The study of dynamic programming algorithms for PHEVs reveals that a linearly decreasing SOC profile with respect to the distance of travel gives optimal performance [13].
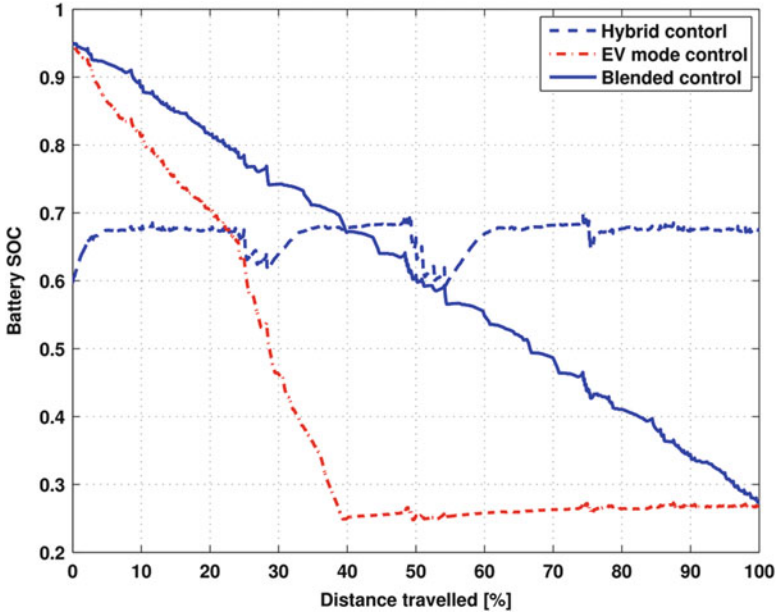
Fig. 1.3 Comparison of battery SOC profile for blended versus EV mode control [11]

The dynamic programming algorithm is a numerical optimization methodology that can compute the optimal solution, but is practically impossible to implement on a vehicle, since it requires complete information on the future driving cycle. Dynamic programming also requires a large amount of memory and computational power to perform the optimization. Other algorithms, such as rule-based algorithms, or online optimization methods like ECMS and stochastic dynamic programming [10], can be implemented onboard a vehicle. These algorithms do require some information to perform off-line optimization, or tuning of the parameters, but the information requirements are typically lower than that those required by dynamic programming.

The performance of the energy management algorithm is closely related to the power demand throughout the driving trip. The power demand depends on the type of road, the weather conditions, and the velocity profile, the latter of which in turn is dependent on traffic and geography. The performance of the energy management can be improved and optimized for the driving conditions and weather patterns [14]. Therefore, information about the driving route, a weather forecast, and traffic conditions are very important in guaranteeing optimal performance of the energy management strategy. Static and dynamic information, including road grade and road surface conditions, speed limits, traffic light locations and timing, and real-time traffic flow speeds, can be used to make a long-term forecast of the overall trip to the destination. Access to such information can improve vehicle energy efficiency and mobility via route planning. Road static information, real-time traffic

Fig. 1.4 Intelligent energy management of PEVs with environment and charging infrastructure awareness

flow, battery charging station locations, and real-time prices and other information are useful in determining an optimal route and energy management. Figure 1.4 shows a concept of such an intelligent energy management with environment and charging infrastructure awareness. Clearly, there is a trade-off between information requirements and algorithm performance. Thus, detailed a priori knowledge of the trip is required for an optimal solution, but clearly this is not a practical scenario, and a trade-off between optimality and level of information is needed.

Finally, for plug-in vehicles, the control strategy should take into account the charging station's location, especially when the chosen state variable is the battery state of charge. In fact, depending on the energy available in the electrical storage system, the vehicle energy management can be controlled in different ways, and the integration of this parameter can bring a relevant benefit in the achievement of the optimal solution. Nonetheless, the integration of the control strategy with the power grid allows considering also grid-related constraints, such as grid stability and capacity, which are often neglected.

1.2.3 Full-Electric Vehicles

An electric vehicle is a vehicle in which the propulsion system converts electrical energy that is stored in a battery into mechanical energy used to move the vehicle; such a vehicle does not have a gasoline engine on board, and thus requires a large

(and expensive) battery to guarantee a still very limited range (up to about 100 miles). Higher cost, limited range, and long recharging time (up to 20 h—using a standard outlet—for 100 miles of driving) represent the main drawbacks. On this regard, in Table 1.1, the total km per charge and the reduction in petroleum use of electric vehicles are reported in comparison with other vehicle technologies.

In fact, a key driver in the development of PEVs will be the consumer. People buy vehicles for a whole variety of reasons; buying decisions are complex, and no one—including the automobile companies—fully understands how it works. It involves a number of psychological factors having to do with the individual's personality and past experiences—as well as some quite down-to-earth considerations such as disposable income and practical needs in a vehicle (cf. Chap. 8). Obviously, people do not buy vehicles based on lifetime costs only, or on the average driving and comfort needs. People might buy vehicles for those "once-in-a-while" trips, and might end up choosing a minivan for the twice-a-year family trip out of state, or a four-wheel drive for two weeks of heavy snow. Table 1.2 shows the factors that make potential PEV drivers most hesitant to choose a PEV as their next vehicle.

Table 1.1 Consumption, autonomy, and reduction in petroleum use for different vehicle technologies

Type of vehicle	km/L	Total km per tank + charge	Reduction in petroleum use
TDI diesel	19	855	–
Hybrid electric	21	945	10 %
Plug-in hybrid electric (10)	36	1180	28 %
Plug-in hybrid electric (40)	67	1255	32 %
Plug-in electric (EVs)	–	150	100 %

Source: US Energy Information Administration [15]

Table 1.2 Answers to the question "Which factor will make you most hesitant to choose a PHEV or an EV as your next vehicle?" raised within an Ernst and Young study [16]

		Access to charging stations	Price	Battery driving range	Reliability/ service ability	Performance and handling	Lack of clear understanding of cost advantage	Battery disposal	Safety	Technological obsolescence	Seating capacity
China		69%	57%	73%	64%	57%	49%	54%	64%	28%	24%
Japan		60%	73%	43%	36%	35%	44%	26%	32%	10%	9%
US		75%	74%	75%	57%	49%	49%	50%	41%	30%	33%
Europe	France	74%	63%	81%	26%	46%	23%	26%	19%	14%	16%
	Germany	74%	66%	75%	46%	52%	48%	36%	26%	27%	20%
	Italy	64%	62%	62%	42%	54%	44%	33%	28%	22%	19%
	UK	71%	60%	71%	47%	50%	44%	36%	31%	23%	27%
Average		69%	67%	66%	49%	48%	45%	41%	41%	22%	21%

■ Highest response rate for each factor   ▢ Lowest response rate for each factor

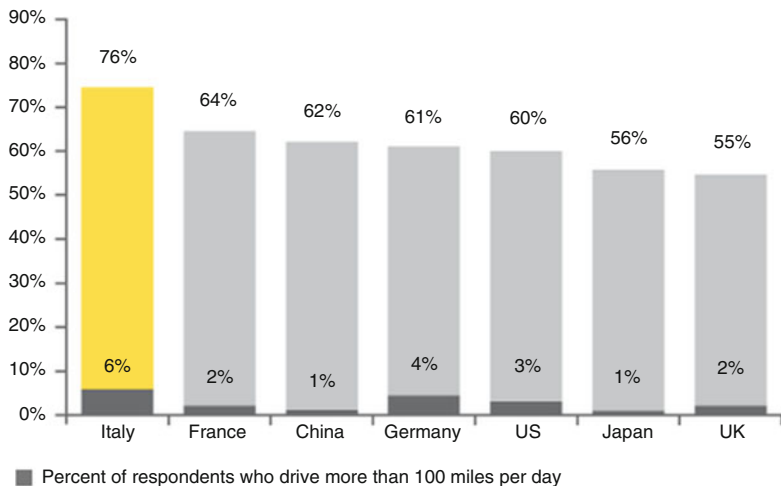Percent of respondents who drive more than 100 miles per day

Fig. 1.5 Answers to the question "Would you consider a driving range of 100 miles to be acceptable?" (percentage of respondents who answered "No") raised within an Ernst and Young study [16]

As expected, respondents provided interesting insights regarding prevailing differences between vehicle adoption in the USA and other countries; however, one major common factor that severely slows down PEV market penetration is that of driving range. Figure 1.5 provides some interesting insights into the ratio between people's actual needs and what people expect from their vehicle, and specifically the percentage of drivers that consider 100 miles of driving range to be *not enough* for their driving needs.

When focusing on US respondents, one can notice that 60 % of all drivers would not be happy with 100 miles of driving range, but at the same time only 3 % actually drive more than 100 miles a day. Is this because *people do not really realize what they need?*

Just to give some numbers: to reach the workplace the average US commuter travels approximately 15 miles one way. Two out of three commuters (68 %) reported a one-way commute of 15 miles or less, 22 % traveled between 16 and 30 miles, and only 11 % actually traveled more than 30 miles. The majority of commuters (81 %) use only their personal vehicle to complete their commute, and most personal vehicle users (86 %) drive alone (Research and Innovative Technology Administration (RITA), "Omnibus Household Survey," U.S. Department of Transportation, Bureau of Transportation Statistics, Vol. 3, Issue 4, 2003).

Technology sometimes moves faster than the pace at which people adjust their habits. People are now used to refueling their vehicle three to four times a month, by driving to the gas station and taking care of the refueling within minutes. But still it is not something people do on a daily basis. PEVs require a more frequent "refueling" and, depending on the specific driving habits, refueling can be a daily routine in order to maximize electric range. The advantage is that, in most cases,

this will happen at home and overnight, thus making the refueling process a part of people's home chores and no more an activity to include in their errands. Let us consider a cell phone: until a few years ago, a phone would go on for days without requiring a charge. Nowadays, people find themselves always looking for a way to charge their smartphone—even when not needed, "just in case"—at the coffee shop, airport, the office, etc. This is called "opportunistic charging," and it is likely the same direction that PEV-charging is heading for. Finally, consumer education is necessary in order to teach owners to not only fully charge each night but also to charge opportunistically in order to maximize electric range.

1.2.4 PEV Charging Options and Infrastructure

Current PEV charging technology offers three types of charging methods ([17, 18]; cf. Table 1.3): level one charging, level two charging,[1] and DC charging. Level one charging usually uses a standard power outlet of 110 V_{AC} and 15 A (12 A usable), which is the lowest voltage one can find in a residential or public building in the USA. It takes about 12–18 hours to fully charge a vehicle, depending on the size of the battery and actual power rate. Level two uses a 220 V_{AC} circuit with 15–30 A and thus takes less time to charge. DC fast charging uses a high direct current (i.e., 200–600 V_{DC}) and requires no more than 30 min to fully charge a vehicle. However, since such a fast-charging method requires special charging equipment and power requirement is beyond the capacity of most residential electric service, DC charging is not expected to be implemented for residential use any time soon.

One of the biggest concerns resulting from vehicle electrification relates to charging stations (of PEVs). Where and how many charging stations should be built to satisfy basic charging needs? What kinds of charging technology should be used? These questions are important in the sense that, as many studies conclude, the availability of a convenient and affordable recharging infrastructure will directly affect customers' purchasing decision and thus also impacts the effective promotion of PEVs. On the other hand, utility companies have always expressed concerns about effects of PEV charging loads on the power system. A location plan might indicate potential power congestion and help utility companies to get ready.

Table 1.3 Charging power levels (based on SAE Hybrid Committee [17])

Charging method	Voltage	Usage	Power (kW)	Charging time
Level one	110 V_{AC}	Home/public	1.4	12–18 h
Level two	220 V_{AC}	Home/public	3.3–6.6	4–8 h
DC levels 1–3 (fast-charging)	200–600 V_{DC}	Public	20–50	15–30 min

---

[1] We refer to level one and two charging as slow charging, and DC charging as fast charging.

The location problem of PEV charging stations, in general, is a refueling infrastructure problem, which has been studied by many papers long before the advent of electric vehicles. Despite the abundant amount of previous researches, there are still numerous issues and nuances that are not well addressed by the earlier models and thus limit their application to PEV charging stations.

First, most of the earlier models are designed for fast-charging refueling systems, where it is assumed that the charging time required by a customer is short enough to ignore, and thus that all the customers arriving at the stations will be served. In other words, any flow that passes through an allocated station will be served. This assumption is generally true for hydrogen and gasoline charging, but not justifiable for PEV charging (at least not for level one and level two). Considering the fact that PEV charging takes a decent amount of time, a flow that arrives or passes through a PEV station might be rejected if there are no free chargers in the station and the customer is unwilling to wait, or a vehicle might only be partially charged because the time it waits is not long enough for full charging. Therefore, a new model is needed to deal with rejection and partial charging.

A second problem with the earlier charging models is that they cannot decide how many chargers are needed for each PEV charging station. This question is important for PEV station design because the number of chargers directly affects the amount of flows that can be served due to the fact that each PEV arriving at the station will occupy a charger for a long period. Also, the number of chargers almost exclusively determines the investment cost for slow-charging stations (i.e., levels one and two) since the fixed cost is relatively low to set up such stations.

Furthermore, many of the earlier studies use conventional vehicle flows or sales data from gasoline charging stations to estimate the new vehicle flows, and an underlying assumption is that the new flows are proportional to the conventional flows. This assumption is problematic for estimating PEV flows, as many recent studies indicate that PEV adoption is strongly related to customers' economic demographic characteristics. Curtin et al. [19] conducted a survey about people's interest in electric vehicles, where economic, demographic and current vehicle usage data were collected for the analysis. The research finds that households with a higher income and education levels are more likely to buy electric vehicles. Besides, vehicle usages, such as the number of cars in the household and the daily highway miles, also have a significant influence. Households with more vehicles and lower average vehicle ages indicate stronger interests in electric vehicles. Gallagher and Muehlegger [20] studied consumer adoption of HEVs in the USA and found that people who are strongly concerned with environmental and energy security issues prefer HEVs. Similar results are also found in other studies of alternative-fuel vehicles (e.g., [21, 22];cf. Chap. 8).

1.3   Energy, Economic, and Environmental Considerations

When connection to the power grid is involved, both the gasoline consumption and the electricity drawn from the grid, with related generation, transportation, and distribution costs and emissions have to be considered. Emissions from a PEV largely depend on the sources used to produce electric power; therefore, various electricity generation options must be considered. The use of PEVs is likely to reduce oil dependency but—in terms of GHG and other pollutant emissions—the primary energy sources used to produce electric power represent the core of the energy dilemma that the smart distribution grid is supposed to relieve (Fig. 1.6).

In the near future, with a still low market penetration of e-vehicles, there should be no major technical problems for PEVs to be recharged. PEVs benefit from an existing infrastructure that can directly use renewable energy: they do not require energy supply infrastructure developments and could obtain substantial public benefits, such as the more rapid introduction of zero-emission vehicles; increase in electric system reliability; lower transportation costs; higher penetration of renewable energy sources in the electric power system; lower dependence on oil importations; and lower pollutant emissions.

However, it is important to understand the ramifications of introducing a number of PHEVs into the grid. Depending on when and where the vehicles are plugged in,
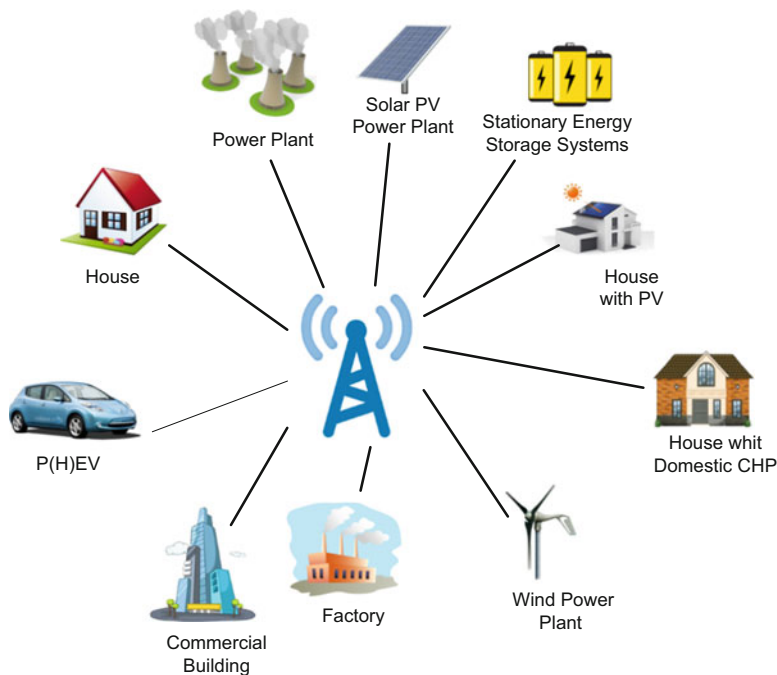

Fig. 1.6   P(H)EVs as part of a smart distributed energy network

they could cause local or regional constraints on the grid. They could also require both the addition of new electric capacity and an increase in the utilization of existing capacity. Local distribution grids will see a change in their utilization patterns, and some lines or substations may become overloaded sooner than expected. Furthermore, the type of generation used to recharge vehicles will be different, depending on the region of the country and the timing when PHEVs recharge, and that will strongly affect PHEV emissions and cost impacts.

One possible behavior, which could be rewarded by appropriate electricity pricing policies, would see PEVs being charged primarily at night, with reduced effects on the grid (controlled charging). Nighttime charging is suitable for the grid because of its unused capacity during the night. On the other hand, nighttime charging requires a charging station or power plug access at home and the installation of a charging facility, and may need to be installed at the vehicle owners' expense. The new load of PEV charging directly impacts the existing primary and secondary distribution networks, with many of these circuits being already saturated without any monitoring and automation capability [23]. Another scenario would be to allow PEV owners to charge at any time, thus resulting in charging mostly during daytime (uncontrolled charging), with the risk of destabilizing the power grid and thus requiring load shedding.

Clearly, the time of charging is a very important factor, since it determines which generators are to be used to satisfy the increased demand; for example, evening charging would increase natural gas combined-cycle generation while nighttime charging would increase coal-fired power generation, with clear implications with respect to cost and emissions [24]. Sioshansi et al. [24], in a case study conducted for the State of Ohio (USA), have shown that PHEVs will yield some reductions in CO_2 relative to conventional vehicles, but that SO_2 and NO_x emissions will rise dramatically, due to high generator emissions of these species. Uncontrolled charging, on the other hand, uses more natural gas-fired generation for PHEV charging, which gives strong reduction in CO_2 emissions compared to controlled charging and CVs. Thus, time of charging can have a significant impact on the emissions and the generation associated with electricity used as a transportation fuel.

These results, however, are not universally true, and the emission impacts will be highly sensitive to the generation mix and economic dispatch policies. It is certain that the increased use of renewable energy generators will help reducing the emissions. Tulpule et al. [25] explored a scenario where solar energy is used to charge PHEVs, and total emission from power grids is measured for nighttime uncontrolled charging, daytime charging without solar, and daytime charging with solar energy. Their results show the benefit of using renewable energy for charging PHEVs, with a CO_2 reduction by approximately 70 % per year through the use of solar charging at the workplace.

Apart from the optimization of energy flows, it is also important to intelligently control the charging behavior. If all vehicle controllers independently decided to charge without any external signal, grid stability could be compromised. Therefore it is necessary to provide a centralized charge-enabling control to each vehicle. Thus, access to real-world data or the ability to generate realistic datasets allows a

better modeling of the situation and therefore a more significant and optimized charging strategy [26]. Another important factor to consider when designing a charging strategy is the likely shift in driving patterns experienced by drivers changing from an internal combustion engine vehicle to an electric or plug-in hybrid electric vehicle. For instance, for EVs the range is limited by battery size and access to charging infrastructure, which leads drivers to better plan daily commutes and adjust their driving style. In terms of generation capacity, no technical challenges are expected for low-volume charging of PEVs with current infrastructure, though larger vehicles (i.e., bigger batteries) may have difficulty completely recharging during off-peak hours when using a standard 115 V/20 A residential outlet. However, highly clustered PEV users in the same neighborhood could cause stress on transmission and distribution systems locally, even at negligible market penetration levels. On a longer term, with a much larger vehicle population, smart metering and charge control at the utility level will likely be required to ensure low-impact charging and so maximize overall system efficiency.

In addition to the use of charging strategies, research is focusing on the use of energy storage to relieve peak loads on the distribution system. Energy storage presents advantages relative to transformer and wiring upgrades. It allows for leveling of distribution-level loads, implying higher capacity factors. Storage can also be used to provide valuable market services, such as energy arbitrage and ancillary services [27, 28]. The introduction of energy storage requires the development of additional and more complex storage control, and optimization algorithms which co-optimize these various competing uses of the storage device.

From this brief state-of-the art assessment it is clear that there are both opportunities in e-mobility as well as some challenges. From the perspective of emissions, the fuel source generating the electricity, be it coal, nuclear, wind, or others, can have a tremendous impact on the overall CO_2 emissions of the vehicle. Moreover, the time of day when the charging happens impacts what mix of electricity will be used to supply the vehicle, which has a direct impact on energy and emissions associated with charging. Customer usage patterns and expectations also play into the issue of PEV charging heavily, as they affect the availability of the vehicle to the grid and owners' expectations of charging rates. Finally, the impact of charging on the local distribution grid is of high importance, as this is a widely acknowledged weakness in the overall distribution grid. With poorly managed charging, even a small number of vehicles on a single residential transformer lead to dramatic loss of insulation life. This leads to reduced reliability and increased costs for the utility provider, which in turn get passed on to customers through rates. Conversely, more sophisticated charging strategies can allow the same transformer to service a large number of vehicles without serious detriment to life. In order for PEVs to become mainstream technology, these issues and many others will need to be addressed by a framework that goes beyond technology issues and aims at investigating the dynamic interactions existing between electric mobility, power grid and infrastructure, individuals and their energy footprint, and multiple energy policies targeting different objectives.

To date, despite the fact that most of the existing research considers both aspects, most of it has focused on either technical or socioeconomic aspects of sustainable mobility. The problem of focusing on one side rather than on both is that in such a turbulent and uncertain situation the risk of not considering the interdependences between technological and socioeconomic issues is strong. To address such intersection of economic, environmental, and technology issues, involving a complex set of trade-offs among cost, air quality, technology, and energy sources, an interdisciplinary and integrated research approach is needed.

1.4 Impacts of PEV Charging on the Power Grid

1.4.1 General Considerations

Vehicle electrification technologies have the potential of making passenger and commercial vehicles more energy-efficient and environmentally friendly. The growing fleet of PEVs needs enhanced charging infrastructure in order to satisfy the electricity demand of these vehicles. Because the electricity infrastructure plays a crucial role in PEV commercialization, the electric utility companies are studying the impacts of charging demand on their distribution networks and are moving to upgrade it and installing smart meters to control and monitor PEV charging [29, 30]. It is necessary to study the effect of different levels of market penetration of PEVs into the automotive sector on the power grid. As the number of vehicles increases, the charging demand may pose serious challenges to grid capacity or may even cause severe constraints on grid operation. The time and location of the vehicles determine whether the effect of the PEV charging will be on a local grid or regional power system. While most electric power systems have sufficient generation and transmission capacities available to accommodate moderate-sized PEV fleets, this assumes that PEV charging is controlled and coordinated with power system operations [27, 31].

Besides all the above-mentioned considerations, the integration of electric vehicles within the power sector depends critically on the policy and regulatory framework. If electric vehicles are charged solely at home, starting immediately after arrival, the resulting uncontrolled charging profile will add to the existing peak load, stressing the existing network infrastructure.

On the other hand, a number of studies have evaluated the potential of dispatching electric vehicle charging during the hours with low electricity demand. This may improve the efficiency of the electricity sector by increasing the load factor of base-load generators, thus reducing the need for expensive peak generation [24]. Another benefit of electric vehicles derives from improving the introduction of more renewable energy sources into the electricity generation mix, reducing costs, and making renewable energy more affordable [32, 33]. The variable nature of natural resources causes large fluctuations in the residual load that is served by

conventional generators. Flexible electric vehicle charging demand can lead to a flatter output profile of dispatchable units. Energy storage can yield similar efficiency benefits by using base-load generators to serve peak loads. A centralized control over vehicle charging could enhance generation efficiency and the introduction of renewable energy sources and could also reduce the issues related with higher peak loads. Controlling the charging profile of electric vehicles requires some form of infrastructure for these vehicles to exchange information with the grid and for remote charging control. It is unclear, however, whether consumers will allow the system operator to have direct control over the charging of their vehicle. Alternatively, the charging decisions could be left to individual consumers, with policy makers defining an adequate set of price incentives to time vehicle charging that considers the interests of the system. Regarding this, small consumers cannot be assumed to be always pursuing cost minimization and will be probably represented by a much smaller number of aggregators. The aggregator, as the intermediate and coordinating entity between individual car owners and other stakeholders, will play a central role in the market. Ultimately, the regulatory framework will have an impact on the operations of the aggregators, for example on which layer of the power system they will operate (generation, transmission, or distribution) and in which market they will trade (day ahead, intraday, or reserve market).

1.4.2 Effects of PEV Charging on Battery Lifetime

By applying intelligent battery charging algorithms, battery lifetime can be increased and at the same time charging costs reduced [34]. The economic impact of a longer battery lifetime is found to be about twice the revenues that can be gained through energy trading. Furthermore, it is found that it is difficult to reach the 10-year battery lifetime intended for vehicle applications without battery oversizing. However, intelligent battery charging strategies can mitigate or altogether avoid battery oversizing, as standstill times are dominating battery operation, and because with uncontrolled battery charging the battery SOC is above 90 % during 80 % of the time. For achieving the intended battery lifetime, intelligent charging strategies are thus paramount. Battery oversizing in order to limit the maximum SOC may be a costly alternative, because either the electric driving range is decreased or the battery costs are increased.

1.4.3 Effects of PEV Charging on Generation and Load Profile

When a vehicle is plugged in and connected to the grid to recharge its battery pack, it is seen as an additional load on the system, and its energy demand has to be

immediately satisfied by increasing the overall electricity production. The charging load corresponding to all the electric vehicles demanding energy for recharging their batteries depends on the number of vehicles present in the market as well as drivers' behaviors and charging strategies. An uncontrolled charging strategy, where all the drivers recharge their batteries whenever they are able to, is the simplest one to implement because it does not need any communication system between the power grid administrator and drivers. This behavior is possible while electric vehicles are a small part of the automotive sector but when the charging load increases with the number of vehicles circulating, the system operator will necessarily need to control the batteries' recharging process in order to optimally align it with the functioning of the power generation system.

In order to estimate the impact of a PHEV fleet on the load profile, it is necessary to know at what time drivers usually park their cars and their driving behaviors. By coupling these data with information on power generators and hourly electricity demand, it is then possible to model the impact of PHEVs on the electric system. An example of such a study is given by Sioshansi et al. [24], for the State of Ohio, USA, supposing that 5 % of the vehicles circulating in the State were recharging the battery from the power grid. Vehicle driving patterns were based upon a household travel survey that was conducted in the St. Louis, Missouri metropolitan area. The vehicle survey tracked second by second driving patterns of 227 vehicles over the course of a number of weekdays [35]. The driving data were used to determine the hours in which PHEVs are driven, the total distance traveled in every hour, and when they are grid connected and could be dispatched to charge their batteries. In doing so, it was supposed that a PHEV has to be parked for at least an entire hour to be considered "grid connected" in that hour. Depending on the state of charge (SOC) of a PHEV battery, the vehicle will be driven in either charge-depleting (CD) mode, in which case the battery is the primary energy source and the gasoline engine is used only on a supplemental basis for quick accelerations, or charge-sustaining (CS) mode, in which case the gasoline engine is used to maintain the same average SOC.

Two different charging strategies were implemented in the analysis:

1. A controlled charging scenario, where the grid administrator co-optimizes PHEV charging load with its normal power demand minimizing the total cost of generation and gasoline burned by PHEVs. In this scenario the grid administrator is forced to completely recharge a PHEV battery before the driver's first trip in the morning.
2. Uncontrolled charging scenarios where PHEVs are recharged whenever they are parked and the grid administrator has to satisfy the PHEVs' charging load, while minimizing generation cost.

In both scenarios it was assumed that public charging stations were available and that all drivers were able to plug in their own vehicles whenever they parked them.

Ohio's power plant generation costs were modeled and implemented in the model to simulate the dispatching process. Generation costs were calculated based on estimated generator heat rates and fuel costs. Nuclear plants were
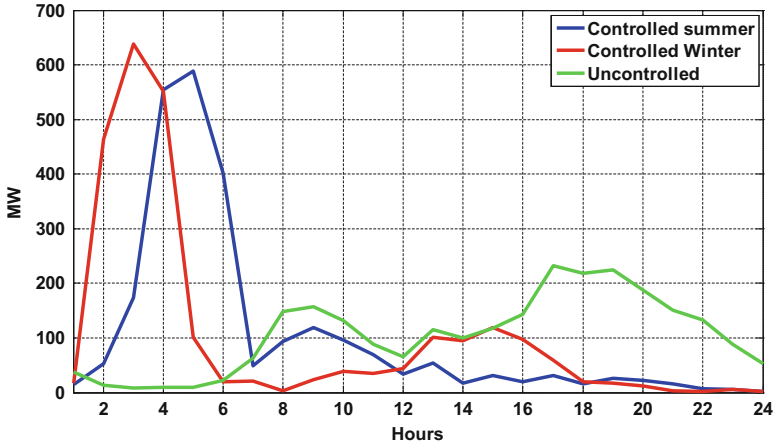
Fig. 1.7 Charging load profile of different scenarios (Sioshansi et al. (2010), p. 6707 [24])

considered as always running at full capacity and not dispatched by the system operator. Heat rates were estimated based on historical continuous emission monitoring system (CEMS) data from the US Environmental Protection Agency. The model simulates the commitment and the dispatching of conventional generators as well as the dispatching of PHEVs to charge when not being driven. As is typical of day-ahead electricity markets, the unit commitment model has a 1-day planning horizon with an hourly time step for the commitment and dispatch variables. Each day in the sample is simulated independently, except that the commitment and dispatching of each conventional generator and the charge level of each PHEV battery at the beginning of each day are fixed based upon the ending values from the previous day's run. PHEV charging decisions are modeled differently in the controlled and uncontrolled charging scenarios (Fig. 1.7).

In the controlled charging scenario, the grid operator makes all charging decisions and coordinates these with power system operations. The controlled charging model also includes a constraint to ensure that each PHEV battery is fully recharged in time for the first vehicle trip of each morning. In the uncontrolled charging scenario, PHEV owners are assumed to make charging decisions by themselves, without any regard for the impact of vehicle charging on the power system. Because PHEV owners face fixed electricity tariffs, it is optimal for them to recharge their vehicles whenever these are plugged in, since electricity is a significantly less costly source of transportation energy than gasoline.

Whereas in the uncontrolled charging scenario charging energy demand is dependent only on drivers' behavior and not affected by the preexisting load on the grid, in the controlled charging scenario the system operator takes the preexisting load into account when deciding how to recharge vehicles' batteries during the day. With 5 % of PHEV penetration in the market the peak load is not increased considerably, but in the future with larger PHEV market penetration
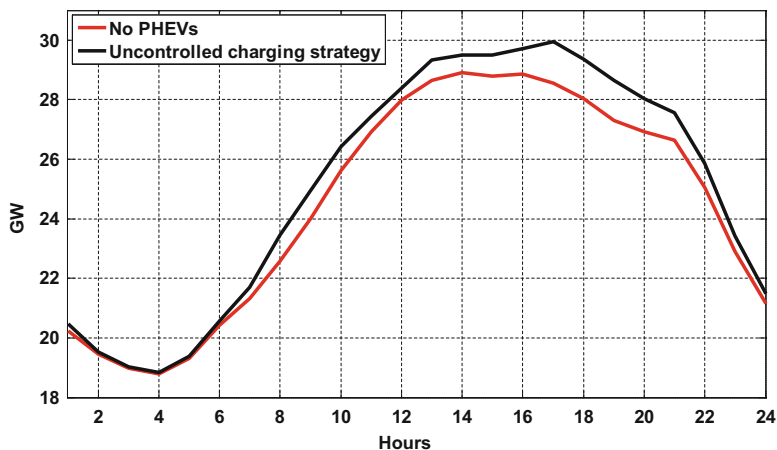
Fig. 1.8 Summer peak load with uncontrolled charging strategy and 30 % PHEV penetration (Sioshansi et al. (2010), p. 6706 [24])

the charging load could start to create considerable problems for grid reliability. The National Research Council has proposed in a recent study that PHEV market penetration could reach 30 % of the light-duty fleet by the year 2050.

The study presents a first estimation of how the load profile could change on the grid in this scenario. The summer peak load is increased by 3.4 %, reaching 30 GW and shifting later in the afternoon ([24]). Even if the generating capacity available in Ohio were to be enough to cover this power demand, the effects of such a load on the transportation lines should be analyzed. This analysis requires very detailed information on the grid scheme and on where exactly generators and loads are located (Fig. 1.8).

PHEVs are supposed to reduce pollutants by using electricity instead of gasoline as a transportation energy source. Their net emission impact will be intimately related with the generation mix in the power system in question, and the mix of generating technologies used to serve the vehicle charging load. In a system with a high penetration of renewable or nuclear power plants, the net emissions associated with PHEVs can be very low, as opposed to a system with predominantly coal which would yield higher PHEV emissions. In some systems the charging scenario will also be an important factor, since different generating fuels can be marginal at different times of the day, which would result in very different generator emissions, depending on when PHEVs are charged.

In Ohio (USA), for instance, a controlled charge will allow charging in periods of low loads, and most of the generation will be supplied by base-load units that usually are nuclear or coal plants. Uncontrolled charging, on the other hand, is done during the afternoon and is covered by peak-load plants, such as gas turbines.

In the case of Ohio the high penetration of coal plants results in an increase of total SO_2 emissions, a decrease of total CO_2 emissions, and minimal variation of NO_x emissions, as shown in [36].
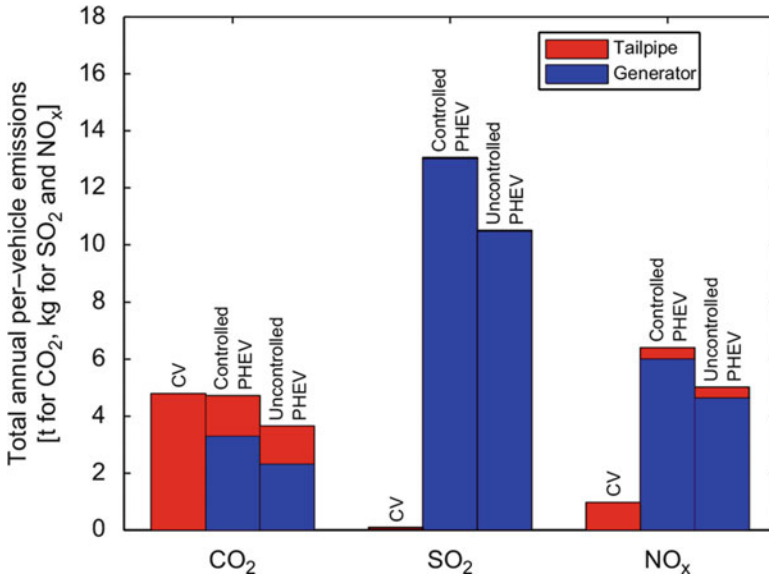
Fig. 1.9 Annual per-vehicle emissions of CO_2 (tons) and SO_2 and NO_x (kg) (*source*: Sioshansi et al. (2010), p. 6708—modified [24])

Figure 1.9 shows the emission impacts on a per-vehicle basis, revealing that PHEV use can yield some CO_2 emissions of around 1.1 tons on an annual basis in an uncontrolled charging case, which corresponds to a 24 % emission reduction. With a controlled strategy, on the other hand, the CO_2 emission reductions are minimal. Annual NO_x emissions will increase around 5 kg in both cases, because emissions connected to power generation are higher than the emission reductions from reduced gasoline use. Due to the high penetrations of coal and heavy oil as generation fuels, annual per-vehicle SO_2 emissions will increase by between 10 and 12 kg with PHEV use.

Looking at the results, it is clear that if the primary goal of PEV use is to reduce emissions, the uncontrolled charging scenario would be preferred, since CO_2 and SO_2 emissions are lower, with a negligible difference in NO_x emissions. This result is not, however, universally true, and the emission impacts will be highly sensitive to the generation mix. In particular, the energy generation mix for different countries is reported in Fig 1.10.

For example, in countries like France or Switzerland where hydroelectricity and nuclear are more abundant, controlled charging may be preferred, since more hydroelectricity and nuclear may be used for vehicle charging. For this reason, using PEVs in these countries may be more beneficial from a net emission standpoint than incountries such as the USA and Germany, which have a large mix of coal-fired generation.
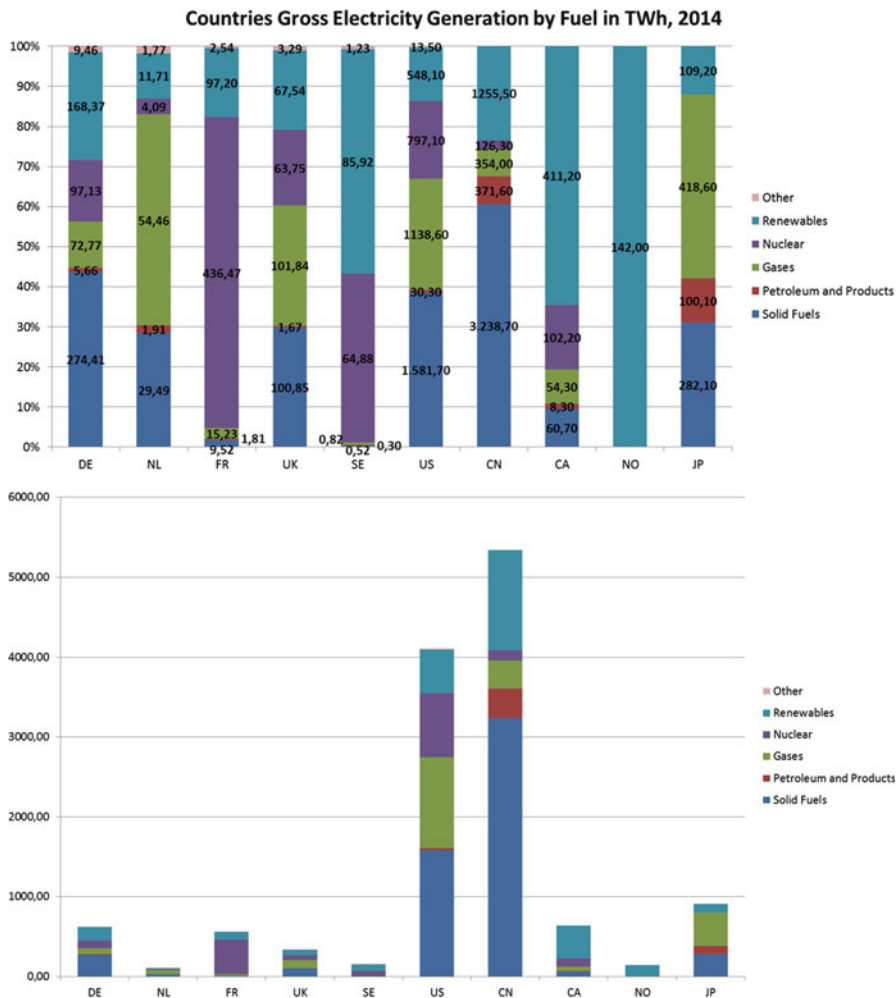
Fig. 1.10 Energy generation mix for France, USA, Switzerland, and Germany (*source*: IEA [36])

1.4.4 Effects of PEV Charging on Distribution Networks

Due to the characteristics of electric power generation, transmission, and distribution, experts have identified local distribution as a likely part of the chain to be adversely affected by unregulated PEV charging [27, 31, 37, 38]. Some research work has been aimed at studying the PEV impact on the local distribution infrastructure [39, 40] and smart charging control strategies considering different objective functions [37, 41, 42]. In particular, Gong et al. [37] used mass simulation approaches (e.g., Monte Carlo) based on stochastic input models to estimate the output also in a stochastic way.

The impact of the increase of PEV market penetration on the power generation system is relatively small. However, the possible impacts on power delivery systems, especially the distribution system, can be an issue including power quality problem, voltage imbalance, and transformer degradation. The PEV charging process involving rectifying the AC signal and running the rectified signal through a DC/DC converter would produce harmonic distortion in the distribution system, causing power quality problems.

The distribution system is the weakest part in the current power grid system, especially the distribution transformer systems. The reason is that the unregulated charging of PEVs can cause a high power load to the current distribution transformer system, which causes the rapid heat up of the transformer winding, thus accelerating the transformer insulation aging. Farmer et al. developed a PEV distribution circuit impact model (PDCIM) to estimate the impact of an increasing number of PEVs on transformers and underground cables [23]. In that paper, the authors mentioned the transformer aging acceleration caused by temperature increase but a detailed study was not carried out. In Shao et al. [40], the authors studied the potential challenges of PEV charging to electric utility at the distribution level, mainly focusing on the transformer efficiency. Roe et al. investigated the impacts of PEVs on the power system infrastructure and the primary fuel utilizations in [43]. A simple transformer thermal model was used for transformer loss-of-life estimation in the paper. However, the inputs to the model were very simple that the ambient temperature was assumed as constant and a random daily load schedule was assumed, making it hard to simulate a more realistic situation in the study.

Since the PEV charging may cause lots of problems in a power grid system, researchers started to find control solutions for PEV charging with different objectives. Some work tried to minimize the power losses in the power system, some tried to minimize the peak load, and some tried to reduce the power generation emission. When the duration of PEV charging is known and the rate of charging can be controlled, authors in [42] proposed smart energy control strategies based on quadratic programming with the objective of minimizing the peak load and flattening the overall load profile. Clement et al. tried to obtain the optimal charge profile of PEVs by using stochastic programming to minimize the power losses and to maximize the main grid load factor in [41]. By defining different objective functions, the authors can utilize the V2G technologies in order to maximize the profit in grid power transactions. Hutson et al. [44] used binary particle swarm optimization (BPSO) with a price curve to maximize profits for vehicle owners for the parking lots case. PEVs can also be used as reactive power support for the distributed power systems when combined with other power devices, such as solar panels. In [45], the smart grid was used to allow the coordination of multiple reactive power devices located on the distribution system in order to restore system voltages. Ma et al. developed a decentralized charging control strategy of autonomous PEVs using noncooperative games theory [46]. They studied the problem as a form of noncooperative game, where a large number of selfish PEVs share electricity resources. They proved that the demand-dependent price scheme drives the system asymptotically to a unique Nash equilibrium. Ito also applied static noncooperative game

theory to the PEV charging problem of allocating the charging activities to the overnight electric demand value [47]. Then, a decentralized charging scheme with guaranteed robustness was proposed. Ahn et al. [48] proposed a decentralized charging algorithm using linear programming in order to reduce power generation cost and carbon emissions. Galus et al. [49] presented an integrated method to assess the impacts of electric mobility on the three domains of power systems, transportation systems, and environment. An agent-based model was proposed in the paper, which comprises models for vehicle fleet evolution, for the development of transport emissions, for the spatial and temporal transportation behavior, and for power systems.

An interesting case study is presented by Gong et al. [50], where a transformer thermal model was used to estimate the hot-spot temperature given the knowledge of load ratio and ambient temperature. Main inputs to the model, including residential load, ambient conditions, and vehicle parameters, were taken from real data. The transformer insulation aging is mainly affected by the hot-spot temperature. A six-vehicle case with a 25 kVA transformer case was studied. Monte Carlo simulation was used to predict the final SOC of daily driving for a PHEV model and an EV model. Different market penetrations of PEVs were studied from the transformer insulation life aspect.

For the transformer thermal model, load ratio and ambient temperature are the two inputs, and the hot-spot and top oil temperatures can be obtained correspondingly. Also, 1-year ambient temperature data and base-load ratio data were available.

One case of charging load comparison of the base load and the load with six PEVs (for six houses which share the same transformer of 25 kVA) with even charging is shown in Fig. 1.11a. The time for this case is the summer, so the ambient temperature would be relatively high. The base load at night is lower than in the daytime. Six PEVs undergoing even charging give a tremendous load to the transformer. The corresponding temperatures of top-oil and hot-spot are reported in Fig. 1.11b. The response of the top-oil temperature is much slower than the hot-spot temperature, since the time constant of oil is much longer than winding. The hot-spot temperature was increased considerably due to the charging load from the six PEVs. The damage impact of this scenario is shown in the next subsection. The transformer insulation life would be compared for different charging conditions.

Similarly, to see how different market penetrations of PEV would affect the transformer hot-spot temperature, a simulation of 2–6 PEVs was carried out and compared with the base-load case. For each market penetration case, half of them are PHEVs (similar to a Chevrolet Volt), and half are EV (similar to a Nissan Leaf). From the results presented in Fig. 1.11, higher market penetration of PEVs would cause much higher hot-spot temperature. The transformer insulation life results for different market penetrations were studied also in the following subsection.

From the aging model, it is estimated that the insulation life is very sensitive to hot-spot temperature. For temperatures much lower than the reference value (110 °C), the expected life can be very long, and for temperatures much higher than the reference value, the expected life can be very short. In our simulation, for

Fig. 1.11 Comparison of
base load to condition with
and without six PEVs even
charging (**A**) with the
corresponding temperature
of top-oil and hot-spot (**B**).
The same evaluations are
also reported for different
market penetrations of
PEVs (**C**, **D**) (*source*: [51])
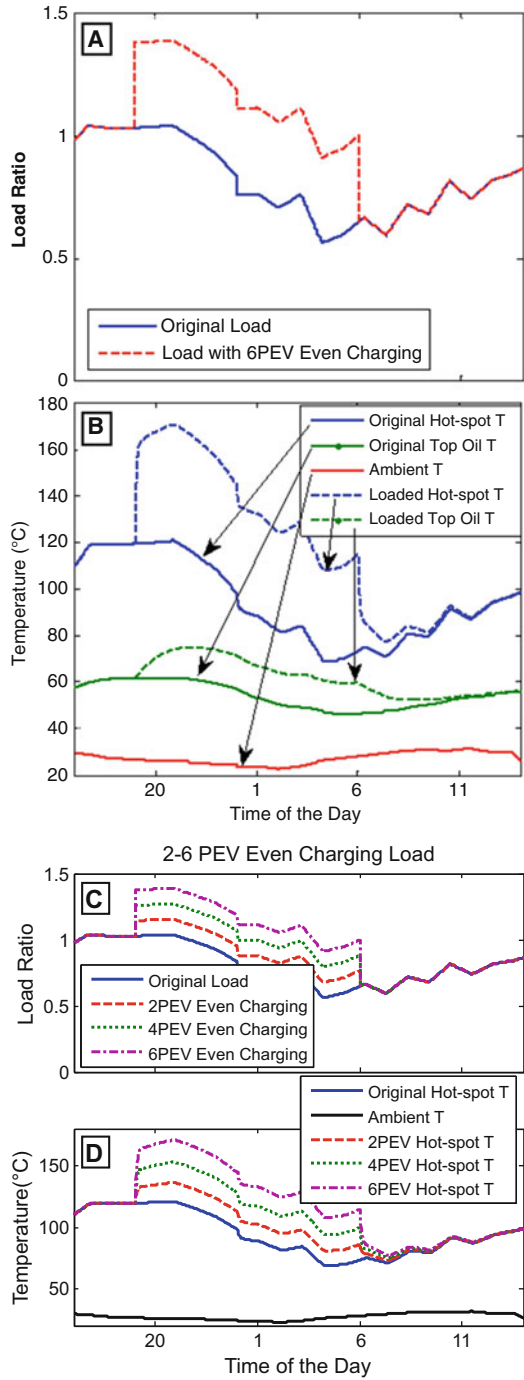
values higher than 100 years, the case is labeled "OK" to avoid the confusion to the real transformer life, which would be dictated by factors other than insulation degradation. For very small values, there would typically be a load-related failure other than the gradual reduction of insulation life. Several charging situations were defined, and the corresponding results were compared to see the necessity of control of the charging:

- Case 1: charging at 7:00 p.m. at the same time, which is the worst case in our study
- Case 2: charging at 12:00 a.m. at the same time
- Case 3: randomized charging strategy with 30-min intervals
- Case 4: randomized charging strategy with 15-min intervals
- Case 5: evenly averaged charging from 7:00 p.m. to 6:00 a.m., which is a nearly optimal case

Level two charging (6.6 kW) was assumed for the PEVs. The expected insulation life for different penetrations of PEVs for the five charging conditions was collected in Gong et al. [50]. In these cases, the PEVs were assumed to require their full usable energy for recharge. From the simulation results, cases with four or more PEVs have great impact on the transformer. In many cases of 4–6 PEVs (out of six houses), the transformer insulation life is very short.

The next step simulation takes the estimated final SOC from the Monte Carlo simulation into consideration. For this simulation, the charging time required for each PEV is not a firm value but a random value, taking the daily driving pattern into consideration. Integrating this factor into the transformer thermal model, the expected transformer insulation life for different market penetrations was simulated and compared in [50]. With Monte Carlo SOC, which is the SOC distribution obtained from the Monte Carlo based mass simulation, the battery of PEVs is usually not completely depleted, so the electric energy required to fully charge the battery is less than the fully depleted case (Table 1.4).

Table 1.4 Expected transformer insulation life for different scenarios (6.6 kW): comparison between vehicle full charge and vehicle charge based on demand predicted by Monte Carlo analysis

Cases	Vehicles assumed to require full charge			Vehicle charge based on demand predicted by Monte Carlo analysis		
	Two PEVs (years)	Four PEVs (years)	Six PEVs (years)	Two PEVs (years)	Four PEVs (years)	Six PEVs (years)
7:00 p.m.	6.7	<1	<1	14.41	<1	<1
12:00 a.m.	OK	<1	<1	OK	<1	<1
Randomized (30 min)	71.04	3.07	<1	OK	13	2.27
Randomized (15 min)	83.07	2.83	<1	OK	20.7	1.36
Average	OK	OK	24.31	OK	OK	OK

Results show that large penetration of the PEVs can have great impact on the power grid—particularly in the case of poor coordination of charging times. Conversely, low market penetration of PEVs is not detrimental to the transformer life, especially if charging is coordinated to some degree. The sensitivity of overall transformer insulation life to the departing SOC was also studied. A randomized strategy shows some improvement of the charging process, and the simulation results also show the potential of using uneven charging, which indicates the necessity of optimization of the charging process considering the transformer insulation life.

1.5 The Role of Smart Charging Technologies and Applications

1.5.1 General Considerations

PEV charging can occur in different locations, such as home charging in the night, workplace charging in the daytime, and shopping center charging during the shopping period. The charging of the PEVs will pose a tremendous load to the local transformers. Thus, smart charging control strategies are necessary.

In the future, power grid administrators will probably need to control when vehicle charging is done, in order to minimize its impact on the power grid. For doing that, a complex communication system between power grid administrator and PEV owners has to be established; with such a system of communication a power grid administrator could start using the energy stored in vehicles' batteries to help meet peak demand when power generation costs are higher, and could recharge these batteries when the load on the grid is lower; PEVs' battery packs could also provide vehicle-to-grid services (V2G), improving the overall generation efficiency. Many studies have proved that PEVs could become a useful asset category for the electrical power grid, providing ancillary services with the distributed energy stored in the vehicles' batteries' [52, 53] . PEVs' batteries could also be used as a distributed energy storage system that can minimize the adverse effects of the intermittent nature of renewable energy resources.

With the two-way communication infrastructure, i.e. smart meters and sensors, the smart grid is a proposed concept which can effectively coordinate and use the available energy resources. V2G technology is a part of this emerging area. V2G technology which not only considers the charging scenarios of PEVs, but also optimizes the impact of PEVs providing electric energy to the power grid, has been widely studied recently. If successfully implemented, V2G can provide benefits, such as to lower electricity generation costs, increase grid reliability, potentially reduce emissions by integrating wind and solar power, and to provide a revenue stream for PEV owners. This broad area has been attracting lots of attention recently. Su et al. [54] presented a comprehensive survey of the role of

industrial informatics systems in the context of PEVs. The survey covers a number of issues, including (1) charging infrastructure and PEV batteries; (2) intelligent energy management; (3) V2G; and (4) communication requirements. The authors introduced a priority-controlled leaky bucket approach for charging PEVs in a smart grid system. The paper introduced the concept of charging quality of service (CQoS) as the charging scheme. Masoum et al. [55] studied the impact of uncoordinated and coordinated PEV charging on substation transformer loading, system losses, and voltage profile in a smart grid with charging stations that are operated based on a real-time smart load management control strategy.

V2G services include acting as an energy storage device that can be charged off-peak and discharged on-peak as well as providing ancillary services, such as regulation, thereby reducing the need of the system to rely on conventional power generators. More important is regulation, which reduces the dependence on conventional generators for capacity and allows the grid administrator to commit fewer generators.

PHEVs can provide regulation of higher quality than currently available for three reasons: (1) It can assure a fast response to a signal; (2) it is available in small increments; and (3) it is distributed.

From the perspective of the electric power sector, this is a new source of high-quality grid regulation [52]; in addition to these savings to the system, PHEV owners can obtain value from making their vehicles available to the system for V2G services; this value comes from energy and ancillary service payment and also from reduced vehicle driving costs, due to conventional generators having more capacity available to charge PHEV batteries, since the grid operator does not have to rely on generators for ancillary services [53]. In this way, V2G services could give PHEV owners an additional income, which would reduce their lifetime ownership costs.

Though V2G is a promising concept, there are several challenges that may delay the real-world implementation in the short term, such as the need for at wo-way communication-enabled system infrastructure, and an unproven business model and economic justification.

In the electric power system, ancillary services are necessary for maintaining grid reliability, balancing of supply and demand, and supporting the transmission of electric power from the seller to the buyer. Regulation is one of the ancillary services that PHEVs could provide; the main purpose of regulation is to adjust the grid to the target frequency and voltage. Regulation helps to maintain interconnection frequency, to balance actual and scheduled power flows among control areas, and to match generation to load [56]. The required amount of regulation service is determined as a percentage of aggregate scheduled demand. Regulation is provided continuously by generators that are online, equipped with automatic control, and will respond within minutes to control center requests to decrease or increase power output.

The basic concept of V2G is that PHEVs provide power to the grid while they are parked. Each vehicle must have three essential elements for V2G: (1) a power connection to the grid for electrical energy flow; (2) a control connection necessary
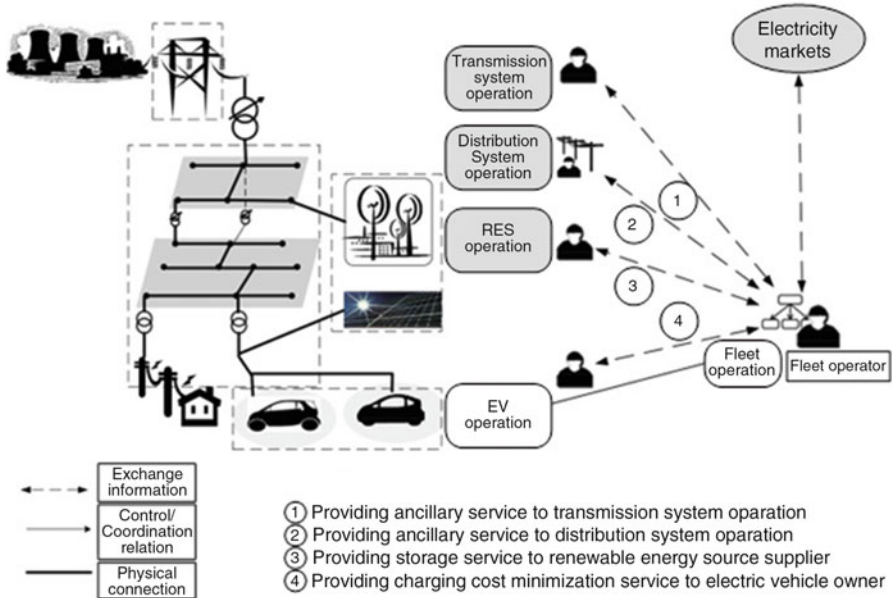
Fig. 1.12 Schematic of power lines and control connections between the electric power grid and vehicles (*source*: [57])

for communications with grid operators; and (3) precision metering onboard the vehicle. In Fig. 1.12, the control signal from the grid operator is shown schematically as a radio signal, but this might be transmitted through a direct Internet connection or other communication media.

In order to schedule the dispatch of power, a grid operator needs to rely on the fact that enough vehicles are parked and potentially plugged in at any minute during the day. In the USA, an average personal vehicle is on the road only 4–5 % of the day, which means that for the great majority of the day the vehicles are parked, and also during peak traffic hours almost 90 % of personal vehicles are parked [58].

Unlike large generators, PHEVs' energy storage and power electronics are already designed to provide large and frequent power fluctuations over short time periods, due to the nature of driving. This makes these vehicles especially well engineered for regulation. Once a signal is received, the vehicle can respond in less than a second to change its power output. A "regulation up" signal would cause the vehicle to provide power to the grid (V2G) and a "regulation down" signal would cause a decrease in the power output or even draw power from the grid (the regular battery-charging mode). In previous studies [59], it has been successfully demonstrated that a single-battery electric vehicle can respond to a regulation signal.

1.5.2 Vehicle Electrification, Impacts on Investments, and Interdependencies in the Power Sector Including Renewables

So far, we have considered the demand side of the electricity market and the impact of the policy framework on the shape of electricity demand. Few studies so far have considered the impact of electric vehicles and their charging patterns on the investments in new generation capacity. A controlled charging strategy will require higher investments in base-load generators, reducing the need for peak units. In contrast, an uncontrolled charging strategy will require more investments in flexible units. Therefore, the regulatory framework governing the charging of electric vehicles will have, *ceteris paribus*, a direct impact on the business of energy utilities and on the generation mix of the electricity sector. Utilizing more base-load generators will increase the emissions of coal-fired units, thereby reducing the load factor of cleaner natural gas generators. Thus, the charging strategy of electric vehicles will also impact carbon emission mitigation policy mechanisms such as the EU Emissions Trading System (EU ETS). Higher emissions may lead to higher carbon prices in the EU ETS, which in turn would cause higher electricity prices, reducing the competitiveness of electric vehicles. Therefore, it is necessary to consider the interrelatedness that exists between the electricity sector and the carbon market when analyzing the resulting pollutant emissions of different charging strategies for electric vehicles [60].

The ability of electric vehicles to enhance the introduction of more renewable energy sources also depends on the existing renewable energy policy. An adequate policy framework is necessary for these generators to respond to market price signals, and to actively participate in the electricity market. This is not the case for many European countries where a feed-in tariff mechanism is in place and generators are paid a fixed price for their electricity independently from demand [61]. Although many of these renewable power generators are intermittent and only biomass-fired units are dispatchable just like conventional generators, exposing these technologies to the electricity price signal - high prices indicating shortage of supply, low prices abundance of supply - will attract investments in those projects which are more valuable for the system.

It is thus necessary to dedicate special attention to the policy and regulatory framework when analyzing the performance of electric vehicles, their impact on the power sector, and their eventual costs to consumers (with and without electric vehicle/s).

1.6 Conclusions

From the considerations reported in this chapter, it is possible to conclude that vehicle electrification is a multifaceted topic, and that there is considerable uncertainty regarding the vehicle mix of the future and the actual market diffusion

dynamics, not least due to the issues of lock-in, habit persistence, interrelatedness with the electricity system, and system transformation. When promoting e-mobility, policy makers need to take the multi-faceted interrelations properly into consideration for maximizing social welfare and avoiding undesirable side effects. They will also need to find out how the impacts change as the number of e-vehicles grows, other flexibility measures arise (that may or may not be cheaper or more easily accessible), and the local grid is renewed. Moreover, it is the concrete (combination of) policy support measures that, additionally to the vehicles and vehicle improvements being offered in the market, all have a crucial impact on the actual technical change happening and the overall benefits of vehicle electrification.

References

1. Mintz M, Han J, Burnham A (2014) Alternative and renewable gaseous fuels to improve vehicle environmental performance, Chapter 4. In: Folkson R (ed) Alternative fuels and advanced vehicle technologies for improved environmental performance. Woodhead Publishing, UK: 90–116
2. Sabri MFM, Danapalasingam KA, Rahmat MF (2016) A review on hybrid electric vehicles architecture and energy management strategies. Renew Sust Energ Rev 53:1433–1442
3. Sadeghinezhad E, Kazi SN, Badarudin A, Oon CS, Zubir MNM, Mehrali M (2013) A comprehensive review of bio-diesel as alternative fuel for compression ignition engines. Renew Sust Energ Rev 28:410–424
4. ICCT (The International Council of Clean Transportation) (2014) Global comparison of light-duty vehicle fuel economy/GHG emissions standards (Update May 2014)
5. Yamamoto M (2010) Development of a Toyota plug-in hybrid vehicle. In: SAE World Congress & Exhibition, Detroit, MI, USA
6. Mi C, Abul Masrur M, Gao DW (2011) Hybrid electric vehicles: principles and applications with practical perspective. Wiley, Chichester
7. Michael AM et al (2011) The GM "Voltec" 4ET50 multi-mode electric transaxle. SAE Int J Engines 4(1):1102–1114
8. Miller JM (2006) Hybrid electric vehicle propulsion system architectures of the e-CVT type. IEEE Trans Power Electron 21(3):756–767
9. Karbowski D, Rousseau A, Pagerit S, Sharer P (2006) Plug-in vehicle control strategy: from global optimization to real-time application. In: 22nd Electric Vehicle Symposium, EVS22, Yokohama, Japan, 2006
10. Moura S, Callaway D, Fahty H, Stein J (2010) Tradeoffs between battery energy capacity and stochastic optimal power management in plug-in hybrid electric vehicles. J Power Sources 195:2979–2988
11. Tulpule P, Marano V, Rizzoni G (2009) Effects of different PHEV control strategies on vehicle performance. In: American Control Conference (ACC'09), 2009
12. Paganelli G, Guezennec Y, Rizzoni G (2002) Optimizing control strategy for hybrid fuel cell vehicle. In: SAE 2002 Transactions Journal of Engines V111-3
13. Tulpule P, Marano V, Rizzoni G (2010) Energy management for plug-in hybrid electric vehicles using equivalent consumption minimization strategy. Int J Elect Hybr Vehicles 2(4):329–350
14. Tulpule P, Marano V, Rizzoni G, Hai Y, McGee R (2011) A statistical approach to assess the impact of road events on PHEV performance using real world data. In: SAE World Congress, April 2011

15. U.S. Energy Information Administration (2015) Annual energy outlook 2015 with projections to 2040
16. Ernst & Young (2010) Gauging interest for plug-in hybrid and electric vehicles in select markets. http://www.ey.com/
17. SAE Hybrid Committee (2011) SAE charging configurations and ratings terminology.
18. Yilmaz M, Jrein P T (2012) Review of charging power levels and infrastructure for plug-in electric and hybrid vehicles. In: Electric Vehicle Conference (IEVC), 2012 I.E. International, Greenville
19. Curtin R, Yevgeny S, Jamie M (2009) Plug-in hybrid electric vehicles. Reuters/University of Michigan, Surveys of Consumers
20. Gallagher KS, Muehlegger E (2011) Giving green to get green? Incentives and consumer adoption of hybrid vehicle technology. J Environ Econ Manage 61(1):1–15
21. Ren W, Brownstone D, Bunch D S, Golob T F (1994) A personal vehicle transactions choice model for use in forecasting demand for future alternative-fuel vehicles. Technical Report UCI-ITS-WP--94-7, California University, Irvine, CA, Institute of Transportation Studies, 1994
22. Melendez M, Milbrandt A (2006) Geographically based hydrogen consumer demand and infrastructure analysis. Final Report, National Renewable Energy Laboratory, Golden, CO, 2006
23. Farmer C, Hines P, Dowds J, Blumsack S (2010) Modeling the impact of increasing PHEV loads on the distribution infrastructure. In: Proceedings of the Annual Hawaii International Conference on System Sciences, 2010
24. Sioshansi R, Fagiani R, Marano V (2010) Cost and emissions impacts of plug-in hybrid vehicles on the Ohio power system. Energy Pol 38(11):6703–6712
25. Tulpule P, Marano V, Yurkovich S, Rizzoni G (2013) Economic and environmental impacts of a PV powered workplace parking garage charging station. Appl Energy 108:323–332
26. Xi X, Sioshansi R, Marano V (2013) Simulation-optimization model for location of a public electric vehicle charging infrastructure. Transport Res D-Tr Environ 22:60–69
27. Sioshansi R, Denholm P, Jenkin T (2012) Market and policy barriers to deployment of energy storage economics of energy and environmental. Econ Energ Environ Policy 1:47–63
28. Xi X, Sioshansi R, Marano V (2014) A stochastic dynamic programming model for co-optimization of distributed energy storage. Energy Systems 5(3):475–505
29. Markel T, Bennion K, Kramer W, Bryan J, Giedd J (2009) Field testing plug-in hybrid electric vehicles with charge control technology in the xcel energy territory. National Renewable Energy Laboratory. Technical Report NREL/TP-550-46345, August 2009
30. National Energy Technology Laboratory (2008) Advanced metering infrastructure. Technical Report, February 2008
31. Kintner-Meyer M, Schneider K, Pratt R (2007) Impacts assessment of plug-in hybrid vehicles on electric utilities and regional U.S. power grids: part 1: technical analysis. Pacific Northwest National Laboratory (a):1–20
32. Marano V, Choi TG, Guezennec Y, Rizzoni G, Panzeri C, Choi W (2007) Opportunities of plug-in hybrids in self-sustaining homes. In: 2nd International Workshop on Hybrid and Solar Vehicles, Salerno, Italy, September 2007
33. Marano V, Rizzoni G (2008) Energy and economic evaluation of PHEVs and their interaction with renewable energy sources and the power grid. In: 2008 I.E. International Conference on Vehicular Electronics and Safety, Columbus, OH, USA, September 2008
34. Hackbarth A, Lunz B, Madlener R, Sauer D-U, De Doncker RW (2012) Plug-in hybrid electric vehicles for CO_2-free mobility and active storage systems for the grid (part 2), E.ON Energy Research Center Series, vol 4, issue 6, 1st ed, December
35. Gonder J et al (2007) Using global positioning system travel data to assess real-world energy use of plug-in hybrid electric vehicles. In: Transportation Research Record: Journal of the Transportation Research Board, pp 26–32
36. International Energy Agency (2015) Electricity Information, IEA/OECD, Paris

37. Gong Q, Midlam-Mohler S, Marano V, Rizzoni G (2012) Study of PEV charging on residential distribution transformer life. IEEE Trans Smart Grid 3(1):404–412

38. Mohseni P, Stevie R G (2009) Electric vehicles: Holy Grail or fool's gold. Power & Energy Society General Meeting, 2009. Calgary, AB, Institute of Electrical and Electronics Engineers, 26–30 July 2009, pp 1–5

39. Hadley S (2007) Evaluating the impact of plug-in hybrid electric vehicles on regional electricity supplies. In: iREP Symposium - Bulk Power System Dynamics and Control - VII, Revitalizing Operational Reliability, Charleston, SC, USA, 2007

40. Shao S, Pipattanasomporn M, Saifur R (2009) Challenges of PHEV penetration to the residential distribution network. In: IEEE Power and Energy Society General Meeting, PES '09, 2009

41. Clement K, Haesen E, Driesen J (2009) Coordinated charging of multiple plug-in hybrid electric vehicles in residential distribution grids. In: IEEE/PES Power Systems Conference and Exposition, PSCE 2009

42. Mets K, Verschueren T, Haerick W, Develder C, De Turck F (2010) Optimizing smart energy control strategies for plug-in hybrid electric vehicle charging. In: IEEE/IFIP Network Operations and Management Symposium Workshops, NOMS, 2010, pp 293–299

43. Roe C, Evangelos F, Meisel J, Meliopoulos AP, Overbye T (2009) Power system level impacts of PHEVs. In: Proceedings of the 42nd Annual Hawaii International Conference on System Sciences, HICSS, 2009

44. Hutson C, Venayagamoorthy GK, Corzine KA (2008) Intelligent scheduling of hybrid and electric vehicle storage capacity in a parking lot for profit maximization in grid power transactions. In: IEEE Energy 2030 Conference, Energy 2008, 2008

45. Rogers KM, Klump R, Khurana H, Aquino-Lugo AA, Overbye TJ (2010) An authenticated control framework for distributed voltage support on the smart grid. IEEE Trans Smart Grid 1 (1):40–47

46. Ma Z, Callaway DS, Hiskens IA (2011) Decentralized charging control of large populations of plug-in electric vehicles. IEEE Trans Control Syst Technol 99:1–12

47. Ito H (2011) Disturbance and delay robustness of gradient feedback systems based on static noncooperative games with application to PEV charging. In: 50th IEEE Conference on Decision and Control and European Control Conference (CDC-ECC), 2011

48. Ahn C, Li C, Peng H (2011) Decentralized charging algorithm for electrified vehicles connected to smart grid. In: American Control Conference (ACC), June 2011

49. Galus MD, Waraich RA, Noembrini F, Steurs K, Georges G, Boulouchos K, Axhausen KW, Andersson G (2012) Integrating power systems, transport systems and vehicle technology for electric mobility impact assessment and efficient control. IEEE Trans Smart Grid 3 (2):934–949

50. Gong Q, Midlam-Mohler S, Marano V Rizzoni G (2011a) PEV charging impact on residential distribution transformer life. In: Energytech, Cleveland, OH

51. Gong Q (2012) PEV charging control considering the distribution transformer life. Doctoral dissertation, The Ohio State University

52. Tomić J, Kempton W (2007) Using fleets of electric-drive vehicles for grid support. J Power Sources 168(2):459–468

53. Sioshansi R, Denholm P (2010) Real-time performance plug-in hybrid electric vehicles as grid resources. Energy J 31:1–22

54. Su W et al (2012) A survey on the electrification of transportation in a smart grid environment. IEEE Trans Ind Inform 8(1):1–10

55. Masoum A S, Siada A, Islam S (2011) Impact of uncoordinated and coordinated charging of plug-in electric vehicles on substation transformer in smart grid with charging stations. In: Innovative Smart Grid Technologies Asia (ISGT), IEEE PES. IEEE, 2011

56. Brendan K, Hirst E (2001) Real-time performance metrics for generators providing the regulation ancillary service. Electr J 14(3):48–55

57. Hu J, Morais H, Sousa T, Lind M (2015) Electric vehicle fleet management in smart grids: a review of services, optimization and control aspects. Renew Sust Energ Rev 56:1207–1226
58. Kempton W, Tomic J, Letendre S, Brooks A, Lipman T (2001) Vehicle-to-grid power: battery, hybrid, and fuel cell vehicles as resources for distributed electric power in California. Technical report for California Air Resources Board and the California Environmental Protection Agency
59. Brooks AN (2002) Vehicle-to-grid demonstration project: grid regulation ancillary service with a battery electric vehicle. California Environmental Protection Agency, Air Resources Board, Research Division
60. Fagiani R, Richstein JC, Hakvoort R, De Vries L (2014) The dynamic impact of carbon reduction and renewable support policies on the electricity sector. Util Policy 28:28–41
61. Hiroux C, Saguan M (2009) Large-scale wind power in European electricity markets: time for revisiting support schemes and market designs? Energy Pol 38:3135–3145
62. Hackbarth A, Lunz B, Madlener R, Sauer D-U, De Doncker RW (2010) Plug-in hybrid electric vehicles for CO_2-free mobility and active storage systems for the grid (part 1). E.ON Energy Research Center Series, vol 2, issue 3, 1st ed, Dec 2010

Chapter 2
AC and DC Microgrid with Distributed Energy Resources

Dong Chen and Lie Xu

Abstract Renewable power generation and the prospect of large-scale energy storage are fundamentally changing the traditional power grid. Arising challenges occur in terms of energy management, reliability, system control, etc. Microgrid, as an active subsystem of modern power grid, has revealed its promising potential in dealing with intermittent clean power generation and emerging energy storage, partially brought by electrical vehicle batteries. In this chapter, the concept of microgrid is introduced. The main focus is placed on the basic issues of control, operation, stability, and protection of DC microgrids.

2.1 AC Microgrid

The arising concerns on environment and sustainable energy issues have promoted the development of distributed renewable power generation and the emerging of microgrid [1]. Since renewable power sources are naturally dispersed, it is very difficult for the power system to manage a countless, yet still growing, intermittent distributed power generation in a traditional way. In order to effectively manage distributed generation sources, load, and possibly energy storages, a systematic view has to be taken. By integrating all these distributed units together, a micro power system is formed from the distribution side, hence the nomination of microgrid. Given that distribution power system is formerly considered as load-only, the inclusion of generation and storage units in microgrids is fundamentally changing the control and operational structure of traditional power system.

As traditional power system is based on AC, microgrids are considered to be naturally AC based at early stage. A three-phase AC bus is commonly employed as the point of common coupling (PCC) [2]. PCC is normally set as the only power interface between a utility grid and the microgrid. The schematic structure is shown

D. Chen (✉)
Glasgow Caledonian University, Glasgow, UK
e-mail: dong.chen@gcu.ac.uk

L. Xu
Strathclyde University, Glasgow, UK
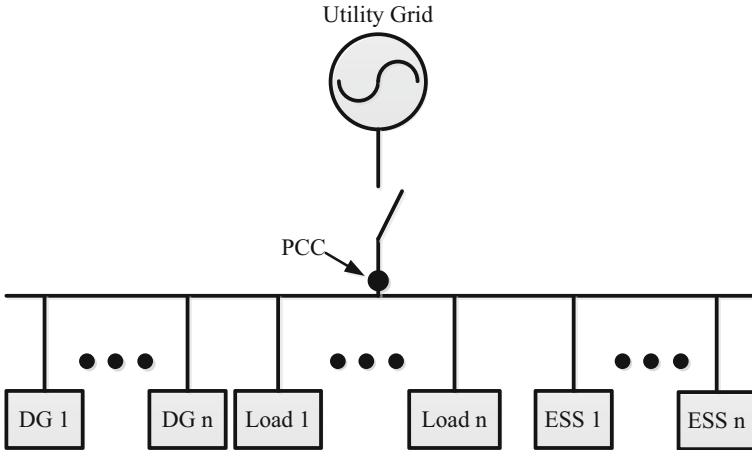e-mail: lie.xu@strath.ac.uk

Fig. 2.1 AC microgrid

in Fig. 2.1. A microgrid can be either operated in grid-connected condition or in some situations, switched to the stage of isolation, i.e., islanding operation [3]. A fast switch can be placed in between PCC and utility grid as the cutoff point between the microgrid and utility grid.

Comparing with traditional power grid, the emergence of DGs and ESSs is the major difference. In a microgrid, renewable DGs and ESSs are interfaced with power electronics converters with distributed control [4].

Renewable DGs extract power from natural environment, blowing wind, or sunshine for instance, and try to maximize the power extraction and integration to the grid. In this sense, the actual power generated mainly depends on instant natural conditions. Therefore, the renewable DGs are generally considered to be nondeterministic from the grid operator's view. The only exception occurs when renewable power must be curtailed or switched off, however, at a certain cost.

ESSs are considered to be a controllable bidirectional source in a microgrid. A high-performance power electronics interface enables an ESS to provide instant support to power grid in addition to storage energy management. This special feature can be employed to cope with the problem caused by intermittent renewable DGs. For example, the EV charging station can use its battery as an energy buffer to absorb intermittent power to avoid voltage instability and discharge it in peak hours to reduce the demand on spinning reverse. It has to be pointed out that a vehicle battery with a one-direction charger is not necessarily an ESS system. A charging-only battery system, though controllable, behaves more like a controllable load in distribution power system due to its lack of discharging capability. However, a vehicle battery, or more likely a group of vehicle batteries in a charging station, with bidirectional "chargers" under certain control can play the role of ESS in a microgrid.

A coordinating scheme, either distributed or centralized, is usually designed to combine all the above-mentioned DGs, loads, ESSs, and relays together to form a subsystem. This feature also defers from a passive distribution power system with

isolated DGs and ESSs. A digital secondary control system is commonly used to supervise, manage, and monitor the whole system [5]. Additional communications and energy management schemes might be applied with relevant supervisory control and data acquisition (SCADA) system of higher power system hierarchy.

2.2   Introduction to DC Microgrids

2.2.1   DC Distributed Sources

The idea of DC microgrid emerged soon after the concept of microgrid was proposed [6]. It is commonly designed for a distributed DC power source connecting intermittent renewable power sources, energy storages, and DC loads. This is due to the fact that many renewable power sources, e.g., directly driven wind generation and photovoltaic system, and energy storage systems, e.g., battery and super-capacitor, normally have DC links at their interface converter stages [4].

2.2.2   The Configuration of DC Microgrids

By connecting all the DC links of the sources and loads, a DC microgrid is formed, as is demonstrated in Fig. 2.2. Unlike the idea of AC microgrids, a DC microgrid does not directly connect to the prevalent three-phase AC utility grid but via a bidirectional DC/AC converter for common integration.
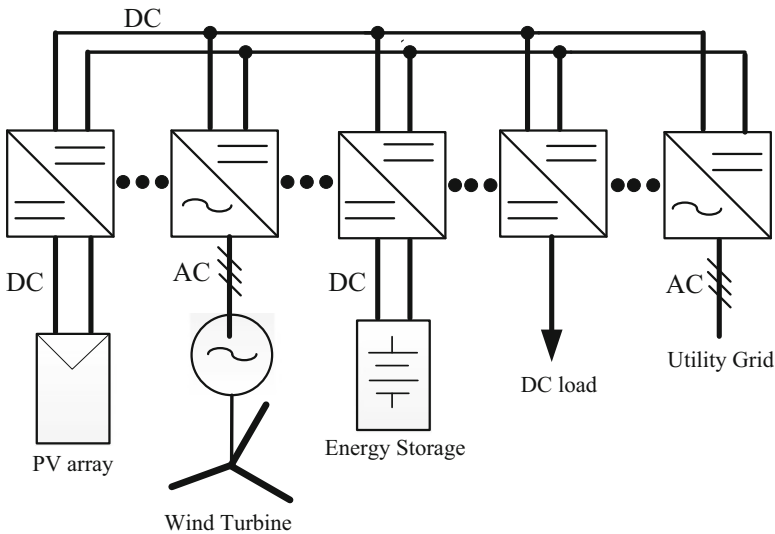
Fig. 2.2   DC microgrid

2.2.3 Comparison of AC and DC Microgrids

(a) Conversion efficiency

DC microgrids are considered to boast its efficiency advantage over AC counterparts in isolated operation mode when energy storage is involved in power flow due to fewer conversion levels. Typically for a PV-to-battery charging case, the power flow in an AC microgrid has to go through DC generation-AC distribution-DC storage process with DC/AC and AC/DC conversions. However, the power flow in a DC microgrid skips the AC stage, thus eliminating the losses brought by DC/AC and AC/DC conversions. One potential additional loss in DC microgrid is on the load side. Additional DC/AC conversion losses may apply if interface convertors are placed between the DC bus and the local AC loads. As a result, the total conversion efficiency between DC and AC microgrids depends on the trade-off between reduced conversion and additional conversion losses.

(b) One-off cost on converters

A common DC/AC converter is normally used for interfacing the DC microgrid to AC utility grid whereas in an AC microgrid, DC/AC converters have to be equipped with every distributed source. As the power rating of the common DC/AC converter in a DC microgrid is normally less than the total power rating but greater than any of the individual unit rating in AC counterparts, the one-off manufacturing and installation cost is reduced in DC microgrids due to higher per-kilowatt cost on converters of lower power ratings.

(c) Transmission/distribution efficiency

A significant feature of DC transmission is that there is no reactive power concern. As a result, the transmission loss caused by reactive current in AC systems is eliminated. In addition, a constant DC current tends to produce less copper loss on power line than AC over the same line resistance when delivering the same amount of real power.

(d) Power supply reliability

One promising feature of microgrids is that it can provide uninterrupted power supply during utility grid outage, which is often referred to as "seamless" switch during islanding operation.

For the AC microgrid system, it is difficult to determine when to switch the energy storage converter to islanded (isolated) mode since there is a contradiction between potential low-voltage ride-through (LVRT) grid code requirement and seamless switch.

Even though the present IEEE 1547 standard does not demand distributed sources to carry out voltage ride through during voltage dip and require renewable sources be tripped for voltage deviations, and the PCC switch of an AC microgrid can be designed and implemented to such requirement accordingly at this stage, it is doubtful that if it is appropriate in future. The reason is that a voltage dip caused by transmission level tends to cause low

voltages over a vast area of distribution systems. The instant and simultaneous trips of AC microgrids along with its DG sources can potentially cause further transient event after the fault. It is better to maintain the generations and possibly loads to avoid severe power imbalance after a grid fault.

A possible case in future is that the utility grid operator would require the distributed sources or microgrids stay connected for a predefined period of time, say a few hundred of milliseconds, before disconnection when voltages stay above a small percentage of nominal, say 15 %, during voltage sag. This could be demanded in a distribution system with high penetration of renewable generations. It is to ensure that a temporary fault would not cause further undesirable disconnection of other distributed generations [7]. That is to say, for a grid-connected AC microgrid, a predefined seam might be required by the grid operator if the voltage drop is not sufficiently low. Therefore, the energy storage system, as is directly coupled with AC utility grid, cannot restore the local voltage by switching to the voltage regulation mode immediately after a voltage dip is detected. Furthermore, the prevalent implementation of instant voltage detection approach, digital phase-locked loop (PLL), either for single or three phase, can cause further delay in voltage detection process [8, 9], which is another unfavorable aspect for seamless transition during islanding operation.

For a DC microgrid not directly coupled with the AC utility grid, the energy storage system on the DC side can take over or facilitate the DC voltage regulation immediately after an abnormal DC voltage variation, say 20 % dip, is detected. It can help to suppress the undesirable variation to a predefined level in a reacting time of milliseconds. This reaction can take place regardless of the operation mode of the common DC/AC converter and whether there is a utility fault or not [10–12]. In addition, enhanced operational control technique [13] may be applied to further improve DC power quality to cater specific power quality standards, MIL-STD-704F for instance, during transients. These features make the DC microgrid to provide a better quality "seamless" power supply to cater commercial [11] and industrial [12] consumers' needs.

(e) Controllability

A good feature of DC power systems is that a constant DC voltage would ensure the stability of the system. As a result, DC voltage regulation is the only essential concern to maintain a stable DC power system. For an AC power system, however, not only the voltage (amplitude) but also the frequency (angle) must be regulated and both regulations must be performed simultaneously. Furthermore, as the AC utility grids are three-phase systems, sophisticated techniques shall be employed to cope with unbalanced components which predominantly come from the vast adoption of single-phase DGs and loads in low-voltage power system. All these fore-cited factors indicate a better controllability for DC microgrids over AC.

(f) Protection arrangement

Protection is currently the major advantage of AC microgrid over DC. For AC protection theory and equipment have been maturely developed and the zero-crossing nature of AC current enables AC circuit breakers to distinguish arc easily. However, zero-crossing does not naturally happen in a DC system. Thus sophisticated technique has to be implemented resulting in higher costs for DC circuit breakers.

(g) Load availability

As power system is predominantly AC based, electric equipment is prevalently designed for standard AC power supply. However, DC load has huge potential. Digital equipment such as computers, routers, LEDs, and TV sets are naturally more compatible with DC power supply. In addition, motor drives including EVs are likely to have DC links. A common DC bus would help to greatly reduce its cost on the rectifying side. The relevant loads, such as converter-fed electric fans, pumps, and air conditioners, can be designed for DC power supply instead of AC with manufacturing cost lowered and efficiency boosted.

The comparison of AC and DC microgrid is generalized in Table 2.1.

Table 2.1 DC microgrid

Microgrid type	AC	DC
Conversion efficiency	Low: Multiple AC/DC and AC/DC conversions have to be used when interconnecting renewable sources and storages	High: AC/DC and DC/AC conversions between renewable sources and storages are reduced
Cost on converters	High: DC/AC converter has to be invested for each of the renewable sources and storages	Low: Reduced conversion stage means less converters are required
Transmission efficiency	Low: Additional loss due to reactive current	High: Loss associated with reactive current eliminated
Power supply reliability	Difficult-to-guarantee seamless transition after a utility fault	A guaranteed smooth transient DC power supply with limited voltage variation
Controllability	Difficult: Both voltage and frequency regulation needed; unbalance compensation needed in a three-phase system	Simple: No frequency, reactive power, or phase unbalance concern
Load availability	High: Available loads are dominantly designed with AC power supply	Low but with great potential: Digital and converter-based loads are highly compatible to DC
Protection	Mature arcing technique with cost-effective circuit breaker and well-developed protection system	High-cost circuit breaker with protection theory and equipment under development

2.3   The Control and Operation of DC Microgrids

2.3.1   Principles of DC Microgrid Operation

As is seen in the previous section, a DC microgrid consists of a number of terminals to achieve certain functions, which are power generation, grid connection, energy storage, and power consumption. DC capacitors which help to maintain system DC voltage are located at each of the terminals. DC lines are set to connect every terminal to form a DC network.

2.3.1.1   The Definition of DC Terminals [13]

DC microgrid terminals can be categorized into four basic types in terms of their functions. They are grid connection, power generation, load consumption, and energy storage.

If we further analyze how the terminals can affect a DC power grid, we can generalize the terminals, in terms of their contributions to system operation stability, into two groups which are named as power terminal and slack terminal.

- Power terminals are defined for those DC terminals that are either outputting or absorbing power on their own merits, which behave as "selfish" terminals.
- Slack terminals are defined for those DC terminals that are actively balancing the power flow within the DC grid, which behave as "generous" terminals.

Care must be taken that the determination of which fore-cited group a certain DC terminal belongs to is based on its instant behavior. Therefore, for a certain DC terminal, it is possible that its category can be switched from one to the other. For instance, the utility grid-side DC/AC converter, normally operating as slack terminal, accommodates the power surplus and deficit within the DC grid. When the surplus exceeds the power rating, the DC/AC converter has to operate at its maximum power (current) point and consequently loses the capability of balancing power and becomes a power terminal.

Obviously, in order to maintain the power balance, there must be at least one slack terminal within the DC microgrid, for the "selfish" power terminals are not capable of balancing the power on their own.

2.3.1.2   Control of DC Microgrids: Central Control and Autonomous Control

One original idea of DC microgrid control scheme was centrally control based [14], which stems from traditional power system control. By using a central controller, the real-time sampling and detections are collected from all the terminals to a general central controller as is illustrated in Fig. 2.3a. The central controller
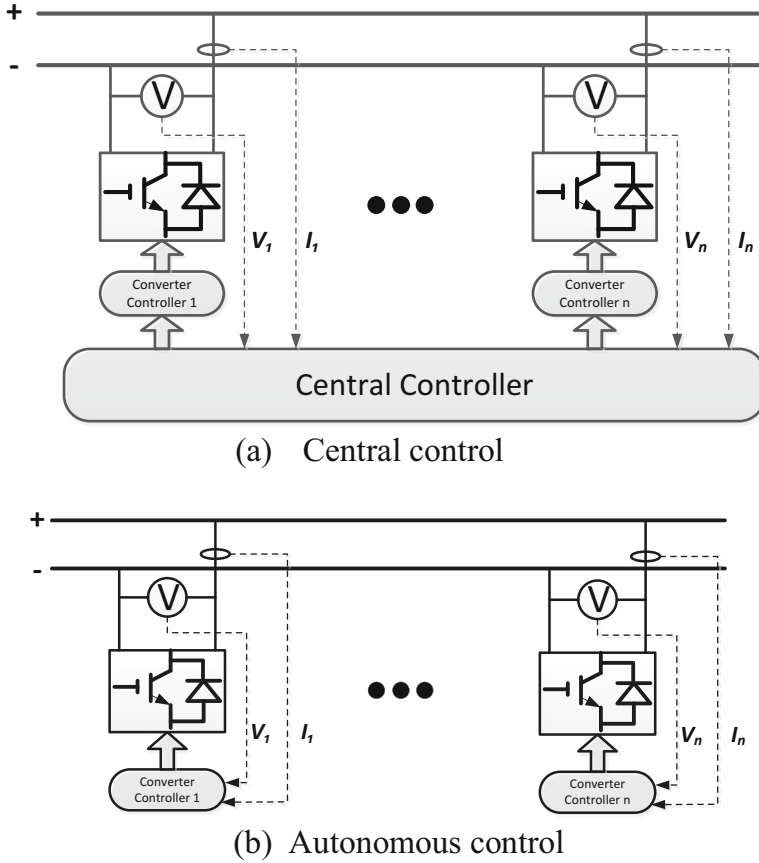
(a)   Central control

(b) Autonomous control

Fig. 2.3 (**a**) Central control. (**b**) Autonomous control

possesses the detected information and manages to output instant orders to each terminal. This idea was soon found unfeasible and unreliable for an expanded DC network with increasing number of DC terminals. Unlike traditional large-scale AC power systems, a DC microgrid does not have significant inertia. The DC voltage can typically drop to zero or rise to double in a few mini-seconds if a steady power mismatch is not addressed. As a result, an extremely high bandwidth and reliable communication channels are demanded in this case. Central control scheme demands duplex communications on the loop of high-bandwidth control between each terminal and the central controller, which would greatly increase the cost and, more importantly, the extra communication system degrades the reliability as unpredictable consequences would occur if there is a communication failure, a packet losing for instance. The overall reliability of a centrally controlled DC microgrid is generally difficult to guarantee as a failure on the central controller on the communication channel may result in system collapse.
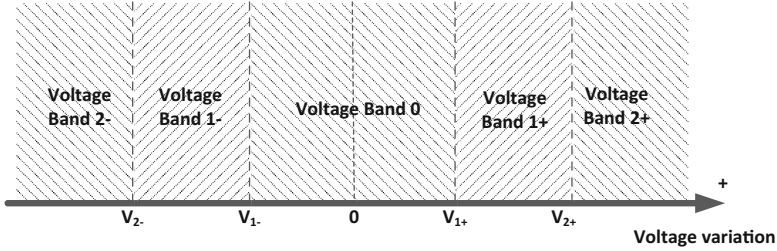
Fig. 2.4 Voltage band definition for autonomous DC microgrid control scheme

Fig. 2.5 Voltage variation-based DC microgrid control scheme
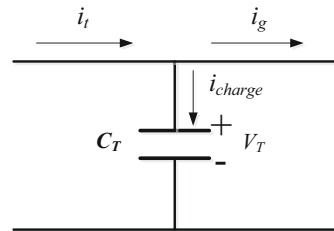
In order to avoid such high communication demand of central control, autonomous control was proposed for DC microgrid control at primary control level, which is illustrated in Fig. 2.3b. Autonomous control is based on local detections only and therefore the primary controls of terminal converters can be incorporated in a "plug-and-play" and expandable manner without the need for communications. With autonomous control methods, the terminal cooperation scheme shall be specially designed and embedded into terminal controllers.

For autonomous control, voltage variation-based technique can be implemented [15–17] which does not need additional communication channel but local voltage detection, hence better reliability and lower cost. Droop control is normally employed throughout voltage variation-based autonomous control scheme. A typical voltage banding scheme is demonstrated in Fig. 2.4, where specific control strategies are determined by which band the local DC voltage detection belongs to [17], and its relevant control is locally embedded within each DC terminal.

2.3.1.3 The Principles of DC Voltage Control [13]

Figure 2.5 shows the basic DC terminal model. The terminal voltage would rise when the capacitor charging current is positive and drop when negative. In other words, voltage variation of a DC microgrid can indicate whether the system power flow is effectively balanced.

Fig. 2.6 DC voltage droop
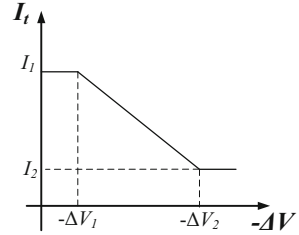
Fig. 2.7 DC voltage droop
control block
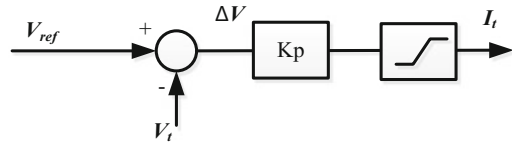
The charging current i_{charge} is subjected to

$$i_{charge} = i_t - i_g \tag{2.1}$$

where i_t is the terminal current and i_g the DC grid current. Once the grid current is given, the charging current can be regulated by controlling the terminal power. Droop control, as is shown in Fig. 2.6, is widely used in the implementation to determine how much current a slack terminal shall be given on a real-time basis. Linear current-voltage control is imposed when the voltage variation is between and ΔV_1 and ΔV_2. Saturation current/voltage is normally added for power rating or control band switching concern.

The corresponding control diagram of droop control can be generalized as a proportional with saturation control shown in Fig. 2.7, where the voltage variation can be calculated with the reference voltage V_{ref} and the detected terminal voltage V_t and K_p refers to the gain of the droop.

2.3.1.4 Operational Criteria

In order to determine the specific control strategy in each operational status, the operational criteria of a DC microgrid is set up in three groups in terms of priority as the following:

- Reliability—of the first priority

  Reliability concerns operational stability and equipment safety, which ensures that the facilities within the microgrid, such as capacitors, power electronics devices, transmission lines, and energy storage systems, are not damaged and are in normal operation. As the reliability is primarily for safety concern, once a DC microgrid is in operation, the criteria of reliability shall be obeyed at all time.

- Function ability—of the second priority

    Function ability concerns satisfactory anytime plug-and-play power supply, maximum renewable power generation, and state of charge (SOC) management of energy storage. As the function ability is proposed for the basic function demand from microgrid customers, it shall be fulfilled upon the state when reliability is ensured.
- Optimization—of the least priority

    Optimization concerns the optimal but not essential operation attributes for a microgrid. Examples are utility grid support, power smoothing, and internal voltage variation suppression.

    During system operation, conflicts among groups of criteria may occur under certain circumstances. The criteria of the lower priority shall be subjected to the higher. One typical example is when the microgrid is operating during islanding operation, load shedding shall be carried out when the load power consumption exceeds the real-time total power supply capability, where the anytime power supply function ability shall give way to the safety criteria to avoid system instability.

2.3.1.5   Autonomous Control Strategy of DC Microgrid [17]

Since the control schemes of the terminals within a DC microgrid can be determined by DC voltage variation, autonomous control for an entire DC microgrid can be established. Assuming that the voltage difference among the terminals is negligible, a certain range of operational voltage can be set and divided into a number of bands. In order to ensure the power balance, certain combination of terminals is assigned into each band acting as slack terminals. Based on the voltage band defined in Fig. 2.4 and the fore-cited control criteria, a typical autonomous voltage control scheme can be established, which is demonstrated in Fig. 2.8.

As is shown in Fig. 2.8, a control structure of three levels within 5 V bands is established by injecting slack terminals into each of the voltage bands. The control levels are:

Level 0: Level 0 control corresponds to voltage band 0, where the system is in normal grid-connected operation. The DC voltage is maintained by utility grid-connected DC/AC converter (GVSC)—the slack terminal.
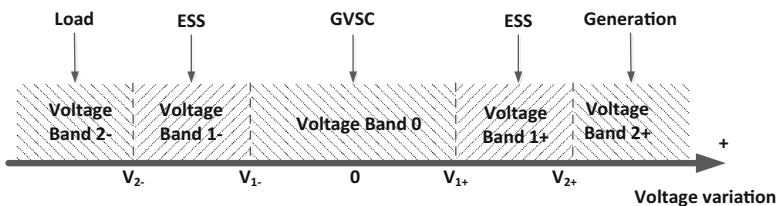

Fig. 2.8 Autonomous voltage control

Level 1: Level 1 control corresponds to voltage band 1+ and 1−, where the G-VSC fails to regulate the DC voltage within band A and energy storage system (ESS), the slack terminal(s), starts to take the place.

Level 2: Level 2 control corresponds to voltage band 2+ and 2−, where both GVSC and ESS cannot maintain DC voltage within band A and an emergency control is performed. Load shedding is carried out in band 2− and generation curtailing in band 2+. Please note that since load shedding is normally an on/off process, it cannot possibly maintain the DC voltage within band 2− but to push the voltage back to band 1−. If the voltage goes below band 2− or above 2+, protection measures shall take place.

It is possible that multiple slack terminals are selected within one band and cooperation strategy is essential in such situation.

2.3.1.6 Enhanced Droop Control for DC Microgrids [13]

Droop control is normally performed in voltage regulation, though it has a number of drawbacks. One obvious fact is that there is always a static error. Another undesirable feature is that the system might be subjected to lack of phase margin when the droop gain is too large for a relatively large control period. In order to correct the undesirable features of droop, enhanced control strategies are proposed for practical implementations.

Adding an integral controller paralleled with the proportional forms a PI controller, as is shown in Fig. 2.9a, which is normally employed by GVSC within a DC microgrid to eliminate static voltage error during AC grid-connected operation. Care must be taken that no more than one PI regulation can be implemented within a DC microgrid simultaneously to avoid conflicts between each other.
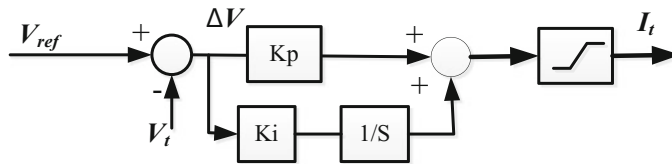
(c) PI voltage control
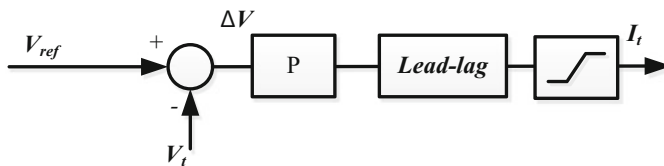
(d) P + Lead-lag control

Fig. 2.9 Enhanced droop control. (**a**) PI voltage control. (**b**) P + lead-lag control
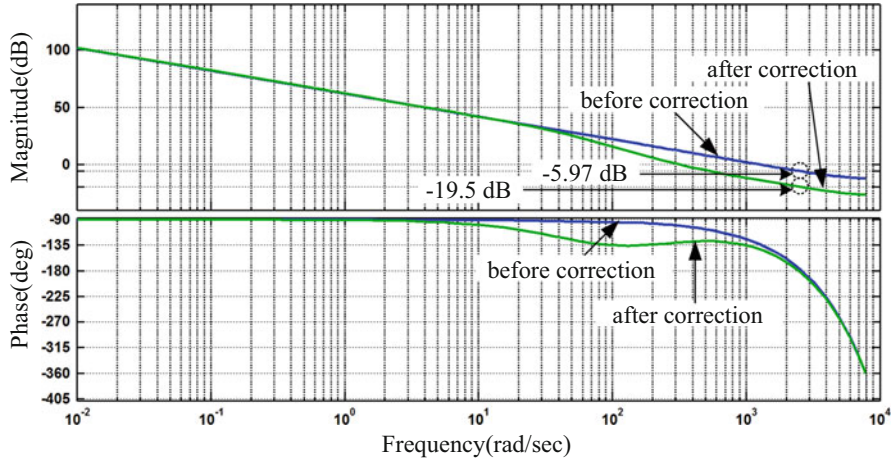
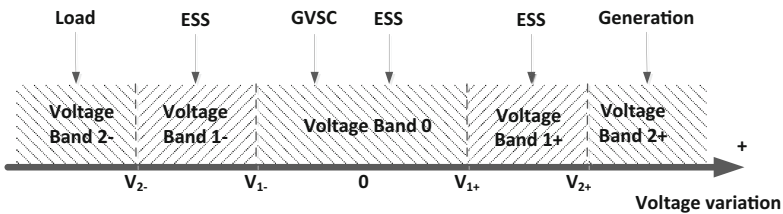**Fig. 2.10** Lead-lag correction

Fig. 2.11 Enhanced operational control

Lead-lag controller is also well employed when a large droop gain is required with a low control frequency, typically 2.5–5 kHz. A lead-lag controller is added to the droop controller to correct the dynamic behavior by increasing phase and gain margin; one example is shown in Fig. 2.10.

2.3.1.7 Enhanced Operational Control of DC Microgrid and Power Smoothing

In order to enhance the output power exchange with the utility grid, ESS can be injected into the voltage band 0 in Fig. 2.8 as Fig. 2.11 shows.

By setting the gain much larger than the GVSC, the ESS can effectively share most of the power fluctuation of higher frequency, hence smoother output power from the GVSC to the utility grid. Besides, the total bandwidth of voltage regulation can be increased, which means that the DC voltage variation can be further suppressed for the same power variation. As the gain can be considerably large, a lead-lag controller shall be added to the ESS controller in the form of Fig. 2.9b.
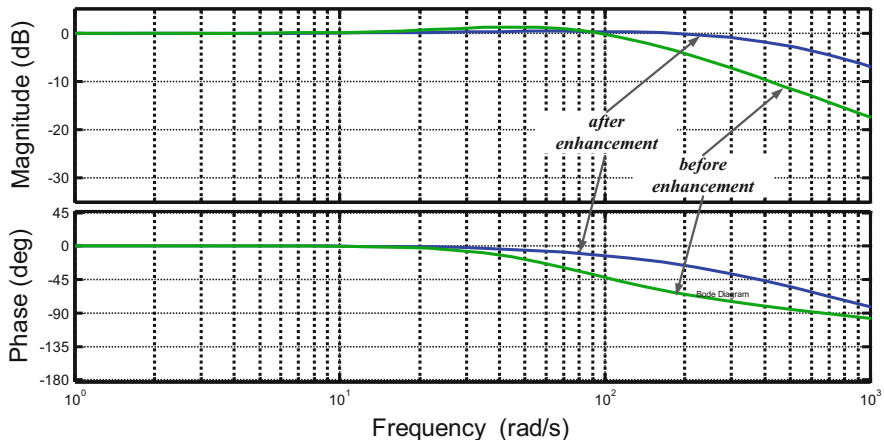
(a) Voltage regulation response $V_{dc}/V_{dc}{}^*$
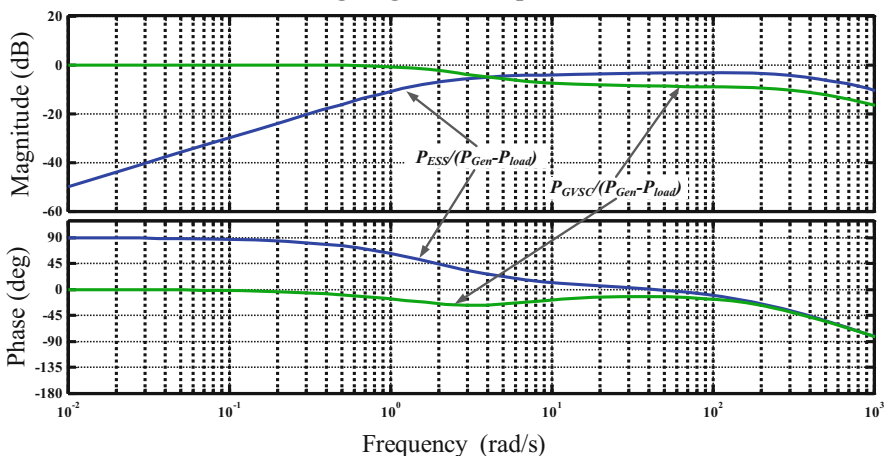
(b) Power sharing of enhancing operation

Fig. 2.12 Close loop Bode plot for enhanced voltage control. (**a**) Voltage regulation response $V_{dc}/V_{dc}{}^*$. (**b**) Power sharing of enhancing operation

Such a voltage regulation and frequency-based power sharing strategy can be assessed by close-loop Bode plot, which is illustrated in Fig. 2.12.

2.3.1.8 Hierarchical Control Scheme with Low-Bandwidth Communication

The major drawback of the fore-cited autonomous control scheme is that a static voltage variation cannot be avoided when the DC system is operating in a certain voltage band other than band 0. Besides, it is also difficult to achieve accurate power sharing among slack terminals in an autonomous manner. A communication
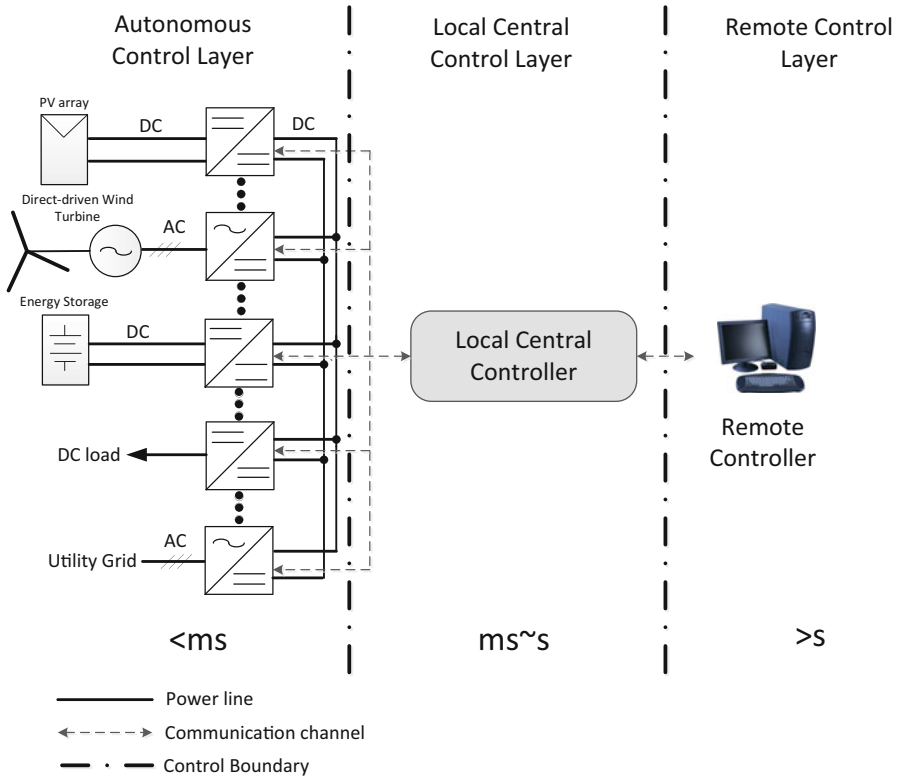
Fig. 2.13 Three-layer DC microgrid control system

network is therefore employed to optimize voltage profile in various timescales, hence a hierarchical control system [18]. A hierarchical microgrid control system can be typically divided into three layers in terms of the control cycle. They are autonomous control layer, local central control layer, and remote control layer, which are demonstrated in Fig. 2.13. As is shown in Fig. 2.13, the fore-cited autonomous primary control scheme is performed by each of the terminal converter in the autonomous control layer. The instant control feedbacks are based on each local voltage and current detections. The control cycle of this layer is normally less than a millisecond. Meanwhile, local central controller collects the current and voltage information from each terminal and provides optimized parametric amendment orders to current and voltage control. A secondary power sharing and voltage adjustment can be performed in this layer [19]. And the overall energy management can also be carried out in this layer if applicable. The control cycle of local central controller is typically between tens of milliseconds to a few seconds depending on communication baud rate and system scale. The remote controller layer allows the system operator or higher but slower level control to access the database uploaded by local central controller and manage the energy management strategy based on a

cycle of a few seconds to a few minutes. The local central control layer is a desirable redundancy for optimization to the autonomous control layer and similar case is the remote control layer to the local central controller.

2.4 Stability of DC Microgrids

2.4.1 Small Signal Model and Stability Assessment

2.4.1.1 Virtual Impedance Method

In order to assess the dynamic performance of a DC system, an appropriate linearized model shall be established for small signal analysis. As is cited in previous sections, the DC microgrid system consists of power terminals and slack terminals. Slack terminal control can actively affect system dynamic performance. A single-slack terminal DC system model can be established with the slack control modeled as virtual impedance in S domain using virtual impedance method [20]. The modeling scheme is demonstrated in Fig. 2.14, where Reg(s) refers to the linear transfer function of the slack terminal control, including both open-loop voltage regulator RegV(S) and close-loop current regulator RegI(S).

The transfer function can be given by

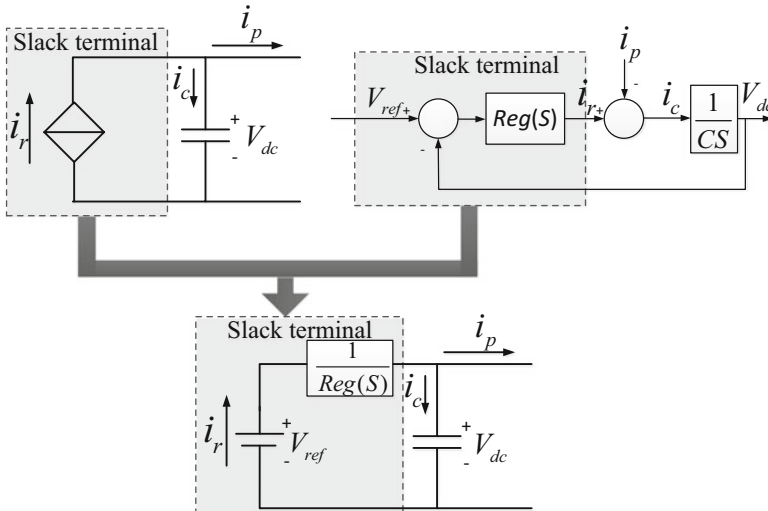$$Reg(S) = RegV(S)RegI(S) \tag{2.2}$$

Fig. 2.14 Single-slack terminal DC microgrid modeling using virtual impedance concept

A high-bandwidth current regulation transfer function can be simplified and modeled as a first-order delay process as

$$\text{RegI}(S) = \frac{1}{1 + T_c S} \tag{2.3}$$

where T_c is the implemented control cycle. $\text{RegV}(S)$ is the linearized open-loop voltage regulator which can be a P control, P with lead-lag control or PI control as is cited in previous sections.

With a simplified model as Fig. 2.14 shows, transfer functions or state space can be established and then system stability can be analyzed with known assessing technique such as phase/gain margin analysis and root locus. One example of single-slack terminal analysis in terms of variable PI regulator band width is shown in Fig. 2.15 using close-loop root locus and open-loop marginal analysis.

For a DC microgrid with multiple slack terminals and complex topology, S-domain model can be set up based on single slack terminals connected to each other via line impedances. By using Thevenin's equivalent from any of the terminal sides, the multiple-terminal system can be transformed into a simplified model in the same form in Fig. 2.14. This process is shown in Fig. 2.16 and then the same stability assessing technique applies.

2.4.1.2 Impacts of Constant Power Load on System Stability

The DC loads in a system are not necessarily linear load. Their behaviors vary and can have significant impact on a DC microgrid operation and stability. One of the commonly seen and severe cases is the constant power loads (CPLs) [17].

Static Consideration of a DC System with CPL

As is previously cited, droop-based control is normally used in autonomous control level. A basic concern about the impact of CPLs is whether they are compatible with droop control. A basic example is demonstrated in Fig. 2.17a where a droop-controlled slack terminal is supplying a CPL R_{CPL} with a cable resistance of R_L. The static characteristic of the simple circuit is shown in Fig. 2.17b with two droops and the CPL considered [17].
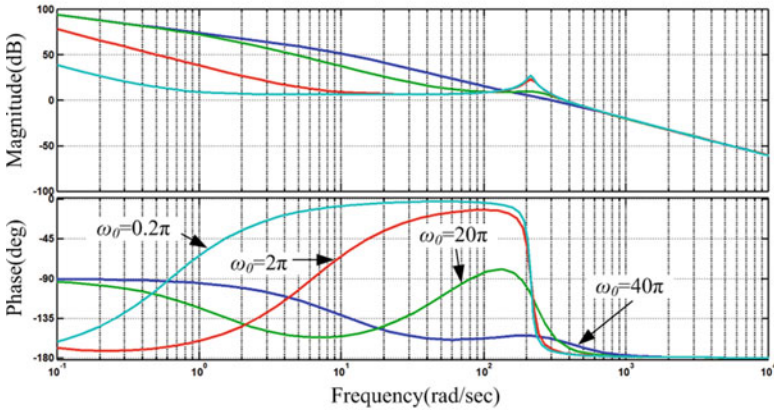
The DC voltage at the load terminal is

$$V_{\text{dc}} = V_{\text{ref}} - \left(R_{\text{eq}} + R_L\right) I_{\text{dc}} \tag{2.4}$$

where R_{eq} is the equivalent slack terminal virtual resistance and per-unit values are used in all the expressions in this section.

As is shown in Fig. 2.17b, the CPL characteristic is given as
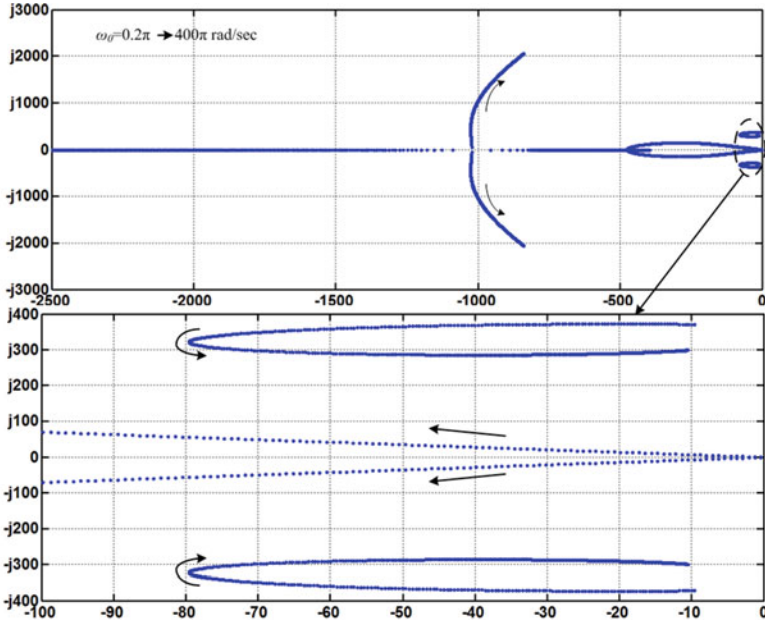
(a) Close-loop Root locus(arrow points to increasing ω_0 value)

(b) Open-loop Bode plot

Fig. 2.15 Stability assessment of single slack terminal. (**a**) Close-loop root locus (*arrow points to increasing ω_0 value*). (**b**) Open-loop Bode plot

$$V_{dc} \cdot I_{dc} = \text{constant} = P_L \tag{2.5}$$

where P_L refers to the load power.

In order to ensure a stable system operation, the characteristic curves of the slack terminal and the load must share a cross point on the V–I plane, using per-unit value
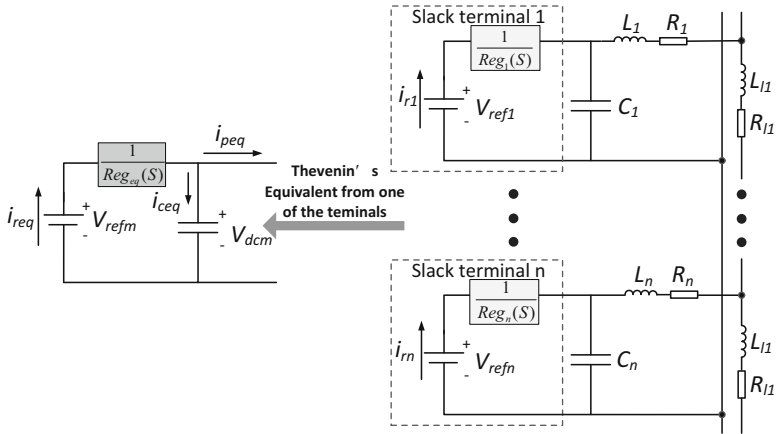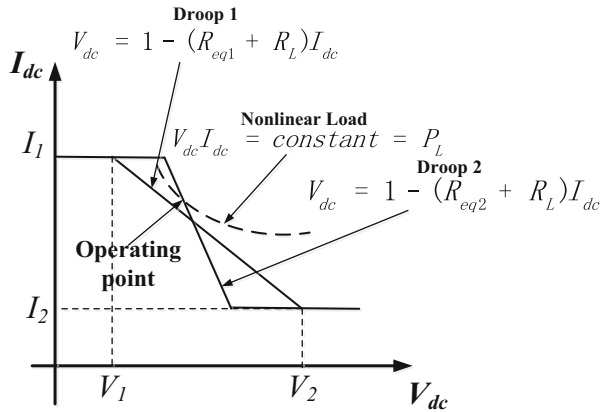
Fig. 2.16 DC microgrid modeling with multiple slack terminals

Fig. 2.17 Simple DC
system with one slack
terminal and one CPL. (**a**)
Circuit diagram. (**b**) V–I
characteristics with
different droop
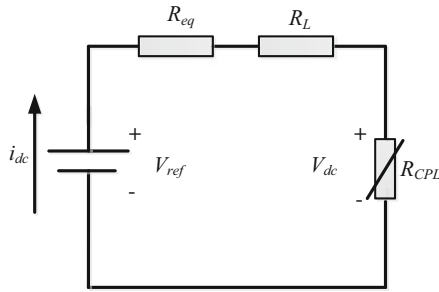
(a) Circuit Diagram

(b) V-I characteristics with different droop

with the superscript of "*" and assigning $V_{dc}* = 1$. The operating voltage can be calculated by combining (Eqs. 2.4 and 2.5) as

$$V_{dc}* = \frac{1 \pm \sqrt{1 - 4(R_{eq}* + R_L*^L)P_L*}}{2} \tag{2.6}$$

To ensure the existence of the operating point, the following condition must be met:

$$R_{eq}* + R_L* \leq \frac{1}{4P_L*} \tag{2.7}$$

Obviously, Droop 1 does not meet the conditions whereas Droop 2 does in Fig. 2.17b. And the operating point can be given as

$$(V_{dc}*, I_{dc}*) = \left(\frac{1 + \sqrt{1 - 4(R_{eq}* + R_L*)P_L*}}{2}, \frac{2P_L*}{1 + \sqrt{1 - 4(R_{eq}* + R_L*)P_L*}} \right) \tag{2.8}$$

Droop can be selected with the guidance of (Eqs. 2.7 and 2.8).

Small Signal Modeling of a CPL with Virtual Impedance Method

By differentiating the equation of $V_{dc} = P_L/I_{dc}$ on both sides, the small signal virtual impedance on a given point can be obtained as

$$R_{CPLeq} = \frac{dV_{dc}}{dI_{dc}} \Big|_{I_{dc}=I_{dc0}} = -\frac{P_L}{I_{dc}^2} \Big|_{I_{dc}=I_{dc0}} \tag{2.9}$$

where I_{dc0} refers to the equilibrium point current. Therefore, when the operational analysis point, that is, V_{dc} and I_{dc}, has been determined, this equivalent virtual resistance can be incorporated into the fore-cited S-domain analytical circuit based on virtual impedance concept.

Dynamic Consideration of a CPL Within a DC Microgrid

In a DC power system, though the static characteristic matches the needs from CPL, there is still a chance that severe oscillation would be caused due to its dynamic behavior caused by the negative resistance brought by CPL. Such oscillation is more likely to happen with larger line impedance, smaller terminal capacitance, and larger constant power load.

In order to prevent undesirable oscillation, damping measurement shall be taken into consideration at the designing stage. The damping implementation varies. However, the damping methods can be generally categorized into two kinds—slack terminal side damping [19–21] and power terminal side damping [22–24]. The power terminal damping methods superimpose an extra damping control into the CPL control, hence a modified and more stable CPL behavior for the global system concern. Such power terminal side method can possibly result in a trade-off of the modified load performance but more adaptive to a system with multiple CPLs and possible reconfigurations [24]. Slack terminal damping methods, on the other hand, superimpose the damping control into the normal voltage control to provide extra damping to the DC system without compromise to load behavior; yet the drawback is that it is case sensitive to system configuration and variable sources and loads may increase the difficulty to ensure its robustness.

2.5 Protection of DC Microgrids

Comparing the protection of traditional AC systems, the theory and implementation of the newly evolved DC microgrid protection are far from maturity. In this section a few issues concerning DC microgrid protection are discussed.

2.5.1 Introduction to DC Faults

The faults within a DC microgrid can occur at terminal units and on any point of the network. The terminal units are DC/DC converters, grid-connected VSC, loads, utility AC grid, or other converters. Network fault concerns those occurring at the DC buses, transmission lines, or feeders.

For converter and AC-side fault, the fault current can normally be limited by the inductive filters along with switching devices.

The DC network faults can further be divided into two types: line breaking and short fault [25].

(a) Line breaking

A line breaking fault will possibly change the system topology and power flow of a DC microgrid. Typically in a radial topology, a breaking fault would essentially intersect the grid into two sub-grids, which is illustrated in Fig. 2.18. The instant autonomous control scheme will continuously be performed within each of the sub-grid. The terminal unit will remain in the operational voltage band shown in Fig. 2.4 as long as there is at least one slack terminal surviving for each sub-grid. Otherwise, the DC system voltage will divert and protection must take place by blocking all the converter sources and tripping the loads. Actually, the system behavior of a DC microgrid after a line

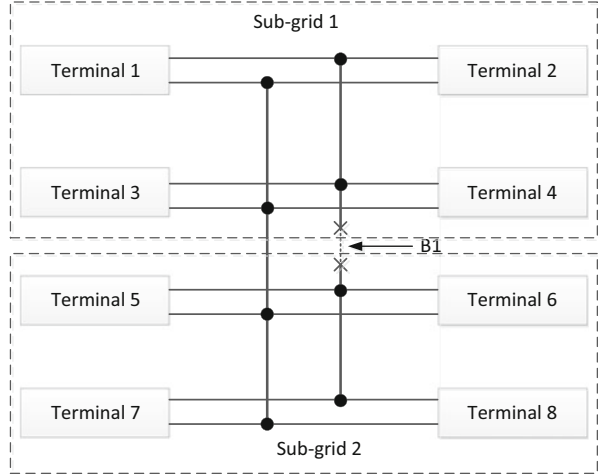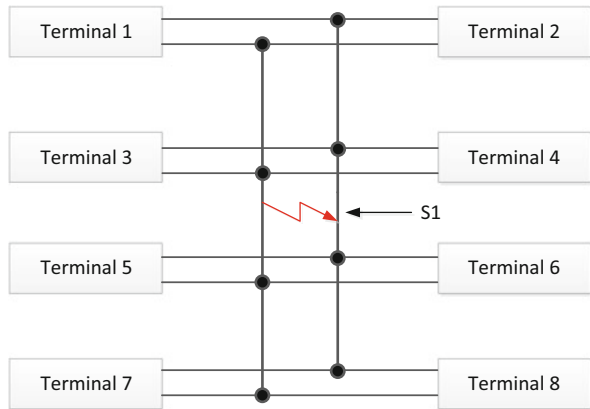**Fig. 2.18** Line-breaking fault in a DC microgrid

Fig. 2.19 Bus fault in a DC microgrid

break seems more like a mode switch and can be handled with predefined autonomous control scheme and voltage protection.

(b) DC short faults

As the DC side impedance is very low, a DC short fault will produce a huge current surge draining into the faulty point in a very short time, typically milliseconds. If a bus fault happens at the point of S1 shown in Fig. 2.19, the current will increase drastically.

Simulation results shown in Fig. 2.20 are given from the GVSC converter side, where it can be seen that the fault current across the faulted cable can rise up to 20 p.u. in 5 ms.

(c) DC arc faults

Arc faults refer to the situation that an electric circuit is maintained via an arc when two conductor ends are very closely located with dielectric medium in between [26–30]. Such situation results from the cause that the
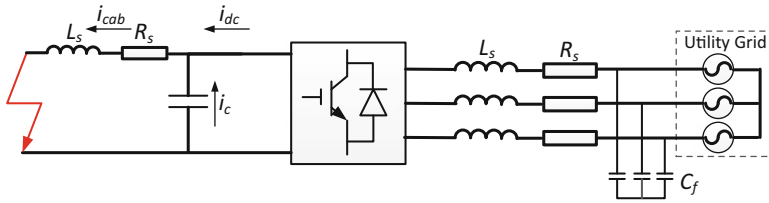
(a) GVSC terminal side model
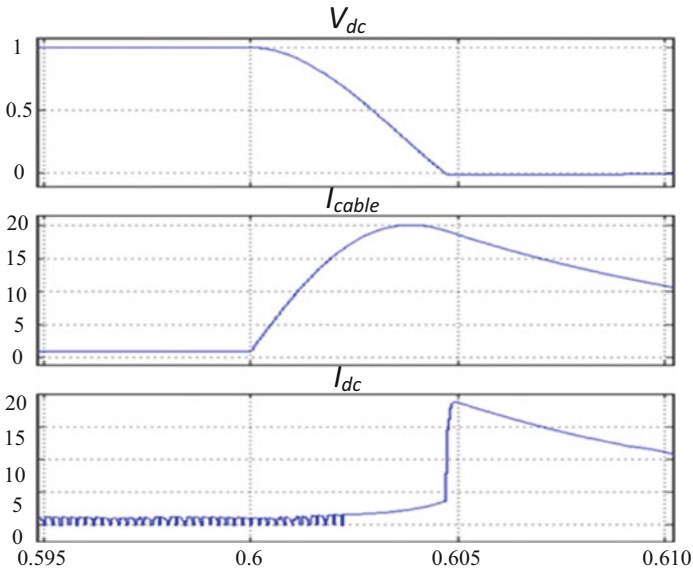
(b) Fault behavior

Fig. 2.20 DC fault behavior from GVSC side. (**a**) GVSC terminal side model. (**b**) Fault behavior

high-temperature arc ionizes the dielectric medium. The arc current is usually not very significant comparing with normal power rating but is able to accumulate high temperature at the faulty point. A lasting arc fault may further damage the adjacent equipment and cause more severe fault event. There are mainly two kinds of arc faults—series and parallel, shown in Fig. 2.21a, b. A series arc fault is more common in a DC system. It can be caused by unintentional conductor discontinuity within DC lines or by a loose contactor that slightly separates the connections, etc.

In order to prevent damage caused by arc fault, the arc fault of a DC microgrid should be detected. However, the detection of DC arc fault, especially a series arc fault, in a DC microgrid is difficult. The reason lies on the fact that the behavior of an arc fault is similar to small nonlinear impedance, causing limited changes to system currents and voltages [26–29]. Reports show that the behavior includes a static resistive characteristic along with high frequency, typically a few kHz, chaotic noise as well [26, 27]. It is still

Fig. 2.21 DC arc fault. (**a**) Series arc fault. (**b**) Parallel arc fault

(a) Series arc fault　　　　　　(b) Parallel arc fault
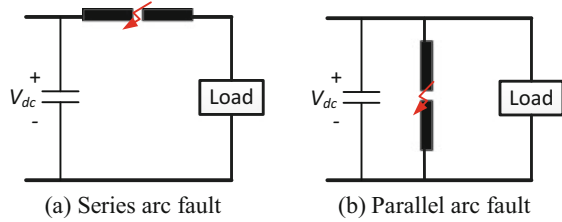
difficult to establish an explicit analytical model to find out its exact signature due to its chaotic behavior and random causes.

2.5.2 DC Circuit Breaking

The key issue of DC protection device is to interrupt fast-increasing DC fault current. There are generally two types of DC current interruption methods, that is, current breaking and current limiting.

Fuse [25] is the most common circuit-breaking device with a fuse link and arc-quenching component. A fuse breaks its circuit by melting when a certain root mean square current goes through, which means that it can be applied in either DC and AC circuit. A fuse uses its heat-absorbing material to break the circuit and quench the arc. The heat-absorbing material is normally silica sand, connecting to conductor links within a ceramic cartridge. The selection of fuse mainly depends on its voltage and current-time ratings. For the DC applications, a shorter current rising time (typically a few milliseconds) rather than a steady large current will result in a quicker melting process and better arc quenching [31]. A quick melting fuse with light overcurrent handling ability is desirable for a DC fault. The major drawback of fuse is that it is nonreversible. Fuse can be applied as the main protection device in small-scale DC microgrid or as the backup device in a relevant large system.

Molded case circuit breaker (MCCB) is the most commonly used low-voltage circuit breaker. Unlike fuses, MCCBs are reversible. An MCCB is able to interrupt current within a time of a few tens of milliseconds under a rated voltage of hundreds of volts and with an interruption current of tens of kilo amperes [32]. MCCB can be used as the main protection device in low-voltage small-scale DC microgrid system.

The idea of current limiting is to insert a device of current-sensitive impedance into DC circuits. The inserted impedance can be resistive or inductive. The value of the inserted impedance is very low when normal current goes through and tends to rise drastically when large fault current passes through, hence limited rising rate of the DC fault current. With the assist of current limiter, the DC current can be interrupted with relevant "slower acting" switchgear. The DC circuit breaker can therefore make the fault current to commutate to the axillary resonant circuit and force a zero-current point to allow arc extinguishing.

2.6   Conclusion

Microgrid, as a promising new power management system, is proposed for accommodating growing distribution generation and energy storages; for example, electric vehicle charging stations can act as an ideal storage resource in microgrids. Distributed renewable generations, energy storage systems, and local loads are key elements of a microgrid. DC microgrid is specially designed for distribution power systems dominated by those generations, storages, and loads that have DC links.

In this chapter, the hierarchical structure of DC microgrids is introduced. With autonomous voltage control scheme at primary control level, a DC system can well operate autonomously. Secondary and higher control levels enable further optimization on accurate power sharing, voltage restoring, and energy management. Virtual impedance method is introduced for assessing DC power system dynamics.

DC microgrids have significant advantages in terms of converter cost, distribution efficiency, power supply reliability, and controllability compared to AC ones, whereas the difficulty in DC protection is the major weakness.

References

1. Lasseter RH (2002) MicroGrids. Proc IEEE Power Eng Soc Winter Meeting 1:305–308
2. Li Y, Vilathgamuwa DM, Loh PC (2004) Design, analysis, and real-time testing of a controller for multibus microgrid system. IEEE Trans Power Electron 19(5):1195–1204
3. Katiraei F, Iravani MR, Lehn PW (2005) Microgrid autonomous operation during and subsequent to islanding process. IEEE Trans Power Del 20(1):248–257
4. Blaabjerg F, Chen Z, Kjaer SB (2004) Power electronics as efficient interface in dispersed power generation systems. IEEE Trans Power Electron 19(5):1184–1194
5. Dimeas AL, Hatziargyriou ND (2005) Operation of a multiagent system for microgrid control. IEEE Trans Power Syst 20:1447–1455
6. Ito Y, Yang Z, Akagi H (2004) DC micro-grid based distribution power generation system. Proc IEEE Int Power Electron Motion Control Conf 3:1740–1745
7. ESB Networks—Distribution Code, Version 1.4, Feb 2005
8. Velasco D, Trujillo C, Garcera G, Figueres E (2011) An active anti-islanding method based on phase PLL perturbation. IEEE Trans Power Electron 26(4):1056–1066
9. Bifaretti S, Lidozzi A, Solero L, Crescimbini F (2015) Anti-islanding detector based on a robust PLL. IEEE Trans Ind Appl 51(1):398–405
10. Kakigano H, Miura Y, Ise T (2010) Low-voltage bipolar-type dc microgrid for super high quality distribution. IEEE Trans Power Electron 25(12):3066–3075
11. Sannino A, Postiglione G, Bollen MHJ (2003) Feasibility of a dc network for commercial facilities. IEEE Trans Ind Appl 39(5):1499–1507
12. Salomonsson D, Sannino A (2007) Low-voltage dc distribution system for commercial power systems with sensitive electronic loads. IEEE Trans Power Del 22(3):1620–1627
13. Chen D, Xu L (2012) Autonomous DC voltage control of a DC microgrid with multiple slack terminals. IEEE Trans Power Syst 27(4):1897–1905
14. Zhou T, Francois B (2011) Energy management and power control of a hybrid active wind generator for distributed power generation and grid integration. IEEE Trans Ind Electron 58 (1):95–104

15. Schonberger J, Duke R, Round SD (2006) DC-bus signaling: a distributed control strategy for a hybrid renewable nanogrid. IEEE Trans Ind Electron 53(5):1453–1460
16. Xu L, Chen D (2011) Control and operation of a DC microgrid with variable generation and energy storage. IEEE Trans Power Del 26(4):2513–2522
17. Chen D, Xu L, Yao L (2013) DC voltage variation based autonomous control of DC microgrids. IEEE Trans Power Del 28(2):637–648
18. Guerrero JM, Vasquez JC, Matas J, Vicũna LG, Castilla M (2011) Hierarchical control of droop-controlled AC and DC microgrids—a general approach toward standardization. IEEE Trans Ind Electron 58(1):158–172
19. Lu X, Guerrero JM, Sun K, Vasquez JC (2014) An improved droop control method for dc microgrids based on low bandwidth communication with dc bus voltage restoration and enhanced current sharing accuracy. IEEE Trans Power Electron 29(4):1800–1812
20. Chen D, Xum L, Yao L (2012) DC network stability and dynamic analysis using virtual impedance method. In: Proceedings of 38th Annual Conference on IEEE Industrial Electronics Society, pp 5625–5630
21. Wu M, Lu DD-C (2015) A novel stabilization method of LC input filter with constant power loads without load performance compromise in DC microgrids. IEEE Trans Ind Electron 62 (7):4552–4562
22. Liu X, Forsyth A, Cross A (2007) Negative input-resistance compensator for a constant power load. IEEE Trans Ind Electron 54(6):3188–3196
23. Liu X, Zhou Y, Zhang W, Ma S (2011) Stability criteria for constant power loads with multistage LC filters. IEEE Trans Veh Technol 60(5):2042–2049
24. Magne P, Nahid-Mobarakeh B, Pierfederici S (2014) Dynamic consideration of DC microgrids with constant power loads and active damping system; a design method for fault-tolerant stabilizing system. IEEE Trans Emerg Sel Topics Power Electron 2(3):562–570
25. Salomonsson D, Soder L, Sannino A (2009) Protection of low-voltage dc microgrids. IEEE Trans Power Del 24(3):1045–1053
26. Yao X, Herrera L, Ji S, Zou K, Wang J (2014) Characteristic study and time-domain discrete-wavelet-transform based hybrid detection of series DC arc faults. IEEE Trans Power Electron 29(6):3103–3115
27. Yao X, Herrera L, Wang J (2015) Impact evaluation of series dc arc faults in DC microgrids. In: IEEE Applied Power Electronics Conference and Exposition (APEC), pp 2953–2958.
28. Yao X, Herrera L, Huang Y, Wang J (2012) The detection of DC arc fault: experimental study and fault recognition. In: IEEE Applied Power Electronics Conference and Exposition (APEC), Twenty-Seventh Annual Meeting, pp 1720–1727
29. Yao X, Ji S, Herrera L, Wang J (2011) DC arc fault: characteristic study and fault recognition. In: IEEE 1st International Conference on Electric Power Equipment Switching Technology (ICEPE-ST), pp 387–390
30. Uriarte FM, Gattozzi AL, Herbst JD, Estes HB, Hotz TJ, Kwasinski A, Hebner RE (2012) A DC arc model for series faults in low voltage microgrids. IEEE Trans Smart Grid 3 (4):2063–2070
31. IEEE Guide for the Protection of Stationary Battery Systems (1998) IEEE Std. 1375-1998
32. ABB—low voltage circuit breakers—working with trip characteristic curves. http://www.tnbpowersolutions.com/sites/default/files/webfm/resources/upload/Cyberex%20Data%20Center/ABB%20Breakers%20and%20Panelboards/ABB%20LV%20Breakers%20working%20with%20trip%20curves.pdf

Chapter 3
Integration of Renewable Energy Sources into the Transportation and Electricity Sectors

Vamsi Krishna Pathipati, Arash Shafiei, Giampaolo Carli, and Sheldon S. Williamson

3.1 Introduction

The challenge for the next few years in the auto industry is to improve vehicle fuel economy, and make them independent of oil supply, as well as reduce carbon dioxide (CO_2) emissions. To achieve these stringent industrial goals, the trend in the auto industry is to move towards transportation electrification, by introducing sustainable and nonpolluting electric and plug-in hybrid electric vehicles (EVs/PHEVs). Innovative transportation penetration has affected energy production in a major way. Energy production is already reaching its peaks. Hence, it has become imperative to find a solution, to manage energy production and usage accurately, especially within the context of EV/PHEV energy storage systems.

The chapter also focuses on EV battery charging from home as well as at work and future public charging stations, covering charging levels I and II, as defined by standards laid out by the Society of Automotive Engineers—SAE J1772. According to SAE J1772, DC charging of EVs/PHEVs can be performed at 200–450 VDC, from 36 kW, 80 A (DC Level I), up to 200 A, 90 kW (DC Level II). A power electronics perspective to interconnect EVs/PHEVs with renewables and the grid is also discussed. Power electronic DC/DC converter topologies for smart and efficient interconnection of EVs to homes as well as the grid and renewable energy systems are introduced. Reduced stages of power conversion are also emphasized upon.

Finally, this chapter presents the advantage of having an EV at home (powered from the AC grid and a rooftop PV panel). Recently, it has become a trend to produce electricity at home, for personal usage, or to sell power to the grid. This is the concept of smart grids. However, there typically exists no energy storage at home. If the EV battery is considered as an element of the household, when the

V.K. Pathipati • A. Shafiei • G. Carli • S.S. Williamson (✉)
University of Ontario-Institute of Technology, Oshawa, ON, Canada
e-mail: sheldon.williamson@uoit.ca

vehicle is connected at home, renewable energy can be stored in the EV battery. Thereafter, this energy can be used for vehicle propulsion or to supply the grid. This power flow is called vehicle-to-home (V2H) or vehicle-to-grid (V2G) power flow. This chapter discusses a real-world test case scenario of an EV connected to a PV/grid-powered home. An optimization formulation for minimal cost power flows is presented.

3.2 On-Board Energy Harvesting Through Renewable Energy Sources

Solar electricity which can be obtained using photovoltaic panels is one of the easiest ways as long as sun is available. They can be easily mounted on the roofs of buildings or rooftops of parking slots generating electric power to charge the battery pack of the EVs while providing shade for the cars. Since solar energy is intermittent and variable, power grid should be involved to ensure that enough power is available. Conventional solar chargers inject power to the grid and use grid as the main source because of its reliability and being infinite. Hence, they use grid as a kind of energy storage system. This approach can lead to problems for grid stability if solar panels are utilized in large scale and comparable to the grid.

For easy understanding, an example approach is taken in this unit, based on the photovoltaic potential as per Pelland et al. [1] and Morris [2] of certain locations in Canada, and the sizing of the PV panel, required for charging a PHEV, for operating in an all-electric mode for 40 miles daily, is discussed. More importantly, scenario-based case studies based on different vehicle structures are carried out to evaluate the possibilities of reducing the costs. Finally, a comprehensive comparison is carried out to summarize the advantages from different points of view.

3.2.1 Introduction

Conventional vehicles (CVs), which use petroleum as the only source of energy, represent majority of the existing vehicles today. As shortage of petroleum is considered as one of the most critical worldwide issues, costly fuel becomes a major challenge for CV users. Moreover, CVs emit greenhouse gases (GHG), thus making it harder to satisfy stringent environmental regulations.

One of the most attractive alternatives includes electric vehicles (EVs) or zero-emission vehicles (ZEVs), which only consume electric energy. However, due to the limited energy densities of the current commercially available battery packs, the performance of EVs is restrained as neighborhood vehicles, with limitations of low speed, short autonomy, and heavy battery packs. As a successful example, Canada-based ZENN's commercialized EV has an average speed of 25 mph and 30–40-mile driving range per charge.

Currently, the most promising and practical solution is the hybrid electric vehicles (HEVs). Its propulsion energy is usually from more than two types of energy storage devices or sources, and one of them has to be electric. HEV drive trains are basically divided into series and parallel hybrids. Series hybrids are electric-intensive vehicles, as the electric motor is the only traction source, and the internal combustion engine (ICE) merely works at its maximum efficiency, as an onboard generator, to charge the battery.

Keeping in mind the goals of creating an energy-wise, cost-effective, and overall sustainable society, plug-in hybrid electric vehicles (PHEVs) are recently being widely touted as a viable alternative to both conventional and regular hybrid electric vehicles. PHEVs are equipped with sufficient onboard electric power, to support daily driving (an average of 40 miles per day) in an all-electric mode, only using the energy stored in batteries, without consuming a drop of fuel. This, in turn, causes the embedded internal combustion engine (ICE) to use only a minimal amount of fossil fuel to support further driving beyond 40 miles, which further results in reduced greenhouse gas (GHG) emissions.

PHEVs can reduce fuel consumption by charging its battery from the grid. It is, thus, a valid assumption that moving into the future, a large number of PHEV users will most definitely exist, and the overall influence of charging the onboard energy storage system (ESS) cannot be neglected. Related literature [3, 4] by L. Eudy and A. Burke firmly states that by the year 2018, the market share of PHEVs will increase to about 25 %. Based on this data, the additional electric energy demanded from the distribution grid for five million PHEVs would be roughly about 50 GWh per day. The typical charging time would be 7–8 h, which might make it hard to accommodate these additional loads in the load curve without increasing the peak load. Also, the required additional charging energy would have a possible impact on the utility system. Expanding the electric system the conventional way, with large generating plants located far from the load centers, would require upgrading the transmission and distribution systems too. Besides the high costs, this can take many years before obtaining the right-of-way. Alternatively, smaller power plants based on renewable energy, such as solar energy, can be installed in a fraction of that time on the distribution system, which is commonly referred to as "distributed generation (DG)." Photovoltaic (PV) presents a modular characteristic and can be easily deployed in the rooftop and facades of residences and buildings. Many corporations are adopting the green approach for distributed energy generation. For instance, *Google* has installed 9 MWh per day of PV on its headquarters, Googolplex, in Mountain View, California. At the moment, it is connected to Mountain View's section of electricity grid. Alternatively, it could be used for charging PHEVs during work hours, being a great perk for environmentally concerned employees. The energy stored in the batteries could also be used for backup during faults. In Canada, the latest projections (2000) indicate that by 2010, renewable DG sources will represent at least 5 % of the total energy produced and 20 % of cogeneration, from the actual figures of 1 % and 4 %, respectively. Therefore, from the environment point of view, charging PHEVs with solar power will be the most attractive solution.

This chapter deals with the sizing of the PV panel required for charging a PHEV for operating in an all-electric mode for 40 miles daily.

3.2.2 Vehicle's Main Features

For the analyses conducted in this chapter, the selected PHEV presents the features of the vehicle's existing state as well as the developing trends in terms of the vehicle size and pure electric autonomy. The typical daily driving mileage for a commuter in North America is approximately 35–40 miles. Thus, PHEV-40, which has 40-mile daily driving in all-electric mode, is proposed. In addition, the midsized sport utility vehicle (SUV) possesses the most significant market share in North America. Therefore, a midsized SUV PHEV-40, configured as a series HEV, is used as the case-study-case vehicle for this chapter. As one of the developing trends, PHEV-40 presents the user favorable features such as long daily driving distance, reasonable onboard battery pack weight, high fuel economy, and environment friendliness.

A typical electrical power system of a PHEV is shown in Fig. 3.1. Charger plugs in the grid to charge the high-energy battery. A bidirectional DC/DC converter connects the battery to high-voltage bus and it is also used to deliver the energy back to battery during regenerative breaking events.

As shown in Fig. 3.2, a series PHEV liberates the ICE, which is disconnected from the shaft, compared to a parallel PHEV, to operate in its optimal efficiency region. The electric motor is the only propulsion source for the vehicle. Fuel energy is used to charge the battery when all the electric energy is drained from the battery. Hence, the electric-intensive structure, which represents the future developing trends, is a combination of different energy sources.
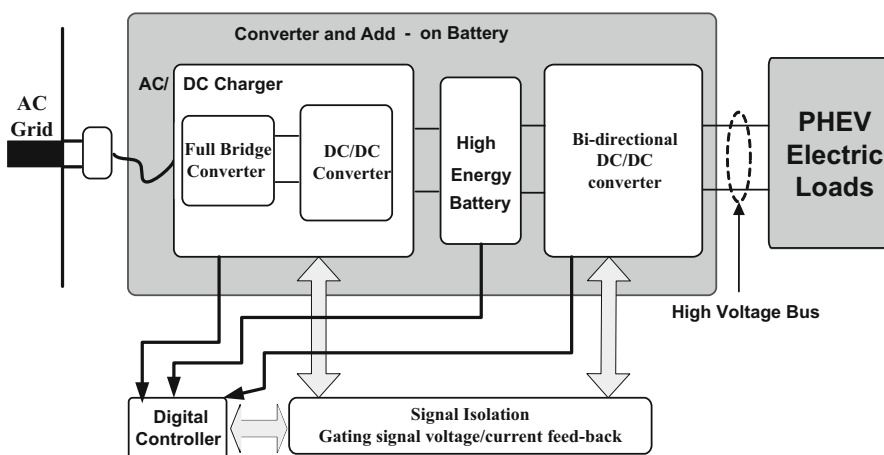

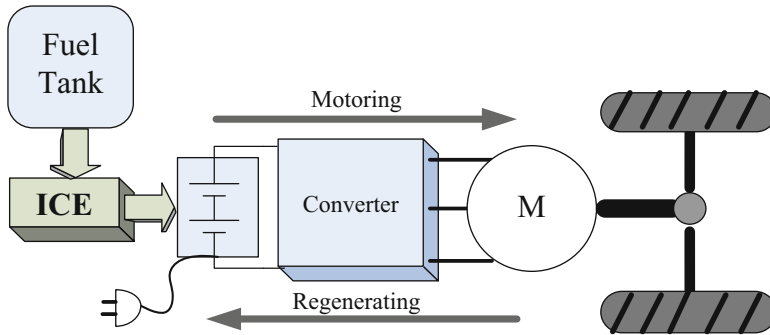**Fig. 3.1** Power system schematic of a plug-in HEV (PHEV)

Fig. 3.2 Block diagram of a typical series PHEV

The proposed SUV employs a lithium-ion battery pack as the onboard energy source, which has a typical energy density of 180 Wh/kg or volumetric energy density of 250 Wh/L. Its price is usually in the range of 3–5 Wh/dollar. Taking the Toyota Highlander and GM Volt as references, on an average, about 15–17 kWh of energy is needed (including regenerative breaking) for driving the first 40 miles in all-electric mode. Here, an important parameter, battery state of charge (SOC), is introduced, to describe the charging state of the battery pack. Due to typical PHEV properties, the upper limit of SOC is 95 % while the lower limit of SOC is 20 %. In other words, only 75 % of the total energy is used and the battery cannot be literally fully charged or completely discharged. Thus, the actual capacity of battery pack is calculated by Eq. (3.1):

$$E_{real} = \frac{E_{req}}{SOC_{hi} - SOC_{low}} \tag{3.1}$$

Here, SOC_{hi} is the battery high SOC and SOC_{low} is the battery low SOC. Hence, the real battery pack range is from 20 to 23.4 kWh.

3.2.3   PV Panel Sizing

Based on the energy requirement, the size of the PV panel, used to charge a PHEV in the worst situation (under minimum solar radiation received during a day), is calculated. The required PV panel size can be proportionally expanded according to the number of vehicles, by simply multiplying the unit PV panel size with the number of vehicles.

A great deal of research with regard to solar power radiation in different areas of Canada has been conducted for years. Reliable data is retrieved from the latest projects for calculation purposes. Figure 3.3 shows the variation of mean daily solar
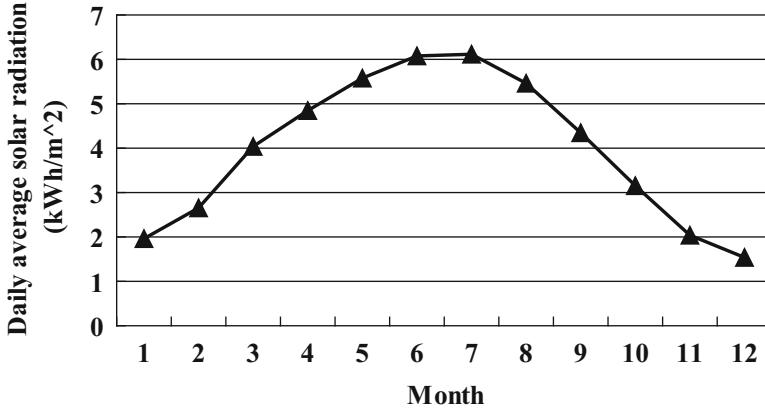
Fig. 3.3 Variation of mean daily solar radiant energy with month in Alberta

radiant energy with respect to each month, in Alberta, which possesses greater solar radiation than many other Canadian cities.

As the required energy (E_{req}) charges the PHEV-40 from low SOC to high SOC, and mean daily radiation (R_{day}) is known, considering the PV array efficiency ($\eta_P V = 15\%$) and DC/DC convert efficiency ($\eta_{DC/DC} = 95\%$), the area of the PV array can be calculated by Eq. (3.2):

$$A = \frac{E_{req}}{R_{day}\eta_{PV}\eta_{DC/DC}} \tag{3.2}$$

It is easy to note from Fig. 3.3 that December is the month with the lowest solar radiation in a year. In contrast, July receives the greatest solar radiant energy. However, in winter, the day hour is considered from 9:00 a.m. to 5:00 p.m., whereas in summer it is from 6:00 a.m. to 8:00 p.m., as shown in Fig. 3.4. By integrating the two curves in Fig. 3.4, it is easy to find that the reduced radiant energy in December is approximately 3/8 of the received solar energy in July. However, since PV can be connected with the grid, one can always charge the battery from the grid with the energy that was injected there before the PHEV arrived in the morning. Therefore, the extra radiant energy in summer from 6:00 a.m. to 9:00 a.m. and 6:00 p.m. to 9:00 p.m. cannot affect the PV panel cost. Consequently, the minimum PV panel size for the best day in a year is 20 m^2.

However, the design should be able to meet the needs in the worst situation. Therefore, the minimum unit PV panel size for all-year operation should take December as a reference, which yields 78 m^2. Keeping the same PV array size in July, the best day, the received solar energy can be used to charge four PHEVs or to inject power into the grid.

In this way, there is no impact on the grid, no fuel expenses, and great perk for the employees. However, there is a cost, which can be reduced in different ways.
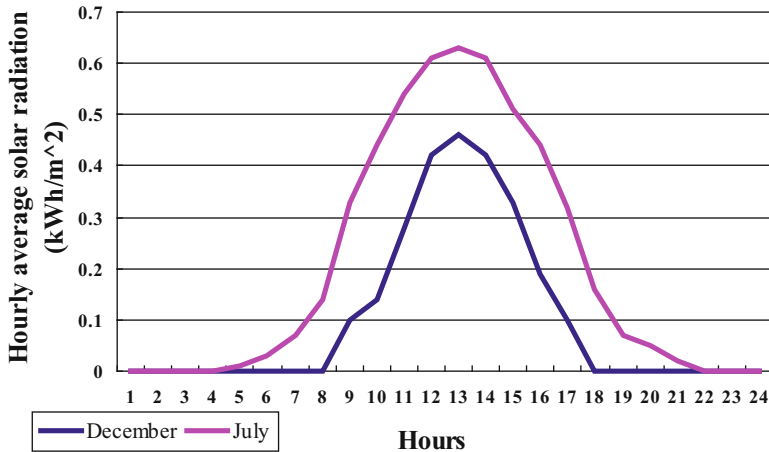
Fig. 3.4 Variation of solar radiant energy with hour

In the next section, different cases are studied to find out the appropriate PV panel size and possible measures to reduce the overall cost.

3.2.4 Case Studies

As mentioned earlier, the typical daily driving mileage in the North America is approximately 35–40 miles. The PHEV-40, if fully charged every day, can cover the daily driving without using any fuel. In this section, the PHEV-40 is compared to different types of vehicles, in order to assess its advantages and disadvantages.

3.2.4.1 Conventional Vehicles

Considering the popular conventional SUV *Highlander* as an example, it employs a 270 hp, 3.5 L, V6 I.E. with an appalling fuel economy of 25 mpg in the city and 35 mpg on highway. The capacity of the fuel tank is 19 gallons, which endows the SUV 475-mile autonomy. Compared to EVs, there is no investment in PV panel installation or maintenance of battery packs. However, the costly fuel and serious environmental problems are the limitations of CVs.

Assuming that a user drives a midsized SUV in a regular manner, the gasoline consumed over 40-mile daily driving is approximately 1.6 gallons. Based on the estimated gasoline price trend, Table 3.1 depicts the estimated average yearly gasoline price and fuel cost in 10 years. The costs incurred due to fuel usage can be saved if the 40-mile daily drive can be replaced by all-electric driving. As the

Table 3.1 Estimated average yearly gasoline price trend (dollar/gallon) and savings on gasoline (dollar)

Year	2007	2008	2009	2010	2011	2012	2013	2014	2015	2016
Estimated average yearly price	2.81	3.22	3.86	4.64	5.80	7.25	9.42	12.24	15.92	22.28
Daily saving	4.50	5.15	6.18	7.42	9.27	11.59	15.07	19.59	25.47	35.65
Yearly saving	1641	1880	2257	2708	3385	4231	5500	7151	9296	13,014

Table 3.2 Typical charging time and energy density of popular battery candidate for EVs

Battery	PbA	Ni-MH	Li-ion	Unit
Charging time	8–10	6–14	5–7	Hours
Energy density	60	80	180	Wh/kg

fuel price increases, the savings on fuel cost will be a justified reason for the consumers to invest in advanced EVs.

Apart from fuel cost, the inefficient operation of ICE, which results in roughly about 15 % overall drive train efficiency, is also not energy-wise. Moreover, from the environmental point of view, a CV emits almost 9 tons CO_2 equivalent greenhouse gas emissions per year, based on 40-mile daily driving. Thus, it is gradually becoming hard for auto manufacturers to meet the stringent requirements of environmental regulations.

3.2.4.2 Pure EVs

A pure EV replaces the petroleum-based CV propulsion system with a pure electric drive train. The commercialized EVs such as the *REVA* and *ZENN* usually employ an AC induction motor with a torque capability of 45–55 Nm at zero speed. As energy sources, they typically use several heavy-duty lead-acid battery packs, with typical sizes of 10–13 kWh, which cost about $7/kWh.

For the purpose of comparison, it is assumed that the electric energy used to drive EVs over the first 40 miles is totally provided by PV. Maintaining the minimum PV cost (20 m^2), as the previously proposed PHEV-40, the users may charge the car at home at their own cost, if further driving distance is needed. Different battery chemistries and their typical charging time from a residential outlet, for 40-mile energy usage, are summarized in Table 3.2. Even though it is the auto industry's preliminary battery, lead-acid (PbA) batteries are out of favor for EV applications, because of its low energy density. In comparison, the nickel-metal hydride (Ni-MH) battery is favored more, because of its higher energy density, shorter charging time, and long life cycle, but it presents an immature recycling system. The lithium-ion (Li-ion) battery chemistry is considered as a definite future trend, but compared to the other two candidates, it has lower durability, which is an issue that needs to be focussed upon.

The performance of commercialized EVs is mainly restrained by the capacity of onboard battery packs. For instance, the *ZENN* can only drive at 25–35 mph and has a limited driving distance with each full charging. In order to have the same performance and autonomy as CVs, the size of battery on an EV has to be at least eight times greater. As is well known, lead-acid battery has the low energy density about 30–40 Wh/kg or 70 Wh/L. As a result, greater vehicle weight and larger space to store battery pack will be accepted neither by the manufacturers nor by the consumers.

3.2.4.3 HEVs

Combining the advantages of CVs and EVs, HEVs are an available alternative to the aforementioned vehicles. Compared to CVs, EVs have higher fuel economy, less GHG emission, and more comfortable driving experience. It is totally disconnected from either PV or the grid. For series HEVs, the onboard ICE works as a generator, to convert the fuel energy to electric energy, when needed. In this way, it ensures that the ICE operates in its maximum efficiency region and provides the vehicle the ability to drive long distances. Consequently, a relatively smaller onboard battery pack can be used, compared to that of pure EVs.

For a mild series hybrid vehicle, the hybridization factor (HF), which is defined as the ratio of the difference between the powers of both the electric motor and the ICE to the power of the electric motor, is no more than 40 %. Assuming that the monitored mild series HEV is driven in a city and highway combined pattern, the sizes of both the ICE and the motor are determined based on the load demands of Fig. 3.5 as well as the HF. Therefore, the sizes of ICE and electric motor are 75 kW
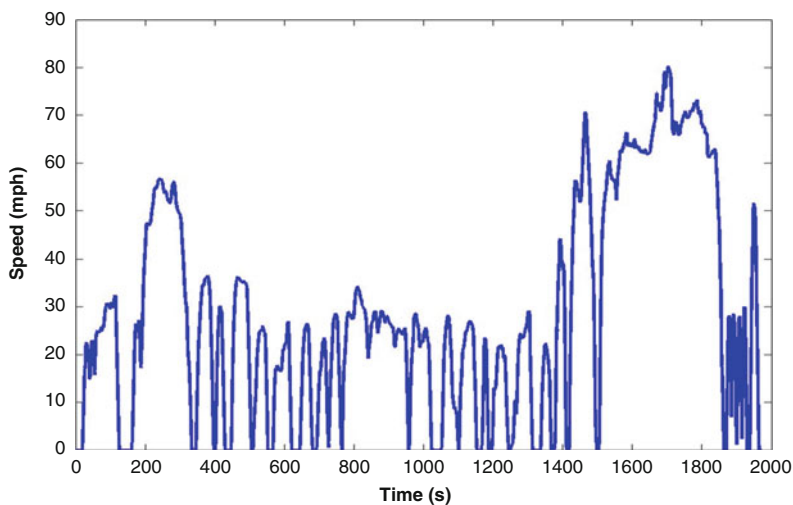

Fig. 3.5 City and highway combined driving schedule (UDDS + HWFET = urban dynamometer driving schedule, also known as FUDS—federal urban driving schedule + highway fuel economy test)

and 125 kW (continuous power), respectively. As the favored battery of the HEV industry, the 25-module NiMH-60, which has a rated voltage of 335 V, 60 A peak current, and 316 kg weight (with 6 kWh stored energy), is used for the abovementioned HEV [].

Unlike the PV-based PHEV, charging from the grid eliminates the limitation of charging from PV. However, charging from grid will be a problem as the number of PHEV users grow. In addition, HEVs save the cost of PV panel, electricity, and huge battery pack, but incurs gasoline costs. The essential difference between an HEV and the proposed PHEV-40 is that more gasoline is involved in the activities of HEVs. 1.3 gallons of gasoline is needed for the 40-mile daily driving for 30 mpg fuel economy. Also, GHG emission, environmental issues, and the increasing gasoline price are the major drawbacks in this case.

3.2.4.4 Grid PHEVs

Simply, an HEV that can be pre-charged from the grid is termed as a PHEV. As one of the HEV families, an advanced attribute of the PHEV is that the control strategy guarantees the usage of electric energy, and is the first priority. Fuel is only used for further traveling after electric energy is drained out. Considering the same battery as that for the HEV, fully charging the battery takes almost 8 h from a conventional residential power outlet. Driving PHEVs in places, such as Montreal and Vancouver, where electricity rates are among the lowest in the world, fully charging the battery only costs approximately $9. However, by employing the aforementioned battery, when fully charged, it is only capable of driving almost 25 miles in all-electric mode. For this reason, either a two times greater onboard battery pack needs to be installed, or the vehicle needs to run in an electric-fuel combined pattern for 40-mile daily driving. In the latter case, based on the above analysis, driving 40 miles per day in Montreal needs two more dollars for gasoline, which is more economic and more environmentally friendly than driving HEVs. However, apart from the fuel cost, GHG emission cannot be eliminated since it is only a half ZEV and if the utility is using thermal generation, charging PHEV from grid eventually contributes to GHG emission.

3.2.4.5 PV-Grid PHEVs

The best solution from both the environmental and fuel economy points of view is that the PHEV can be fully or partially charged regularly from a renewable energy source. For example, when charging with solar energy, the user drives the car to work in the morning and back in the evening. Hence, the vehicle can be charged during the day.

Keeping the same size of PHEV as that in previous sections, the first case (case 1) presented here is that a large PV panel is needed to guarantee the ability of fully charging a PHEV all year long. Thus, the PV panel is designed based on the worst

situation of a year. As mentioned earlier in the chapter, 78 m^2 is required for charging a PHEV all year long.

Also, the proposed PHEV-40 is armed with a 23.4 kWh Li-ion battery pack, used to store the 17 kWh electric energy, which can be used to satisfy 40 miles of daily driving. In summer, the surplus solar energy can be injected into the grid. During the best days of the year, the surplus energy generated by the 78 m^2 solar panel is 67 kWh. This is able to create at least $4.6 revenue per day in Montreal, or $22.1 per day in New York City.

From the vehicle point of view, the onboard battery would be the major element that needs to be considered into cost. However, benefit of driving a PHEV-40 is irresistible, such as no fuel cost over regular daily driving, zero greenhouse gas (GHG) emission in pure electric mode, and comfortable driving experience.

The second case (case 2) presented here is that the PV panel is designed based on the best day of the year, which means that the PHEV can only be fully charged for 40-mile daily driving during the sunniest day of the year. In this way, as described in the second section of this chapter, one can obtain the minimum PV panel size, which is 20 m^2. Keeping the same onboard battery capacity as in previous case, a PHEV is able to operate as the normal pure PV-based PHEV-40 in July, but as the solar radiation decreases during rest of the year, the PHEV needs to be charged from grid. Table 3.3 lists the average daily solar-generated energy with respect to the month, based on the minimum PV panel design. Assuming that users need 40-mile daily driving, it is clear to see that in the worst situation, only 4.3 kWh is generated and therefore the remaining 12.7 kWh needs to be charged from grid. Only in June and July can surplus energy be generated, and in the worst case of December, user needs to pay $0.9 for charging from the grid.

In summer, a vehicle can be fully charged by PV, and charged by both PV and grid when solar radiation is not satisfied. It reduces the impact of PHEVs on the power grid as well as helps companies reduce the costs on energy saving. However, from the PV panel's point of view, the second case saves the cost of PV modules. The typical lowest cost of solar modules as of May 2008 is approximately $4.9 CAD/W. For case 1, when solar power is designed based on the worst day of the year, the initial cost for PV panel would be almost $20,000. For the latter case, the initial cost for PV panel is only $10,000. However, for the first case, surplus energy can be injected into grid, to balance the final cost. It is important to note that the solar electricity sales rate in May 2007 was 27.33 cents/kWh, assuming that users fully charge their vehicles for 40-mile driving every day and use PV as first priority. Table 3.4 elaborates the operation costs for the two above cases during a year. Apparently, case 1 suppresses case 2.

Table 3.3 Average daily solar energy with month in kWh

Month	January	February	March	July	August	September
Generated PV energy	5.56	8.31	11.54	17.40	15.53	12.41
Month	April	May	June	October	November	December
Generated PV energy	13.85	15.90	17.31	8.95	5.86	4.37

Table 3.4 Final operation costs during a year

Month	January		February		March		April		Total grid electricity sales (dollars)	
	Case 1	Case 2	Case 1	Case 2	Case 1	Case 2	Case 1	Case 2	Case 1	Case 2
Generated PV energy	21.67	5.56	29.45	8.31	45.02	11.54	54.02	13.85	2662.10	−241.43
Energy injected (+) or drawn (−) from grid	4.67	−11.44	12.45	−8.69	28.02	−5.46	37.02	−3.15		

Month	May		June		July		August		Total grid electricity sales (dollars)	
	Case 1	Case 2	Case 1	Case 2	Case 1	Case 2	Case 1	Case 2	Case 1	Case 2
Generated PV energy	62.02	15.90	67.52	17.31	67.86	17.40	60.58	15.53	6309.21	−15.94
Energy injected (+) or drawn (−) from grid	45.02	−1.10	50.52	0.31	50.86	0.40	43.58	−1.47		

Month	September		October		November		December		Total grid electricity sales (dollars)	
	Case 1	Case 2	Case 1	Case 2	Case 1	Case 2	Case 1	Case 2	Case 1	Case 2
Generated PV energy	48.46	12.41	34.90	8.95	22.84	5.86	17.06	4.37	1820.44	−310.92
Energy injected (+) or drawn (−) from grid	31.46	−4.59	17.90	−8.05	5.84	−11.14	0.06	−12.63		

	Case 1	Case 2
Total solar energy sales during a year (solar electricity sale rates: $0.27/kWh)	10,791.75	−568.29
Initial PV panel cost	20,781.23	5328.52
Final cost during a year operation	9989	5897

[a]Grid electricity rates: $0.07/kWh (based on Montreal market)

It is critical to note that although the proposed PV-based PHEV needs the investment for the solar panel integration with buildings, the enormous environmental impact is non-negligible. Moreover, as the years go by, it is easy to notice that the full-size design in the former case presents a more promising future, due to the feature of injecting energy into the grid rather than only drawing energy. In addition, energy storage systems with higher energy densities, such as ultracapacitors and flywheels, also provide the PHEV the ability to drive as a ZEV for a longer distance.

In general, Table 3.5 briefly summarizes the key elements compared in the above analyses. As shown in Table 3.5, the potential of PHEVs is definitely very promising.

3.3 Opportunities and Challenges for Photovoltaic-Based EVSEs

3.3.1 Introduction

As different electrical sources, loads, and storage devices have different characteristics, power electronics plays a key role in reliable and efficient operation of electrical systems. Power electronics have dramatically developed over the previous decades in different aspects such as speed, reliability, performance, and control. Besides, enormous effort has been put into development in different areas of power electronics such as novel converter topologies, converter control and modeling, and power flow management to improve the performance, increase the efficiency, and reduce the cost of power converters. Without reliable and low-cost power converters, deployment of renewable energy sources for residential and industrial applications is impossible. Power electronic converter systems can be categorized based on different criteria. For single-input single-output converters power flow is a general criterion for classification which leads to two important classes, namely, unidirectional converters and bidirectional converters. Multi-input single-output, single-input multi-output, and multi-input multi-output converters are generally classified under multiport converter category.

For the EV/PHEV battery pack charger application using solar energy, PV panels are not used to charge the battery pack directly because of the intermittent nature of renewable sources. This is because of the necessity of the presence of enough power during the charging process. If the PV panels are directly connected to battery pack using an MPPT stage, when the required power by the battery pack is more than the available power from the PV panels, the battery pack cannot be charged based on the specified charging algorithm by the manufacturer. This will lead to battery degradation and reduced life cycle over time and also prolonged charging times which is not acceptable for users. Due to this fact, what is being applied in solar charging stations currently is injecting the available power from PV

Table 3.5 Summary of cost comparison

Vehicles		PV size (m²)	Battery pack (kWh)	Estimated fuel economy per 40 miles	GHG emission	Motor size	Engine size	Equivalent ZEV driving rang/charge (miles)	Fuel equivalent price/mile
CV		0	N/A	1.6 gallons	9 tons per year	N/A	200 kW @ 5600 rpm	0	$0.13/mile
EV		0	17	No fuel usage	ZEV	200 kW continuous	N/A	30	$0.04/mile
HEV		0	6	1.2 gallons	6.4 tons per year	125 kW continuous	75 kW @ 5600 rpm	14	$0.09/mile
Grid PHEV		0	23	No fuel usage	ZEV	125 kW continuous	75 kW @ 5600 rpm	40	$0.04/mile
PV-grid PHEV	Case 1	78	23	No fuel usage	ZEV	125 kW continuous	75 kW @ 5600 rpm	40	$0/mile
	Case 2	20	23	No fuel usage	ZEV	125 kW continuous	75 kW @ 5600 rpm	40	$0.02/mile

[a]Electricity prices are based on the electricity rates in Montreal

panels to the grid using inverters and charging the battery packs from the grid separately which can be considered an infinite source providing any amount of required power to the load. Using this method is like using the grid as a storage device which stores power from PV panels when available and delivers power to the load when required, specifically if the charging process does not coincide solar irradiation. This configuration has some problems or may cause some other problems for the grid in future. First, all of the injected power from the PV panels to the grid will not necessarily enter the battery pack and may flow through other paths and other loads far from the source which involves electric losses. In some cases the generation plant and charger can be very far from each other which will lead to lots of electrical losses in the transforming cables. Second, if the number of these charging stations increases a lot over time, assuming that each house installs a solar charger and they all utilize the grid as storage, this can cause problems for the stability of the grid. What author has in mind is to propose a structure which forces the available power from PV panels to enter the battery pack directly and obtain the remaining required power from the grid simultaneously.

3.3.2 Solar Maximum Power Point Tracking for EV/PHEV Battery Charging

Solar energy is one of the most interesting types of renewable energy because of relatively well-established technology and efficiency enhancement every day with great efforts towards higher performance photovoltaic (PV) panels. However, nonlinearity of PV panel characteristics and their dependence on atmospheric conditions such as sunlight irradiance level and temperature variations need a maximum power point tracking (MPPT) unit, which is usually a converter to track the maximum power to ensure maximum efficiency of the system. Direct connection of PV panels to the load involves oversizing the panels to ensure load supply or in other words increased loss of the whole system. A typical PV panel characteristic is plotted in Fig. 3.6.
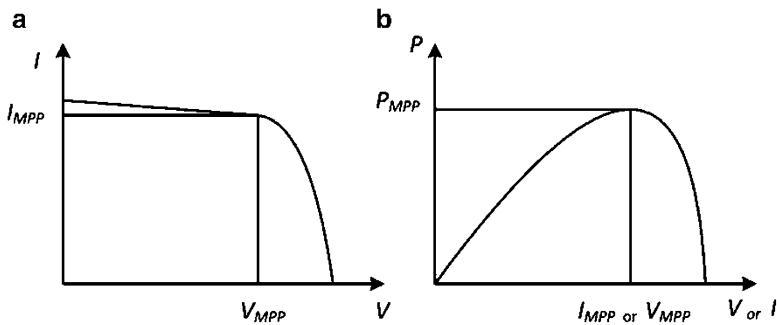
Fig. 3.6 Typical photovoltaic cell characteristics: (**a**) *I–V* curve and (**b**) *P–V* or *P–I* curve

In general, the task of MPPT technique is to automatically shift the operating point to the maximum power point. There are numerous techniques in the literature. They may be categorized in different ways. In [5] MPPT methods are classified into two major groups based on the size of the system: (1) large-scale PV systems which utilize digital signal processors (DSP) and (2) small-scale PV systems which do not use DSP-based methods. However, based on operation principles MPPT methods can be divided into various categories [6]: (1) hill climbing/P&O, (2) incremental conductance, (3) fractional open-circuit voltage, (4) fractional short-circuit current, (5) fuzzy logic control, (6) neural network, (7) ripple correlation control (RCC), (8) current sweep, (9) DC-link capacitor droop control, (10) load current or load voltage maximization, (11) dP/dV or dP/dI feedback control, (12) array reconfiguration, (13) mathematical calculation of MPP, (14) state-based MPPT, (15) best fixed voltage (BFV) algorithm, (16) linear reoriented coordinates method (LRCM), etc. All these methods are summarized and briefly described in [6] along with their major characteristics such as PV array dependence, true or approximate MPPT, analog or digital implementation, periodic tuning, convergence speed, implementation complexity, and sensed parameters. Based on MPPT technique characteristics, one or more types are more suitable for a specific application.

One of the most common applications is battery charging which may be the main purpose of the whole PV system such as PHEV battery pack charger (stand-alone system), or a subsidiary part of the PV system as an energy storage element for storing extra energy produced, such as power injection to the grid in distributed generation systems (grid-connected system). A novel MPPT algorithm is introduced in this chapter and the first scenario is of interest of this thesis. However, this technique can be easily applied to more complex PV systems [7]. According to [8] among single-pole double-switch converters, the buck-boost converter has the highest energy conversion efficiency; however, since our goal here is not to investigate the energy conversion efficiency of the proposed algorithm among different topologies, we have chosen a simple buck converter as the MPPT stage just to prove the validity of the proposed algorithm. However, this algorithm is independent of the converter topology as will be described later. As concluded in [9] the MPPT can be achieved only with sensing one of the output variables, output voltage or output current. This method mainly falls into load current maximization category, however, with some advantages such as independence from circuit topology and high degree of simplicity of low-level controller. Besides, it can be easily implemented using low-cost analog circuits with low implementation complexity.

3.3.3 Power Electronics Interface

3.3.3.1 Conventional Structures of PV Systems

In this section, we have an overview on the existing PV structures. A general PV system consists of PV panels, power converters, filters, controllers, and electrical load or power system. Different configurations can be utilized to convert solar
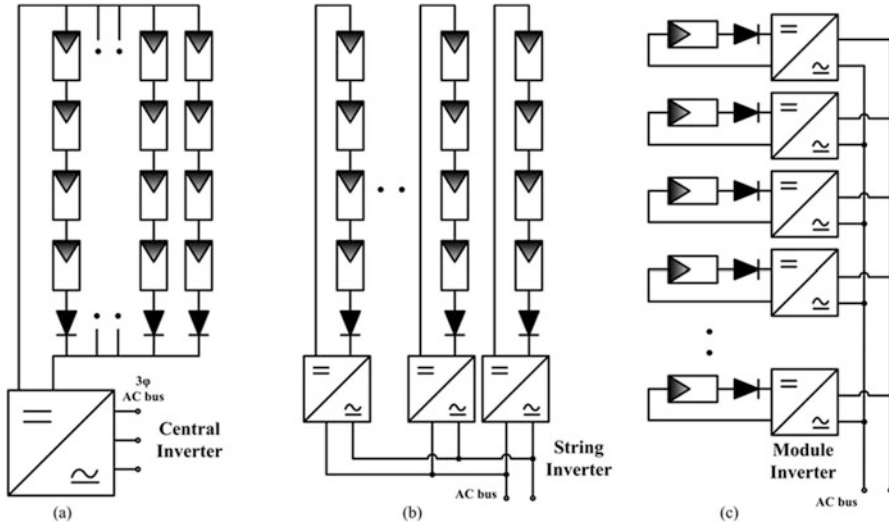
Fig. 3.7 Conventional PV structures: (**a**) Central inverter, (**b**) string inverter, and (**c**) module inverter

power to processed electrical power. They are mainly [10] (a) central inverters, (b) string inverters, and (c) module-integrated inverters as shown in Fig. 3.6. It is important to understand various inverters so as to implement them in the

In Fig. 3.7 the converters are shown as DC–AC inverters. However, they do not have to be necessarily an inverter. They can also be DC–DC converters implementing MPPT based on the nature of the load, coupling of sources, or power system connected to the other side.

3.3.3.2 Central Inverters

In this configuration (usually for more than 10 kW), some PV strings are paralleled and connected to a single converter. This has some advantages and some disadvantages. According to initial and maintenance cost, it is beneficial because of single converter. On the other side, this topology has lower efficiency compared to others because of inherent characteristic mismatch among different PV panels. In addition, partial shading in this case cannot be handled in an efficient manner [11]. After all, according to reliability point of view, this configuration is not reliable, since failure of the converter will result in failure of the whole system.

3.3.3.3 String Inverters

As depicted in Fig. 3.7b in the case of string inverters, the whole PV arrays are divided into parallel strings of series connected PV panels and each string is connected to a singular converter. This increases the whole energy harvested

Fig. 3.8 Multi-string
inverter structure
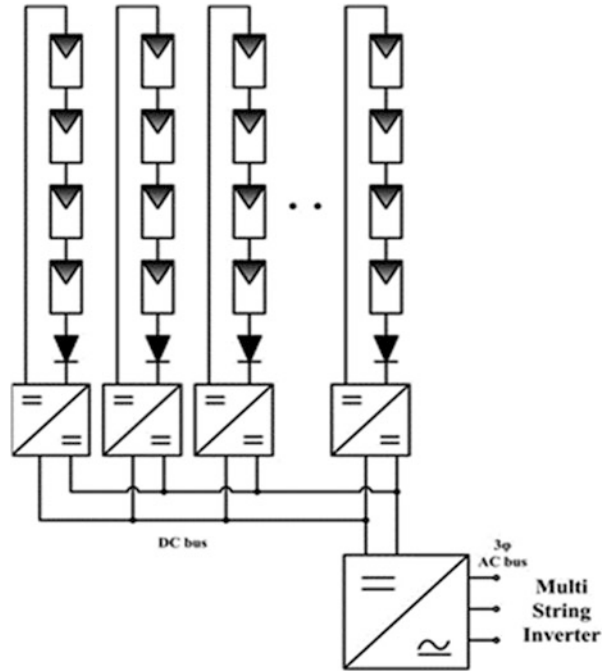
from solar energy due to better and more accurate MPPT capability, since each
string is controlled separately and partial shading and PV panel mismatch can be
considered in a more efficient manner. Because of utilization of multiple converters
the whole system has higher reliability compared to centralized configuration.

A subclass of string converters exists and is called multi-string inverters. In this
category a DC–DC converter is utilized for each string and finally only one DC–AC
inverter is used for conversion to AC as shown in Fig. 3.8. This configuration
combines the benefits of both string and centralized configurations. This multi-
string topology allows the integration of different technologies of PV panel strings
and also different orientations. The typical operating power range of multi-string
topology is 3–10 kW.

3.3.3.4   Module-Integrated Inverters

This configuration uses one converter for each PV panel and according to energy
point of view the maximum possible electrical energy is harvested out of each panel
because of implementing MPPT at panel level. This eliminates the losses due to
panel mismatch. This system has a very high reliability; however, maintenance
procedure is very complicated. Although this configuration is very costly at the
moment, some researchers believe that according to progressing technology of
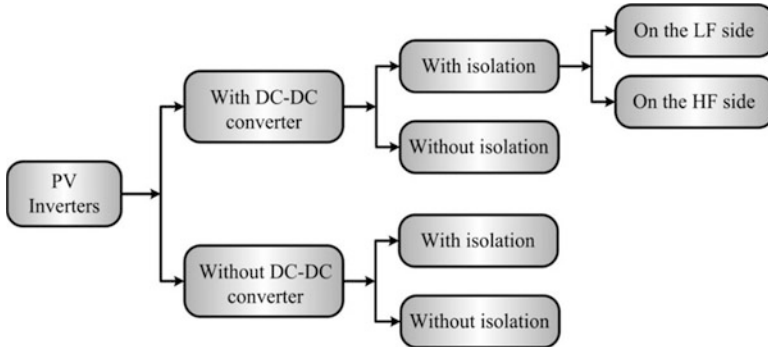
Fig. 3.9 Power configurations for PV inverters

packaging and everyday decreasing price of semiconductors, this topology will be the most suitable one for the future of PV plants according to modularity and plug and play capability.

3.3.4 Topologies for PV Inverters

During recent years PV inverter technologies have evolved increasingly [12]. There are various power configurations possible. These can be summarized as shown in Fig. 3.9.

Using or not using a DC–DC converter depends on the configuration of PV panels and number of PV panels in series. If the number of PV panels in series is high enough to produce higher voltage than load-side voltage for most of the times the use of a boost DC–DC converter can be avoided. The isolation depends on the safety standards and requirements.

3.3.4.1 PV Inverters with DC–DC Converter and Isolation

Isolation is usually achieved using a transformer. This transformer can be on the low-frequency (LF) side (Fig. 3.10a) or interleaved in the high-frequency (HF) side (Fig. 3.10b) which is an intermediate AC stage. The second configuration is smaller and lighter due to smaller transformer; however, transformer should be of higher quality because of higher losses.

3.3.4.2 PV Inverters with DC–DC Converter and Without Isolation

Depending on the safety regulations, if isolation is not mandatory the transformer can be eliminated and a more simple system will be achieved as shown in Fig. 3.11.
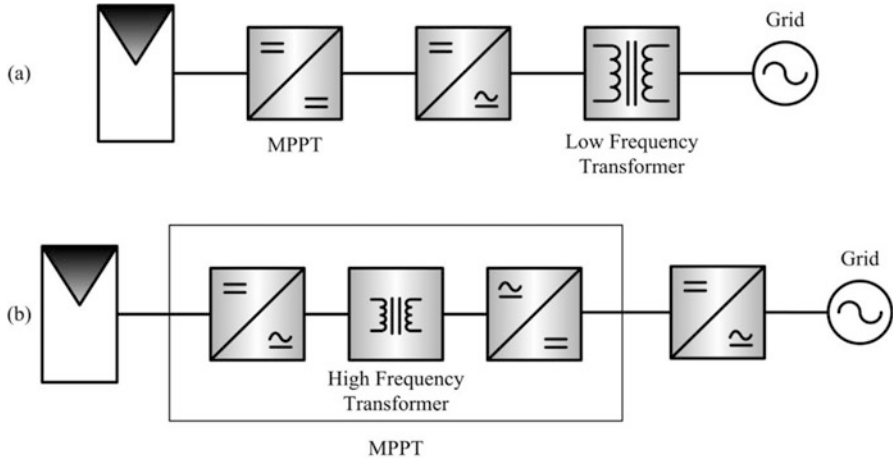
Fig. 3.10 PV inverter configurations with DC–DC converter and isolation: (**a**) Transformer on LF side and (**b**) transformer on HF side
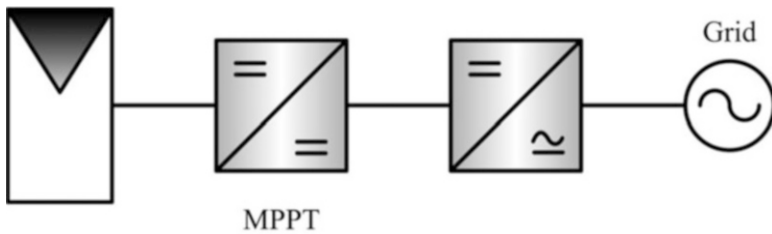
Fig. 3.11 PV inverter configuration with DC–DC converter and without isolation

3.3.4.3 PV Inverters Without DC–DC Converter and with Isolation

Eliminating the DC–DC converter stage and using only the DC–AC inverter involve MPPT and inversion stages to be integrated resulting in a more complex control algorithm. Besides, since the transformer is on the low-frequency side it is bigger and heavier. A typical block diagram of this configuration is illustrated in Fig. 3.12.

3.3.4.4 PV Inverters Without DC–DC Converters and Without Isolation

This configuration is the simplest configuration possible and at the same time has the least reliability comparing to its counterparts. Any fault in the source side or load side can easily expand to the other side and endanger the operation of the system. So an efficient protection system is required. Besides, any DC current can
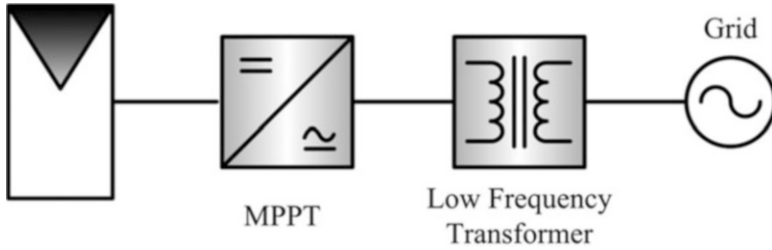
Fig. 3.12 PV inverter configuration without DC–DC converter and with isolation

Fig. 3.13 PV Inverter configuration without DC–DC converter and without isolation
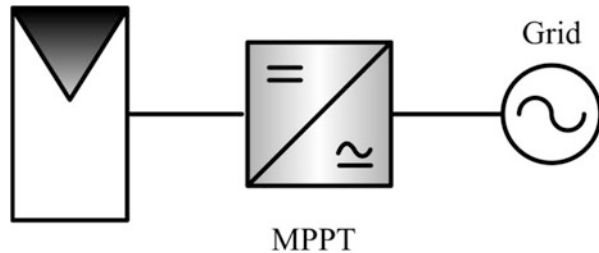
be injected to the load or power system side. This configuration can be utilized if the number of PV panels in series is high enough to produce a voltage higher than AC-side voltage level. This configuration is shown in Fig. 3.13.

3.3.4.5 Possible PV Interconnection Schemes

Comparing output power and energy results from PV systems obtained using simulations during design stages with the real experimental results over the previous decades has exposed a significant difference [13]. This is due to numerous reasons, one of which is mismatch losses. Mismatch losses are mainly constituted of two main reasons [14–19]. The first reason is dispersion of electrical properties and nonuniform PV cell illumination among the array. This is mainly due to the manufacturer's tolerances or degradation processes. The other important reason is partial shading of the PV array and variation of the tilt angles of different PV panels. Test results from various commercially available inverters show that the power loss due to partial shading can be as high as 70 % [19]. If partial shading happens in a PV array or different PV panels with different angles are connected to one converter this will cause the power versus voltage/current characteristics of the PV array to have multiple local maximum point as shown in Fig. 4.8; however only one of them is the global peak (GP) [20].

The existence of such local maximums can cause some MPPT techniques especially perturb and observe (P&O) or incremental conductance methods to fail tracking the global maximum point ($P_{max,2}$ in Fig. 3.14). Eliminating or reducing
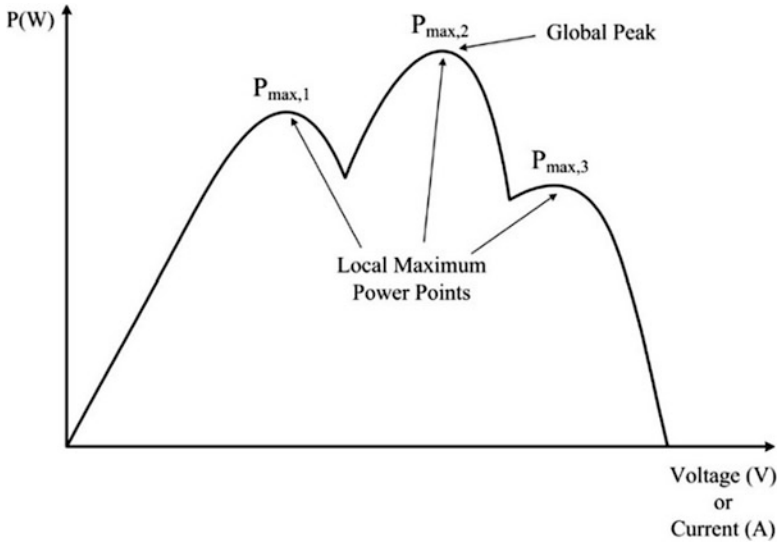
Fig. 3.14 A typical *P*–*V* curve of a partially shaded PV array

this power loss resulting from mismatch of panels or different tilt angles can be performed by utilizing more efficient MPPT techniques, adding more converters or static/dynamic reorganizing cell/module connections. The usual interconnection of panels is connecting them in series and making strings of cells and paralleling the strings as was previously shown in Figs. 3.6 and 3.7. This interconnection is called series–parallel (SP). Other cell interconnections have been proposed which can reduce the mismatch power loss [14–16, 21–23]. They are called total cross-tied (TCT) and bridge-link (BL). They are shown in Fig. 3.15.

3.3.4.6 Latest Research and New Proposed Topologies

The system diagram of the proposed structure is depicted in Fig. 3.16. This configuration has some advantages. First, the PV power can be directly injected to the battery pack and not to the grid and then from the grid to the load which reduces the overall losses. Second, this configuration provides great flexibility for different power flows. Depending on the amount of available power from PV panels and required power by the battery pack, different modes of operation may happen.

If available power from PV is more than the required power for charging the battery pack the remaining can be injected to the grid (mode 1). If PV power is not enough, grid will be involved to supply the remaining power (mode 2). If there is no power available from the PV panels battery pack can be charged solely by the grid (mode 3). If the battery pack is not connected to the system, PV power can be injected to the grid to reduce the electricity bill of the house (mode 4). If needed, the battery pack can be discharged to the grid during specified times performing as a configuration supporting vehicle to grid (V2G) (mode 5). Even in the case of
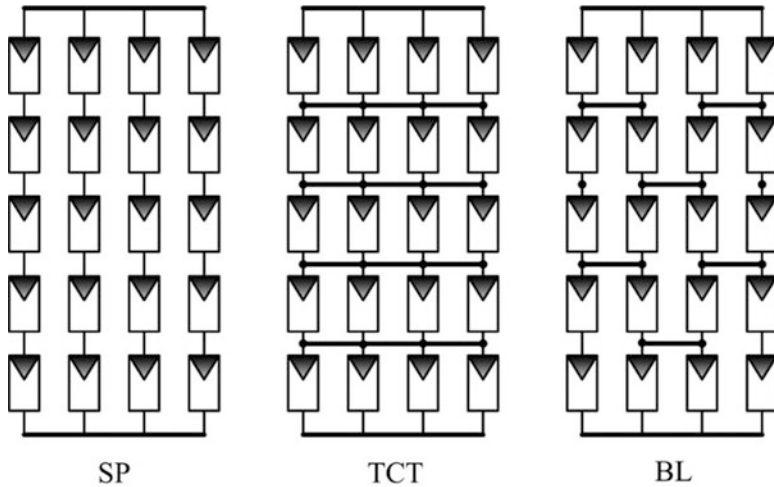
Fig. 3.15 Different cell interconnections: series–parallel (SP), total cross-tied (TCT), and bridge-link (BL)
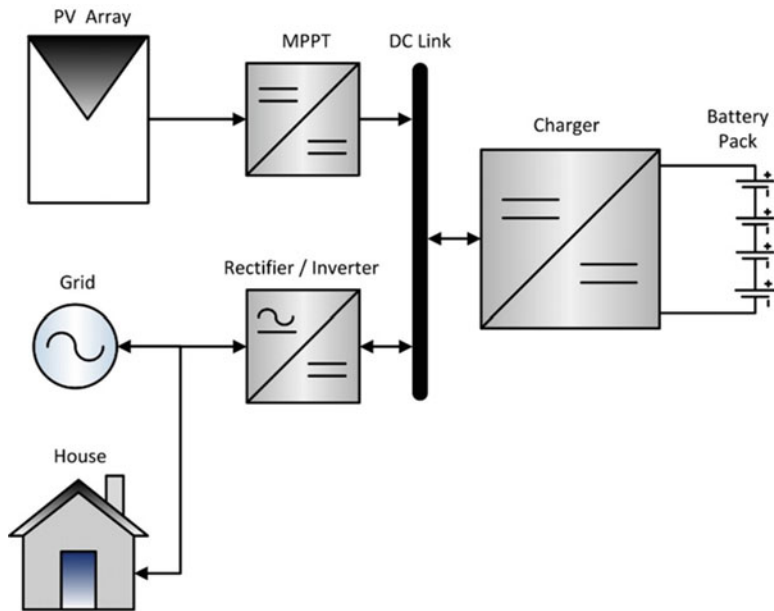

Fig. 3.16 System structure

blackouts the battery pack can perform as an energy source and supply the power to the house for some time depending on the battery pack capacity (mode 6). This flexibility in power flows and modes of operation facilitates implementing concepts like smart grid. Different modes of operation are illustrated in Fig. 3.17.
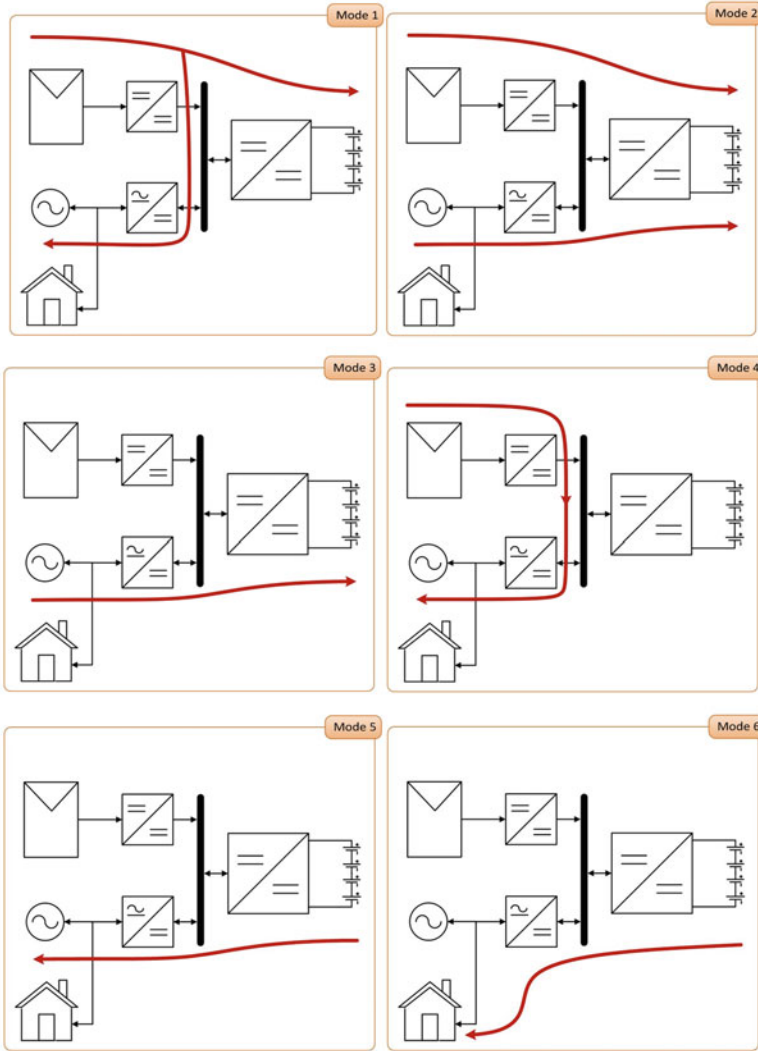
Fig. 3.17 Modes of operation

3.4 Renewable Energy and Electric Mobility into the Smart Grid: Enabling Factors Towards Sustainability

3.4.1 Introduction

Solar electricity which can be obtained using photovoltaic panels is one of the easiest ways as long as sun is available. They can be easily mounted on the roofs of

buildings or rooftops of parking slots generating electric power to charge the battery pack of the EVs while providing shade for the cars. Since solar energy is intermittent and variable, power grid should be involved to ensure that enough power is available. Conventional solar chargers inject power to the grid and use grid as the main source because of its reliability and being infinite. Hence, they use grid as a kind of energy storage system. This approach can lead to problems for grid stability if solar panels are utilized in large scale and comparable to the grid.

Earth temperature has risen by 1.1–1.6 °F over the past century as assessments by Intergovernmental Panel on Climate Change (IPCC) show. This has caused noticeable climate change evidences such as ice mass loss and decreasing snow cover in both the northern and southern hemispheres, rising sea levels, more frequent extreme weather events, floods, more sever tropical storms and hurricanes, volcanoes, acidification of oceans, and much more. These are all due to increased greenhouse gases made by human activities. Since large-scale industrialization began around 150 years ago, levels of several important greenhouse gases have increased by about 40 %. Fossil fuels constitute around three-fourth of human-made emissions during the past 20 years. Some of the emitted greenhouse gases can be absorbed by natural processes happening in the nature but the remaining will be added to the atmosphere. On an annual average basis, 7.2 billion metric tons of greenhouse gases are produced each year, 4.1 billion metric tons of which are added to the atmosphere annually. The process which increases the earth temperature can be simply described by extra absorption of radiations coming from the sun by additional greenhouse gases made by human activities and converting them to heat.

Greenhouse gas emissions include different types of gases, each of which includes a portion of the total emissions. Considering the USA, a highly industrial country emitting large amounts of pollutants each year as an example, the latest available data provided by U.S. Energy Information Administration (EIA) shows that carbon dioxide (CO_2) emissions constitute 81.5 % of total gas emissions in the USA as shown in Fig. 3.18. Other gases include methane, nitrous oxide, fluorinated gases, and other carbon dioxide gases constituting 11.1 %, 3.3 %, 2.7 %, and 1.3 %, respectively. According to the big portion of CO_2 emissions the sources of this gas
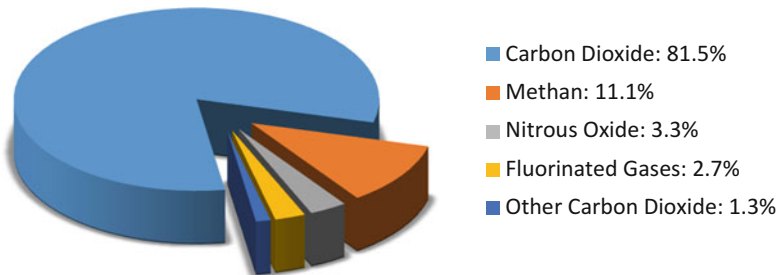

U.S. Greenhouse Gas Emissions, 2009

- Carbon Dioxide: 81.5%
- Methan: 11.1%
- Nitrous Oxide: 3.3%
- Fluorinated Gases: 2.7%
- Other Carbon Dioxide: 1.3%

Fig. 3.18 US greenhouse gas emissions by gas type

U.S. Energy-Related Carbon Dioxide Emissions by Major Fuel, 2011
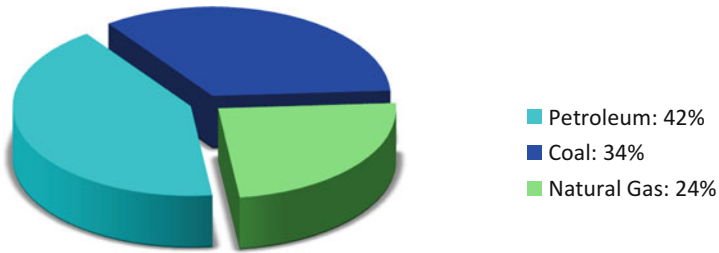

■ Petroleum: 42%

■ Coal: 34%

■ Natural Gas: 24%

Fig. 3.19 US energy-related carbon dioxide emissions by major fuel, 2011

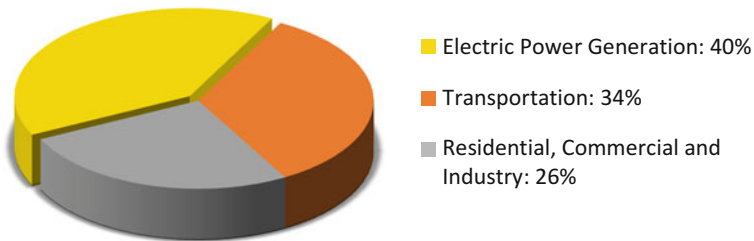**U.S. Energy-Related Carbon Dioxide Emissions by Sector, 2011**

■ Electric Power Generation: 40%

■ Transportation: 34%

■ Residential, Commercial and Industry: 26%

Fig. 3.20 US energy-related carbon dioxide emissions by sector fuel, 2011

should be considered. The biggest carbon dioxide-emitting sector in the USA is the energy sector. About 87 % of the total amount of US greenhouse gases emitted in 2010 has been energy related and 91 % of those energy-related gases have been carbon dioxide from the combustion of fossil fuels.

Main energy-related fossil fuels used in the USA are petroleum, coal, and natural gas as depicted in Fig. 3.19. The major fuels are used in different sectors of the US economy, each one contributing to the greenhouse gas emissions. Electric power generation is the biggest part emitting 40 % of the total carbon dioxide and transportation stays on the second level with 34 % as illustrated in Fig. 3.20. The remaining is due to the direct use of fossil fuels in residential and commercial buildings and by industry. Emissions by electric power generation and transportation section together have increased at an average rate of 0.8 % per year in the period of 1990–2011.

Related literature [1, 2] by L. Eudy and A. Burke firmly states that by the year 2018, the market share of PHEVs will increase to about 25 %. Based on this data, the additional electric energy demanded from the distribution grid for five million PHEVs would be roughly about 50 GWh per day. The typical charging time would be 7–8 h, which might make it hard to accommodate these additional loads in the load curve without increasing the peak load. Also, the required additional charging energy would have a possible impact on the utility system. Expanding the electric

system the conventional way, with large generating plants located far from the load centers, would require upgrading the transmission and distribution systems too. Besides the high costs, this can take many years before obtaining the right-of-way. Alternatively, smaller power plants based on renewable energy, such as solar energy, can be installed in a fraction of that time on the distribution system, which is commonly referred to as "distributed generation (DG)." Photovoltaic (PV) presents a modular characteristic and can be easily deployed in the roof top and facades of residences and buildings. Many corporations are adopting the green approach for distributed energy generation. For instance, *Google* has installed 9 MWh per day of PV on its headquarters, Googolplex, in Mountain View, California. At the moment, it is connected to Mountain View's section of electricity grid. Alternatively, it could be used for charging PHEVs during work hours, being a great perk for environmentally concerned employees. The energy stored in the batteries could also be used for backup during faults. In Canada, the latest projections (2000) indicated that by 2010, renewable DG sources will represent at least 5 % of the total energy produced and 20 % of cogeneration, from the actual figures of 1 % and 4 %, respectively. Therefore, from the environment point of view, charging PHEVs with solar power will be the most attractive solution.

3.4.2 Smart Grid and EVs/PHEVs

3.4.2.1 Grid-Tied Infrastructure

Assuming that fast charging through direct DC connection becomes the method of choice, car owners will have two options. They may still prefer to slow-charge their vehicles overnight by plugging it into an AC–DC charger (or electric vehicle supply equipment: EVSE), most probably in their homes. This converter will deliver relatively low power of the order of 5–10 kW because of the limitations of the residential connection, as mentioned earlier. However, as further explained in Sect. 15.5, this method might involve some financial returns. The alternative method will be to use a fast-charging public facility, corresponding to a familiar service gas station that is capable of multi-megawatt power transfers. Although the cost per kWh will be high, the owner benefits from charge times in the order of minutes rather than hours.

In both cases, V2G capability enabled by smart grid technology will become a standard feature with all EVSEs, whether they are public, commercial, semipublic, or private. This will allow the subsistence of a very significant distributed storage resource at the disposal of electric utilities. More specifically, the PEV fleet will be optimally positioned to become a significant provider of some ancillary services and play a role in offering dispatchable peak power. These services to the electricity supplier will be analyzed separately.

3.4.2.2 PEVs as "Peakers"

A peaker is a small but nimble generating unit that can supply the grid with relatively fast response. Historically, natural gas turbines or small hydroelectric plants were the devices of choice for this task. They are active for only a few hours every day and therefore provide only limited energy. Thus, a substantial fleet of PEVs can carry out this task as a highly distributed resource without significantly depleting their batteries. Unfortunately, as long as peak power is not considered a "service," the utility operator will compensate the car owner solely for the energy sold, albeit at a higher peak demand rate [24]. This might not constitute a strong incentive to the car owner who has to consider other factors, such as the additional battery and power electronics wear and tear, for his or her vehicle. Nevertheless, future adjustments in energy market models are understood to address this among many other issues.

3.4.2.3 PEVs as Spinning and Non-spinning Reserve

One of the most lucrative ancillary services is the spinning and non-spinning reserve. The former consists of generators that are online, but normally run at very low capacity. In the case of a disruption, such as a failure in base load generation or transmission, these generators are commanded to provide the missing power. They must be able to ramp up in less than 10 min and provide power for as long as 1 h or more. Non-spinning reserves are not online and are required to ramp up to full power within 30 min. Because this is a service, the utility company will pay for the availability of the power as well as its amount. In fact, this service is paid even when no power is ever delivered. A PEV owner can provide this service naturally and be reimbursed starting at the time he or she plugs his or her vehicle into the grid, even if the battery is never discharged. Additionally, it must be noted that PHEVs have smaller battery capacity than AEVs, but contain an ICE that can be started on a V2G command to generate electricity and function as a spinning reserve as well.

3.4.2.4 PEVs as Voltage/Frequency Regulation Agents

An ancillary service that is even better tailored for PEVs is regulation. It consists of delivering or absorbing limited amounts of energy on demand and in real time. Normally, the request is automated in order to match exactly the instantaneous power generation with the instantaneous load. Failure to do so results in dangerous shifts in line frequency and voltage. The dispatched amount of energy has short duration, only of the order of a few minutes, but it is requested relatively frequently. Therefore, this is a continuous service. It is important to underline that the amount of energy involved is relatively small and changes direction quite rapidly and

regularly, implying minimal PEV battery discharge for any reasonably short time interval. The near-instantaneous response time and the distributed nature of the PEV fleet explain why regulation is probably the most competitive application for V2G from the point of view of the utility operators.

3.4.2.5   PEVs as Reactive Power Providers [25]

Most electronic topologies used for the inverter/rectifier function in the interface of the PEV to the grid are fully capable of shaping the line current to have low distortion and varying amounts of phase shift with respect to the AC line voltage. This implies that reactive power can be injected into the grid on demand and in real time. Furthermore, as reactive power translates in no net DC currents, this service can be provided without any added stress to the PEV battery.

3.4.3   Vehicle-to-Grid (V2G) and Vehicle-to-Home (V2H) Concepts

The advantages described in the preceding sections are not presently exploitable owing to a general lack of the required hardware infrastructure, as well as the thorny transition to new business models that include the V2G concept. The roadmap towards achieving this goal will probably consist of the following several milestones.

1. The first milestone is rather rudimentary because it does not yet require bidirectional converters. It will consist of a simple owner-selectable option afforded by the vehicle BMS user interface that allows the grid to schedule when to activate and deactivate charging. In return, the owner pays lower per-kWh rates. Communication between the grid operator and the BMS can be done through existing cell phone technology, requiring no additional infrastructure or hardware.
2. The straightforward "grid-friendly" charging time-window strategy described above will evolve to include more sophisticated algorithms. For instance, the grid might broadcast any updates to the current per-kWh cost and let the vehicle's BMS choose whether to activate charging. Some ancillary services, such as regulation "down," could become feasible, while regulation "up" will be limited by the lack of reverse power flow capability of the EVSE at this stage. The use of aggregators will also become widespread. Aggregators are intermediate communication and power distribution nodes between a group of vehicles, located in proximity to each other and to the grid. This allows the grid to macro-manage a single installment of several vehicles, corresponding to significant power-level blocks with somewhat predictable behavior, akin to other distributed energy resources. Furthermore, because the aggregator's consumption will

be in the MW range, it will allow purchases of power on the wholesale market, reducing the cost for each participant vehicle.

3. Eventually, directionality will become a standard feature for all EVSEs. However, this capability will not be harnessed immediately to achieve controlled reverse power flow to the grid. Rather, the PEV battery will, most likely, initially service the surrounding premises, probably the owner's home. This scenario, called V2H, will probably precede the full implementation of V2G [26], because it effectively bypasses several large infrastructure and technical issues needed for V2G while achieving many of the same results. Through pricing incentives, a PEV, parked at the residential premises and connected on the customer's side of the meter could be exploited to absorb energy from the grid during times of low demand and transfer it to the household appliances during times of high demand. Indirectly, this will shrink the power peaking for the grid while reducing the electricity bill for the user. It will also reduce overall transmission losses over the V2G strategy, because line current will flow only in one direction, from grid to vehicle, and will then be consumed locally.

   Moreover, if the household is geared with renewable source generators, the vehicle can immediately serve as storage and, during blackouts, as backup power. Although one can find some similarities between the concepts of V2H and V2G, there are important distinctions. In practical terms, these differences stem from the fact that V2H cannot take advantage of the high predictability deriving from statistical averages afforded by very high numbers of vehicles available for V2G operations. Simply stated, the real benefits of V2H are not easily estimated because they are dependent on many exceedingly uncertain variables, which include the number of available vehicles, commute schedule, time duration and distance, PEV energy storage capacity, presence and quantity of quasi-predictable local generation (example: solar panels), presence and quantity of unpredictable local generation (example: wind power), residence-specific energy consumption profile, and presence, of additional storage. Despite the fact that these issues will require complicated management algorithms in order to optimize the use of V2H, some benefits such as emergency backup are available immediately with relatively minor upgrades to the residential infrastructure. These upgrades consist mainly of the installation of a transfer switch to disconnect the residence from the grid during backup operation, and to expand the design of the power converter to detect islanding conditions. Furthermore, the EVSE must be capable of controlling output current into the line when connected to the grid, but reverting to controlling output voltage when acting as a backup generator.

4. Full V2G implemented with automated options for V2H: The connection would be metered and it could include any locally generated renewable energy management.

3.4.3.1   Grid Upgrade

The electric transmission and distribution networks in most industrialized nations must consider changes and upgrades in order to benefit fully from the introduction of PEVs as distributed resources. First, we must consider the extent by which the current production capacity will have to be expanded. Various studies [27] have suggested that once the typical charging profile for a PEV is scrutinized and hopefully optimized—charging mostly at night—the installation of a new generation will be unnecessary or minimal at most. In fact, it will have the effect of diminishing reliance on more expensive load-following plants, as the overall 24-h demand curve will average closer to the base load. Therefore, the main effort should be in effectively introducing intelligence into the grid. The hardware and communication standards for implementing such intelligence are still under study. A wideband digital interface can take the form of power line communication (PLC) or utilize separate communication channels that have some market penetration already. In either case, the EV will most likely be treated as any other managed load by this smart grid, with the exception of a sophisticated onboard metering device that will have to be reconciled with the utility's pricing model. Presently the two major obstacles to the utilization of PEVs as distributed resources are the lack of directionality in the power converters and the lack of recognized standards, both software protocols and hardware, for the smart grid function. Of the two, the former is by far the easiest to implement, given the well-established characterization of suitable power electronic topologies.

3.4.3.2   Renewable and Other Intermittent Resource Market Penetration

Owing to recent well-known trends, renewable resources are becoming increasingly prominent in the complex energy market mosaic. As long as their penetration level is low, they can be handled easily by the current infrastructure, but at present incremental rates, this will not be the case in the future. The intermittent nature of solar and wind generation will require a far more flexible compensation mechanism than is currently available. Because of this, large battery banks that act as buffers between the generator and the grid invariably accompany today's renewable energy installations. Wind power, in particular, is not only intermittent but it has no day-average predictability, as winds can differ hour to hour as easily at night as during the day, adding an extra amount of irregularity to an already varying load. This suggests that PEVs will be called on to not only perform the more manageable regulation tasks, but also aid in providing peak power. As noted earlier, this might not find approval with PEV owners unless the pricing model is modified. Nevertheless, it is reasonable to ask whether a large PEV-contracted fleet could perform this task on a national (US) level. Studies have shown [28] that the answer is yes. With an overconfident 50 % estimation for the market penetration of wind energy

and 70 million PEVs available, peak power could be provided at the expense of approximately 7 kWh of battery energy per day or about 10–20 % of an average PEV reserve.

3.4.3.3   Dedicated Charging Infrastructure from Renewable Resources

The traditional microgrid often relies on diesel generators as a single source of energy. Even in this case, any load fluctuations are quite difficult to negotiate, relying solely on the intrinsically slow ramp-up speeds of the generator itself. The new trend towards integrating renewable resources into microgrids greatly amplifies this problem owing to their notorious intermittent nature. On the other hand, the dedicated generation from renewables for the explicit purpose of PEV charging is gaining more credibility as a means to eliminate transmission losses and greatly reduce the overall carbon footprint associated with EVs. Such installations would fall into two categories: (1) small installations with or without a grid tie and (2) large installations with grid tie. Small installations can be somewhat arbitrarily defined at less than a total of 250 kW of peak production. This would be sufficient to slow-charge about 20 vehicles and would certainly require local external storage in order to buffer the peaks and troughs in local energy production. This is more evident in the case of islanded installations; if any energy is produced in excess, it cannot be sent back to the grid, so it will need long-term storage capability. Large installations with a grid tie can inject or draw power to and from the grid as a means to equalize the grid during overproduction and draw from the line. However, depending on the number of vehicles connected, which can be accurately predicted with statistical methods, some of the PEV resource could be utilized to minimize the size of the external storage. Nonetheless, it appears that PEVs could alleviate the inherent issues associated with local renewable production for the dedicated purpose of PEV charging, but not eliminate them.

3.4.4   Power Electronics for GRID and PEV Charging

The PEV charging process will be enabled by the sophisticated power electronics circuits found in the EVSE. Such equipment will be optimally designed depending on the different possible sites and types of power connection. We will begin by looking at EVSE connected to the main power grid and then analyze dual-sourced systems such as grid-tied renewable energy installations dedicated to PEV charging. A short discussion on basic safety compliance strategy follows.
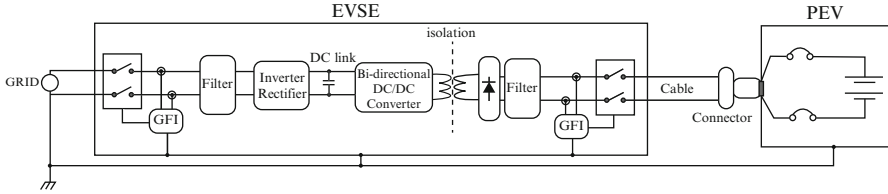
Fig. 3.21 Typical EVSE safety configuration

3.4.4.1   Safety Considerations

For off-board chargers, only a few important safety needs affect significantly the power converter design: (1) isolation of the battery pack with respect to the chassis and the grid terminals, (2) ground fault interrupters (GFI) to detect any dangerous leakage current from either the grid or the battery circuit, (3) connector interface, and (4) software. A typical EVSE and related connections are shown in Fig. 3.21.

Two GFIs detect any breakdown or current leakage on either side of the isolation barrier in order to ensure complete protection to the user and to disconnect the high-power circuit immediately in case of fault. The battery pack is fully isolated from the chassis because it cannot be grounded properly during charging without heavily oversizing the connector cable. In fact, some existing safety recommendations require that an active breakdown test be performed on the battery pack prior to every charging cycle. At the time of writing, the de facto standard for Level 3 DC charging is the CHAdeMO standard developed by the Tokyo Electric Power Company. Although competing standards may eventually overtake it in popularity, the description of the CHAdeMO connector demonstrates the safety concerns involved. The connector itself will have the mechanical means to lock itself onto the car receptacle in order to prevent accidental removal when energized. It will carry the power leads, but also the communication wires that include a CAN bus digital interface as well as several optically isolated analog lines for critical commands, such as on/off and start/stop. Every analog signal sent by the PEV to the charger (or vice versa) is received and acknowledged through the analog lines. This analog interface is sturdier than a digital one and less susceptible to electromagnetic interference. The CAN bus is activated only when more complex information is exchanged. Prior to the start-charge command, the EVSE communicates its parameters to the PEV (maximum output voltage and currents, error flag convention, etc.) and the PEV communicates its parameters to the EVSE (target voltage, battery capacity, thermal limits, etc.) and a compatibility check is performed. During charging, the PEV continuously updates the EVSE with its instantaneous current request (every 100 ms or so) and all accompanying status flags. Once charging is finished, the operator can safely unlock the connector and drive away.

As can be seen, the presence of safety devices, such as the GFIs, as well as the sturdy method of analog and digital communication render the charging process

extremely safe, leaving the power electronic designer of the EVSE with the relatively simple task of ensuring only the isolation barrier between the grid voltage and the PEV floating battery. In fact, the utilization of an isolation transformer can actually simplify some designs owing to the added voltage amplification capability afforded by the transformer's turns ratio. This could prove very beneficial if much higher battery voltages become necessary in order to increase storage capacity.

3.4.4.2 Grid-Tied Residential Systems

As noted earlier, only Levels 1 and 2 are feasible within the confines of a residential setting. This can be accomplished through integrated chargers when available or by an external EVSE. In the latter case, the most obvious circuit configuration is a single-phase bidirectional rectifier/inverter powered by a 240 V AC/60 A circuit that is readily available from the distribution transformer. The DC-link voltage is then processed by a bidirectional DC–DC converter that performs the isolation function. This simple topology, shown in Fig. 3.22, can be called the canonical topology as it will be repeated, with minor changes, for most grid-tied systems irrespective of power rating.

In North America, the 240 V from the residential distribution transformer is in the form of a split 120 V supply, suggesting small modifications to the canonical topology. Figure 3.23 shows two possibilities.
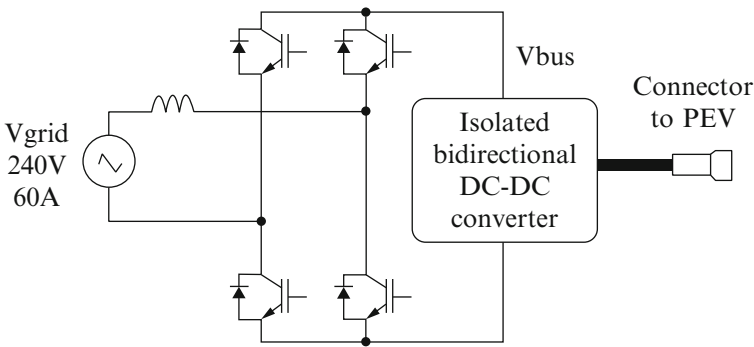
Fig. 3.22 Canonical single-phase EVSE configuration
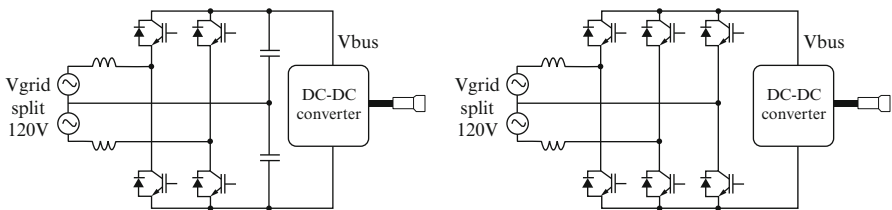
Fig. 3.23 Split phase-sourced EVSE configurations
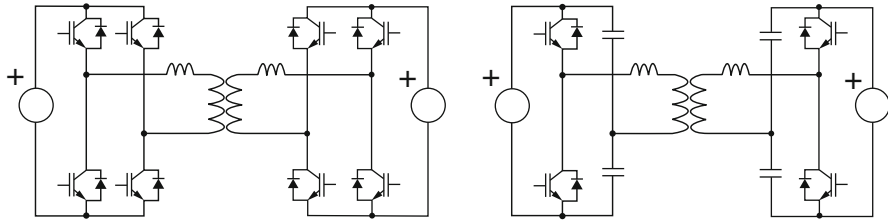
Fig. 3.24 Typical isolated bidirectional buck-boost DC–DC converter topologies

The two topologies in the figure are similar, but the one on the right has better voltage utilization and is better equipped to counter unbalanced loads on the split supply [29]. For the DC–DC converter, many bidirectional isolated circuit topologies have been proposed [30]. Typical circuits are shown in Fig. 3.24.

When the two controlled bridges are driven independently in phase-shift modulation (PSM), these are generally referred to as dual active bridge (DAB) topologies. In their simplest operation mode, when power needs to be transferred from the left-side circuit to the right-side circuit, for instance, the right-side IGBT switches are left undriven, leaving their antiparallel diodes in the form of a regular diode bridge. Under these circumstances, the topology becomes identical to a regular PSM converter, which is simple to operate, but not very flexible in terms of voltage gain. On the other hand, when both bridges are modulated, power transfer can be accomplished in both directions and with great variability ranges on the input and output voltages. In addition, zero voltage switching (ZVS) can be assured for all switches for reduced switching loss and generated electrical noise (EMI). Other topologies [31, 32] based on the DAB have been proposed with purported additional benefits, such as better switch utilization, extended ZVS operating range, and more flexible voltage amplification.

3.4.4.3 Grid-Tied Public Systems

A public parking/charging installation would deliver only Level 2 power, given the relatively long plug-in times. Because there are several parking locations in close proximity, the power configuration used for residential use might not be optimal. Rather, a single transformer can be installed at the grid, delivering isolated power to all vehicles in the facility. This way, cheaper and more efficient non-isolated DC–DC converters can be used without violating safety rules. Figure 3.25 illustrates this configuration for each charging station. For the entire installation, the architectures shown in Fig. 3.26 are possible.

In the centralized architecture [33], a single, large polyphase 50/60 Hz step-down transformer connects to the grid, providing isolation for the entire facility. A large bidirectional rectifier that produces a single high-voltage DC bus follows this. Each parking station uses inexpensive high-efficiency non-isolated DC–DC converters to process this bus voltage into the appropriate charging current for the
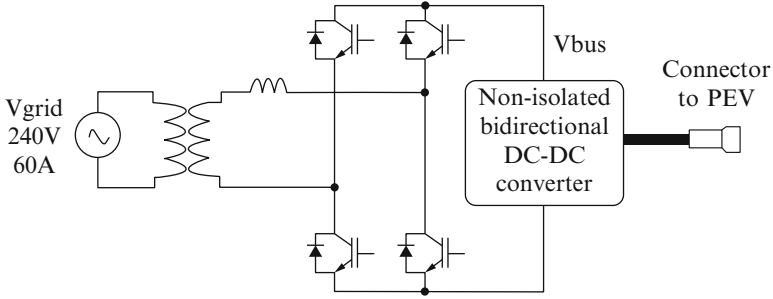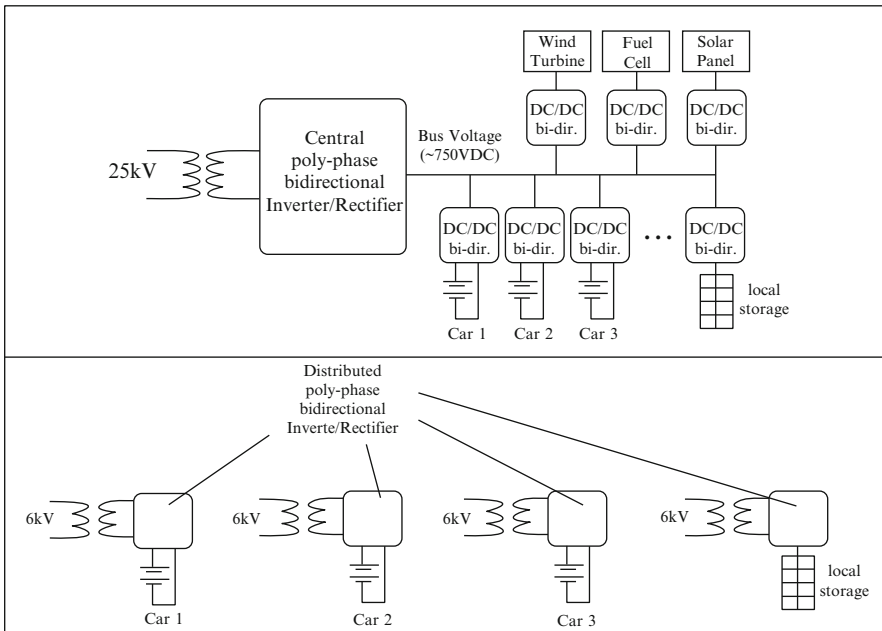
Fig. 3.25 Configuration with isolation at the grid

Fig. 3.26 Central architecture (*top*); distributed architecture (*bottom*)

individual PEVs. Because isolation is either desirable or required, especially on PV panels depending on local electrical codes, additional storage or generating resources, such as wind turbines and fuel cells, could also benefit from a simpler interface to the DC bus. Moreover, the single-transformer connection guarantees that no DC current is injected into the grid, doing away with complicated active techniques to achieve the same purpose.

However, these advantages of the centralized configuration are somewhat offset by the following drawbacks: (1) the need for a bulky and usually inefficient line-frequency transformer, (2) an expensive high-power polyphase inverter/rectifier, (3) single-fault vulnerability in the transformer and central inverter rectifier, and
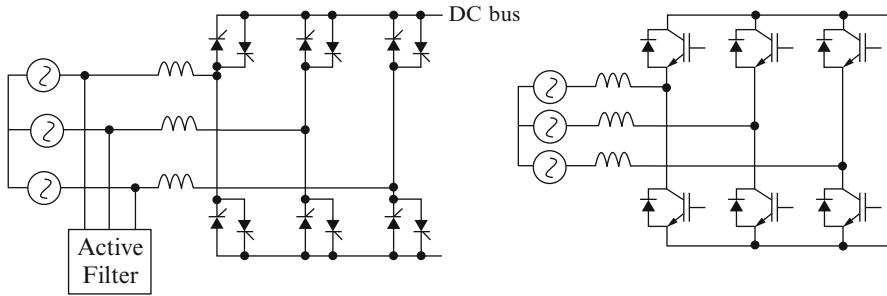
Fig. 3.27 Thyristor bridge and active line filter (*left*); IGBT bridge (*right*)

(4) lack of voltage amplification in each non-isolated DC–DC converter (otherwise afforded by the turns ratio of the high-frequency transformer in isolated topologies).

In a Level 3 (fast-charging) public facility, other technical challenges must be considered. For instance, with battery pack rated voltages in the range of 200–600 V, the overall currents required for fast charging will be of the order of thousands of amps [34]. These currents must necessarily flow through cables and especially connectors, causing local thermal issues and loss of efficiency owing to ohmic losses. In addition, the charging stations will appear as concentrated loads to the grid, such that any power transients produced by the stations are very likely to cause local sags or surges.

The first issue can be countered partially by brute force methods such as the development of advanced sub-milliohm connectors and by minimizing cable lengths by placing the grid step-down transformer in physical proximity to the vehicle. It is obvious that any intervening power conditioning electronic circuitry should be added only when necessary. This suggests immediately that the architecture of the charging station should be distributed rather than central. As can be seen from Fig. 3.27, a distributed architecture could potentially reduce the number of processors from grid to battery from two to one. To be fair, this single stage may not be feasible when managing large input–output voltage ranges, especially if buck-boost operation is required (see discussion on the Z-converter later in this section). Nevertheless, if an additional DC–DC stage should prove necessary, it will be easily integrated locally with the inverter for improved efficiency. Furthermore, a central processor, in addition to constituting a single point of failure, as already noted, would have to be rated for the full service station power, which could be of the order of a megawatt. In contrast, a distributed architecture benefits from repeated circuitry (economies of scale), redundancy for higher reliability, and possibility of power conditioning in physical proximity to the vehicles, thereby reducing ohmic losses.

The issue of the deterioration of power line quality caused by the service station operating transients has only been studied for specific geographic locations [35], but possible voltage fluctuations of up to 10 % have been reported, depending on the length of the feeding high-voltage transmission line. The obvious and perhaps sole approach to mitigate this problem is the integration of flywheel, battery, or

ultracapacitor banks into the charging station. This storage will smooth out the load transients by delivering local power when needed and storing power during periods of lower demand. Moreover, it will average out the draw from the grid, such that the distribution equipment can be rated at much lower peak powers (by as much as 40 %) [36].

The task of discriminating between the various available electronic topologies is made easier when considering the sheer power handled by fast chargers, to wit, up to 250 kW. Obviously, a good candidate must be very efficient, inherently of low noise with low component count, and be capable of high-frequency operation in order to control physical size. For the inverter/rectifier section, we must also add the requirement that no significant harmonic content should be present in the line current. In order to obtain input currents that are sinusoidal and free of ripple noise, several methods of increasing complexity exist.

One method uses a three-phase thyristor bridge. The devices are very rugged and efficient in terms of conduction loss and have enough controllability to regulate approximately the DC bus [37]. In order to remove unwanted current harmonics, an active filter is added. This filter is based on IGBT devices, but it only processes a small proportion of the total power. A second method uses a fully controlled IGBT bridge in order to achieve excellent input current shaping for extremely low input current distortion and well-regulated, ripple-free DC bus voltage.

Moreover, fewer components and much higher switching frequencies can be achieved resulting in smaller magnetic components. On the other hand, IGBTs have switching losses and more significant conduction losses than thyristors. However, other techniques, although less sophisticated, have the potential of realizing the required low-current distortion limit without the addition of an active filter. The uncontrolled 12-pulse rectifier shown in Fig. 3.28 can certainly do this, albeit with the addition of significant inductive filtering. Because the output DC bus will not be regulated, the subsequent DC–DC converter design cannot be optimized. Using thyristors can achieve regulation of the bus and possibly still achieve the required input current shaping. It is important to note that of the four topologies mentioned here, only those in Fig. 3.27 are bidirectional and therefore are the only choices if
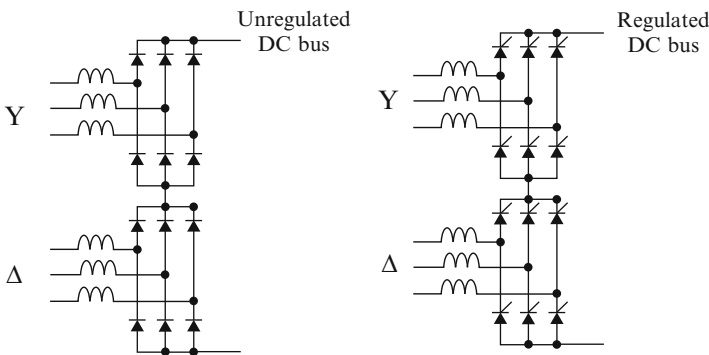

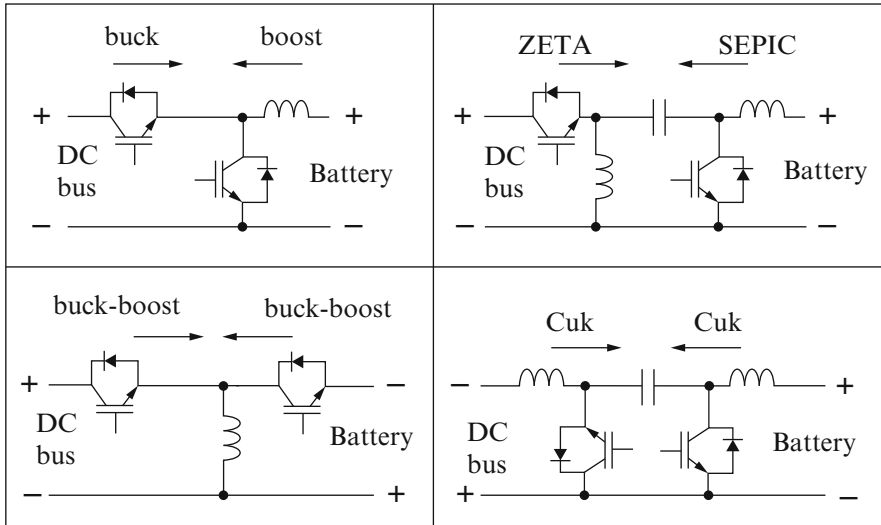**Fig. 3.28** 12-Pulse rectifier circuits

Fig. 3.29 Basic bidirectional non-isolated topologies

V2G is to be implemented. For the final DC–DC converter, all common basic topologies, boost, buck-boost, buck, Cuk, SEPIC, and ZETA, can be used, so long as they are rendered bidirectional by replacing the diode with a transistor device. In this case, these topologies function differently, depending on the direction of the power flow, Fig. 3.29.

Different design requirements might suggest different topologies [33], but some of these are more difficult to justify objectively. For instance, using the buck-boost/buck-boost (bottom left in Fig. 3.29) produces a voltage inversion from positive to negative that might be undesirable. It also places higher electrical stress on the switches, it requires a more sophisticated design for the inductor, and it draws pulsed current from the battery. Similarly, the ZETA/SEPIC topology has a higher part count, including a capacitive, rather than inductive, energy-transferring element. On the other hand, as long as the DC bus is guaranteed to exceed the battery voltage—a requirement that is assured by the use of the controlled bridge discussed earlier—the buck-boost topology (top left in the figure) is quite attractive. Furthermore, this topology is readily modified in order to divide the task of handling a very large power flow among paralleled modules [35].

This is shown in Fig. 3.30. The amount of converted power can be split among n identical sections and the battery ripple current reduced greatly by the well-known technique of phase-shift interleaving. Using this circuit with $n = 3$ and a switching frequency of 2 kHz, for a typical 125 kW application, efficiencies as high as 98.5 % have been reported.
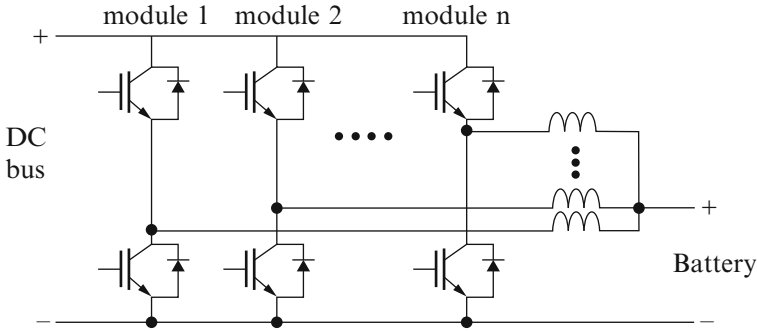
Fig. 3.30 Interleaved modular approach for the DC–DC converter

3.4.4.4 Grid-Tied Systems with Local Renewable Energy Production

As noted earlier, when relatively large energy production from intermittent sources is to be tied into the grid, a statistically predictable PEV presence could serve the purpose of minimizing on-site dedicated storage. This would be the case for municipal carports powered by wind and/or solar generation, and where the vehicles must be able to interact intelligently with both locally generated and grid distributed power at the same time. The possible scenario described in Fig. 3.26 may not be ideal when the renewable resource is meant to generate the dominant share of PEV charging energy. Rather, by realizing the advantages of the distributed configuration, as in Fig. 3.26, one stage of conversion can be eliminated as long as a conversion topology with wide input–output voltage range capability can be found.

Figure 3.31 shows some possible configurations for one of the several charging stations in a solar carport. The architecture depicted on the left has the disadvantage of inserting a DC–DC converter into the main intended power flow, from PV to battery. Moreover, the power drawn from a single-phase connection is pulsed at twice the line frequency. This pulsating power takes the form of an undesirably high ripple current into the battery. The configuration shown in the middle of Fig. 3.31 removes the ripple issue, but adds an additional conversion stage between the grid and the battery. The configuration on the right requires a converter that is capable of bidirectional flow between the PEV and the grid, as well as the steering of PV power to either the PEV or the grid in a controlled fashion. Furthermore, ideally, this should be achieved by a single conversion stage for all power flow paths and with wide voltage range capability. A good candidate for this task is the Z-loaded inverter/rectifier topology shown in Fig. 3.32.

The operating characteristics of the Z-loaded converter have been described extensively in the literature [38–41]. The most salient feature of this conversion topology is its controllability through two distinct modulation modes within the same switching cycle, designated by duty cycle D and "shoot-through" duty cycle Do. The gating patterns shown in Fig. 3.32 describe the meaning of D and Do. As can be seen, during period Do, all four switches are closed simultaneously, causing
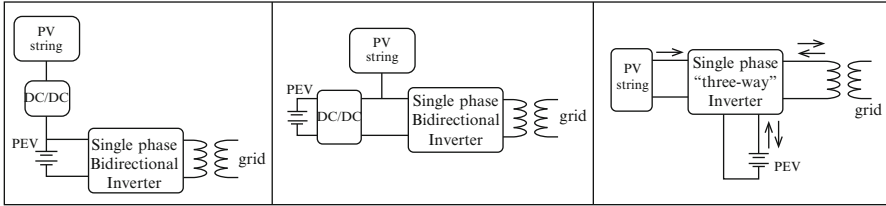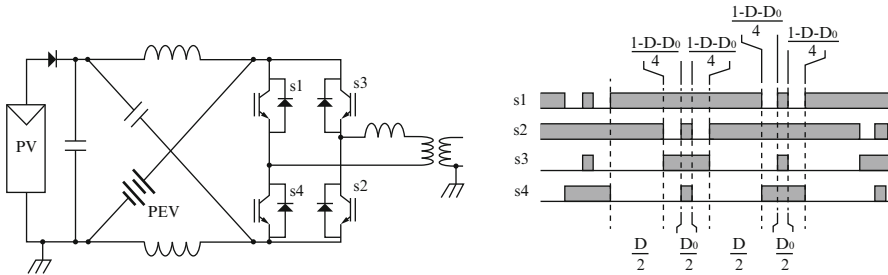
Fig. 3.31 Possible configurations for solar carport

Fig. 3.32 Z-loaded rectifier (*left*); gating pattern (*right*)

the inductors to charge and ultimately boost the voltage across the capacitor, the battery, and the grid terminals. Thus, Do can be understood as the duty cycle associated with operation, akin to that of a current-sourced inverter. During period D, on the other hand, the bridge operates in a manner similar to that of a voltage-sourced inverter, which is essentially a buck. Therefore, with the appropriate utilization of D and Do, both buck and boost operation can be achieved, such that the battery voltage can be either higher or lower than the peak of the line voltage. This allows a wide line and battery voltage range. Most significantly, owing to the double modulation, both the grid and the battery current can be controlled precisely in amplitude and shape (sinusoidal for the line current and ripple-less DC for the battery). The MPPT function for the PV string can then be achieved by managing the simple addition of these two power flows.

The topology shown in Fig. 3.32 must be modified in order to achieve isolation of the battery pack. Therefore, the DAB converter shown in Fig. 3.24 can be integrated, resulting in the detailed schematic of Fig. 3.33. The apparent complexity of the isolation stage is deceptive. In fact, it is a simple bidirectional converter using a small and inexpensive high-frequency transformer, which runs in open loop at full duty cycle, where all eight switches are driven by the same signal. In addition, as the duty cycle is always 100 %, ZVS is assured, resulting in efficient operation executed by relatively small devices.

With the inclusion of the isolated DC–DC converter, the need for the 50/60 Hz isolation transformer might be called into question. In North America, the grounding of one side of the PV panel has traditionally been the required norm. Although the National Electric Code has allowed recent conditional exceptions to this safety
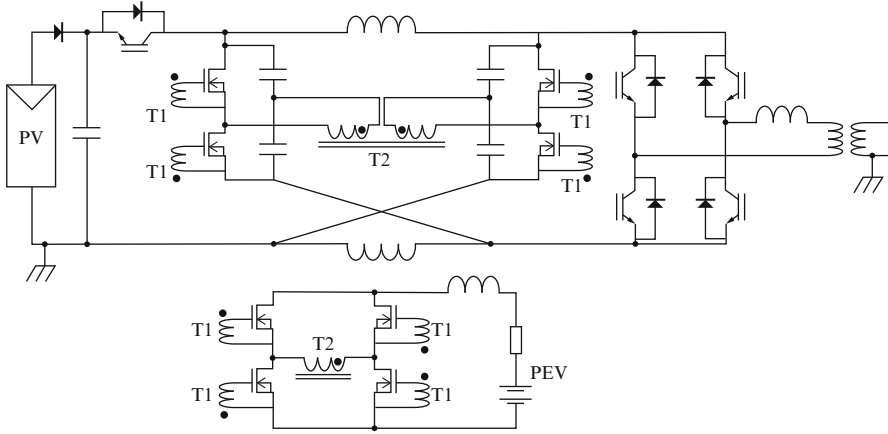
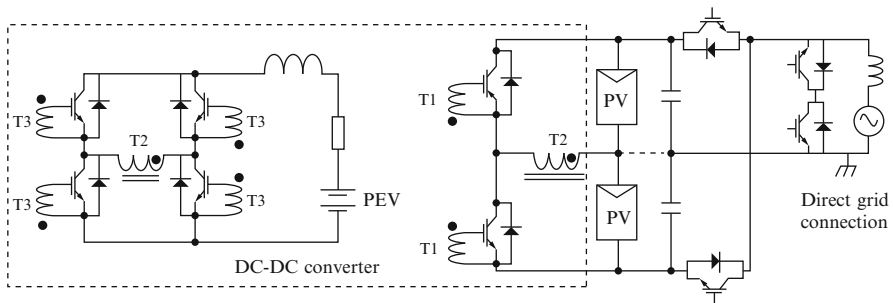**Fig. 3.33** Z-converter application to single-phase, grid-tied PV charging station

Fig. 3.34 Transformerless topology

regulation, utility companies have resisted this change, mainly because a direct connection to the AC–DC bridge converter can inject dangerous levels of DC current into the distribution transformer. On the other hand, should this constraint become less binding in North America, as it is currently in Europe, other circuits could be proposed that could prove more reliable and efficient. Many so-called transformerless topologies have been proposed [42, 43], and Fig. 3.34 depicts a simplified schematic for one such possibility.

In this case, the DC–DC conversion and the rectifier/inverter section are controlled separately, rendering the control strategy much simpler. On the other hand, the DC–DC converter is now governed by a feedback loop, meaning that it no longer takes advantage of the low switching loss normally associated with 100 % duty cycle operation. With allowances from the regulatory safety agencies, the PV panels can be floating, as long as the circuit has additional protection afforded by GFIs and that it produces no leakage currents to ground during normal operation.

The last requirement is attained only if the topology guarantees very little common-mode voltage on the PV panels during normal operation (note that this cannot be achieved with the Z-converter). Nevertheless, the midpoint can still be grounded, as indicated by the dashed line in the figure, but at the expense of performance.

Whichever architecture is chosen, it is clear that the energy transfer cannot be controlled to satisfy fully any arbitrary current demands of the PV, the grid, and the EV/PHEV battery, simultaneously. In fact, many renewable resources are themselves subject to MPPT control, such that the simple power balance in Eq. (3.3) must be satisfied:

$$P_{\mathrm{MPPT}} = P_{\mathrm{PEV}} + P_{\mathrm{G}} \tag{3.3}$$

Here, MPPT is the power draw requested by the distributed resource. It has to equal the sum of the power absorbed by the grid and the PEV battery (PPEV and PG, respectively). As MPPT is determined by external factors, such as clouding in the case of PV, either PPEV or PG can be controlled independently, but not both. Which of these is controlled will depend heavily on how the PEV owner decides to utilize his or her vehicle storage resource. Thus, in installations where charging power comes primarily from intermittent sources, the need for a significant presence of additional storage on the premises will be diminished, but not eliminated.

3.5 Conclusions

This chapter started off by presenting the arrangement and basic design aspects of EV charging infrastructures. Future trends in EV charger manufacturing were also discussed. Integration of EVs with green, renewable energy sources was presented, along with an introduction to the design of such systems, focusing on power electronic converters and control. Various charging scenarios for EV batteries were discussed, when charging at home, at work, or in between routes. Future advanced battery charging infrastructure, such as from combined PV and grid sources, were introduced and studied in detail.

Shortage of petroleum is considered as one of the most critical worldwide issues today. At the same time, as of today, car owners in Canada and North America, in general, spend more money at the gas station than they have done ever before. The most practical solution to the oil crisis problems lies in commercially available electric and plug-in hybrid electric vehicles (EVs and PHEVs). EVs and PHEVs present a significant opportunity to reduce greenhouse gases and dependence on foreign oil. Major car companies have already developed exciting new EVs, such as the Chevy Volt, Nissan Leaf, Tesla Model S, just to name a few of the many manufacturers of electric cars. The Tesla Model S is a brand new product in the market as a result of a successful start-up company project. Finally, Toyota most recently developed the plug-in hybrid electric model of the popular Prius. Thus, it is clear that new EVs are being introduced at an increasing rate in the market.

In order to convince customers to buy EVs, urban communities will need to enable the necessary large-scale charging infrastructure. An EV can reduce fuel consumption by charging its battery from the utility grid. The typical battery charging time for EVs and PHEVs is 6–8 h, if charged at home. However, if the charging is required to be done at a faster rate, it can be performed in less than 20 min, at a suitably sized charge station. However, the required charging energy will have a major impact on the utility. Alternatively, green renewable energy sources, such as photovoltaics (PV) and wind energy, could be used to provide the necessary charging energy at a cleaner and cheaper rate. Such energy sources can also be installed at home or in urban buildings in large cities, thereby allowing for battery charging during work hours.

References

1. Pelland D, McKenney W, Poissant Y et al (2006) The development of photovoltaic resource maps for Canada. In: Proceedings of 31st Annual Conference of the Solar Energy Society of Canada, Montreal, Canada, 20–24 Aug 2006
2. Morris R (2006) The solar and wind resource in Canada. National Archives and Data Management Branch, Atmospheric Monitoring and Water Survey Directorate Meteorological Service of Canada
3. Eudy L, Zuboy J (2004) Overview of advanced technology transportation, 2004 update. Technical report on advanced vehicle testing activity, energy efficiency and renewable energy. U.S. Department of Energy, DOE/GO-102004-1849, Aug 2004
4. Burke A (2004) Present status and marketing prospects of the emerging hybrid-electric and diesel technologies to reduce CO_2 emissions of new light-duty vehicles in California. Institute of Transportation Studies, University of California, Davis. http://repositories.cdlib.org/itsdavis/UCD-ITS-RR-04-2. Accessed June 2004
5. Lee D-Y, Noh H-J, Hyun D-S, Choy I (2003) An improved MPPT converter using current compensation method for small scaled PV-applications. In: Applied power electronics conference and exposition, 2003. APEC '03. Eighteenth Annual IEEE, 9–13 Feb 2003. 1: 540–545
6. Esram T, Chapman PL (2007) Comparison of photovoltaic array maximum power point tracking techniques. IEEE Trans Energ Convers 22(2):439–449
7. Chiang SJ, Chang KT, Yen CY (1998) Residential photovoltaic energy storage system. IEEE Trans Ind Electron 45(3):385–394
8. Enrique JM, Durán E, Sidrach-de-Cardona M, Andújar JM (2007) Theoretical assessment of the maximum power point tracking efficiency of photovoltaic facilities with different converter topologies. Sol Energy 81(1):31–38
9. Shmilovitz D (2005) On the control of photovoltaic maximum power point tracker via output parameters. IEE Proceed Electric Power Appl 152(2):239–248
10. Iov F, Ciobotaru M, Sera D, Teodorescu R, Blaabjerg F (2007) Power electronics and control of renewable energy systems. In: Power electronics and drive systems, 2007. PEDS '07. 7th International Conference on, 27–30 Nov 2007, pp P-6, P-28,
11. Shimizu T, Hirakata M, Kamezawa T, Watanabe H (2001) Generation control circuit for photovoltaic modules. IEEE Trans Power Electron 16(3):293–300
12. Haeberlin H (2001) Evolution of inverters for grid connected PV systems from 1989 to 2000. In: Proceedings of Photovoltaic Solar Energy Conference, 2001
13. Picault D, Raison B, Bacha S, de la Casa J, Aguilera J (2010) Forecasting photovoltaic array power production subject to mismatch losses. Sol Energy 84(7):1301–1309

14. Chouder A et al (2009) Analysis model of mismatch losses in PV systems. J Sol Energy Eng 131:024504
15. Gautam NK et al (2002) An efficient algorithm to simulate the electrical performance of solar photovoltaic arrays. Energy 27:347–361
16. Kaushika ND et al (2003) Energy yield simulations of interconnected solar PV arrays. IEEE Trans Energ Convers 18(1):127–134
17. Kaushika ND et al (2007) An investigation of mismatch losses in solar photovoltaic cell networks. Energy 32:755–759
18. Meyer EL et al (2004) Assessing the reliability and degradation of photovoltaic module performance parameters. IEEE Trans Reliab 53(1):83–92
19. Van der Borg NJCM et al (2003) Energy loss due to shading in BIPV application. In: 3rd World Conference on Photovoltaic Energy Conversion, Osaka, Japan, 11–18 May 2003, pp 2220–2222
20. Bruendlinger R, Bletterie B, Milde M, Oldenkamp H (2006) Maximum power point tracking performance under partially shaded PV array conditions. In: Proceedings of 21st EUPVSEC, Dresden, Germany, Sept 2006, pp 2157–2160
21. Xiao W, Ozog N, Dunford WG (2007) Topology study of photovoltaic interface for maximum power point tracking. IEEE Trans Ind Electron 54(3):1696–1704
22. Karatepe E et al (2007) Development of a suitable model for characterizing photovoltaic arrays with shaded solar cells. Sol Energy 81:977–992
23. Nguyen D et al (2008) An adaptive solar photovoltaic array using model-based reconfiguration algorithm. IEEE Trans Ind Electron 55(7):980–986
24. Kempton W, Kubo T (2000) Electric-drive vehicles for peak power in Japan. Energy Pol 28:9–18
25. Kisacikoglu1 MC, Ozpineci B, Tolbert LM (2010) Examination of a PHEV bidirectional charger system for V2G reactive power compensation. In: IEEE Applied Power Electronics Conference, Palm Springs, California
26. Tuttle DP, Baldick R (2012) The evolution of plug-in electric vehicle-grid interactions. The University of Texas at Austin Department of Electrical and Computer Engineering
27. Jenkins SD, Rossmaier JR, Ferdowsi M (2008) Utilization and effect of plug-in hybrid electric vehicles in the United States power grid, vehicle power and propulsion conference
28. Kempton W, Tomic J (2005) Vehicle-to-grid power implementation: from stabilizing the grid to supporting large-scale renewable energy. J Power Sources 144(1):280–294
29. Wang J, Peng FZ, Anderson J, Joseph A, Buffenbarger R (2004) Low cost fuel cell converter system for residential power generation. IEEE Trans Power Electron 19(5):1315–1322
30. Han S, Divan D (2008) Bi-directional DC/DC converters for plug-in hybrid electric vehicle (PHEV) applications. Applied Power Electronics Conference and Exposition, APEC
31. Peng FZ, Li H, Su G-J, Lawler JS (2004) A new ZVS bidirectional DC–DC converter for fuel cell and battery application. IEEE Trans Power Electron 19(1):54–65
32. Xiao H, Guo L, Xie L (2007) A new ZVS bidirectional DC–DC converter with phase-shift plus PWM control scheme. Applied Power Electronics Conference, APEC
33. Du Y, Zhou X, Bai S, Lukic S, Huang A (2010) Review of non-isolated bi-directional DC–DC converters for plug-in hybrid electric vehicle charge station application at municipal parking decks. Applied Power Electronics Conference and Exposition (APEC)
34. Buso S, Malesani L, Mattavelli P, Veronese R (1998) Design and fully digital control of parallel active filters for thyristor rectifiers to comply with IEC-1000-3-2 standards. IEEE Transactions on Industry Applications Vol 34, Issue 3.
35. Aggeler D, Canales F, Zelaya H, Parra DL, Coccia A, Butcher N, Apeldoorn O (2010) Ultra-fast DC-charge infrastructures for EV-mobility and future smart grids. Innovative Smart Grid Technologies Conference Europe (ISGT Europe), IEEE PES
36. Bai S, Du Y, Lukic S (2010) Optimum design of an EV/PHEV charging station with DC bus and storage system. Energy Conversion Congress and Exposition (ECCE)

37. Moore SW, Schneider PJ (2001) A review of cell equalization methods for lithium ion and lithium polymer battery systems. In: Proceedings of SAE 2001 World Congress, Detroit, MI
38. Peng Z (2003) Z-source inverter. IEEE Trans Ind Appl 39(2):504–510
39. Peng FZ, Shen M, Holland K (2007) Application of Z-source inverter for traction drive of fuel cell – battery hybrid electric vehicles. IEEE Trans Power Electron 22(3):1054–1061
40. Carli G, Williamson S (2009) On the elimination of pulsed output current in Z-loaded chargers/rectifiers. In: Proceedings of IEEE Applied Power Electronics Conference and Exposition, Washington, DC
41. Carli G, Williamson SS (2013) Technical considerations on power conversion for electric and plug-in hybrid electric vehicle battery charging in photovoltaic installations. IEEE Trans Power Electron 28(12):5784–5792
42. González R, López J, Sanchis P, Marroyo L (2007) Transformer-less inverter for single-phase photovoltaic systems. IEEE Trans Power Electron 22(2):693–697
43. Kerekes T, Teodorescu R, Borup U (2007) Transformer-less photovoltaic inverters connected to the grid. Proceedings of IEEE Applied Power Electronics Conference and Exposition.

Chapter 4
Charging Architectures for Electric and Plug-In Hybrid Electric Vehicles

Sebastian Rivera, Samir Kouro, and Bin Wu

Abstract This chapter provides an overview of the different charging architectures available for electric vehicles and plug-in hybrid electric vehicles. The charging architectures are addressed following two main categories: onboard chargers, used mainly for slow and semi-fast charging (generally AC connection), and off-board chargers, used for fast charging (DC connection). The chapter focuses on the mainstream solutions available in the industry, and also presents some recent advances and trends found in the literature. In addition, the chapter provides an introduction to well-established charging standards being used by manufacturers. Finally, the control schemes used in charging configurations, including the control schemes for DC–DC and AC–DC converter stages, are discussed, the latter considering both single- and three-phase control schemes.

4.1 Introduction

One of the most critical components in electric vehicles (EV) and plug-in hybrid electric vehicles (PHEV) is the battery storage system. Its energy density, charging time, lifetime, and cost are currently the main drivers behind EV technology development to increase their penetration in the market. The energy density and charging time are closely related to the range of the EV, and are perceived as the main limitations by a broad segment of the market for the adoption of EVs over fossil-fueled cars. In addition, the charging time and lifetime of a battery are strongly related with the characteristics of the battery charger. Hence, by extension,

S. Rivera
University of Toronto, 10 King's College Road, Toronto, ON, Canada, M5S 3G4
e-mail: s.rivera.i@ieee.org

S. Kouro (✉)
Technical University Federico Santa Maria, Av. Espana 1680, Valparaiso, Chile
e-mail: samir.kouro@ieee.org; samir.kouro@usm.cl

B. Wu
Ryerson University, 350 Victoria Street, Toronto, ON, Canada, M5B 2K3
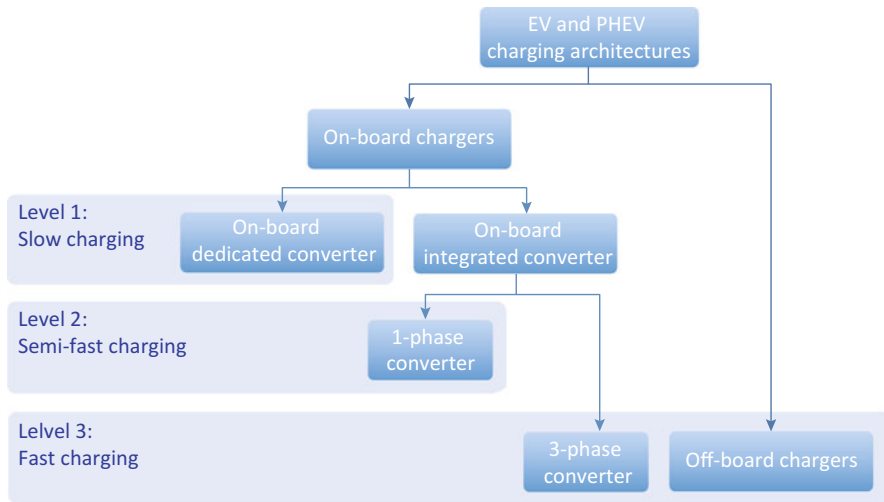e-mail: bwu@ee.ryerson.ca

Fig. 4.1 Classification of EV and sperm charging architectures

the battery charger has also become a key player for the present and future of EV and their widespread acceptance.

For these reasons research and development of different charging architectures is one of the most important topics in EV evolution. Their structure, power rating, charging times, and type of connection can lead to different classifications. Nevertheless, the most conventional classification accepted currently for chargers is based on their power ratings as shown in Fig. 4.1. The division according to the power levels that the charger can deliver to the battery is given by level 1 for powers below 1.92 kW, level 2 up to 19.2 kW, and level 3 for chargers that deliver power above 20 kW. Additionally, depending on the nature of the electrical input to the vehicle, these chargers can be either AC or DC. Furthermore, based on the location of the charger components or stages, they are also divided between onboard and off-board chargers.

Onboard chargers, as the name suggests, are located inside the vehicle, and provide flexibility and simplicity, as they require minimal external equipment besides the power outlet. There are two main types of onboard chargers, depending on whether an exclusive or dedicated power converter is used to charge the batteries as shown in Fig. 4.2a, or if its integrated, by using the existing power converters already available in the power train that drives the power from the batteries to the motor, as shown in Fig. 4.2b.

Dedicated onboard chargers are usually small in power (as illustrated by the size of the DC–AC converter connected to the grid in Fig. 4.2a) due to size and weight limitations of adding additional equipment to the vehicle, and therefore are considered level 1 slow chargers. Dedicated chargers are typically single phase and intended for overnight home AC charging. Integrated chargers, in turn, use the motor drive converters, hence their power ratings are increased, without adding
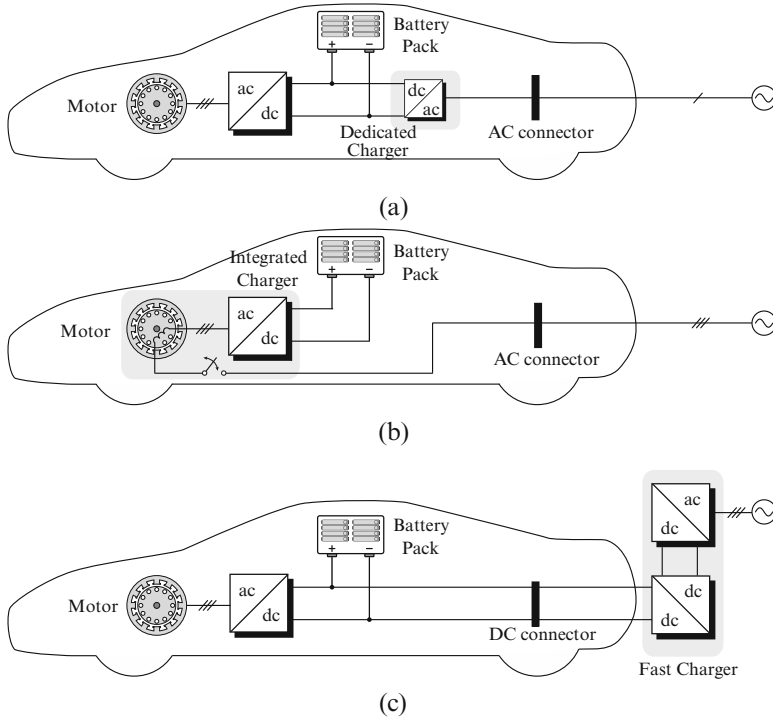
Fig. 4.2 Electric vehicle charging configurations: (**a**) onboard dedicated converter, (**b**) onboard integrated converter, and (**c**) off-board fast charger

cost, size, and weight, while reducing the charging time. This architecture can be found with single- and three-phase grid connection and they are considered both slow and semi-fast level 2 chargers. Their charging time can go from ten to a couple of hours and therefore are targeted for use at home, work, or shopping (parking).

Finally, off-board chargers consist of dedicated charging architectures that reside outside the vehicle as shown in Fig. 4.2c. Because of this reason there are no strict restrictions related to weight and volume, compared to their onboard counterparts. The connection to the vehicle is performed directly to the battery; hence the vehicle connector is of DC nature. The higher converter power capacity allows deliver shorter charging times of less than an hour, hence the name DC-fast chargers and classification as level 3. Because of their size and power levels, they are designed considering a three-phase connection to the grid, and therefore cannot be easily accommodated at home and even work. Instead, they are installed at parking lots and public locations that resemble the conventional gas-filling stations.

Table 4.1 summarizes the main features, parameters, and characteristics of level 1, 2, and 3 chargers, including an example of the hardware required outside the vehicle, to easily recognize which type of charging system that is being used.

Table 4.1 Charging level parameter comparison

Item description	Level 1	Level 2	Level 3
Speed	Slow charging	Slow/semi-fast charging	Fast charging
Charger location	Onboard	Onboard	Off-board
Connection to vehicle	AM	AM	DC
Typical use	Home	Home and work	Charging station
Typical charging time	6–10 h	30 min to 4 h	15-50 min
Power level	1.1 to 3.3 kW	3.3 to 19.2 kW	20-150 kW
Voltage	120 V	208 or 240 V	480 V
Number of phases	Single phase	Single/three phase	Three phase
External equipment	Source: Roperld	Source: Bosch	Source: Blink
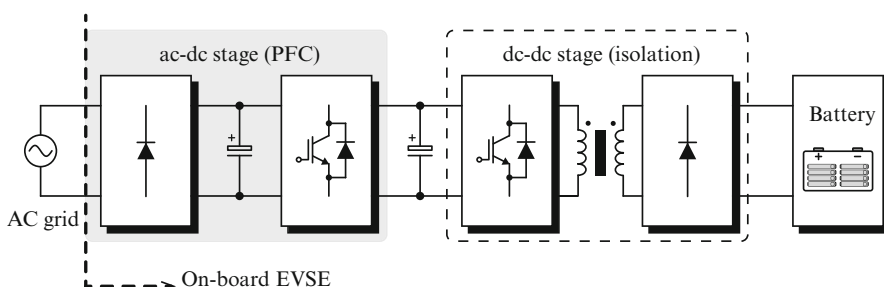
Fig. 4.3 general structure of a two-stage onboard battery charger

4.2 Onboard Chargers

Onboard chargers provide flexibility to the drivers, as they do not require any special equipment other than a traditional power outlet. This allows to charge anywhere, with the drawback that the stringent concerns of cost, volume, and weight of vehicles typically restrict the size and capacity of the charger. Therefore, usually onboard chargers are found for power levels below 3.5 kW [1], and feature long charging times. The general structure of an onboard conductive charger is presented in Fig. 4.3. It can be seen that it is composed by a rectifier stage that also features power factor correction (PFC), for unity power factor operation. Then, this intermediate DC voltage is adapted using a DC–DC stage to the voltage levels required by the battery management system (BMS), which regulates the charging

process [2, 3]. Additionally, the latter stage features high-frequency isolation, in order to isolate the battery from the AC grid for safety issues [3–5]. In the following sections different onboard charger power converter topologies will be analyzed and commented.

4.2.1   Level 1: Dedicated Converter (Slow Charging)

The simplest and most straightforward concept for onboard battery chargers is the use of a dedicated power converter, which exclusively performs the battery charging tasks. As mentioned earlier, these converters are based on a two-stage power conversion structure as shown in Fig. 4.4, where the first generates an intermediate DC voltage while generating a low distortion current and unity power factor at the AC grid side, and the second regulates the battery charging current. Additionally, these onboard chargers include a galvanic isolation towards the main distribution network [3, 4] in order to comply with safety regulations.

The 3.3 kW topology presented in Fig. 4.4a is proposed in [6]. As illustrated, it can be seen that it consists of a two-channel interleaved boost performing the rectification and PFC, which allows to reduce the input and output current ripples and share the input power between the two channels. This is achieved by a phase shift introduced between the PWM carrier signals controlling both boost converters. The reduced current ripple allows a reduction of the size of the boost inductor and the output capacitor, as well as an extension of its life span. Because the power is divided between two boost converters, lower current rated semiconductor devices can be used, which feature shorter commutation times, higher switching frequency, and hence smaller magnetic components, such as the inductor core. Higher capacity chargers can include even more boost converter channels in interleaved connection to allow more power without increasing the size of the converter. The second stage of the charger is a high-frequency (HF) isolated full-bridge DC–DC converter with zero voltage switching. This discontinuous switching mode operation greatly reduces the switching losses, increasing the efficiency of the charger. Operating at rated load, the overall reported efficiency of the system is up to 93.6 % [6].

Following a similar structure, Fig. 4.4b presents an alternative onboard charger [7]. In this topology, the high-frequency isolated DC–DC stage has been changed to a series-loaded resonant full-bridge DC–DC converter, while the PFC stage is composed by a single-phase rectifier bridge and boost converter. As in the previous case, the converter features unidirectional power flow imposed by the diode rectifier and boost converter. The PFC ability provided by the boost converter enables adjustable power factor operation up to 0.995. The HF isolated DC–DC converter requires a special frequency control method for the resonant characteristic that reduces switching losses. The reported efficiency for this topology at rated load is 93 % [7].

A different approach is presented in [8], where the boost PFC stage has been shifted to the lower voltage end in order to reduce the size of the DC-link capacitor
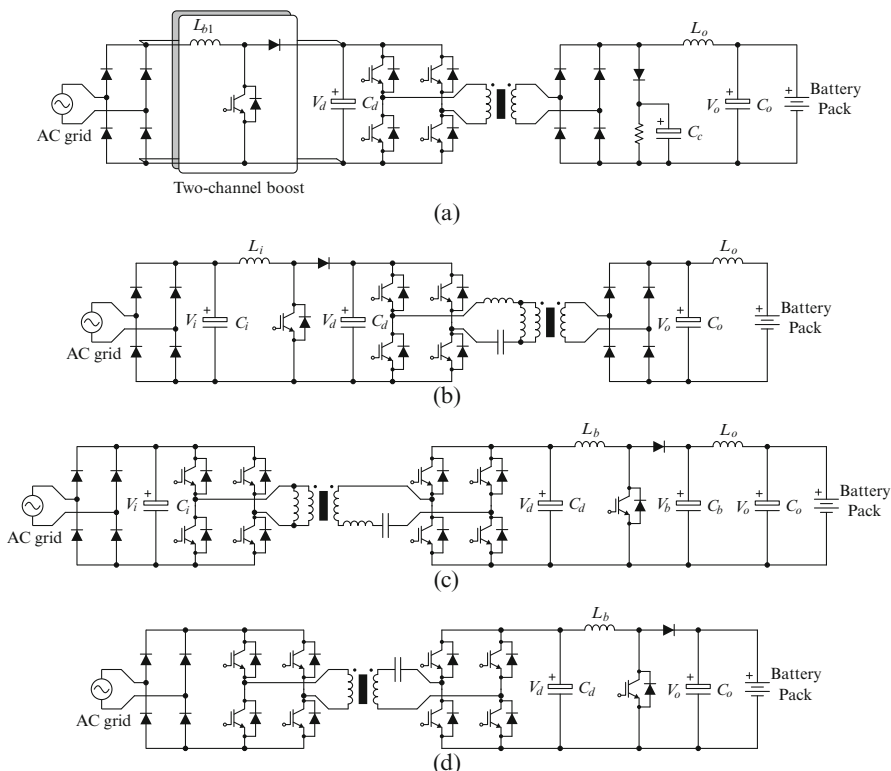
Fig. 4.4 Two-stage onboard chargers with high-frequency galvanic isolation and dedicated charging converter. (**a**) Full-bridge converter with interleaved boost PFC. (**b**) Series resonant converter with boost PFC. (**c**) LLC full-bridge resonant converter with low-voltage boost PFC. (**d**) Uncontrolled LLC resonant converter with low-voltage boost PFC

and extend its life span. As it can be seen in Fig. 4.4c, the 3 kW charger has a reverse structure compared to the conventional two-stage topologies. It uses a passive front end followed by an LLC full-bridge resonant converter that operates with fixed switching frequency, and finally a low-voltage boost PFC stage that performs the output voltage regulation and the harmonic control. This scheme allows to reach an efficiency of 93.6 % with a power factor of 0.996 operating at full load. The reduction on the DC-link voltage allows to replace the electrolytic capacitor with a film capacitor, extending the life span of the converter.

A similar charger structure is shown in Fig. 4.4d, where a cascade structure of a high-frequency resonant converter is employed [9]. The topology is composed of a single-phase rectifier bridge connected in cascade to an uncontrolled LLC resonant converter, which provides the step-down of the voltage while introducing galvanic isolation. This is followed by the second stage which includes a boost converter performing the PFC control. The charger is able to deliver output voltages in the

range from 150 to 450 V, with a peak efficiency of 92.5 %, when operating at full load and with a 220 V input.

As can be appreciated from all the topologies in Fig. 4.4, a common feature of onboard chargers is the galvanic isolation achieved using high-frequency transformers, instead of low-frequency transformers, which would add too much weight and volume to the vehicle. Nevertheless, HF isolation requires more power converter stages through which all the power is transmitted, resulting in additional switching, conduction, and magnetic losses reducing the converter efficiency.

4.2.2 Level 2: Integrated Converter (Semi-fast Charging)

A different approach for onboard chargers is to use part of the drive inverter and machine windings for charging purposes, considering that in normal operation the driving and charging do not happen simultaneously, with the exception of regenerative braking [2]. This has motivated the development of integrated drive system and battery charger. This integration offers the possibility of reducing the problems of additional cost, space, and weight by using a single converter for both driving and charging. Since the power converter used for the drive system is rated at nominal machine power, the same power capacity can be used for charging, increasing the power level compared to dedicated chargers. However, depending on the level of integration, the voltage adaptation, and torque pulsations in the motor during charging, efficiency considerations should be properly addressed. Additionally, the random connection of these higher power chargers in different places of the city has to be taken into consideration, so the grid may absorb the EV charging load properly [10, 11].

As discussed earlier there are different levels of integration regarding onboard battery chargers. This level of integration will depend on whether they use exclusively the power electronics devices of the drive, or also make use of the motor windings.

Among the partially integrated topologies, which fractionally use the power electronics on board as a part of the charging circuit, several topologies have been proposed. The idea is to maximize the usage of the components, leading to a reduction in cost, size, and weight. In this category, the charging circuit is reduced to a single-stage topology that is combined with the bidirectional DC–DC stage, which is also used by the power train. This leads to a further reduction in the size of the converter and the component count; however, as stated earlier, this sets the restriction that the vehicle cannot be charged while driving or it cannot be driven while the battery is being charged.

Despite the two-stage power converter configuration with HF transformer approach appears a mainstream solution for onboard chargers, there is no explicit requirement for such characteristics in standards for safety of EVs as specified in SAE J1772 [12]. This has motivated the research and development of different high-efficiency non-isolated single-stage topologies, which feature important
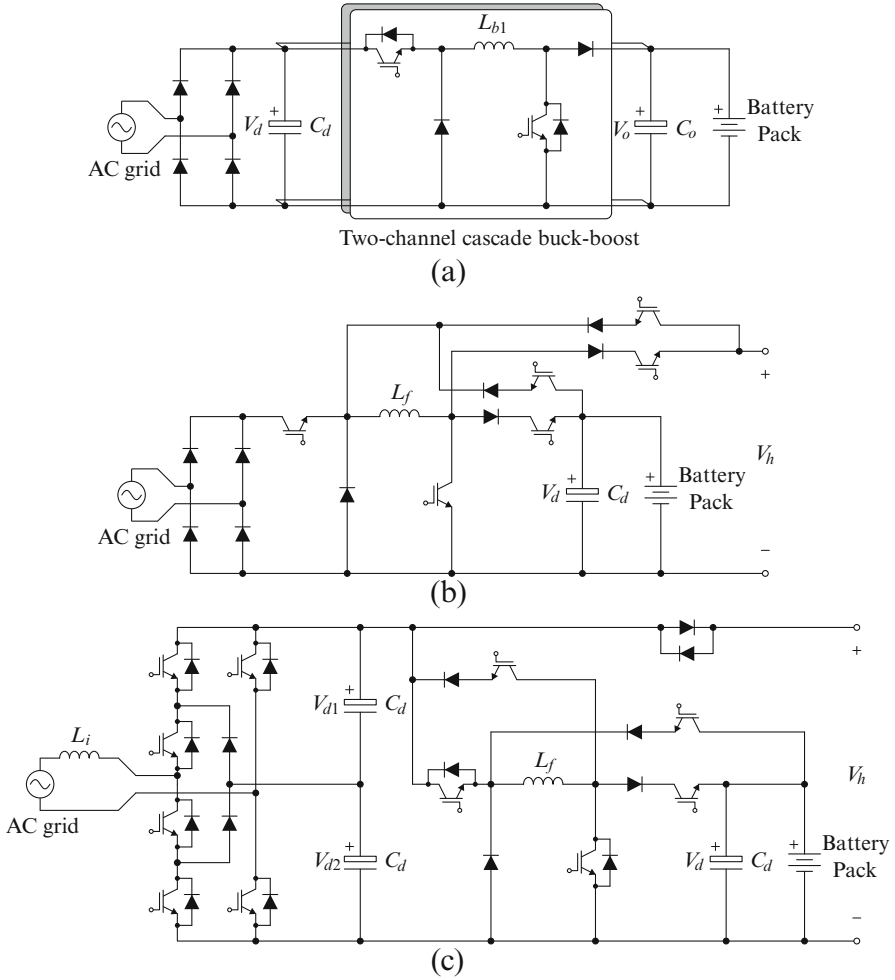
Two-channel cascade buck-boost

(a)

(b)

(c)

Fig. 4.5 Onboard partially integrated charging topologies without galvanic isolation. (**a**) Single-phase rectifier with interleaved buck-boost. (**b**) Bidirectional AC-DC/DC-DC converter for PHEVs. (**c**) Non-isolated buck-boost with a three-level active front end

advantages in increasing the power density and converter efficiency through the elimination of the HF transformer.

The topologies shown in Fig. 4.5 correspond to partially integrated onboard chargers. From the figure it is possible to see that part of the DC–DC converter featured in the topology is already part of the power train; more precisely they provide a voltage ratio conversion between the battery DC voltage and the motor drive inverter DC voltage. They do not use the full power converter and motor windings as the integrated onboard chargers, hence the name.

The non-isolated onboard charger presented in Fig. 4.5a features a diode bridge rectifier, followed by an interleaved buck-boost stage [13]. The two-channel interleaved connection allows reduction in the current and voltage ripples while reducing the size of the converter inductors. The buck-boost converter also provides a wider input and output voltage range. This topology has been reported to be rated at 3.7 kW, with a peak efficiency of 97.6 % and a power factor of 0.99. Since the converter has no HF isolation it requires less converter stages and therefore has a reduced component count compared with previously reviewed onboard chargers.

Another non-isolated buck-boost active rectifier employed as battery charger is shown in Fig. 4.5b. The topology shares the inductor L_f with an integrated bidirectional DC–DC converter [14]. This structure allows to meet the three requirements of the PHEV system: buck-boost operation for the charging of the battery; boost operation from the battery to the higher voltage DC bus of the electric traction system; and buck operation from this bus to the battery for regenerative braking. Is important to mention that this approach assumes that none of the three previous modes happen simultaneously. In comparison with traditional topologies this approach has the drawback of additional losses because of the extra switching devices and also a poor harmonic performance at the AC side if no filter is employed. Aiming to improve the harmonic performance at the grid side, a three-level active front end is incorporated into the charger [15], which along with reducing the total harmonic distortion (THD) below 3% provides a bidirectional power flow allowing vehicle-to-grid (V2G) operation. This comes at the expense of an increased number of switching devices and the need of controlling the midpoint voltage.

A higher level of integrated onboard chargers use the traction inverter together with the motor windings, as shown in the topologies in Fig. 4.6. For this category, the main concern is the minimal addition of external elements to allow the reconfiguration of the circuit aiming to reduce the size and weight of the power electronics used in the vehicle. Moreover, as the motor drive is normally designed for higher power ratings, this approach allows the use of higher charging power levels (i.e., shorter charging times) and either single- or three-phase power outlets.

The idea behind the integrated charger presented in Fig. 4.6a is to use the induction motor (IM) stator leakage inductances as a set of filters, which along with the inverter operate as a boost converter [16]. It can be seen how the drive system is reconfigured with the use of inexpensive relays to operate as a battery charger.

This charger can be fed either by a single-phase supply, as shown in Fig. 4.6a, or the three phases of the converter as an interleaved three-channel boost converter, with the drawback of generating torque in the machine during charging. It is reported that the single-phase alternative has an input voltage in the range of 100–250 V and is rated up to 20 kW.

A similar single-phase concept based on a dual-IM system, either with two machines or using a single one with split phases and two inverters, is shown in Fig. 4.6b. In this topology, the three-phase sets of inductors are connected to the AC grid through the neutral point, acting as a power factor correction DC–DC stage that
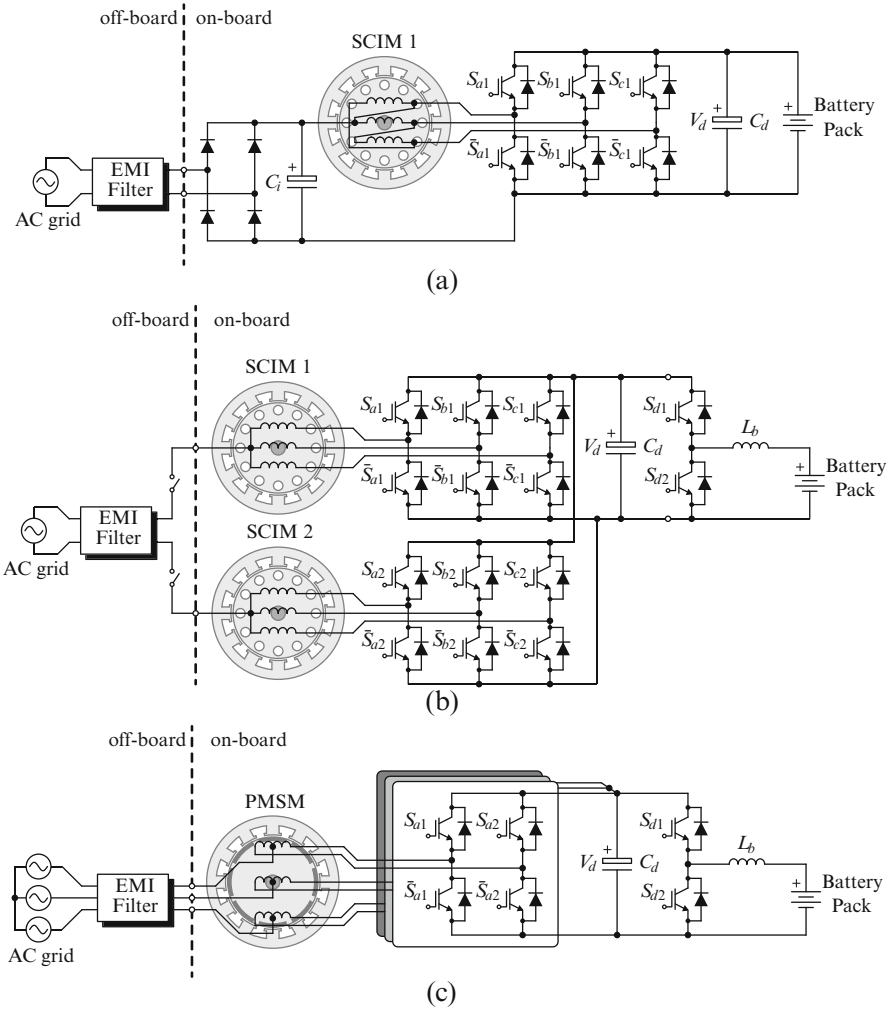
Fig. 4.6 Integrated onboard chargers using the drive inverter and motor windings (part 1).
(**a**) Based on a SCIM. (**b**) Multiphase/Dual SCIM. (**c**) Open-ended PMSM

recharges the battery [17]. This approach has the benefits of allowing a bidirectional
power path and unity power factor operation; however there is no galvanic isolation
provided.

A different integrated charger is presented in Fig. 4.6c, in which each of the split
phases of a permanent-magnet synchronous motor (PMSM) are connected to a dual
set of two-level voltage source converters [18–20]. This generates an intermediate
DC-link voltage V_d that reaches up to 900 V. This voltage is converted by a
bidirectional buck-type DC–DC stage that performs the battery charging. An
additional EMI filter is normally added in order to improve the quality of the grid
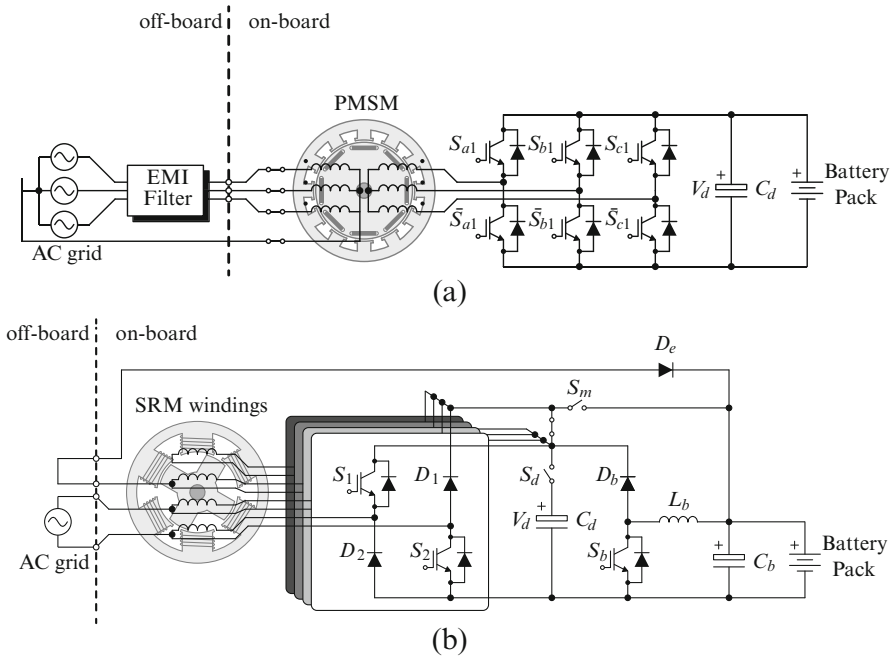
Fig. 4.7 Integrated onboard chargers using the drive inverter and motor windings (part 2). (**a**) Isolated IPMSM combined system. (**b**) SRM based integrated charger

currents. Despite having a total traction power of 40 kW, this scheme limits the battery charging power to only 30 kW.

The use of the split-winding configuration leads to the cancellation of the rotational magnetic field in the motor while charging. Additionally, this scheme does not require any additional relays or contactors, thereby reducing the hardware requirements. This scheme is also available in a single-phase version [21].

Another onboard solution that uses the power train for charging purposes is illustrated in Fig. 4.7a. The approach is based on an interior permanent-magnet synchronous motor (IPMSM) with reconfigurable stator windings [22, 23]. The use of relay-based switching devices and a mechanical clutch allows to use the machine as an isolation transformer connected to the grid and the traction components operate as a battery charger. The IPMSM has six stator windings, which are connected in series in order to constitute a three-phase set, while charging a relay reconfigures these windings as shown in Fig. 4.7a. It can be seen that in this configuration, the drive inverter operates as an active front end, allowing to control the battery voltage, while generating high-quality currents at the AC side. It is important to mention that this scheme does not require a mechanical brake, as the machine rotates freely at synchronous speed, while inducing voltages in the secondary side. For a 25 kW drive system, this charger is restricted to operate at 12.5 kW. The reconfigurable charging system has been patented in [24].

The switched reluctance machine (SRM) has emerged as a promising alternative for the IM or PMSM in drive applications, because of its simple control and robustness. A compact single-phase integrated SRM-based onboard charger is presented in Fig. 4.7b. During charging mode, the switch S_m is connected to the charging point, while S_d remains permanently off (the boost stage connected to the battery pack is not used during charging mode) [25]. Three out of the four phases of the SRM are reconfigured to compose a buck-boost PFC charger; the first two motor windings act as input filters while the third one operates as an energy storage for the SRM converter. This leads to improved power quality at the AC side.

4.3 Off-Board Chargers

The previous sections covered the different charging topologies with a dedicated or integrated power converter installed inside the vehicle, responsible for the charge of the batteries. These onboard chargers provide flexibility and availability, as they only require a conventional power outlet and minimal additional hardware to recharge the battery. Nevertheless, the additional volume and weight on the vehicle limit its power ratings, hence increasing the charging times. An alternative to recharge the battery pack of an EV or PHEV is through the use of a dedicated infrastructure located externally. This offsets weight and volume from the car to the electric vehicle supply equipment (EVSE) which delivers power from the grid to the vehicle.

Additionally, the presence of a vast charging infrastructure network in the future will support the adoption of PEVs, as the availability of quick-charge stations in different parts of the cities will provide drivers more flexibility in using their cars, address range anxiety, and allow occasional longer trips without the need of batteries with larger capacities. This is expected to happen regardless fast charging becomes the main alternative for replenishing batteries or remains as a complementary process to conventional level 1 and 2 charging [26].

The general structure for off-board chargers is illustrated in Fig. 4.8. Depending on the architecture, the chargers are connected to the grid through a transformer, followed by a rectifier stage composed by the input filter to mitigate the grid-side harmonic injection, and the AC–DC stage to control the input currents and generate the regulated DC voltage. Then, a DC-DC converter is connected to this regulated DC voltage, in order to regulate the battery voltage and control its charging currents, following the requirements of the vehicle's BMS. The latter stage does not require galvanic isolation in the presence of a grid-side transformer, as shown in Fig. 4.8a. Finally an output filter for the regulation of the battery current and voltage ripples is included.

In case the galvanic isolation is part of the DC–DC stage, then the off-board charger can eliminate the bulk line frequency transformer, as exhibited in Fig. 4.8b. The differences between the isolation location, and the different converter topologies for both AC–DC and DC–DC stages are discussed next.
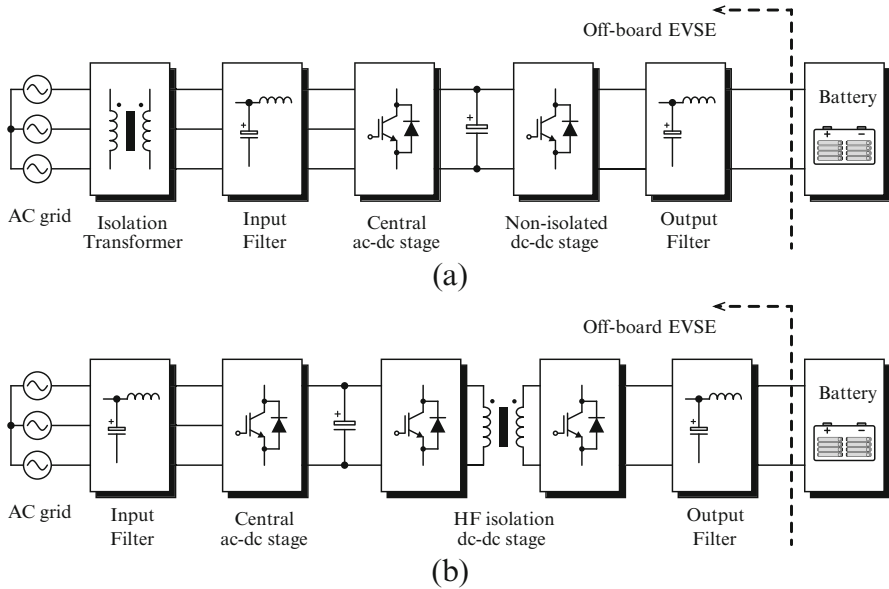
Fig. 4.8 General structure of an off-board battery charger. (**a**) LF isolation. (**b**) HF isolation

4.3.1 Level 3: Dedicated Off-Board DC Chargers (Fast Charging)

4.3.1.1 Concept of Fast-Charging Stations

As established in the previous sections, the fast charging of EVs and PHEVs might not be conceivable as an onboard solution, due to cost, size, and weight constraints in the vehicle. Therefore, studying the concept of a public installation with installed off-board high-power chargers that operates as a filling station is relevant. These stations will provide EVs the equivalent of a *fuel stop* by feeding their batteries directly with DC currents, which refuel the car in the shortest possible time [4]. This concept, along with emerging battery technologies that accept higher charging rates and several thousands of charging cycles, makes fast charging a realistic possibility [27].

Two possibilities can be identified for fast-charging station (FCS) architectures, as shown in Fig. 4.9. The first uses the secondary windings of the step-down/isolation transformer as an AC bus, where each load is connected to the bus via independent AC–DC stages. The second uses a single AC–DC stage in order to provide a common DC bus for all the loads of the system.
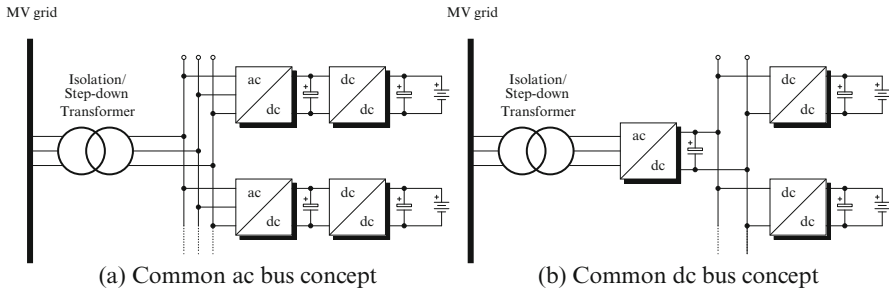
Fig. 4.9 Charging station architectures. (**a**) Common AC bus concept. (**b**) Common DC bus concept

4.3.2 Common AC Bus Architecture

One alternative for the FCS architecture is the use of a common AC bus, as depicted in Fig. 4.9a. In this structure, each charging unit has its own rectifier stage that is connected to a common AC coupling point in the secondary windings of the step-down transformer. This architecture represents a simple concept and has been used for years, and well-developed standards and technologies are available. Furthermore, it needs lower power rating front-end stages, which can be either passive or active.

However, the presence of several battery chargers, with independent rectifier stages and inherent low power-factor operation, may produce unwanted harmonic effects on the utility grid [28, 29], particularly for high-power fast chargers. Moreover, the cost of several converter units with lower power ratings is higher than that of a single high-power converter unit, due to the need of several filter sets, control stages, and sensors.

In addition, in the presence of distributed generation units in the station, such as photovoltaic panels or fuel cells, or even the usage of energy storage systems, will also require their independent AC–DC stage, thereby further increasing the number of the conversion stages in the system and consequently, the cost and complexity of the AC bus architecture.

4.3.2.1 Common DC Bus Architecture

The alternative approach uses a single AC–DC stage with a higher power rating to provide a common DC bus, as illustrated in Fig. 4.9b. This bus feeds several battery chargers and provides a more flexible structure, which can easily integrate distributed renewable energy conversion systems, or energy storage devices, since these systems are essentially DC, as depicted in Fig. 4.10. In addition, the DC connection is characterized by the lack of synchronization and reactive power problems. These features allow the charging station to act as an intelligent system that can mitigate
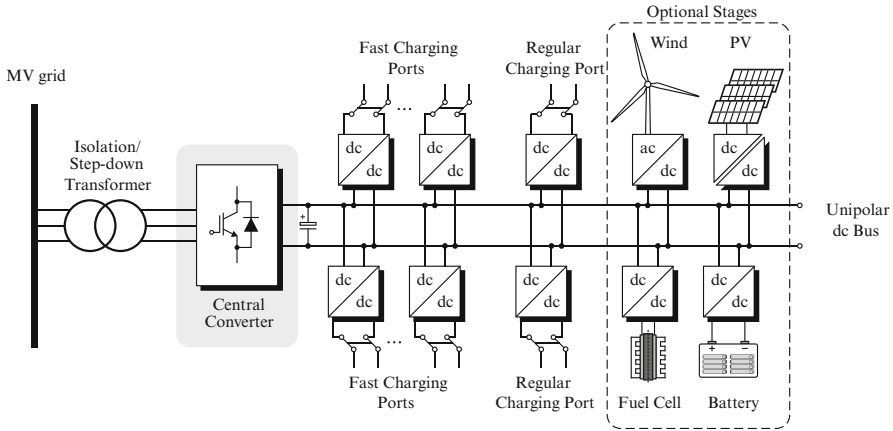
Fig. 4.10 Common DC bus charging station concept with distributed generation microgrid

the negative effects of a deeper EV penetration in the existing utility grid, and also to be a part of a future smart grid.

The system in Fig. 4.10 is better in reducing device count and costs in comparison to the AC bus architecture, as a result of the fewer power conversion stage requirement [30–33], but at the expense of an increase in the power rating of the central grid-tied converter. The lower number of power conversion stages also improves the overall efficiency of the charging station. However, the higher power ratings of the single rectifier unit lead to more stringent requirements by the grid code, in terms of harmonic components amplitude and THD. Moreover, limits are imposed on the switching frequency of the devices because the switching losses become relevant when the power is in the megawatt range. Another issue with the DC bus concept is that it requires more complex protection devices than the AC bus, because no zero crossing of the voltage exists [34].

In general, a much lower number of converters is needed in comparison to the AC bus architecture, making the system simpler. Moreover, energy delivery at DC is characterized by reduced losses and voltage drops in lines [35]. Furthermore, assuming that the DC system has generation units, in case of the abnormal operation of the utility grid, the DC system can be switched to stand-alone operation, and the loads are supplied with the generated power [36].

On the other hand, regarding the application, the current development in DC charging standards [12, 37] also supports the idea of a centralized charging station serving as an active front end and providing DC power to several battery chargers, which can be either semi-fast or fast solutions. In addition, this allows to concentrate these potentially large loads in strategic places to minimize their impact on the grid, as opposed to the case of residential fast chargers that are randomly connected in different areas of the city.

Fig. 4.11 Off-board charger central grid-connected two-level voltage source converter
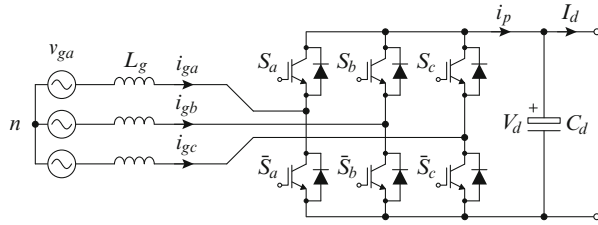
4.3.3   Central Converter Topologies

The central converter stage has a fundamental role in the DC charging architecture of Fig. 4.10, and is desirable to provide several features, such as distortion-free operation, fully adjustable power factor, and reduced size of the input filters, while simultaneously featuring a reduced number in both active and passive components [2, 38]. The following section provides a brief review of the most common converters used as the central converter of the charging station.

4.3.3.1   Two-Level Voltage Source Converter

One of the most widely used topologies in the industry is the two-level voltage source converter (2L-VSC), whose power circuit is presented in Fig. 4.11. As shown in the figure, the circuit consists of an array of six switching devices, typically insulated-gate bipolar transistors (IGBTs) and a DC-link capacitor. The presence of these active switches, along with a proper control scheme, generates sinusoidal currents at the input side, a fully adjustable power factor, and a bidirectional power flow [39]. This converter also steps up the voltage to higher values than the input grid voltages. These characteristics make this topology a valid alternative as the grid-tied converter for a high-power off-board charger [38], or as the central converter of the charging station.

Both carrier-based pulse-width modulation (PWM) and space vector modulation (SVM) can be applied to generate the switching patterns for the 2L-VSC [40]. In addition, variable switching frequency methods, such as table or prediction-based methods, can also be used [41, 42]. As the name suggests, this converter generates a binary pulse train, which alternates between 0 and V_d, whereas the line-to-line voltage presents a three-level waveform. This impacts the THD of the input current, as larger active/passive filters or higher switching frequencies are needed in order to meet the limits imposed by the grid code.

This configuration typically operates at low AC voltage (690 V), which allows a power rating of up to 0.8 MW, without paralleling switching devices or converters, limiting the number of chargers that the station is able to feed. To reduce the current stress on the devices, the converter can be connected to higher AC voltages; however, this also implies a larger DC voltage as well, thereby increasing the
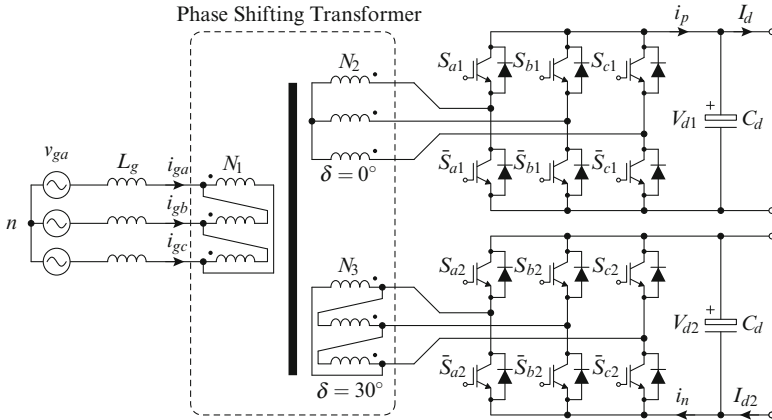
Fig. 4.12 Off-board charger central grid-connected dual two-level voltage source converter

voltage blocking requirement of the devices and the step-down effort of the DC–DC stages of the chargers, which is not desirable since it reduces the conversion efficiency.

Moreover, future megawatt charging stations will also demand higher power ratings for the central grid-tied converter, for which the power ratings, power quality, and efficiency requirements cannot be met using a 2L-VSC. Therefore, the use of several two-level converters is needed, which also means more power electronics, control systems, sensors, filters, larger size, and higher cost.

In order to extend the power ratings of this converter topology, some alternative configurations can be used, which are based in the use of multi-winding transformers. A phase-shifting transformer is included to share the power between two AC–DC stages, as presented in Fig. 4.12. Each 2L-VSC stage is connected to a different secondary winding of the transformer. The presence of this transformer, along with a symmetrical gating pattern of both converters, leads to the significant mitigation of certain harmonic components in the grid currents, in this case those with order $6n \pm 1$, with n odd, which is similar to that achieved when using a diode front end in the 12-pulse configuration [40]. The DC output of the converters can be connected either in parallel, to have a single DC bus, or in series to generate a split DC bus.

Although the phase-shifting transformer significantly improves the power quality at the grid side, the limited power that this topology is able to withstand without paralleling devices is still low for the application. The result is a higher cost of the grid interface assuming a 2 MW charging station, as the paralleling of devices or converters may be needed. In addition, the presence of the transformer is not optional because it is required for the harmonic improvement at the AC side, which results in the higher cost and size of the station even if the fast chargers provide isolation to the battery.
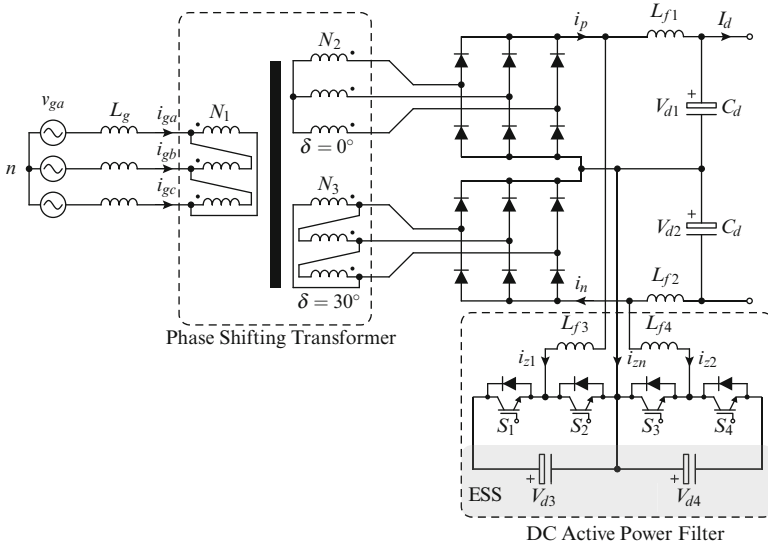
Fig. 4.13 Off-board charger central grid-connected Vienna rectifier

4.3.3.2 Vienna Rectifier

Some authors suggest that in the case of fast charging applications, the bidirectional operation is not mandatory, considering that its main functionality is to charge the batteries as quick as possible and also because vehicle-to-grid (V2G) operation is still not considered as a short-term solution. Therefore, the bidirectional rectifier stage is replaced by a Vienna converter [2, 38]. The power circuit of the converter is shown in Fig. 4.13.

This topology shares the operating principle of stepping up the voltage with the 2L-VSC. It features a lower active switching device count, at the expense of sacrificing the reverse operation characteristics. Moreover, this topology features a highly sinusoidal input current, three-level voltage waveform, reduced voltage stress in the devices, and a high-power factor operation. The input filter size is reduced because of the multilevel voltage waveform [43].

The control scheme is based on controlling the magnetization of the inductor by using high-frequency PWM [38]. One important advantage is that this topology offers operation without a neutral connection. Furthermore, the commutation of diodes takes place as soon as the switches are turned off, which removes any dead-time problems [43]. The disadvantages include the lack of regeneration and relatively high assembly effort exhibited by the circuit when a realization with discrete components is considered. In addition, the high switching frequency required limits its potential for high-power applications.

4.3.3.3 Multipulse Rectifier with DC Active Power Filter

Another approach for central converter considers a nonregenerative 12-pulse decoupled rectifier system which provides the common DC bus for a 1.1 MW charging station [32, 44]. A DC active power filter (DC-APF) stage is also included to eliminate the harmonics at both DC and AC side. The circuit diagram is shown in Fig. 4.14.

Fig. 4.14 Off-board charger central grid-connected multipulse rectifier with DC active power filter

This harmonic cancellation is achieved through the triangular shaping of the currents i_p and i_n. The result is a grid-tied converter with reduced complexity and cost, which generates high-quality sinusoidal input currents. The resulting converter complies with the limits imposed by IEEE 519-1992 standard and produces a DC bus with reduced voltage ripple and improved dynamics.

This topology also includes an energy storage system (ESS), in order to design the converter such that it withstands only the average demanded power, while this additional stage provides the extra power during peak instants.

However, the inability to control the DC bus voltage and the lack of power factor adjustment and regeneration capabilities limit the potential of the charging station, given that it becomes unable to inject power into the utility grid or perform reactive power compensation.

4.3.4 High-Power DC–DC Converters

Once the grid connection and the DC voltage regulation have been performed by the central converter stage, the fast-charging ports must be enabled through the use of high-power DC–DC converters. These converters will have a tremendous impact on the system efficiency and on the charging times. The DC voltage output range remains the same as with conventional charging levels, covering the range from 200 to 600 V; however for the reduction of the charging time, the power ratings are in the range from 50 to 240 kW [3, 4]. Considering this, the cost, efficiency, and

isolation requirements should be properly taken care of. In terms of cost, the size of passive elements can be reduced while featuring higher switching frequencies in the operation of the DC–DC stage or with the use of interleaved topologies [4, 27, 45]. On the other hand, the fast charger efficiency will put strong limitations in the switching frequency, in order to keep the turn-on and turn-off losses within acceptable levels. This has led to the use of soft switching techniques[2, 27, 46, 47].

Finally, the galvanic isolation requirement between the distribution grid and the battery pack will depend on the selected architecture, as it was mentioned earlier that this could be achieve either through a low-frequency transformer at the input side or this could be included in the DC–DC stage with a high-frequency transformer [4, 32]. The following sections cover different high-power DC–DC stages considered for EV and PHEV charging applications.

4.3.4.1   Non-isolated Multichannel Interleaved Buck Converter

The central high-power charging station usually includes an isolation transformer in its AC–DC stage; thereby the galvanic isolation requirement is already covered, leading to the use of non-isolated DC–DC stages [27]. The multichannel interleaved buck converters share the high charging power between multiple modules [4, 27, 45]. Its power circuit is shown in Fig. 4.15a, where it can be seen that three bidirectional buck channels are sharing the output power of the fast charger. By means of this configuration it is possible to reduce the filter size, as the interleaved operation increases the output equivalent frequency. This leads to a smooth output current, which allows the reduction in the output inductor by a factor of $1/n$, for an n-channel converter.

Another advantage of interleaving DC–DC converters is the possibility of power shedding, which is the management of the number of active stages depending on the partial load of the fast charger. This allows to achieve higher efficiencies in a wider load range.

4.3.4.2   Phase-Shifted ZVS Full-Bridge Converter

If the central AC–DC stage does not include an isolation transformer, the DC–DC stage must provide a galvanic isolation stage. In this category falls the phase-shifted ZVS full-bridge converter, which is shown in Fig. 4.15b. This topology uses the parasitic capacitance of the switching devices and the leakage inductance of the HF transformer to conform a resonant tank which is controlled in ZVS operation [38]. It is reported to have higher efficiency than the conventional full-bridge topology in a specific load range. Through the phase-shifting of the switching signals between the converter legs (S_3 and S_4 with respect to S_1 and S_2), the minimization of the oscillations, which take place between the aforementioned inductance and capacitances, is achieved. However, its soft-switching characteristic is only valid over a specific power level, as it depends on the output current.
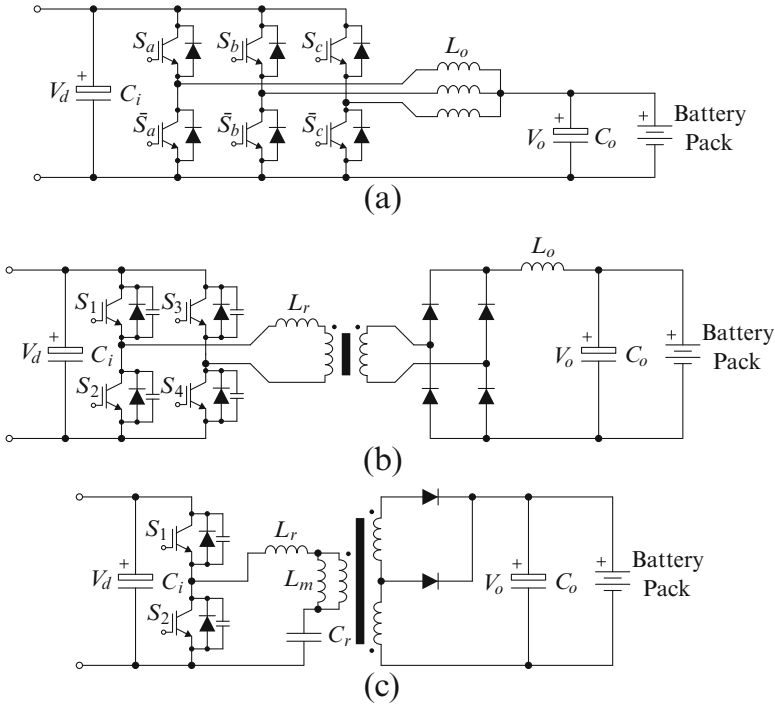
Fig. 4.15 High-power DC–DC stages for off-board fast chargers. (**a**) Non-isolated multi-channel interleaved buck converter. (**b**) Phase-shifted ZVS full bridge converter. (**c**) Half-bridge LLC resonant converter

4.3.4.3 Half-Bridge LLC Resonant Converter

Another option to enable the fast-charging ports in a fast-charging station is the topology illustrated in Fig. 4.15c. The half-bridge LLC resonant converter is composed by an active half bridge at the primary side, followed by three passive components: the resonant inductor L_r, the resonant capacitor C_r, and the magnetizing inductor L_m [38]. The secondary side of the converter is composed by a center-tapped rectifier and the output filter capacitor C_o. This topology features a wide load range for ZVS operation and high efficiency at high input voltage along with no reverse recovery losses. However, the output voltage is a function of the switching frequency, which complicates the design of the transformer and the filter.

4.3.5 Challenges for Fast-Charging Stations

As stated earlier, it is expected that the development of a vast fast-charging infrastructure will have a key role in the large-scale adoption of EVs in the near

future [26]. However, high-power fast charging is a challenging task due to large currents being injected to the battery pack, as well as generating them in a wide output voltage range efficiently [27]. Additionally, this process implies challenges not only to the vehicle itself but also to the distribution system. To start with, the power rating involved in the fast-charging process makes it unlikely to be adopted as an onboard solution because of the requirement for larger, heavier, and costly additional equipment [2, 3]. Furthermore, studies show that conventional overnight charging (AC levels 1 and 2) are expected to remain as the preferred charging method [26]; thus, installing an additional high-power charger on board is not needed. Even if the vehicle features an onboard integrated fast charger, the random connection of high-power fast chargers in different places of the cities will have adverse effects on the utility grid (e.g., demand and energy price increase, voltage stability decreased, power quality issues) [26, 48].

On the other hand, quick charging is not suitable for residential applications due to several reasons. First, dedicated equipment must be installed at the homes, as a result of the increase in the power consumed by the charger in order to reduce the charging time of the battery. In addition, this power consumption exceeds the typical power ratings of the conventional appliances. Moreover, a three-phase power connection is required because of the power levels involved. Furthermore, the electric system in these areas is not designed for high-power levels; therefore, if fast chargers operate in residential areas, then transformers and other distribution elements need to be replaced; otherwise they will be damaged by repetitive overload operation [49]. This additional infrastructure makes the cost of the fast-charging solution excessive, so that a different approach is required.

Finally, from the perspective of the utility grid, a large-scale penetration of EVs results in increased power demand, thereby leading to additional coordination methods of absorbing the EV charging load, and does not merely require having sufficient generation capacity [11]. The reason for this is the stochastic behavior of the EV load, and if this issue is not addressed properly, the actual electric system will be unable to satisfy this demand. For example, a larger EV fleet will require additional operating reserves in order to cope with the increased power demand and the uncertainty associated with the EV charging [26]. This also affects the transformers and lines loading and the protection settings. In order to minimize these effects the addition of generation or energy storage units becomes necessary.

4.4   EV / PHEV charging Standards

A crucial part of the operation of the EVs is the recharging of their battery pack. This process can be carried out in two different ways: conductively or inductively. The first charging method uses electrical contact between the charging port of the vehicle and the charger connector to transfer the energy into the battery pack. The second method uses wireless energy transfer through electromagnetic field coupling, eliminating the plug-in cord [3, 50]. This type of charger has been explored

for level 1 and 2 devices, and is still under development and therefore will not be discussed in detail in this chapter.

Conductive charging has already been adopted by the EV industry, including mainstream EV manufacturers. Depending on the rate at which the EV battery is charged, conductive chargers can be generally classified into slow chargers and fast chargers. The slow or conventional chargers are able to recharge the battery in 8 h, while the fast chargers can do this process within 30 min (although generally not allowed up to full charge). More specifications on the power levels and charging times for the available charging methods can be found in some of the existing charging standards [12, 51].

To regulate and standardize the conductive chargers several organizations, such as the Institute of Electrical and Electronics Engineers (IEEE), the Society of Automotive Engineers (SAE), and the International Electrotechnical Commission (IEC), have been developing standards to regulate the utility/customer interface.

4.4.1   SAE J1772 Standard

The SAE has published the standard SAE J1772™ [12], which defines practices regarding the conductive charging architecture for electric vehicles. This standard defines three charging methods: AC level 1, AC level 2, and AC level 3, aside from the DC fast-charging levels, which are still under development. The details of the charging levels included in SAE J1772 are presented in Table 4.2.

Levels 1 and 2 in general fall into the category of slow charging, except for level 2 DC charging. A European standard IEC 62196 has also been developed promoting different charging levels (up to 690 V AC and 1000 V DC) that are analogous to

Table 4.2 SAE charging configurations and rating terminology (as in [12])

Charging method	Input voltage (V)	Charger location	Power level	Sperm (EV) charging time
AC Level 1	120	Onboard	1.4 kW, 12 A 1.9 kW, 16 A	7 (17) h
[a]DC Level 1	200-450	Off-board	36 kW, 80 A	0.3 (1.2) h
AC Level 2	208-240	Onboard	19.2 kW, 80 A	0.4–3 (1.2–7) h
[a]DC Level 2	200-450	Off-board	90 kW, 200 A	10 (20)
AC Level 3	208-240	Onboard	96 kW, 400 A	(15)
[a]DC Level 3	200-600	Off-board	240 kW, 400 A	(<10) min

EV (25 kWh usable pack size) charging always starts at 20 % SOC, faster than a 1C rate will also stop at 80 % SOC instead of 100 %

PHEV (10 kWh usable pack size) can start from 0 % since the hybrid mode is available

[a] Not finalized

those in SAE J1772. Additionally, there is an ongoing coordination between the two standards in order to develop a combined charging system (CCS)[52].

4.4.2 CHAdeMO Standard

Other than the SAE and IEC standards, an association named CHAdeMO proposed a quick charging method as a global industry standard. The name CHAdeMO is an abbreviation of *Charge de Move*, equivalent to *charge for moving* [37].

CHAdeMO was formed by Tokyo Electric Power Company (TEPCO), Nissan, Mitsubishi, and Fuji Heavy Industries. Toyota later joined as its fifth executive member. TEPCO has developed a patented technology and a specification for high-voltage high-current automotive fast charging via a DC fast charge connector from the Japan Automotive Research Institute (JARI). The connector from JARI is apparently the basis for the CHAdeMO protocol. Additionally, its technical specifications are provided by the Japan Electric Vehicle Standard (JEVS) G105-1993 from the JARI.

The maximum output compatible with CHAdeMO protocol is 500 V/125 A, with power reaching 62.5 kW.

At present, this standard is gaining wide acceptance, and several leading industrial manufacturers are commercializing CHAdeMO standard DC fast chargers (e.g., ABB-Terra 53CJ, Fuji Electric—FRCH50B-2-01, Siemens—CP300D3xB05-4xxx). According to [37], over 10000 chargers and more than 57,000 compatible EVs are available on the road around the world. Additionally, there are ongoing efforts of increasing the charging power ratings above 150 kW [37].

4.5 Control Schemes for Charging Converters

The following sections covers the main control schemes used for the regulation of the different converters involved in the charging process of the battery. First, the main schemes used for the grid-tied AC–DC stages, both single and three-phase approaches, followed by the regulation of the DC–DC stage that performs the charging of the battery pack, are given.

4.5.1 AC–DC Converter Control

The main function of a grid-tied power converter is to generate a regulated DC voltage, and control the grid currents (active and reactive power). However, the requirements for these converters have increased through time because of more stringent grid codes and the increased use of generated electric energy to feed loads

through rectifier stages, traditionally based on diodes and thyristors, thereby increasing the presence of harmonic currents in the utility grid. Some of these additional requirements are as follows:

- The reduction of the harmonic content because of its negative effect on the electric system (e.g., voltage distortion, electromagnetic interference, increased power ratings of power system equipment)
- Adjustable power factor
- Bidirectional power flow

The emergence of these requirements has resulted in new challenges for the control schemes and has prompted researchers to improve them to meet the control objectives and at the same time maintaining high performance.

4.5.1.1 Single-Phase AC–DC Converter Control

The voltage-oriented control (VOC) for single-phase grid-tied converter control scheme is presented in Fig. 4.16. It can be seen that the outer control loop regulates the DC-link voltage V_d, using a linear proportional integral (PI) controller, while the inner one regulates the grid-side current i_g with a proportional resonant (PR) controller, given the sinusoidal nature of this variable. Additionally, in order to avoid the distortion of the grid current reference, a notch filter with a cutoff frequency of $2\omega_g$ is needed in the feedback of DC-link voltage V_d due to the rectified power pulsation that generates voltage ripples with twice the grid frequency. Finally, to ensure the unity power factor operation, a phase-locked loop (PLL) is used for the synchronization with the grid voltage v_g.
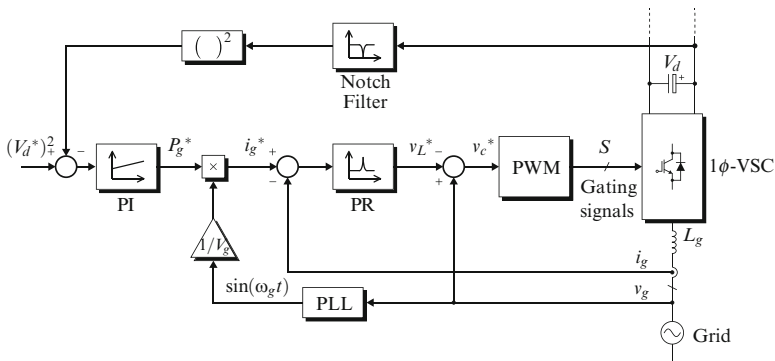
Fig. 4.16 Single-phase AC–DC converter-stage VOC control scheme

4.5.1.2 Three-Phase AC–DC Converter Control

Regarding the regulation of a three-phase grid-tied voltage source converter, the problem is similar to the generation of a controlled AC waveform from a DC power supply. In fact, a dual version for the rectifier side exists for all of the inverter control schemes [53]. However, two mainstream schemes dominate the industry applications: voltage-oriented control (VOC) and direct power control (DPC).

Voltage Oriented Control

Derived from the flux-oriented Control (FOC) of an induction motor [54], VOC is based on a cascade control structure and a coordinate transformation between the $\alpha\beta$ stationary frame and the dq synchronous frame. The result is fast transient response and high static performance, with no steady-state error, as a result of the DC nature of the controlled quantities [41].

The VOC block diagram is presented in Fig. 4.17. As displayed in the figure, the measured signals are transformed to the synchronous frame, using a PLL for proper synchronization with the grid voltage vector v_g. This synchronization leads to the decomposition of the current vector i_g into the orthogonal components i_{gd} and i_{gq}, which are related with the AC-side active P_g and reactive power Q_g, respectively. In addition, the outer DC voltage loop indirectly generates the active power reference, through i_{gd}^*, whereas i_{gq}^* can be set arbitrarily depending on the application requirements, usually set to zero for unity power factor operation.

Both the dq current components and the DC-link voltage V_d are regulated using PI controllers, as they are DC variables, which lead to zero steady-state tracking

Fig. 4.17 Three-phase AC–DC converter-stage VOC control scheme

errors. Finally, the actuations of the currents PI are transformed back into a three-phase coordinate frame and then given to the modulation stage. This modulation stage can be either PWM or SVM, for the generation of the gating signals. For its application to multilevel converters, the basic structure of VOC is kept, and this latter stage is changed accordingly [55].

Additionally, in order to facilitate the controller design, the elimination of the cross-coupling between the synchronous components of the input current and a decoupling block is necessary. To solve the problem, a decoupled controller shown in Fig. 4.17 can be implemented.

Direct Power Control

Given that the direct torque control (DTC) regulates directly the torque and flux of an inverter fed induction machine using a switching table, it is possible to extend the same operating principle and control the active power and reactive power at the input of a grid-tied converter. This scheme is called direct power control (DPC) [56]. The performance of this method can be improved by using the virtual flux concept [57], which results in the virtual flux direct power control (VFDPC).

The control scheme is shown in Fig. 4.18. The scheme is also based on the cascade control structure, except that the inner loop controller is nonlinear. The DC-link voltage V_d is controlled by a linear PI controller, which provides the reference for the active power P_g^*, whereas the reactive power reference Q_g^* can be set arbitrarily. Both powers are estimated from measurement feedback and controlled with nonlinear hysteresis comparators. Its outputs h_P and h_Q along with θ_s are used to access the voltage vector lookup table. Finally, the table delivers
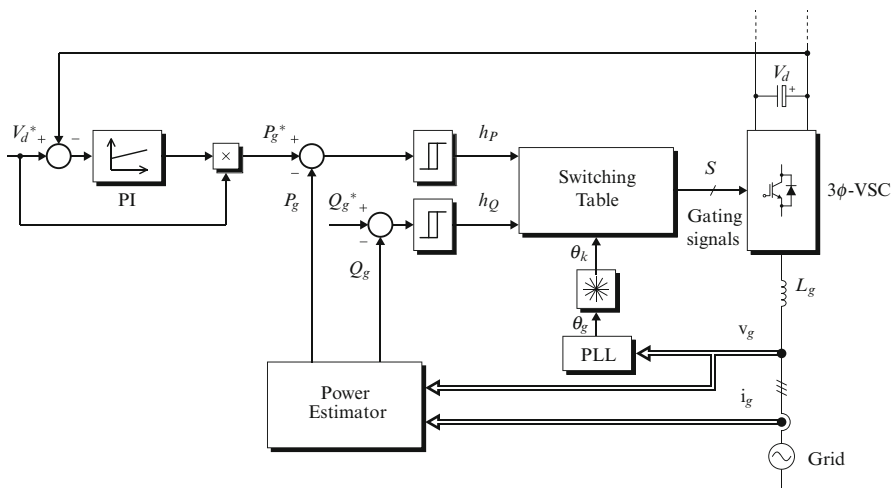
Fig. 4.18 Three-phase AC–DC converter-stage DPC control scheme
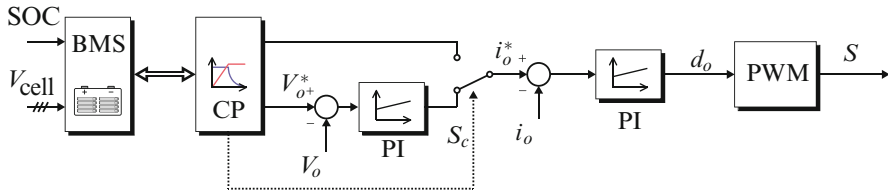
Fig. 4.19 Battery-side DC–DC converter control scheme

the gating signals to generate the selected voltage vector. Although this method is designed for the conventional 2L-VSC, some adaptations for the multilevel converters exist [58–61].

4.5.2 DC–DC Converter Control

Finally, the conventional control scheme for the DC–DC power conversion is shown in Fig. 4.19. Once again the cascaded control architecture can be observed, using exclusively linear PI controllers for regulating the battery voltage and current. In order to safely recharge the battery, this control scheme communicates with the battery management system (BMS) of the vehicle, which sets the charging profile (CP) and the reference signals. The most conventional charging profile is called constant current–constant voltage mode [38], and it basically divides the charging process into two segments: the first one injects the maximum allowed current to the battery, hence bypassing the outer voltage loop, until a certain voltage threshold is reached; the latter one changes to voltage control mode, where the outer loop sets i_{or}^* which exponentially decays as the battery reaches its full charge. The transition between these two modes is also controlled by the BMS, depending on the battery state of charge (SOC).

4.6 Latest Developments and Future Trends

4.6.1 Inductive Charging

The conductive charging is not the only method to recharge the batteries inside the PEV. An alternative to this is through the magnetic power transfer, which is also known as inductive power transfer (IPT). In such systems, the power is transferred from the primary coil to the secondary coil through electromagnetic induction, as demonstrated by Nikola Tesla in 1891 [5, 62, 63]. Even though it is hard for such systems to match the efficiency or power ratings of conductive chargers, this family of devices provides several features: they can be completely autonomous while
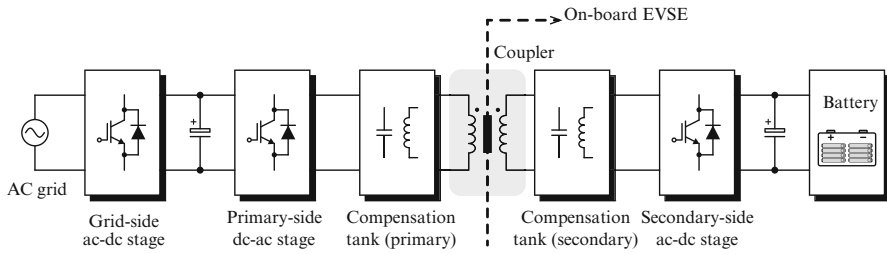
Fig. 4.20 General structure of a loosely coupled inductive battery charger

providing a safer charging process (e.g., cables and cords have been eliminated, galvanic isolation, no risks of electric sparks, higher reliability). Moreover, the inductive charging allows to recharge the battery while the vehicle is moving, thereby reducing the battery size and the requirement for fast-charging infrastructure.

Two categories can be identified in IPT chargers, based on the coupling existing between the two coils: closely or tightly coupled systems, like a transformer or an induction motor; and loosely coupled systems, which use the air as coupling medium instead of a common core made of ferromagnetic materials. Given the physical separation between primary and secondary sides, loosely coupled systems have the advantage of free movement with one respect to the other, making it suitable for EV charging applications. Additionally, the inherent lack of galvanic contact is an obvious advantage, from the perspective of safety, reliability, low maintenance, and long product life [64, 65].

The typical structure of a loose IPT is presented in Fig. 4.20. It can be seen that it is composed by an indirect AC–AC conversion stage, typically a rectifier with PFC capability and an inverter generating a high-frequency output. This stage is followed by a compensation tank, which is a combination of reactive elements (inductors and capacitors) helping to reduce the stress in the coupling inductor, distributing the VA ratings between more components [63].

Then, on the secondary side, another compensation tank is implemented before the final AC–DC conversion stage, which shapes the current for the battery pack. Additionally, this secondary side could be either stationary or moving with respect of the primary side [3]. The latter category leads to the road-embedded charging concept [66–69], which allows to supply power to the vehicle while it is moving. With this system, the electric vehicle is charged on the road by wireless power charging, and the battery can hence be downsized and no waiting time for charging is needed. The study in [69] reports a 100 kW road-embedded charger with an efficiency of 80 %.

4.6.2 Multilevel Converters

The remainder of this section gives an overview of the most relevant high-power converter topologies that are widely used in the industry. However, despite the potential benefits of these topologies for EV applications, they have not been fully applied to produce EV fast-charging solutions.

4.6.2.1 Cascaded H-Bridge Converter

Among the multilevel converter topologies, the cascaded H-bridge (CHB) is currently one of the most widely used topologies in MV applications. As its name indicates, the CHB is composed by the series connection of single-phase full-bridge converters (HBs). Each one of these cells enables an independent DC voltage, as displayed in Fig. 4.21. One of the main features of the CHB is its modularity; it can easily reach medium voltage by adding more power cells to each phase. This particular topology is commercially available to reach different voltage levels: 3.3 kV (3 cells per phase), 6.6 kV (6 cells per phase), and up to 11 kV (11 cells per phase).

In [70], a CHB-based architecture is proposed to enable the fast charging of several EVs. The architecture uses the CHB as the grid interface, which is directly connected to the MV AC grid, intermediate ESSs as power buffers, and interleaved dual-half-bridge DC–DC converters as fast-charging units. No issues with the asymmetrical operation have been found because of the connection of the DC–DC stages. This configuration makes the three phases of the converter to always deliver the same power. However, to increase the number of charging units three

Fig. 4.21 Grid-connected cascaded H-bridge converter
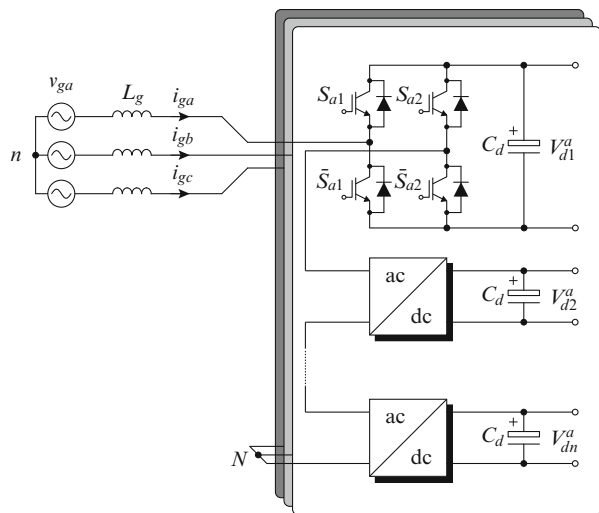
additional cells, with their corresponding energy buffer and isolated DC–DC, stages must be considered, which consequently limits the modularity offered by the CHB.

4.6.2.2   Modular Multilevel Converter

One of the most promising multilevel converter topologies for medium- and high-voltage high-power applications is the modular multilevel converter (MMC) [71, 72]. The generalized structure of modular multilevel converter is displayed in Fig. 4.22, which consists of several two-level full-bridge submodules in cascade. The number of submodules in each phase is increased to achieve the higher operating voltage without the use of a transformer. Additionally, the higher number of submodules leads to better input power quality, as the voltage and current waveforms have minimal total harmonic distortion values. The main features of this converter are high modularity, common DC bus, possibility of back-back operation, and direct connection to the high-voltage network without transformer [71, 72].

In [73] an integrated charging system based on the use of a split-winding configuration motor and a battery-based split integrated storage (SIS) is presented.

Fig. 4.22 Grid-connected MMC-based integrated charger for split integrated battery pack
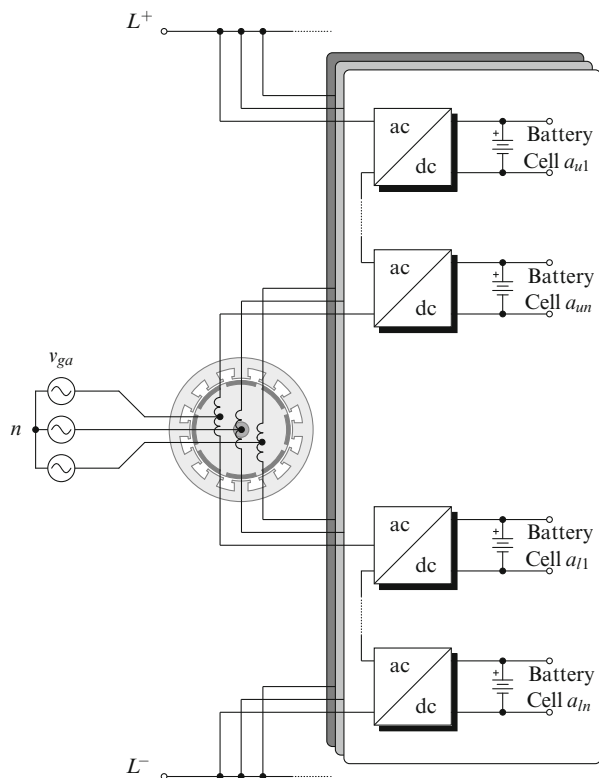
As it is displayed in Fig. 4.22, during the charging mode the stator windings of the machine are used as the input filter of the MMC, while each cell of the converter feeds a module of the split battery pack. The result is a configurable MMC, which performs the traction, charging of the battery, and also the balancing of the battery cells. The result is a converter that offers modularity, flexibility, a bidirectional power flow, and enhanced efficiency given the active balancing of the battery. The concept allows a universal and flexible charging, allowing higher power ratings and increased power quality at the input side. This has been validated in driving mode and in charging mode as reported in [73].

4.6.2.3 Neutral-Point Clamped Converter

The three-level neutral-point clamped converter is currently one of the dominant topologies in MV drives. Its wide presence in the industry makes it a natural candidate for EV charging applications. Originally introduced at the beginning of the 1980s [74], the three-level NPC is considered to be the first multilevel converter to be used in MV applications. At present, commercial NPCs reach voltages in the range of 2.2–6.6 kV, within a wide power rating range (3–50 MW), and these NPCs can be found in several processes, which are used either as an inverter that feeds an AC load or as an active front-end converter that interfaces with the utility grid [75].

A different DC bus concept to enable high-power fast charging is proposed and validated in [31]. The structure is based on the use of a central NPC converter enabling a bipolar DC bus, which is shown in Fig. 4.23. The use of this split DC bus provides flexibility to the connection of the loads, has higher voltage and power handling capabilities, has reduced step-down effort of the DC–DC stages. However, given the adoption of the bipolar structure and the intended application, the balance
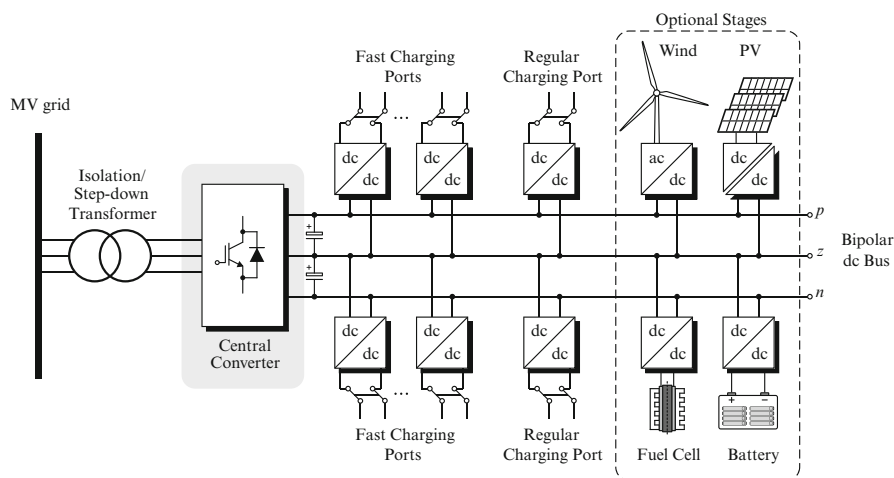
Fig. 4.23 Fast-charging station architecture with bipolar DC bus
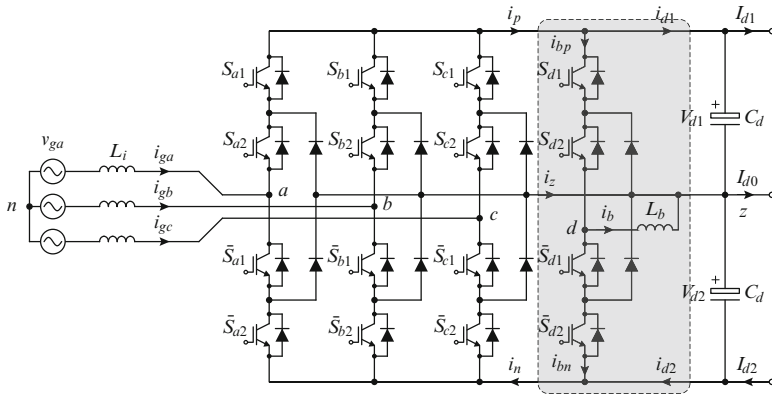
Fig. 4.24 Dual DC bus three-level NPC central converter with a balancing leg
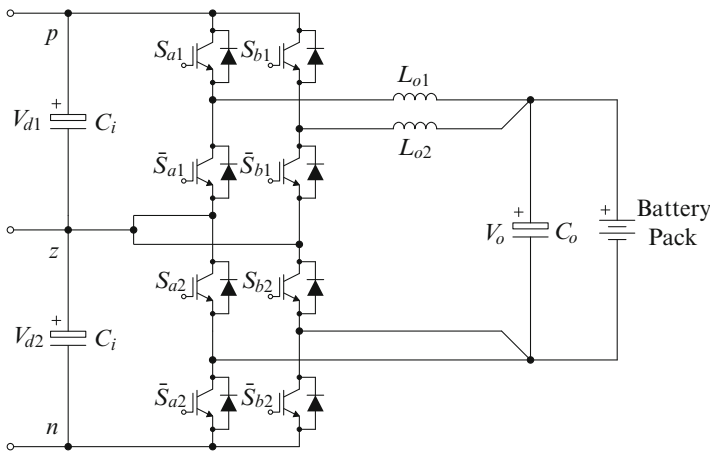
Fig. 4.25 Two-channel interleaved three-level DC–DC converter for EV fast charging

control becomes essential. In [31] this was done by adding an additional circuit to the system, which enhances the balancing capabilities of the grid-tied converter. The converter topology is presented in Fig. 4.24, where it can be seen that a fourth leg has been added in order to perform the additional balancing functions. The result led to balanced DC voltages even under severe unbalanced load conditions.

Regarding the DC–DC stage, this converter has also been considered for EV fast charging. In [76] a two-channel interleaved three-level DC–DC converter unit is proposed to operate as a level 3 charger. The converter shown in Fig. 4.25 is able to handle the high charging current, and given the three input terminals it directly fits the bipolar DC bus of the central charging station shown in Fig. 4.23. In addition to improving the output power quality, reducing the current stress and the filter size, and its modularity, this three-level topology can assist the central NPC to perform
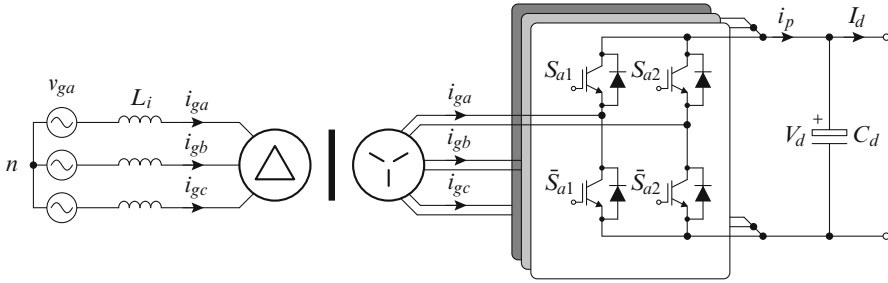
Fig. 4.26 Three-phase H-bridge central converter

the DC power balancing, allowing to improve the overall system efficiency and the grid-side currents. However, as it is a non-isolated structure, it requires an LF isolation stage at the line side of the central converter to provide galvanic isolation between the battery and the grid.

4.6.2.4 Single DC-Link H-Bridge Converter

The work in [77] proposes a different concept of interfacing a common DC bus charging station, where open-end secondary winding transformers are used, along with two 2L-VSC stages, in order to generate a single DC-link H-bridge converter, as presented in Fig. 4.26. This approach leads to a multilevel waveform generated at the AC side, which improves the power quality while eliminating any possibilities of asymmetrical DC loads. Additionally, this configuration reduces the requirements on the DC-link voltage, allowing to reduce the step-down effort of the DC–DC stages that are performing the fast charging of the batteries. However, its power handling capabilities are still limited for the intended power ratings of the FCS.

4.7 Summary

A general overview of the EV and PHEV charging architectures has been provided in this chapter. Depending on the charging power levels, additional equipment, location, and the time required to recharge the battery pack, different approaches are available. First, the most simple and straightforward way to recharge the battery is through a dedicated onboard charger, which provides the flexibility of only requiring the minimal external equipment to perform this task, i.e., a conventional power outlet. However, given the onboard location of this equipment, it is strongly limited in terms of cost, size, and weight, thereby limiting its power rating to be less than 3.3 kW. Considering the high-energy batteries present in the EVs, this kind of chargers take several hours to fully replenish the battery.

The next category uses part of the drive train to perform the charging of the battery. This is based on the premise that, with the exception of regenerative braking, the driving and charging tasks do not happen simultaneously, therefore allowing to use the idle equipment for charging purposes. Integrated chargers have the benefit of reducing the additional equipment for recharging the battery, along with higher power capability, as typically the drive has higher power ratings. This approach also features either single- or three-phase solutions, allowing to reduce the charging times to only a few hours.

Finally, the fastest charging methods require the use of dedicated EVSE located off-board the vehicle. By means of off-loading the cost, volume, and weight from the vehicle higher power levels can be reached (over 50 kW). Considering the particularities of the fast charging process, the implementation of this charging method is using the concept of public and commercial installations similar to conventional gas-filling stations. However, the design, operation, and location of these stations must be addressed properly in order to avoid altering the stability of the utility grid.

The chapter continues with a brief review of the main charging standards. The North American standard clearly defines three charging levels, which are categorized depending on its power ratings, location, and charging times: level 1 chargers are intended for home overnight charging, using a common household type and a reduced power rating that completes a full charge in 8 h or more, and level 2 increases the power ratings, using single- and three-phase approaches, which enable the charging either at home or at working places and reduce the charging time to a couple of hours. Finally level 3 charging employs dedicated equipment for restoring up to 80 % of the battery SOC within 30 min.

Then, the state-of-the-art control methods for the different power converter stages involved in the charging architectures are covered. First, the gird connection methods are analyzed, both single- and three-phase solutions, covering the additional objectives that this equipment has considering the large-scale penetration of nonlinear loads in the system. Then, the general DC–DC stage control scheme is depicted.

Finally, future trends in charging architectures are covered. In order to replace the conductive charging methods, different inductive power transfer methods are being developed. First, stationary IPT methods consider both the transmitting and receiving ends to be still while the charging takes place. Additionally, moving IPT methods consider the receiving end to be in constant moving, leading to the road-embedded charging methods. Despite the reduced efficiency and power ratings, IPT alternatives to recharge the offers attractive benefits that may lead to a reduction in the necessity for fast-charging stations and also smaller battery packs in the vehicles. Additionally, the application of high-power medium-voltage converters to fast-charging applications is covered. The improved power quality, efficiency, and higher power handling capabilities along with its proven high performance in other power conversion areas make this family of converters the natural candidate to enable quick-charging ports through the cities under the charging station concept.

References

1. Haghbin S, Lundmark S, Alakula M, Carlson O (2013) Grid-connected integrated battery chargers in vehicle applications: review and new solution. IEEE Trans Ind Electron 60 (2):459–473
2. Khaligh A, Dusmez S (2012) Comprehensive topological analysis of conductive and inductive charging solutions for plug-in electric vehicles. IEEE Trans Vehicular Technol 61 (8):3475–3489
3. Yilmaz M, Krein PT (2013) Review of battery charger topologies, charging power levels, and infrastructure for plug-in electric and hybrid vehicles. IEEE Trans Power Electron 28 (5):2151–2169
4. Aggeler D, Canales F, Zelaya-De La Parra H, Coccia A, Butcher N, Apeldoorn O (2010) Ultra-fast DC-charge infrastructures for EV-mobility and future smart grids. Gothenburg, Sweden, pp 1–8
5. Aditya K, Williamson SS. Design considerations for loosely coupled inductive power transfer (IPT) system for electric vehicle battery charging—a comprehensive review. In: Transportation Electrification Conference and Expo (ITEC), 2014 IEEE, June 2014, pp 1–6
6. Gautam DS, Musavi F, Edington M, Eberle W, Dunford WG (2012) An automotive onboard 3.3-kw battery charger for PHEV application. IEEE Trans Vehicular Technol 61 (8):3466–3474
7. Kim J-S, Choe G-Y, Jung H-M, Lee B-K, Cho Y-J, Han K-B (2010) Design and implementation of a high-efficiency on-board battery charger for electric vehicles with frequency control strategy. In: Vehicle Power and Propulsion Conference (VPPC), 2010 IEEE, Sept 2010, pp 1–6
8. Chae H-J, Moon H-T, Lee J-Y (2010) On-board battery charger for PHEV without high-voltage electrolytic capacitor. Electron Lett 46(25):1691–1692
9. Chae HJ, Kim WY, Yun SY, Jeong YS, Lee JY, Moon HT (2011) 3.3 kw on board charger for electric vehicle. In: 2011 I.E. 8th International Conference on Power Electronics and ECCE Asia (ICPE ECCE), May 2011, pp 2717–2719
10. Bae S, Kwasinski A (2012) Spatial and temporal model of electric vehicle charging demand. IEEE Trans Smart Grid 3(1):394–403
11. Qian K, Chengke Z, Allan M, Yuan Y (2011) Modeling of load demand due to EV battery charging in distribution systems. IEEE Trans Power Syst 26(2):802–810
12. SAE electric vehicle and plug in hybrid electric vehicle conductive charge coupler (2012) SAE Std. J1772, Oct 2012
13. Oh C-Y, Kim D-H, Woo D-G, Sung W-Y, Kim Y-S, Lee B-K (2013) A high-efficient nonisolated single-stage on-board battery charger for electric vehicles. IEEE Trans Power Electron 28(12):5746–5757
14. Lee Y-J, Khaligh A, Emadi A (2009) Advanced integrated bidirectional ac/dc and dc/dc converter for plug-in hybrid electric vehicles. IEEE Trans Vehicular Technol 58 (8):3970–3980
15. Onar OC, Kobayashi J, Erb DC, Khaligh A (2012) A bidirectional high-power-quality grid interface with a novel bidirectional noninverted buck-boost converter for PHEVs. IEEE Trans Vehicular Technol 61(5):2018–2032
16. Rippel WE (1990) Integrated traction inverter and battery charger apparatus. US Patent 4,920,475, 24 Apr 1990
17. Rippel WE, Cocconi AG (1992) Integrated motor drive and recharge system. US Patent 5,099,186, 24 Mar 1992
18. De Sousa L, Bouchez B (2011) Combined electric device for powering and charging. US Patent App. 13/127,850, 15 Sept 2011
19. De Sousa L, Silvestre B, Bouchez B (2010) A combined multiphase electric drive and fast battery charger for electric vehicles. In: Vehicle Power and Propulsion Conference (VPPC), 2010 IEEE, Sept 2010, pp 1–6

20. Bruyre A, De Sousa L, Bouchez B, Sandulescu P, Kestelyn X, Semail E (2010) A multiphase traction/fast-battery-charger drive for electric or plug-in hybrid vehicles: solutions for control in traction mode. In: Vehicle Power and Propulsion Conference (VPPC), 2010 IEEE, Sept 2010, pp 1–7

21. Lacroix S, Laboure E, Hilairet M (2010) An integrated fast battery charger for electric vehicle. In: Vehicle Power and Propulsion Conference (VPPC), 2010 IEEE, Sept 2010, pp 1–6

22. Haghbin S, Lundmark S, Alakula M, Carlson O (2011) An isolated high-power integrated charger in electrified-vehicle applications. IEEE Trans Vehicular Technol 60(9):4115–4126

23. Haghbin S, Khan K, Zhao S, Alakula M, Lundmark S, Carlson O (2013) An integrated 20-kw motor drive and isolated battery charger for plug-in vehicles. IEEE Trans Power Electron 28 (8):4013–4029

24. Alaküla M, Haghbin S (2011) Electrical apparatus comprising drive system and electrical machine with reconnectable stator winding. WO Patent App. PCT/SE2011/050,745, 22 Dec 2011

25. Chang H-C, Liaw C-M (2009) Development of a compact switched-reluctance motor drive for EV propulsion with voltage-boosting and PFC charging capabilities. IEEE Trans Vehicular Technol 58(7):3198–3215

26. Silva V, Kieny C (2011) Impacts of EV on power systems and minimal control solutions to mitigate these. Essen, Germany, RWE Deutschland AG. http://www.g4v.eu/downloads.html

27. Christen D, Tschannen S, Biela J (2012) Highly efficient and compact DC-DC converter for ultra-fast charging of electric vehicles. In: 2012 15th International Power Electronics and Motion Control Conference (EPE/PEMC), Sep 2012, pp LS5d.3–1–LS5d.3–8

28. Chan CC, Chau KT (1997) An overview of power electronics in electric vehicles. IEEE Trans Ind Electron 44(1):3–13

29. Gomez JC, Morcos MM (2003) Impact of EV battery chargers on the power quality of distribution systems. IEEE Trans Power Del 18(3):975–981

30. Du Y, Zhou X, Bai S, Lukic S, Huang A (2010) Review of non-isolated bi-directional DC-DC converters for plug-in hybrid electric vehicle charge station application at municipal parking decks. Palm Springs, CA, USA, Feb 2010, pp 1145–1151

31. Rivera S, Wu B, Kouro S, Yaramasu V, Wang J (2015) Electric vehicle charging station using a neutral point clamped converter with bipolar DC bus. IEEE Trans Ind Electron 62 (4):1999–2009

32. Bai S, Lukic SM (2013) Unified active filter and energy storage system for an MW electric vehicle charging station. IEEE Trans Power Electron 28(12):5793–5803

33. Williamson SS, Rathore AK, Musavi F (2015) Industrial electronics for electric transportation: current state-of-the-art and future challenges. IEEE Trans Ind Electron 62(5):3021–3032

34. Kakigano H, Miura Y, Ise T (2010) Low-voltage bipolar-type DC microgrid for super high quality distribution. IEEE Trans Power Electron 25(12):3066–3075

35. Sannino A, Postiglione G, Bollen MHJ (2003) Feasibility of a DC network for commercial facilities. IEEE Trans Ind Appl 39(5):1499–1507

36. Ito Y, Zhongqing Y, Akagi H (2004) DC micro-grid based distribution power generation system. 3:1740–1745

37. CHAdeMO Association. CHAdeMO Association & Protocol. http://www.chademo.com/wp/wp-content/uploads/2016/04/brochure_04.2016.compressed.pdf. Accessed Jul 2016

38. Dusmez S, Cook A, Khaligh A (2011) Comprehensive analysis of high quality power converters for level 3 off-board chargers. In: Vehicle Power and Propulsion Conference (VPPC), 2011 IEEE, Sep 2011, pp 1–10

39. Wilson JWA (1978) The forced-commutated inverter as a regenerative rectifier. IEEE Trans Ind Appl IA-14(4):335–340

40. Bin W (2006) High-power converters and AC drives. Wiley-IEEE Press, Chichester, West Sussex

41. Marian P. Kazmierkowski, Ramu Krishnan, Frede Blaabjerg (eds) (2002) Control in power electronics: selected problems. Academic Press, New York

42. Rodriguez J, Cortes P (2012) Predictive control of power converters and electrical drives. Wiley-IEEE Press, Chichester, West Sussex

43. Kolar JW, Ertl H, Zach FC (1996) Design and experimental investigation of a three-phase high power density high efficiency unity power factor PWM (Vienna) rectifier employing a novel integrated power semiconductor module. In: Applied Power Electronics Conference and Exposition, 1996. APEC'96. Conference Proceedings 1996, Eleventh Annual, vol 2, pp 514–523

44. Bai S, Lukic SM (2013) New method to achieve ac harmonic elimination and energy storage integration for 12-pulse diode rectifiers. IEEE Trans Ind Electron 60(7):2547–2554

45. Garcia O, Zumel P, De Castro A, Cobos JA (2006) Automotive dc-dc bidirectional converter made with many interleaved buck stages. IEEE Trans Power Electron 21(3):578–586

46. Kutkut NH, Divan DM, Novotny DW, Marion RH (1998) Design considerations and topology selection for a 120-kw IGBT converter for EV fast charging. IEEE Trans Power Electron 13 (1):169–178

47. Pahlevaninezhad M, Das P, Drobnik J, Jain PK, Bakhshai A (2012) A novel ZVZCS full-bridge DC/DC converter used for electric vehicles. IEEE Trans Power Electron 27 (6):2752–2769

48. International Energy Agency (2015) Hybrid and electric vehicles annual report. http://www.ieahev.org. Accessed May 2015

49. Dickerman L, Harrison J (2010) A new car, a new grid. IEEE Power Energy Mag 8(2):55–61

50. Mohagheghi S, Parkhideh B, Bhattacharya S (2012) Inductive power transfer for electric vehicles: potential benefits for the distribution grid. In: Electric Vehicle Conference (IEVC), 2012 I.E. International, 2012, pp 1–8

51. Plugs, socket-outlets, vehicle connectors and vehicle inlets—conductive charging of electric vehicles—part 2: dimensional compatibility and interchangeability requirements for a.c. pin and contact-tube accessories (2011) IEC 62196–2, Oct 2011

52. Botsford C, Szczepanek A (2009) Fast charging vs. slow charging: pros and cons for the new age of electric vehicles. In: Battery, hybrid and fuel cell electric vehicle symposium (EVS), 2009 24th International, May 2009

53. Malinowski M (2001) Sensorless control strategies for three-phase PWM rectifiers. PhD thesis, Warsaw University of Technology

54. Blaschke F (1972) The process of feldorientirung to regleung the asynchronous machine. Siemens researchers Dev 1 (1): 184-193

55. Rodriguez J, Franquelo LG, Kouro S, Leon JI, Portillo RC, Prats MAM, Perez MA (2009) Multilevel converters: an enabling technology for high-power applications. Proceed IEEE 97 (11):1786–1817

56. Ohnishi T (1991) Three phase PWM converter/inverter by means of instantaneous active and reactive power control. In: Industrial electronics, control and instrumentation, 1991. Proceedings. IECON'91, 1991 International Conference on, Oct/Nov 1991, vol 1, pp 819–824

57. Malinowski M, Kazmierkowski MP, Hansen S, Blaabjerg F, Marques GD (2001) Virtual-flux-based direct power control of three-phase PWM rectifiers. IEEE Trans Ind Appl 37 (4):1019–1027

58. Serpa LA, Barbosa PM, Steimer PK, Kolar JW (2008) Five-level virtual-flux direct power control for the active neutral-point clamped multilevel inverter. In: Power Electronics Specialists Conference, 2008. PESC 2008. IEEE, Jun 2008, pp 1668–1674

59. Serpa LA, Kolar JW (2007) Virtual-flux direct power control for mains connected three-level NPC inverter systems. In: Power conversion conference—Nagoya, 2007. PCC '07. pp 130–136

60. Eloy-García J, Arnaltes S, Rodríguez-Amenedo JL (2007) Extended direct power control for multilevel inverters including dc link middle point voltage control. IET Electron Power Appl 1 (4):571–580

61. Rivera S, Kouro S, Wu B, Alepuz S, Malinowski M, Cortes P, Rodriguez J (2014) Multilevel direct power control—a generalized approach for grid-tied multilevel converter applications. IEEE Trans Power Electron 29(10):5592–5604
62. Kar NC, Iyer KLV, Labak A, Lu X, Lai C, Balamurali A, Esteban B, Sid-Ahmed M (2013) Courting and sparking: wooing consumers? Interest in the EV market. IEEE Electr Mag 1 (1):21–31
63. Lukic S, Pantic Z (2013) Cutting the cord: static and dynamic inductive wireless charging of electric vehicles. IEEE Electr Mag 1(1):57–64
64. Pedder DAG, Brown AD, Skinner JA (1999) A contactless electrical energy transmission system. IEEE Trans Ind Electron 46(1):23–30
65. Wang C-S, Stielau OH, Covic GA (2005) Design considerations for a contactless electric vehicle battery charger. IEEE Trans Ind Electron 52(5):1308–1314
66. Green AW, Boys JT (1994) 10 khz inductively coupled power transfer-concept and control. In: Power Electronics and Variable-Speed Drives, 1994. Fifth International Conference on, Oct 1994, pp 694–699
67. Pantic Z, Bai S, Lukic SM (2009) Inductively coupled power transfer for continuously powered electric vehicles. In: Vehicle Power and Propulsion Conference, 2009. VPPC'09. IEEE, Sept 2009, pp 1271–1278
68. Huh J, Lee SW, Lee WY, Cho GH, Rim CT (2011) Narrow-width inductive power transfer system for online electrical vehicles. IEEE Trans Power Electron 26(12):3666–3679
69. Shin J, Shin S, Kim Y, Ahn S, Lee S, Jung G, Jeon S-J, Cho D-H (2014) Design and implementation of shaped magnetic-resonance-based wireless power transfer system for roadway-powered moving electric vehicles. IEEE Trans Ind Electron 61(3):1179–1192
70. Vasiladiotis M, Rufer A (2015) A modular multiport power electronic transformer with integrated split battery energy storage for versatile ultrafast EV charging stations. IEEE Trans Ind Electron 62(5):3213–3222
71. Abu-Rub H, Holtz J, Rodriguez J, Baoming G (2010) Medium-voltage multilevel converters—state of the art, challenges, and requirements in industrial applications. IEEE Trans Ind Electron 57(8):2581–2596
72. Perez MA, Bernet S, Rodriguez J, Kouro S, Lizana R (2015) Circuit topologies, modeling, control schemes, and applications of modular multilevel converters. IEEE Trans Power Electron 30(1):4–17
73. Tsirinomeny M, Rufer A (2015) Configurable modular multilevel converter (CMMC) for flexible EV. In: Power Electronics and Applications (EPE'15 ECCE-Europe), 2015 17th European Conference on, Sept 2015, pp 1–10
74. Nabae A, Takahashi I, Akagi H (1981) A new neutral-point-clamped PWM inverter. IEEE Trans Ind Appl IA-17(5):518–523
75. Kouro S, Malinowski M, Gopakumar K, Pou J, Franquelo LG, Wu B, Rodriguez J, Perez MA, Leon JI (2010) Recent advances and industrial applications of multilevel converters. IEEE Trans Ind Electron 57(8):2553–2580
76. Tan L, Wu B, Rivera S, Yaramasu V (2015) Comprehensive dc power balance management in high-power three-level dc-dc converter for electric vehicle fast charging. IEEE Trans Power Electron 31(1):89–100, Jan 2016
77. Rivera S, Wu B, Kouro S (2014) Distributed DC bus EV charging station using a single DC-link H-bridge multilevel converter. In: 2014 I.E. 23rd International Symposium on Industrial Electronics (ISIE), June 2014, pp 1496–1501

Chapter 5
Battery Technologies for Transportation Applications

Javier Campillo, Erik Dahlquist, Dmitri L. Danilov, Nima Ghaviha, Peter H.L. Notten, and Nathan Zimmerman

Abstract More than a fifth of the greenhouse emissions produced worldwide come from the transport sector. Several initiatives have been developed over the last few decades, aiming at improving vehicles' energy conversion efficiency and improve mileage per liter of fuel. Most recently, electric vehicles have been brought back into the market as real competitors of conventional vehicles. Electric vehicle technology offers higher conversion efficiencies, reduced greenhouse emissions, low noise, etc. There are, however, several challenges to overcome, for instance: improving batteries' energy density to increase the driving range, fast recharging, and initial cost. These issues are addressed on this chapter by looking in depth into both conventional and non-conventional storage technologies in different transportation applications.

Nomenclature

Constants

Symbol	Explanation	Value	Units
e	Elementary charge	1.6022×10^{-19}	$^{\circ}$C
F	Faraday's constant	9.6485×10^{4}	$^{\circ}$C mol^{-1}
N_A	Avogadro's number	6.022×10^{23}	mol^{-1}
R	Gas constant	8.3144	K mol^{-1}

J. Campillo (✉) • E. Dahlquist • N. Ghaviha • N. Zimmerman
School of Business, Society and Engineering, Mälardalen University, Västerås 72123, Sweden
e-mail: javier.campillo@mdh.se

D.L. Danilov • P.H.L. Notten
Department of Chemical Engineering and Chemistry, University of Technology Eindhoven, Eindhoven 5600 MB, Netherlands

Symbols

Symbol	Explanation	Units
a_i	Activity of species i	–
c_i	Molarity (or concentration) of species i	mol/m^3
E	Energy	W h
E^o	Standard electrode potential	V
$E^{o\prime}$	Formal electrode potential	V
$\triangle G$	Molar Gibbs free reaction enthalpy	$J\,mol^{-1}$
$\triangle G^o$	Free energy change	$J\,mol^{-1}$
$\triangle Hr$	Reaction enthalpy	J
$\triangle H$	Change in enthalpy	J
$\triangle Hr^o$	Molar reaction enthalpy (STC)	$J\,mol^{-1}$
I	Current	A
K	Equilibrium constant	–
M	Molality	$mol\,kg^{-1}$
M_i	Molar mass of species i	$kg\,mol^{-1}$
N	Number of moles of electrons	–
N_i	Molar flow rate of species i	$mol\,s^{-1}$
P	Power	W
Q	Electrolyte flow rate	m^3/s
Q_c	Charge	C
S	Entropy	$J\,K^{-1}$
$\triangle S$	Change in entropy	$J\,K^{-1}\,mol$
$\triangle Sr^o$	Molar reaction entropy (STC)	$J\,K^{-1}\,mol$
SoC	State of charge	%
T	Time	s
T	Temperature	K
U	Voltage	V
V	Volume	m^3
x_i	Molar fraction	–
y_i	Activity coefficient of the species i	–

1 Introduction

Rechargeable batteries are already widely used while metal-air systems are on the rise. A common feature of these systems is that the stored chemical energy at any time can be converted to electrical energy if the equipment demands. Recent introduction of hybrid (HEV) and full electric vehicles (EV) have increased the demand for high-performing rechargeable batteries. A lightweight rechargeable Li-ion battery is the only feasible long-term technology that offers high energy density, high cell voltage, low self-discharge rate, and long cycle life. By this reason mathematical modelling of Li-ion rechargeable batteries became popular

topic during last few years. Simulating discharge voltage curves of Li-ion batteries already dates back to the early 1980s [25]. Detailed reviews dealing with mathematical modelling of Li-ion batteries can be found in the literature [66, 77, 13].

At the same time, equivalent electronic network (EN) models have been presented for various types of rechargeable batteries [44, 60, 9, 10, 20]. These models are all based on macroscopic descriptions of the fundamental electrochemical and physical processes occurring inside these systems, enabling quantification of the relevant processes. The EN models were elegantly used to visualize these processes, reporting good agreement between simulations and experimental results [44, 60, 9, 10, 20]. In addition, the degradation (aging) process of Li-ion batteries has also been considered [69, 64].

Another promising technology for transportation applications, but more focused on heavy vehicles, are flow batteries. In conventional batteries, the energy capacity (kWh) and power output (kW) are strongly integrated. As a result, one of the main disadvantages is that everything is densely packed and contained in one box that contains both the electrodes and electrolytes.

Flow batteries use a different approach; energy capacity and power output are two separate components. The cell-pack is designed to handle the peak power consumption, but to have as much stored capacity as required, by storing liquid electrolytes in separate tanks. This separate-component design allows for the additional flexibility of recharging the battery by reversing the process and use electricity for recharging the electrolyte. Another alternative is to simply replace the *discharged* liquid electrolyte with a *charged* one, thus allowing for a pumping recharging process that is similar to conventional vehicles. Making this particular battery, very attractive for electric transportation applications.

Although the technology seems simple enough, its drawback for transportation applications is that the electrolyte requires a high storage capacity, and in vehicle applications, volume and weight is a limiting factor. In this chapter, we will discuss both the technology around different types of flow batteries and the system aspects when these types of batteries are used for transportation application. A different logistic chain is required when compared to the use of conventional batteries. Dimensioning examples will be performed to give a brief idea of what can be expected from this technology.

Additionally, the thermal management issue when large battery packs are used in modern Battery-Electric Vehicles (BEV) and hybrid vehicles (HEV) is also addressed. The BMS should be able to predict changes in the temperature of the battery and intervene if necessary. It requires simple and efficient models of the thermal behavior of the battery pack to be available.

Other technologies used in transportation applications will be discussed as well.

2   Battery Parameters

In this section, the parameters most commonly used to describe battery technologies will be explained.

2.1   Storage Capacity

This is one of the most important battery parameters. It determines for number of hours for which the battery can be discharged at a constant current to a defined cutoff voltage. It is represented by the Coulomb SI unit (Amperes per second) but since this unit is usually very small, the Ampere-hour (Ah) unit is used instead (1 Ah represents 3600 C). The value of this capacity depends on the ambient temperature, the age of the battery, and the discharge rate. The higher the discharge rate, the lower the capacity, although it affects each battery technology differently [22]. Additional to the Ampere-hour unit, the storage capacity can also be defined in Watt-hours (Wh = V×Ah), where 1 Wh represents 3600 J.

2.2   Energy Density

The energy density is the amount of energy that can be stored, per cubic meter of battery volume, expressed in Watt-hour per cubic meter (Wh m^{-3}) [46]. This is a very important parameter to select a specific battery technology for transportation applications, where space availability is critical.

2.3   Specific Power

This parameter is defined as the power capacity per kilogram of battery, in W kg^{-1}. Some battery technologies offer high energy density but low specific power, which means that even though they can store a large amount of energy, they can only supply a small amount of power instantly. In transportation terms, this would mean that a vehicle could run for a long distance, at low speed. On the contrary, batteries with high specific power usually have low energy density, because high discharge currents usually reduce the available energy rapidly (e.g., high acceleration) [46].

2.4   Cell Voltage

The cell voltage is determined by the equilibrium thermodynamic reactions that take place inside the cell, however, this value is often difficult to measure and

therefore, the open circuit voltage (OCV) measured between the anode and cathode terminals is used instead. For some battery technologies (e.g., lead-acid), the OCV can be used as a basic estimate of the state of charge (SoC). Another measure often used is the closed circuit voltage (CCV), which depends on the load current, state of charge, and cell's usage history. Finally, battery manufacturers provide the nominal voltage value, from the cell's characterization and therefore, cannot be experimentally verified [42].

2.5 Charge and Discharge Current

During the discharging process in a battery, electrons flow from the anode to the cathode through the load, to provide with the required current and the circuit is completed in the electrolyte. During the charging process, an external source supplies with the charging current and the oxidation takes place at the positive electrode while the reduction takes place at the negative electrode [22]. For practical purposes, the term C-rate is used to express the charge or discharge current relative to the rated capacity. For example, a discharge rate of 1 C means that the battery will be fully discharged in 1 h.

2.6 State of Charge

The state of charge (SoC) defines the amount of stored energy relative to the total energy storage capacity of the battery. Depending on the battery technology, different methods are used to estimate this value, some of which will be discussed throughout this book chapter.

2.7 Depth of Discharge

Often referred to as DoD(in %), this parameter expresses the battery capacity that has been discharged relative to the maximum capacity. Each battery technology supports different maximum recommended levels of DoD to minimize its impact on the overall cycle life.

2.8 Cycle Life

The cycle life determines the number of charge/discharge cycles that the battery can experience before it reaches a predetermined energy capacity or other performance

criteria. The current rate at which the battery is charged/discharged as well as environmental conditions (e.g., temperature and humidity) and the DoD can affect this number, since it is originally calculated by the manufacturer based on specific charge and discharge conditions.

2.9 Self-discharge

This parameter defines the reduction in energy capacity of the battery under no-load conditions (e.g., open circuit), as a result of internal short-circuits and chemical reactions. This parameter can be affected by environmental conditions such as temperature and humidity, as well as the DoD and the battery's charge/discharge history. Additionally, this parameter is particularly important for long-term shelf storage of batteries.

2.10 Round-Trip Efficiency

Due to internal losses and material degradation, not all the energy supplied to the battery during charging can be recovered during discharge. The amount of energy that can be taken from the battery during the discharging process over the energy supplied determines the round-trip efficiency. This efficiency is sensitive to the charging and discharging currents. At higher currents, thermal losses increase and therefore the efficiency is reduced [23].

2.11 Overpotentials

The total cell overpotential (η) is the difference between the equilibrium voltages and the current-driven voltages. For example, in Li-ion batteries, the equilibrium voltage is the difference between the equilibrium voltage of the positive and negative electrodes, i.e., $E_{eq} = E_{LiMeO_2}^{eq} - E_{LiC_6}^{eq}$

$$\eta = E_{bat} - E_{eq} \tag{5.1}$$

The total cell overpotential (η) is, normally, a sum of four contributions, according to four main processes occurring inside the cell: the charge transfer reactions at the surfaces of electrodes, the ionic flow through the electrolyte, diffusion in the intercalation electrodes, and ohmic voltage drop in the electrodes.

$$\eta_t = \eta^{ct} + \eta^d + \eta^{mt} + \eta^{\Omega} \tag{5.2}$$

$$\eta^{\Omega} = IR \tag{5.3}$$

where I equals the cell current [A] and R is the ohmic series resistance inside the cell [Ω]. Note that by definition $I > 0$ while charging, $I < 0$ while discharging.

3   Battery Technologies

3.1   Lead Acid

This battery technology was invented in 1859 by the French electrochemist Gaston Plante who placed two sheets of pure lead, separated by a linen cloth, inside a glass jar that contained sulfuric acid solution [22]. Since then, multiple improvements on these type of batteries have been carried out and today are by far, the most used battery technology in multiple applications, representing approximately 40–45 % of the total global battery sales [24].

Lead-acid batteries use lead dioxide (PbO) as the positive active material and lead (Pb) as the negative active material immersed in sulfuric acid which acts as electrolyte. The two half-cell reactions are as follows [22]:

At the positive electrode:

$$PbO_2 + HSO_4^- + 3H^+ + 2e^- \underset{\text{Discharge}}{\overset{\text{Charge}}{\rightleftharpoons}} PbSO_4 + 2H_2O \tag{5.4}$$
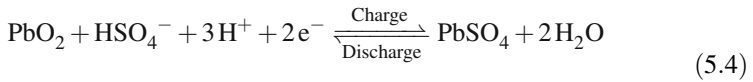
$$E^\circ = +1.690V$$

At the negative electrode:

$$Pb + HSO_4^- \underset{\text{Discharge}}{\overset{\text{Charge}}{\rightleftharpoons}} PbSO_4 + H^+ + 2e^- \tag{5.5}$$
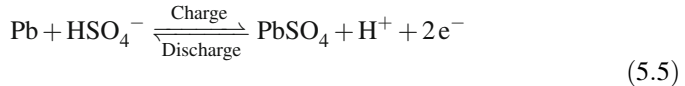
$$E^\circ = -0.358V$$

where E^o is the standard electrode potential for each cell reaction. The overall cell reaction is, therefore:

$$Pb + PbO_2 + 2H_2SO_4 \underset{\text{Discharge}}{\overset{\text{Charge}}{\rightleftharpoons}} 2PbSO_4 + 2H_2O \tag{5.6}$$
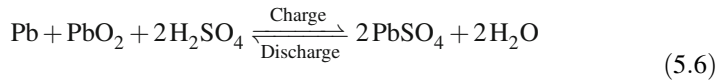
$$V^\circ = +2.048V$$

where V^o is the standard cell voltage.

Some of the main advantages of lead-acid batteries include: easy estimation of the SoC, since it has a direct relation with the specific density of the electrolyte; good charge retention, suitable for intermittent recharging; cell components are easily recyclable; low cost, and high OCV cell voltage.

This battery technology also has several limitations, for example: most lead-acid battery types require periodic maintenance, since they tend to lose water while in operation, so it needs to be replenished; lead is heavy and therefore these batteries tend to be heavier than other technologies, which limits their portability; relatively low cycle life, although some types can achieve up to 2000 cycles, most used ones have a considerably lower number; the thermal runaway issue in this battery technology, when the internal heat generation from the charging current flowing through the resistive components; among others.

In the transportation sector, modified lead-acid batteries with high cycle life and high DoD capabilities have been used for decades in battery-powered trucks, forklifts, elevating trucks, and other vehicles for internal factory transportation as well as leisure vehicles, such as golf carts. However, due to technology developments in other battery technologies, specially Li-ion, the use of lead-acid batteries in most vehicles sold today has been limited to start, lighting and ignition (SLI) operations.

3.2 Nickel-Cadmium (Ni-Cd)

Historically, Nickel-cadmium batteries go almost as far back as lead-acid ones. They were developed in the beginning of the twentieth century and still hold a large market share. They are manufactured in two main versions: unsealed batteries, where the electrolyte and gas can escape through a vent; and a fully sealed battery which do not require refilling the electrolyte with water. The first version is often used in traction applications as a flooded battery, while the latter is used as a portable power source [42].

Nickel-cadmium batteries are considered to be very reliable and to have a long cycle life. One important characteristic is that they exhibit voltage suppression, also known as *memory-effect*. This means that the battery can only provide with the capacity that was used during the repeated charge/discharge cycles before. Due to this, the battery should be fully discharged before recharging again, to avoid losing storage capacity. In consequence, this battery technology is not suitable for applications that do now allow complete discharge [24].

Some of the advantages of this battery technology include: longer life time, lower maintenance, and broader temperature operating range than lead-acid batteries; low self-discharge rate and high sturdiness, which makes them ideal for heavy-duty applications. Its main limitations include its memory-effect and the fact that cadmium is an environmentally hazardous material, so the final disposal of these batteries is a major issue [24].

The cell reaction that takes place in nickel-cadmium batteries can be expressed as:

$$2\,Ni(OOH) + 2\,H_2O + Cd \xrightleftharpoons[\text{Discharge}]{\text{Charge}} 2\,Ni(OH)_2 + Cd(OH)_2 \qquad (5.7)$$
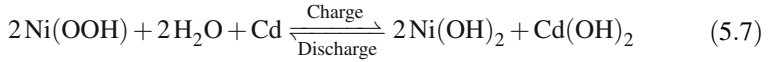
And the equilibrium or open circuit voltage is $V^o = 1.32\,V$.

3.3   Nickel-Metal Hydride (Ni-MH)

Nickel-metal hydride (Ni-MH) batteries are very similar to nickel-cadmium batteries, because they share the same positive electrode and the same electrolyte, however, for the negative electrode, hydrogen is used instead of cadmium. Furthermore, the negative electrode corresponds to a fuel cell electrode rather than to a conventional battery. In the charged state, hydrogen remains as gaseous gas within the cell, therefore nickel-metal hydride batteries must be hermetically sealed. In the discharged state, the hydrogen is absorbed by the nickel hydroxide [42]. Another difference with Ni-Cd batteries is that in Ni-MH batteries, the cell reaction exothermic and therefore, the internal temperature of Ni-MH cells rises during operation [24].

There are several advantages for Ni-MH batteries over Ni-Cd ones. First, Ni-MH do not pose the same environmental hazards as Ni-Cd batteries do. Additionally, Ni-MH batteries have higher energy density and specific energy, and most importantly, they do not exhibit the same level of *memory-effect* as Ni-Cd batteries do.

There are, however, several limitations for this battery technology, for instance: overcharging can overheat the battery and release hydrogen that would pose a serious fire hazard. Therefore, complex charging circuitry is required; when discharged at high-current levels, its life time reduces significantly (200–300 cycles); higher self-discharge rate than Ni-Cd; among others [24].

The cell reaction can be expressed as [42]:

$$2\,NiOOH + H_2 \xrightleftharpoons[\text{Discharge}]{\text{Charge}} 2\,Ni(OH)_2 \qquad (5.8)$$
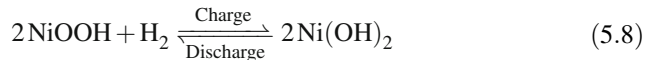
When the battery is being charged, NiOOH is reduced to $Ni(OH)_2$ and hydrogen is consumed. When the battery is being discharged, Eq. (5.8) is reversed and hydrogen (H_2) is stored as gas in each cell. The equilibrium cell voltage is $V^{(o)}$ = 1.34 V [42].

Ni-MH batteries have been very popular in electric vehicles, such as the Toyota "RAV-EV" as well as in hybrid vehicles, like the popular "Prius." This has helped Ni-MH batteries gain an important position in the transportation sector and has displaced other technologies, like lead-acid and Ni-Cd. Today, its main competitor are Li-ion batteries.

3.4 Lithium-Ion (Li-Ion)

This battery technology has been available since 1991 and today, is the most popular technology for portable electronics, such as mobile phones and portable computing [84]. Lately, thanks to the cost reduction in lithium-ion batteries manufacturing and high incentives towards clean transportation, this battery technology is becoming very popular among electric vehicle manufacturers.

The most frequently used lithium-ion battery type is the lithium-nickel-manganese-cobalt-oxide. These batteries use a new chemistry commercialized since 2004 [19]. The cathode of these batteries is made of mixed oxide $Li(Ni_{1/3}Mn_{1/3}Co_{1/3})O_2$. The elementary processes, occurring inside such Li-ion battery, are schematically shown in Fig. 5.1. The main electrochemical storage reactions at the positive electrode can be represented by:

$$Li(Ni_{\frac{1}{3}}Mn_{\frac{1}{3}}Co_{\frac{1}{3}})O_2 \xrightleftharpoons[\text{Discharge}]{\text{Charge}} Li_{1-x}(Ni_{\frac{1}{3}}Mn_{\frac{1}{3}}Co_{\frac{1}{3}})O_2 + xLi^+ + xe^- \qquad (5.9)$$
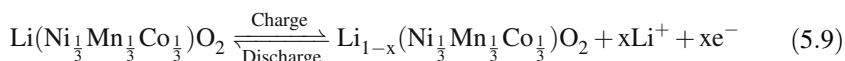
for $0 \leq x \leq 0.5$, describing the extraction of Li-ions from the positive electrode during charging and the insertion of Li^+ ions during discharging. The corresponding reactions at the negative, graphite, and electrode can be described by:

$$C_6 + zLi^+ + ze^- \xrightleftharpoons[\text{Discharge}]{\text{Charge}} Li_zC_6 \qquad (0 \leq z \leq 1) \qquad (5.10)$$
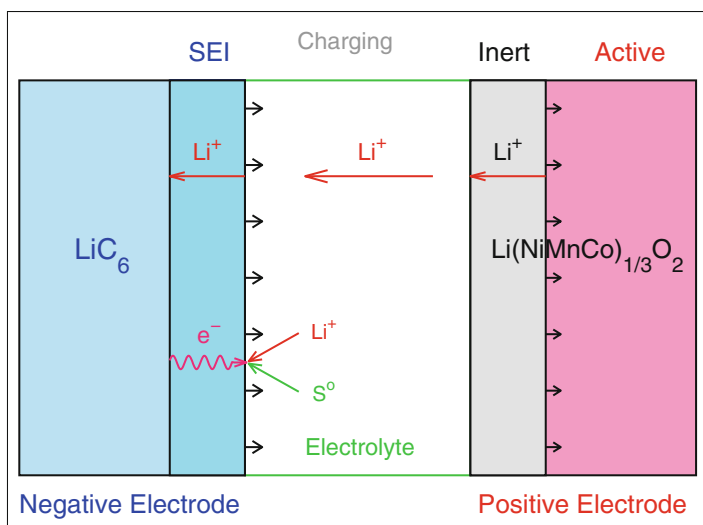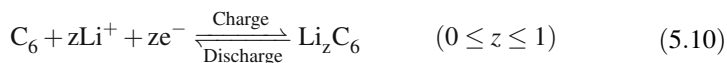
Fig. 5.1 Schematic representation of nickel-manganese-cobalt based battery, indicating the movements of Li-ions inside the $LiPF_6$ salt-containing electrolyte during charge and discharge

As a result of these electrochemical charge transfer reactions, Li-ions must cross the electrolyte under current-flowing conditions (see Fig. 5.1). The electrolyte in Li-ion batteries is based on a dissociated Li-salt, e.g., $LiPF_6$ or $LiClO_4$, which cannot be considered as a well ionic-conductive medium. The ions in the electrolyte are transported both by diffusion and migration, this latter process being induced by the electric field between the electrodes across the electrolyte. The positive electrode generally consists of trivalent mixed-oxide species, in which lithium ions are intercalated ($Li(Ni_{1/3}Mn_{1/3}Co_{1/3})^{III}O_2$) to provide electroneutrality. During charging, trivalent metal is oxidized into four-valent (($Ni_{1/3}Mn_{1/3}Co_{1/3})^{IV}O_2$) and the excess of positive charge is liberated from the electrode in the form of Li^+ ions. The Li^+ ions cross the electrolyte and are reduced into lithiated graphite at the negative electrode. The reverse reactions take place during discharging.

3.5 Flow Batteries

The first known flow battery prototype was developed in 1884 by the French scientist Charles Renard [12]. He used zinc and chlorine as the reactive elements and was connected to an electric motor to drive the propeller of a war airship. Years later, the German scientist, Walter Kango, built a flow battery using a solution of titanium-chlorine and hydrochloric acid.

Other flow batteries such as the uranium, zinc bromine redox flow battery, and the polysulfide bromide flow battery were developed by different researchers and commercial manufacturers, but the early developed flow batteries had many limitations. Those flow batteries used hazardous chemicals and operated at high temperature under high pressure. Different types of electrolytes were used in the negative and positive half-cell but membrane failures and molecular transfer through the membrane caused cross-contamination of the electrolytes.

To address this issue, the vanadium redox flow battery, developed at the University of New South Wales in 1984, used the same species in the electrolyte in both parts of the cell and therefore, it avoids cross-contamination of the electrolyte.

Their findings proved to be valuable and since then, several groups have taken special interest in developing this renewable technology by looking into four main aspects: electrolyte optimization, membrane development, electrode development, and optimization of the constituent parts in the stack design [67].

3.6 Fuel Cells

Fuel cell technology goes as far back as 150 years, when W.R. Grove tested the first fuel cell in 1842, however, it could not compete with the energy capacity of lead-acid batteries [42]. One century later, space programs in different countries put a lot

of effort and research into developing this technology, to the point that it has been successfully used in multiple applications.

Fuel cells are built with two electrodes (anode and cathode) separated by a semi-permeable membrane. The electrodes are connected to each other through an external load that closes the circuit and allows the flow of current.

There are multiple types of fuel cells, however, recent developments have focused on the mass commercialization of proton-exchange membrane (PEM) and solid-oxide (SOFC) type fuel cells. Both have advantages and disadvantages for its use in electric vehicles. PEM can be started from ambient temperature and operate at a relative low temperature (80 °C), which makes it very convenient, however, the main challenge with this fuel cell type is that it requires pure hydrogen (H_2) as fuel and therefore, it requires a major infrastructure for production, distribution, and storage of hydrogen. SOFC fuel cells solve this issue by operating with any type of fuel, thanks to its ceramic electrolyte, which conducts oxygen ions that burn any fuel. Its main disadvantage, however, is that it operates at a high temperature (500–800 °C) [42].

Fuel cells are well suited for their use in large electric vehicles, for instance, delivery trucks, trains, and buses. Recently, several automotive manufacturers have developed smaller fuel cells to build fuel cell electric vehicles (FCEVs) to compete with conventional, hybrid, and electric vehicles.

FCEVs are very similar to battery-electric vehicles (BEVs), however, instead of storing electricity on internal batteries, FCEVs use hydrogen, stored onboard in high pressure tanks and convert it into electricity using a fuel cell stack. FCEVs also have an internal battery, but it is considerably smaller than the one used in BEVs and only used for storing excess electricity produced by the fuel cell or from the energy recovered from regenerative braking systems [31].

There are, however, several challenges to address before the technology reaches a high market penetration, being the most significant one, the high cost of the vehicles, and the lack of hydrogen refueling infrastructure [36].

3.7 Super Capacitors

Super capacitors (SC) are electrochemical capacitors normally used to provide peak power for short periods of time, for instance, when start–stop operations in EVs. SCs are electrically similar to conventional capacitors and can be built using double layer capacitors made of non-porous materials, such as activated carbon. It is also possible to use capacitors that use transition metal oxides, nitrides, and polymers with high surface areas [81].

Compared with other battery technologies, SCs offer several advantages, for instance: high life cycle ($> 500,000$); high charge/discharge rate; low internal resistance; round-trip efficiencies of around 90 %, and high power density. However, this technology also has some limitations, being the most important one is that SCs have very low energy density, about 50 times lower than a Li-ion battery [35] and high self-discharge rates.

For these reasons, SCs are not suitable as a stand-alone storage device, however, when used in transportation applications, combined with other battery technologies, it increases the overall technical performance significantly. For instance, when used in combination with fuel cells, which have high energy density but can only supply a relatively low peak power, SCs can provide with the *extra boost* required to provide a higher torque during fast acceleration start-up. Similarly, when combined with Li-ion or Ni-MH batteries, it can help increase the batteries life cycle, by reducing the peak currents required to provide high acceleration torque in the vehicle.

4 Battery Management

In order to guarantee the batteries safe operation, maximize its life time and optimize its usage, it is necessary to supervise each cell using a battery management system (BMS). The BMS supervises single cell voltages, monitors, and controls current in (charging) and out (discharging) of the cell stack, supervises temperatures, and analyzes the battery usage in order to maintain the battery within its operation limits at all times [15].

4.1 Battery Charging

4.1.1 Charging Methods

Float Charge This method is commonly used in non-sealed lead-acid batteries, since they can operate at a high voltage level for long periods. The charging current depends on the SoC of the cells and its value gradually reduces as the cells become fully charged. This charging mode, however, produces gassing inside the cells and therefore, requires filling up the battery with water to maintain the electrolyte level [24].

Trickle Charge This method is used to maintain the battery at a full state of charge. This is accomplished by supplying a small current to offset the self-discharge characteristics of the battery. This method is often used in lead-acid batteries when stored for large periods.

Bulk Charge This method is used to charge the majority of the total energy capacity of the battery.

Equalization Charge This method is used to bring the SoC of all individual cells to the same value. The techniques used to accomplish this vary between battery technologies. In lead-acid batteries, for instance, this can be achieved simply by using a higher charging voltage. In other technologies, like Li-ion, the

process is not so simple and active equalization methods, where external circuits transport energy among the internal cells in order to maintain them at the same level, are required [87].

4.1.2 Charging Techniques

Constant Current This technique uses a constant current during the charging process. While the chargers required for this are relatively simple and inexpensive, it is challenging to determine the right current value. If too low, the charging time will be too long, on the contrary, if too high, it might overheat the battery or cause gassing inside the cells. To solve this issue, usually a high current is used during the first period of the charging process (bulk charge) followed by a smaller current at the later stages (trickle charge).

Constant Voltage In this technique, since the voltage is maintained constant, the current supplied is determined by the voltage difference by the voltage difference between the charger and the battery. The supplied current starts at a high level and decreases exponentially as the battery gets charged. Due to the initial high current, this technique is often used for fast bulk charging, however, it might cause overheating and gassing.

Constant Current–Constant Voltage This technique uses constant current charging until the battery reaches a predefined value, then, it switches to constant voltage charging allowing the current to decrease exponentially. By using this technique, the advantages of both methods are combined, so that the battery charges fast enough, without using high currents that can cause overheating and gassing.

4.2 SoC Estimation

There are several techniques to determine the SoC and they depend on measuring one or several parameters that vary with the state of charge, often particular to each individual battery technology. Some of the most important techniques are listed below.

Voltage Measurement In several battery technologies, there is an almost a linear relationship between cell terminal voltage and SoC and therefore, the SoC can be directly determined by measuring the terminal voltage of the battery. However, in other technologies, such as Li-ion, they have a flat voltage profile during discharging and simple voltage measurement fails to determine the SoC accurately.

Specific Gravity Measurement This technique is used in lead-acid batteries, since the sulfuric acid is used as the battery discharges and therefore, its specific density reduces. By measuring the specific gravity of the sulfuric acid, it is possible

to estimate the SoC in lead-acid batteries. This method does not work with valve-regulated lead-acid type batteries [24].

Current Measurement Also known as *Coulomb-counting*, it is possible to estimate the SoC by integrating the current supplied to the cell during a period of time. This method offers high accuracy for determining the SoC and can also be useful to determine battery's ageing by comparing the current supplied to the battery with the current extracted from it.

Kalman Filtering The Kalman filter is an algorithm that estimates the inner states of a dynamic system. When applied to batteries, each cell is represented by a state-space model, where the SoC is a state of the system. In electric vehicles, the Kalman filter model for the battery is started with initial state estimates when the vehicle is turned on, based on the previous states, terminals' OCV, a look-up table, self-discharge parameters, temperature, etc. The algorithm then proceeds to update the states of the battery parameters as the system runs. This technique has proven to offer highly accurate SoC estimation [24].

Internal Impedance Measurement The composition of active chemicals inside the battery change as it gets charged or discharged. In consequence, the internal impedance of the battery also changes. The internal impedance of the battery can provide information about the SoC of each cell, however, the internal impedance can also be affected by other parameters, such as temperature, which can lead to erroneous measurements [24].

5 Battery Models

5.1 Li-Ion Battery Models

5.1.1 Experiments

Experiments were carried out on 2.2 Ah cylindrical CGR 18500CG cells from Panasonic. These cells contain nickel-manganese-cobalt oxide cathode (Panasonic solid-solution) and traditional graphite anode. The cell was charged and discharged according to the following regime: constant current constant voltage (CCCV) charging with a 1.5 A current until the maximum voltage level of 4.2 V was reached, followed by a 150 min relaxation period and a Current Constant (CC) discharge until 2.5 V was reached. The following discharge rates were successively applied: 0.05, 0.10, 0.15, 0.20, 0.30, 0.50, 0.75, 1.00, 1.50, and 2.00 C. The C-rate is normally used to describe battery loads or battery discharging currents. One C-rate denotes the current rate at which a nominal capacity of the battery can be discharged in 1 h.

In the experiment, the cycling of the cells was performed on an 8-channel MACCOR battery tester. The temperature development of the cell was measured by the potential drop across PT100 type thermo-resistors connected to the battery tester via the auxiliary voltage input. A water bath was used to control the ambient
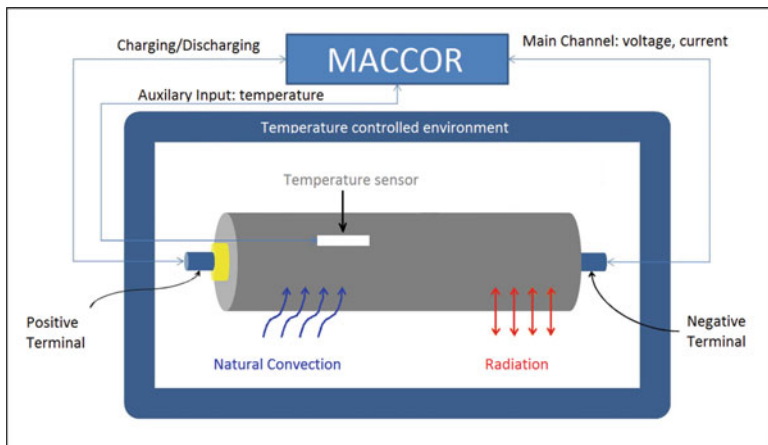
Fig. 5.2 Measuring thermal behavior: experimental setup

temperature (i.e., 23°C) in a climate control box, the scheme is similar to the one shown in Fig. 5.1. To evaluate the thermal behavior of the cell at different temperatures, three different ambient temperatures were selected: 0, 20, and 40 °C. Figure 5.2 illustrates the measurement setup and equipment connections.

5.1.2 Lumped-Sum Models

Thermal modelling of a cell is a procedure that derives the temperature evolution of the cell and possibly, the distribution of the temperature in various parts of the cell as a function of time. Thermal modelling starts by defining the heat flows. Where the heat flow generated inside the cell is given by [10]:

$$H_t^{in} = \sum_{n=i} \frac{-T\Delta S_i}{n_i F} + In_t \tag{5.11}$$

where H_t^{in} is the heat flow, i.e., the intensity of heat generation inside the cell [W], T the cell temperature [K], ΔS_i denotes the entropy change associated with electrochemical charge transfer reactions given by Eqs. (5.9) and (5.10) [J mol^{-1} K^{-1}], n_i the number of electrons exchanged in particular electrochemical reaction i, n_t the total overpotential [V]. Note that, $E_{bat} \leq E_{bat}^{eq}$ while charging and $E_{bat} \geq E_{bat}^{eq}$ while discharging, resulting always in $In_t \geq 0$. That means that the heat flow given by the second term of Eq. (5.11) is always positive and the cell always heats up because of this term. The first term can be either positive or negative. It is positive when $\Delta S_i < 0$ which is valid for an exothermic reaction. In this case, the cell heats up by this heat flow. However the cell will cool down as the result of an endothermic reaction, for which $\Delta S_i > 0$. A reaction that is exothermic during charging is endothermic during

Fig. 5.3 Charging and discharging curves obtained with various C-rates: 0.05, 0.10, 0.15, 0.20, 0.30, 0.50, 1.00, and 2.00 C
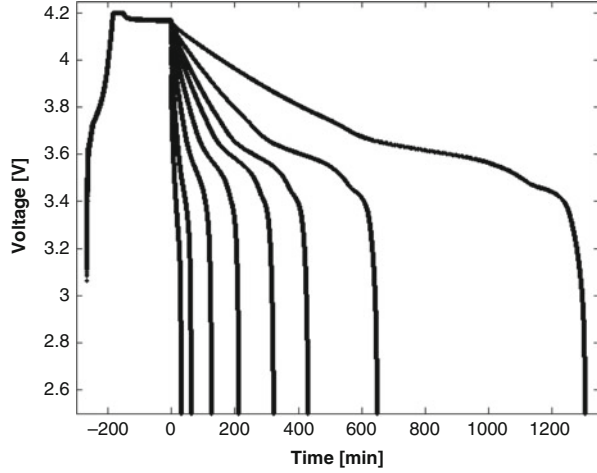
discharging and vice versa. For Li-ion cells ΔS_i is usually small and therefore the first term in Eq. (5.11) can be neglected. The heat flow from the cell to the environment H_t^{out} is, in general, determined by heat conduction, convection, and radiation [74]. In the experiment, a cylindrical cell was held horizontally, keeping its side walls exposed to the air. For such conditions, the heat conduction from the top and the bottom can be neglected. For the side walls, the heat conduction is described by the equation:

$$H_t^{out} = hA(T - T_0) + \sigma A(T^4 - T_0^4) \tag{5.12}$$

where H_t^{out} is the heat flow outside the cell [W], T_0 is the ambient temperature [K], A is the surface area of the cell [m^2], h is the heat transfer coefficient [W m^{-2} K^{-1}], $\sigma = 5.67 \times 10^{-8}$ [J s^{-1} m^{-2} K^{-4}] is the Stefan–Boltzmann constant, and ε is the emissivity. When heat fluxes are determined, the evolution of cell temperature is determined by the standard heat balance equation:

$$mC_p \frac{dT}{dt} = H_t^{in} - H_t^{out} \tag{5.13}$$

where C_p is the specific heat capacity of the cell [J g^{-1} K^{-1}] and m is the mass of the cell [g]. Ordinary differential equation (ODE) Eq. (5.13) has to be solved with respect to initial conditions, representing cell temperature at $t = 0$, which equals the ambient temperature $T(0) = T_0$. Then, the solution of the ODE Eq. (5.13) determines the evolution of the cell's temperature. Figure 5.3 shows the charge and discharge voltage curves as a function of time where, for convenience reasons, $t = 0$ corresponds to the start of each discharge cycle. Figure 5.4 shows the same discharge curves but plotted as a function of the amount of extracted charge (Q_{out}). The equilibrium voltage has been determined by regression extrapolation [20, 69]. The regression extrapolation was applied separately on the flat and steep

Fig. 5.4 Discharging voltages and estimated EMF
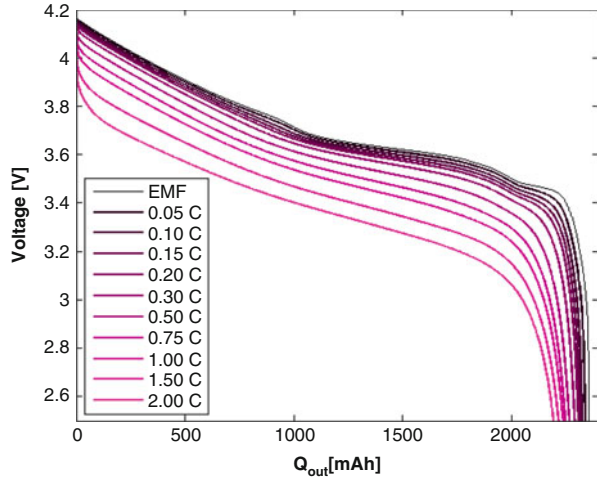
Fig. 5.5 Influence of the ambient temperature on the EMF
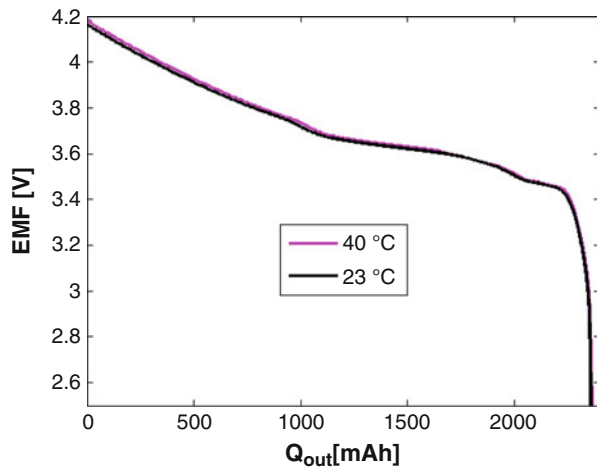
parts of the equilibrium voltage curve. The thin black line in Fig. 5.4 corresponds to the estimated equilibrium voltage (EMF). The obtained EMF is, in principle, temperature dependent, however, within moderate temperature range this influence is small and can be neglected, as illustrated in Fig. 5.5.

The difference between the equilibrium voltage and the discharge voltage is the overpotential, see Eq. (5.11). The dependence of the total experimental overpotential as a function of Q_{out} at various discharge rates is shown in Fig. 5.5. For all currents, a wide flat interval, consisting of two sloping plateaus, is followed by a sharp decrease at the end of the discharge process. Thermal modelling starts by calculating the thermal fluxes. The intensity of heat generation or heat flow into the battery is calculated according to Eq. (5.11). The experimentally measured currents

Fig. 5.6 Discharge overvoltages as a function of extracted charge for the various applied discharge currents
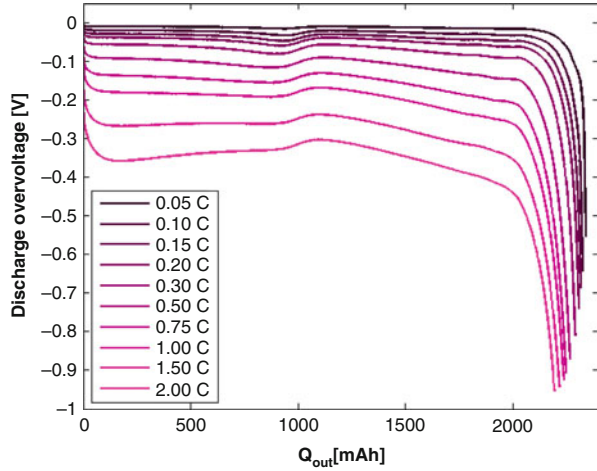
Fig. 5.7 Temperature evolution during discharging with various C-rates. Experimental data are *dashed lines*, simulations are *solid lines*
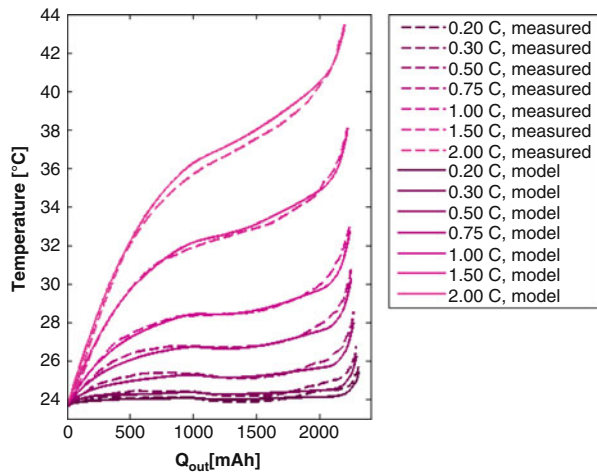
and estimated overpotentials (see Fig. 5.5) are used as inputs. In Fig. 5.6 the solutions of Eq. (5.13) are compared with the experimentally measured cell temperatures during the discharging process (Fig. 5.7).

The dashed lines indicate measurements while the solid lines represent the model fit. The heat transfer coefficient and specific heat capacity of the battery were used as the parameters for the function to be minimized. The (non-linear) ordinary least squares minimization was applied. The estimated values of the heat transfer coefficient and specific heat capacity are $13\,\mathrm{W\,m^{-2}\,K^{-1}}$ and $1.25\,\mathrm{J\,g^{-1}\,K^{-1}}$ accordingly, which agrees well with recent results from literature [64]. The fit quality is good, with deviations of modelled temperature less than 1 °C for all considered C-rates at any moment of time. If the heat transfer coefficient is assumed

Fig. 5.8 Temperature increase during 2 C-rate discharge for various ambient temperatures
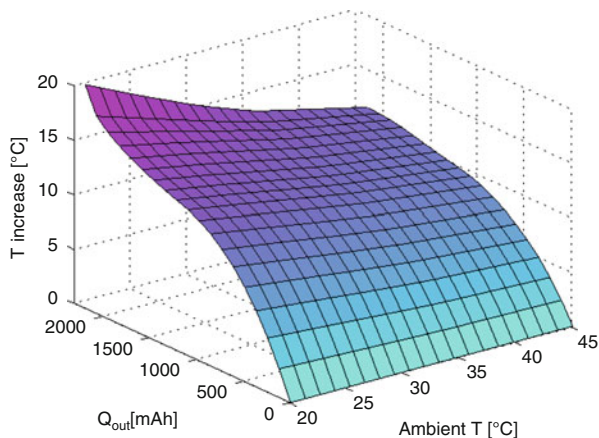
to be a linearly increasing function of the cell surface temperature $W\,m^{-2}\,K^{-1}$, then the fit function improves uniformly for all C-rates with the error below 0.75 °C.

The experiment illustrates a simple and accurate method for adaptive thermal modelling of the Li-ion batteries. The performance of the thermal model is illustrated for the commercially available Panasonic CGR18650CG 2.2 Ah cells. For all available C-rates model predictions from the measured temperature deviate less than 1 °C. Note that for this high energy density cell, the increase in temperature while discharging can be considerable, up to 20 °C, see Fig. 5.8. For that particular cell, the entropy effect is small and the heat generated from the overvoltage explains the experimentally observed data. If this model is combined with an adaptive algorithm that could determine the capacity fade, it would represent an adaptive thermal model. This type of model would provide a proper temperature prediction during the whole lifespan of the battery using a single EMF measurement when the cell was new. A battery management system (BMS) equipped with a thermal model would be able to predict the battery's temperature evolution and apply preventive cooling when necessary, thus reducing the wear of the battery.

5.1.3 High Power Cells, Importance of Entropy-Related Terms

For high energy cells the entropy term can be neglected [19]. However, there are situations where the entropy contribution is considerable and may not be omitted, [74]. As an illustration, the case of 7.5 Ah ultra-high power Li-ion batteries is considered in this section. The anode of this battery system is made of graphite, while the cathode consists of $Li_{1-x}(Ni_{0.8}Co_{0.15}Al_{0.05})O_2$ which in general is known as NCA Li-ion. The basic electrochemical charge transfer reactions at the positive and negative electrode can be represented by:

$$\mathrm{Li(Ni_aCo_{1-a-b}Al_b)O_2} \xrightleftharpoons[\mathrm{Discharge}]{\mathrm{Charge}} \mathrm{Li_{1-x}(Ni_aCo_{1-a-b}Al_b)O_2) + xLi^+ + xe^-} \quad (5.14)$$

$$\mathrm{c_6Li_y + xLi^+ xe^-} \xrightleftharpoons[\mathrm{Discharge}]{\mathrm{Charge}} \mathrm{C_6Li_{y+x}} \quad (5.15)$$
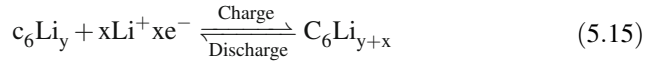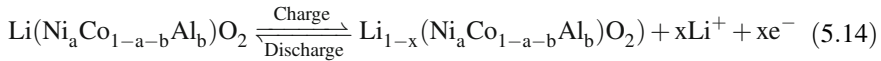
for $0 \le x \le 0.5$, respectively.

The positive electrode generally consists of mixed-metal oxide species in which lithium ions are stored to provide electroneutrality. During charging, the metal oxide is oxidized and the excess of positive charge is liberated from the electrode in the form of $\mathrm{Li^+}$ ions. These ions cross the electrolyte and enter the negative electrode. There, $\mathrm{Li^+}$ ions are inserted during charging and extracted from the negative electrode during discharging. As a result of both electrochemical charge transfer reactions, Li-ions must cross the electrolyte by means of diffusion and migration.

For this experiment, CCCV was used. CC charging is carried out at 5.25 A ($= 0.7$ C-rate) until the maximum cell potential of 4.2 V is achieved. Charging continues under constant voltage conditions at 4.2 V until the charging current dropped below 0.376 A. Subsequently, CCCV-charging is followed by a relaxation period of 180 min. Then constant current (CC) is applied to discharge the battery at various C-rates. Discharging was terminated at 2.7 V. The following C-rates were employed for discharging: 0.05, 0.10, 0.15, 0.2, 0.3, 0.5, 0.75, 1.00, 1.50, and 2.00 C-rate. The results of these measurements are used to determine the EMF (equilibrium voltage) based on the voltage extrapolation towards zero current [20, 69]. The resulting charging and discharging curves are illustrated in Fig. 5.9.

The observed temperature development can be seen in Fig. 5.10. One can see that temperature development of the ultra-high power cell has complex non-uniform shape. For moderate C-rate, a temperature drop can be observed soon after the discharging process starts, in contrast with high-energy cells (Fig. 5.7), where the temperature increase during discharging is constant. Therefore the overvoltage heat alone is not sufficient to explain such temperature behavior.

Cell potential curves at various C-rates have been plotted as a function of extracted charge (Q_{out}) in Fig. 5.11. The same method of extrapolation towards zero current as in the previous section was applied to obtain the equilibrium voltage. The resulting E_{eq} is shown in the upper black line in Fig. 5.11. The difference between each cell potential curve and E_{eq} represents the overpotential η_t, which is one of the sources of heat generation inside the cell (see Eq. (5.11)), especially important at high C-rates and at the end of discharging. In the plateau region η_t is only about 4 mV at 0.05 C-rate discharge, while it grows to 40 mV at 2 C-rate, see Fig. 5.12. At the end of discharging at high C-rates the overpotentials increase rapidly to very high values of more than 500 mV due to slow diffusion of $\mathrm{Li^+}$ ions in electrode(s). The second source of the heat in thermal balance equation Eq. (5.13) is, according to Eq. (5.11), the entropy term $-\frac{I_t \Delta S}{\eta F}$. Note that ΔS is a
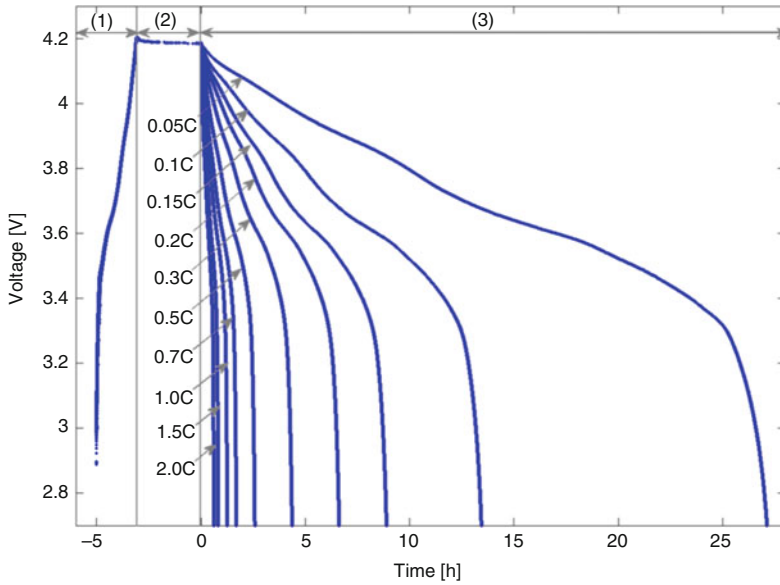
Fig. 5.9 Voltage development during (1) charging under 0.7 C, (2) relaxation, and (3) discharging at various C-rates
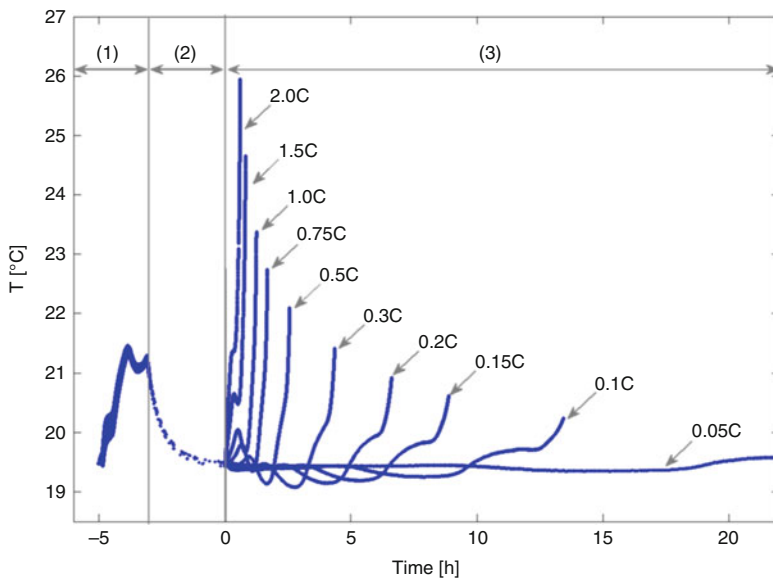
Fig. 5.10 Temperature development. Ambient temperature is 20 °C

Fig. 5.11 Measured voltages during discharge at various C-rates, as-determined equilibrium voltages, simulated 4 and 6 C-rate discharge voltages re-plotted as a function of Q_{out}
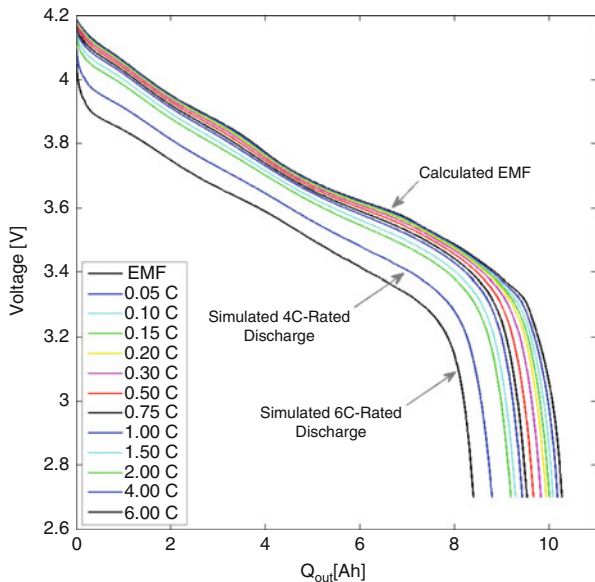
Fig. 5.12 Calculated $-\eta$ at various C-rates during discharge
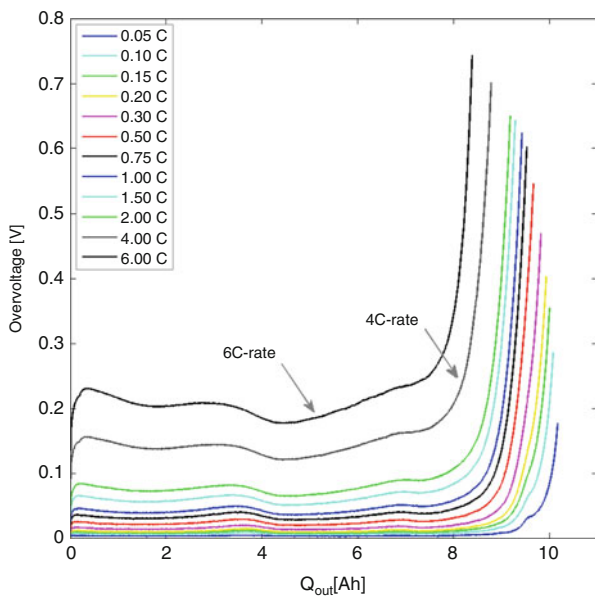
function of the state-of-charge (SoC) of the battery. To estimate ΔS as a function of SoC we use an optimization procedure. In this method the SoC range is divided into ten intervals and ΔS is estimated in the middle of each interval by minimizing the (squared) differences between the simulated (according to Eq. (5.13)) and measured
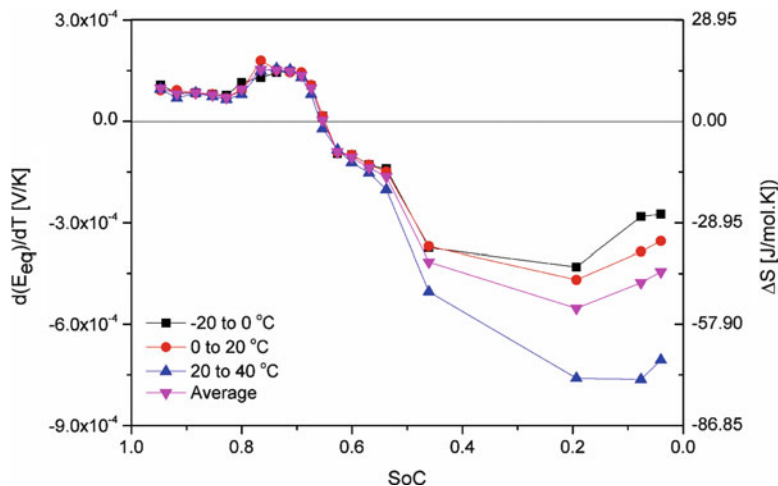
Fig. 5.13 Estimated $\frac{\partial E_{eq}}{\partial T}$ and ΔS values as a function of SoC

temperatures by unconstrained non-linear optimization using MATLAB software. The as-determined values for dE_{eq}/dT and ΔS are shown in Fig. 5.13.

Three regions can be recognized in this figure: at $SoC \geq 0.35$, in the interval $0.25 < SoC < 0.35$ and when $SoC \leq 0.25$. In the first region, E_{eq}/dT is positive, whereas around $SoC = 0.3$ it sharply turns into negative values. At $SoC \leq 0.3$, ΔS is in between 40 and 10 J mol^{-1} K^{-1}. The highest value of 17 J mol^{-1} K^{-1} is obtained at about 50 % SoC.

Phase transition at different SoC has been observed for $LiCoO_2$, $LiCo_{0.5}Ni_{0.5}O_2$ and $LiNi_{0.65}Co_{0.25}Mg_{0.05}Ti_{0.05}O_2$ cathode materials [37, 90, 82, 39]. Similar observations have been reported for graphite electrodes [64, 39, 5]. Several studies have been carried out to experimentally describe the phase transition of electrodes in Li-ion and Li-polymer batteries [45, 17, 2, 32, 26]. The analyzed entropy changes in the present work can be related to these phase transitions.

Figure 5.14 illustrates the contribution of both the overpotential and entropic heat (Eq. (5.11)). These individual contributions and the summation are plotted for the charging process at 0.7 C and discharging at 1 C-rate at the ambient temperature 40 °C. The overvoltage heat is always positive (red curve in Fig. 5.14). In the initial stages of the charging process (SoC < 30 %) and main part of discharging (SoC > 30 %) the entropy heat is negative, i.e., it neutralizes the overpotential heat generation and even makes the total heat generation negative in these regions; the battery therefore should cool down. Hence, in spite of positive overvoltage heat the temperature drops as the entropic contribution is dominant. In calculating the overpotential at each SoC, both the cell potential (from measurements) and the determined EMF terms are at the corresponding battery temperature at that SoC in our model. It means that the calculated overpotential takes into account the effects from the temperature development.

Fig. 5.14 Overpotential, entropic, and total heat generation inside the cell at 40 °C during charging at 0.7 C-rate and discharging at 1 C-rate
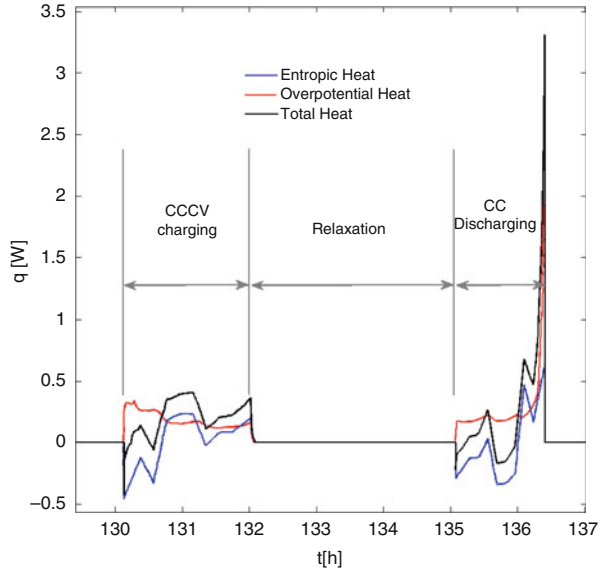
Fig. 5.15 Temperature profile for charging at 0.7 C and discharging at 2 C, $T = 0$ °C
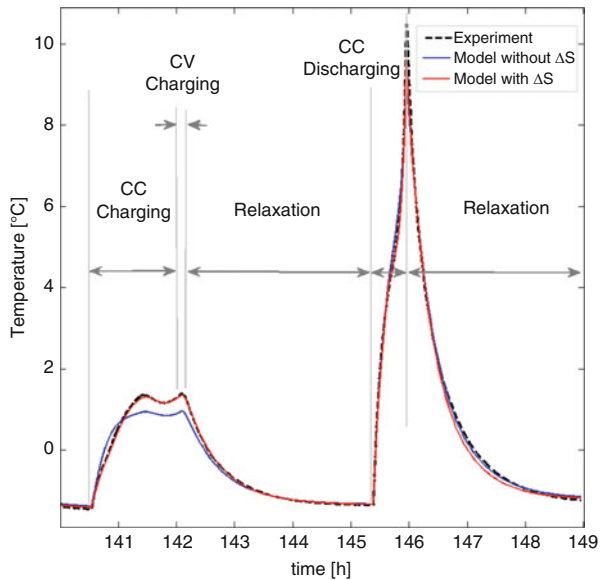
The temperature profiles are presented as a function of time in Figures 5.15 and 5.16 at ambient temperatures of 0 and 40 °C, respectively. The simulated temperatures upon charging at 0.7 C-rate and discharging at 2 C-rate are compared. The temperature deviations are much higher at 40 °C, indicating that the ΔS contribution to heating is much more pronounced than at higher temperatures. The temperature profile improves significantly at all battery conditions by

Fig. 5.16 Temperature
profile for charging at 0.7 C
and discharging at 2 C, $T = 40\,^\circ$C
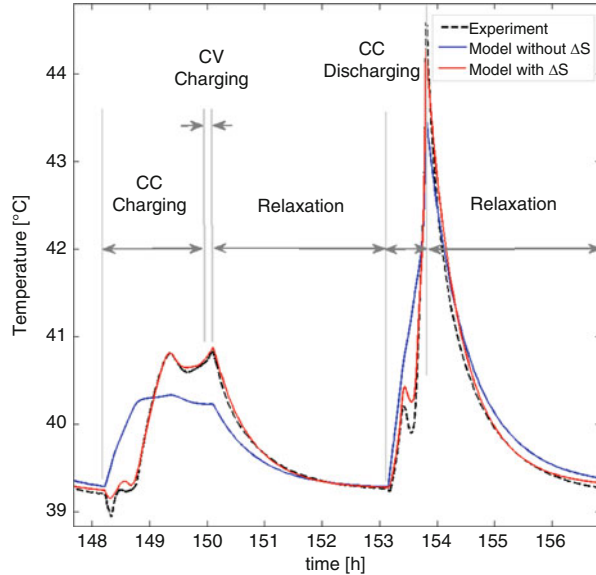
introducing $\Delta S = \Delta S$ (SoC) into the model, especially at elevated temperatures. Thus the model can predict both the temperature evolution under all SoC conditions.

To analyze the temperature profiles with and without considering $\Delta S = \Delta S$ (SoC) it is useful to plot the temperature development as a function of Q_{out}. Figure 5.17 shows sets of temperature profiles at 0.2, 1, and 2 C-rate at an ambient temperature of $20\,^\circ$C. This figure gives an overview of the SoC-dependent entropic heat contribution on the temperature evolution. While the current and overpotential have the same sign during charging and discharging, the overvoltage heat is always positive, i.e., it always generates heat inside the cell. The overpotential heat generation subsequently can only predict the gradual temperature increase but not the temperature drop. On the other hand, the entropy is changing from negative to positive dependent on the battery SoC. Thus the entropic heat can be either endothermic or exothermic and this is the only reason explains that the temperature drop.

5.1.4   Pack Modelling

When modelling a battery pack, the temperature distribution across various parts of the cell and the pack must be taken into account. Therefore, instead of using the lumped-sum model described by Eq. (5.13), more advanced 3D derivations must be carried out. The point in space $\mathbf{r} = (x, y, z)$, where the location in the cell is denoted by $\mathbf{r} \in R^3$. The temperature in point $\mathbf{r}$ at the time t is denoted as $T(r, t)$ [K]. The conductive heat flux $\mathbf{Q}(\mathbf{r}, t)$ [$\mathrm{W\,m}^{-2}$] follows standard Fourier's law, according to:
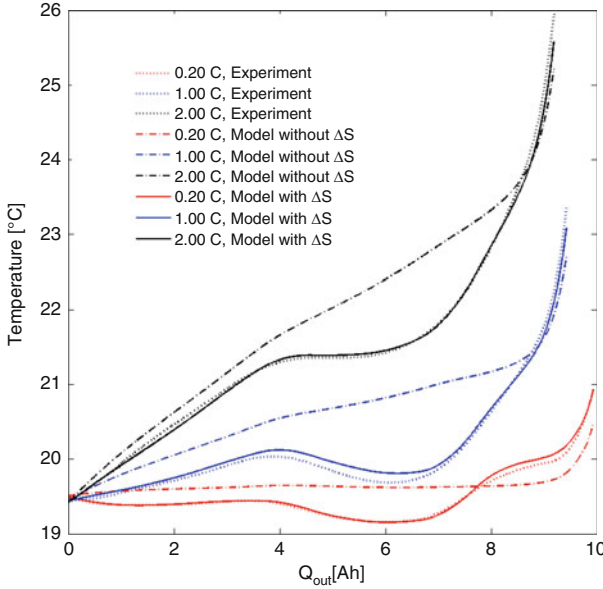
Fig. 5.17 Temperature profile during discharge versus extracted charge from the battery at 0.2, 1 and 2 C-rate, $T_a = 20\,°C$

$$\mathbf{Q}(\mathbf{r}, t) = -k\nabla(r, t), \tag{5.16}$$

where ∇T is the gradient of the temperature $[\mathrm{K\,m^{-1}}]$, and $k = k(\mathbf{r})$ is the thermal conductivity of the particular part of the cells and module $[\mathrm{W\,m^{-1}\,K^{-1}}]$. Specifically, it is assumed that the thermal conductivity is constant within each part of the cells and casing. Denote the bulk heat source term as $H^{in} = H^{in}(\mathbf{r}, t)$ $[\mathrm{W\,m^{-3}}]$. The law of energy conservation leads to the following partial differential equation (PDE) for temperature distribution:

$$\rho C_p \frac{\partial T}{\partial t} = \nabla \cdot (k\nabla T) + H^{in}, \tag{5.17}$$

where ρ is the density of the material $[\mathrm{g\,m^{-3}}]$ and C_p is the specific heat capacity $[\mathrm{J\,g^{-1}\,K^{-1}}]$. Equation (5.14) states that the rate of temperature variations within the system is due to the rate of heat diffusion and rate of heat generation in the battery.

If the outside area of the cells (or module) contains air or liquid, then heat exchange at the interface is determined by convective H_c and radiation H_r heat transfer, that is:

$$-\mathbf{n} \cdot \mathbf{Q}(\mathbf{r}, t)\Big|_{\mathbf{r} \in \Gamma_{\max(i \in J_c)}} = H_c + H_r \tag{5.18}$$

$$H_c = h(T - T_a) \tag{5.19}$$

$$H_r = \sigma(T^4 - T_a^4), \tag{5.20}$$

where T_a is the ambient temperature at the surface of the cell K.

In several cases the properties of the cooling fluid media were considered. It is assumed that velocity of cooling medium $\mathbf{u}$ can be described by the system of Navier–Stokes equations for compressible flow, according to:

$$\rho_E \frac{\partial \mathbf{u}}{\partial t} + \rho_E (\mathbf{u} \cdot \nabla) \mathbf{u} = \nabla \cdot \left[-p\mathbf{I}_3 + \mu_E \left(\nabla \mathbf{u} + (\nabla \mathbf{u})^T \right) - \frac{2}{3} \mu (\nabla \cdot \mathbf{u}) \mathbf{I}_3 \right]$$
$$\nabla \cdot (\rho \mathbf{u}) = 0 \tag{5.21}$$

or by

$$cropenup5pt \rho_E \frac{\partial \mathbf{u}}{\partial t} + \rho_E (\mathbf{u} \cdot \nabla) \mathbf{u} = \nabla \cdot \left[-p\mathbf{I}_3 + \mu_E (\nabla \mathbf{u} + (\nabla \mathbf{u})^T) \right]$$
$$\nabla \cdot \mathbf{u} = 0 \tag{5.22}$$

for incompressible flow. ρ_E is the fluid density [kg m^{-3}], μ_E the dynamic viscosity [Pa $\times$ s], p is the pressure [Pa], and $\mathbf{I}_3$ is the three-dimensional unit matrix. The heat generation term $H^{in}(\mathbf{r}, t)$ in the right-hand side of Eq. (5.17) determines the heat sources which is only applied to the electrochemical core of the cell. The casing, plastic cover, pack, and terminals of the battery do not contribute in heat generation. $H^{in}(\mathbf{r}, t)$ is composed of two parts according to:

$$H^{in}(\mathbf{r}, t) = \frac{H_\eta(t) + H_S(\mathbf{r}, t)}{V_O}, \tag{5.23}$$

where $H_\eta(t)$ [W] represents overpotential heat, $H_S(\mathbf{r}, t)$ [W] entropic heat, and V_O [m^3] the volume of electrochemical core of the cell. $H_\eta(t)$ is defined by:

$$H_\eta = \eta_t I, \tag{5.24}$$

where $\eta_t(t)$ [V] gives the total overpotential. $H_S(\mathbf{r}, t)$ represents the entropic heat [W] and is defined by:

$$H_S(\mathbf{r}, t) = -I(t) T(\mathbf{r}, t) \frac{\Delta S(t)}{nF}, \tag{5.25}$$

where n is the number of electrons that are transferred in the electrochemical reaction during battery operation and F is the Faraday constant. $\Delta S(t)$ [J mol^{-1} K^{-1}] expresses the entropy change induced by the electrochemical charge transfer reaction during battery operation and, as shown in the previous section, this can be positive or negative, depending on SoC.

5.1.5 Cell Thermal Simulations

This section describes simulations made for the case of ultra-high power NCA automotive cells, described in detail in the previous section. Figure 5.18 illustrates development of the temperature of this cell under 2 C discharge and ambient temperature of 20 °C. Figure 5.18 contains four lines. The blue line corresponds to the temperature at the surface of the cell, where the thermistors are usually placed. The red line indicates temperature of the core of the cell, in the geometrical center of the battery. The magenta line shows the average temperature of the cell, while the black dotted line gives the experimentally measured temperature. It can be seen that applied 3D model predicts the development of surface temperature quite well. It also can be seen that there is a considerable difference between surface (measured) and core temperature.

Figure 5.19 contains the temperature profiles at the end of 6 C discharge when two cooling regimes are applied to the cell. Figure 5.19a corresponds to natural air cooling with $h = 10$ [W m^{-2} K^{-1}] h while Fig. 5.19b relates to a forced-cooling case with $h = 45$ [W m^{-2} K^{-1}]. One can see that 6 C discharge causes much higher temperatures than 2 C case. In the case of natural air cooling the surface temperature reaches almost 37 °C. The core in this case is around 45 °C. The introduction of
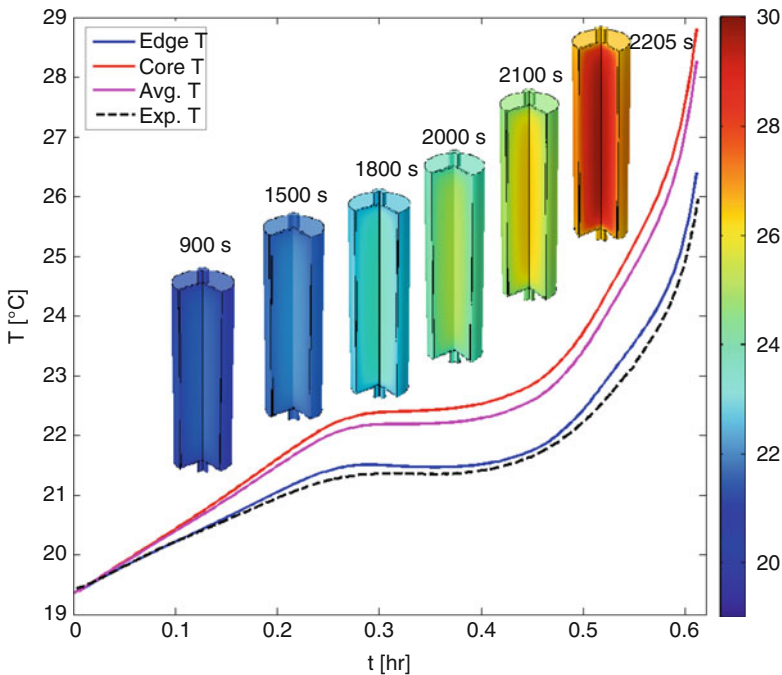
Fig. 5.18 Edge, core, and average temperature profiles during discharge at 2 C-rate and comparison with measured temperatures

A)   B)

t = 760 s   Centerline T   t = 760 s   Centerline T
▲ 44.9 °C   (r direction)   ▲ 41.5°C   (r direction)

▼ 36.9°C   ▼ 27.4°C
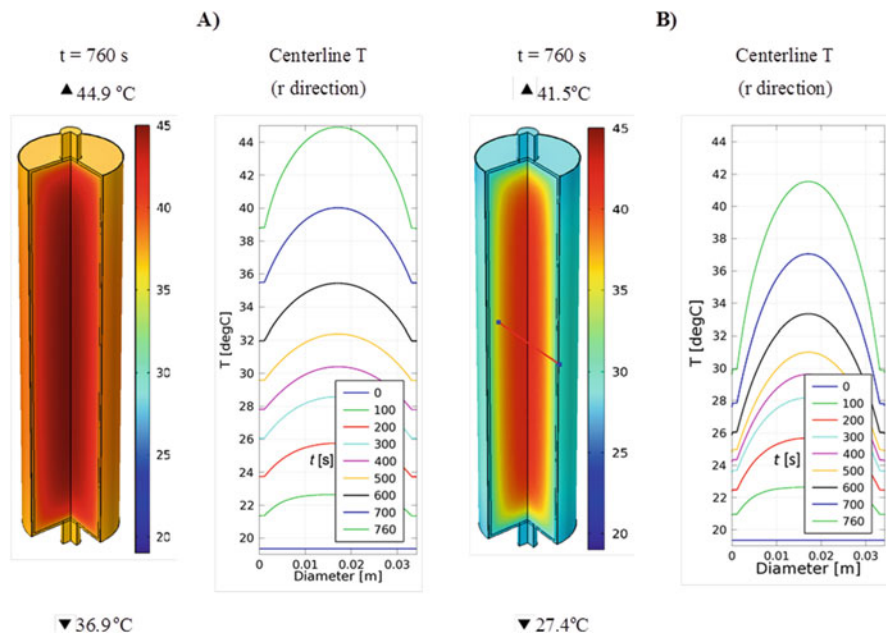
Fig. 5.19 Temperature profile of the cell at 6 C-rated current discharge; (**a**) air natural convection, (**b**) air forced convection, $h = 45$ [W m^{-2} K^{-1}]

forced cooling helps reduce the surface temperature of the cell down considerably to 37 °C. However the core temperature is not affected by the surface cooling, declining only to 42 °C. That means that intensive cooling in many situations only help to control the surface temperature, while the core temperature remains high.

5.1.6 Pack Thermal Simulations

In this section, simulation results developed at cell level in the previous section are applied to pack modelling. Figure 5.20 illustrates the thermal behavior of the 12 cell pack in a 3×4 arrangement. Figure 5.20a shows the layout of the pack and the location of its cross section. The temperature distribution at that cross section is plotted in Fig. 5.20b, it is assumed that the cells are surrounded by air and no external airflow is assumed.

Figure 5.21 represents the same modelling assumptions, but provides with temperature profile along the center of the middle 4-cells row during 6 C discharge (Fig. 5.21a) followed by 3 h of relaxation. One can see that for large battery packs, the temperature drops slowly in the absence of forced cooling, and even after 3 h of relaxation, it still remains almost 10 °C higher than the ambient temperature.
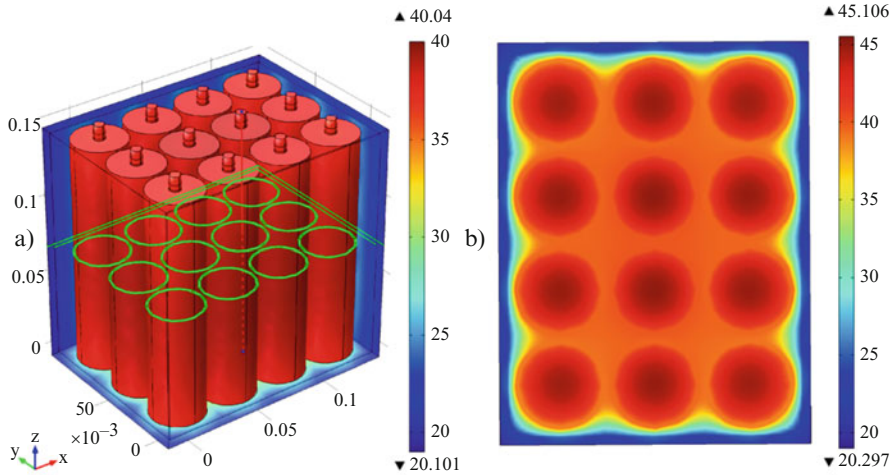
Fig. 5.20 (**a**) Module structure under static air conditions and temperature distribution on the surfaces of the cells and ABS pack at the end of discharge under 6 C-rate; (**b**) temperature distribution within air and a cross section of the cells under static air conditions
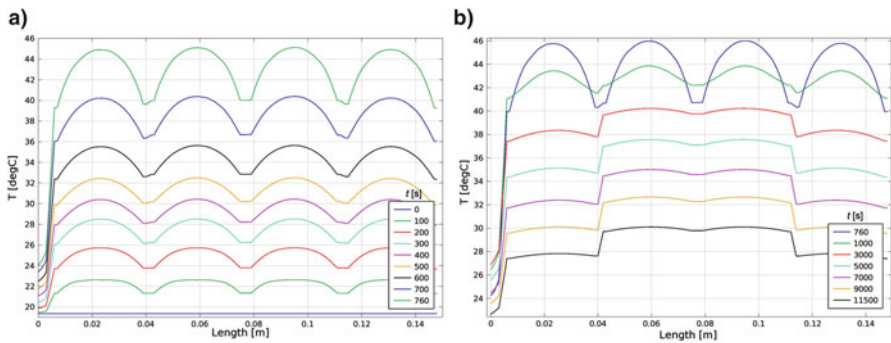
Fig. 5.21 Centerline (*x* direction) temperature development during 6 C-rated current in the battery module occupied by air, (**a**) during discharge (**b**) during 3 h relaxation (legend shows time in seconds)

The last figure, Fig. 5.22 reports the influence of the force cooling by constant flow of the air (Fig. 5.22a) and water (Fig. 5.22b) in 3×3 cells arrangement during 6 C discharge. Temperature of the cooling media on the inlet is 20 °C, laminar flow is assumed. The inlet of air and water is located at the top of the pack and outlet is at the bottom. It can be seen that water is better cooling media than air, since maximal core temperature for water cooling pack is reduced from 42 to 35 °C. At the same time, the temperature gradients across the cell are still considerable; there is a large difference between temperatures of the core and the surface. In addition, in the case of force cooling there is a clearly visible temperature gradient in the vertical direction: the top parts of the cells are better cooled than the bottom ones.
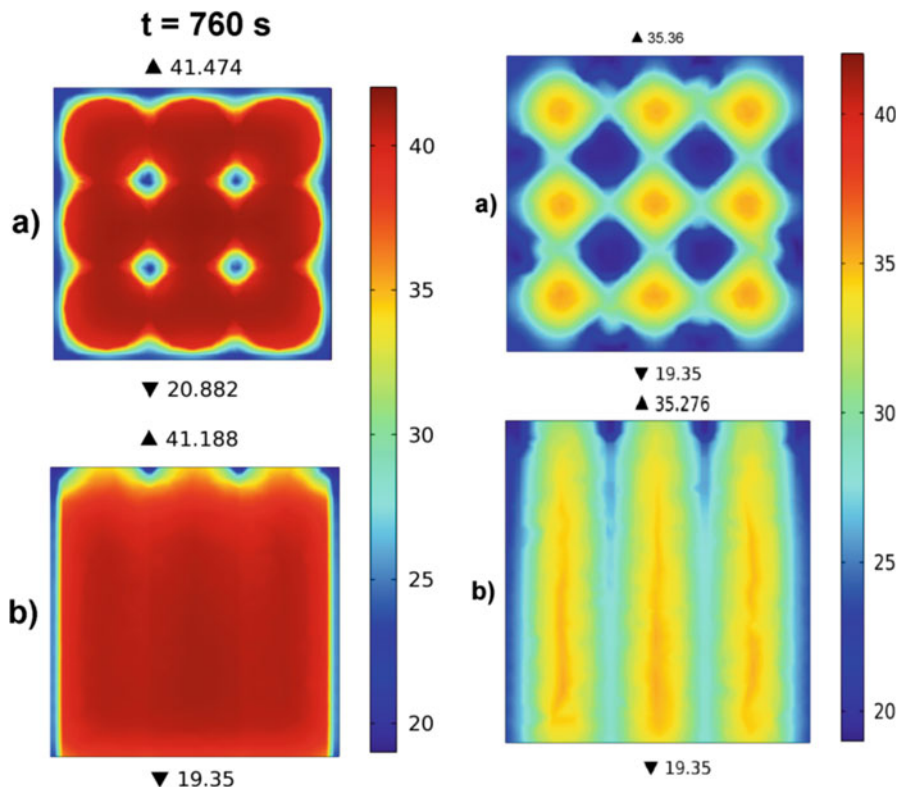
Fig. 5.22 *Left*: Temperature distribution in the battery module under predictive speed air flow at 20 °C under 6 C-rated current discharge. (**a**) Structure of the battery module and surface temperature distribution at the last moment of discharge. (**b**) Temperature development during discharge and relaxation periods on horizontal and vertical cross sections. *Right*: Temperature distribution in the battery module under predictive speed water flow at ambient temperature of 20 °C under 6 C-rated current discharge. (**a**) Horizontal cross sectional view, (**b**) side view (vertical cross sectional)

All that observations point out that measuring the temperature of the cells with surface sensors do not provide with the true thermal condition of the cell. Moreover, in the case of large battery packs, considerable thermal gradients can occur even in the presence of forced cooling. Therefore, methods to access the integral, or average, temperature of the cell [70] are of high interest. The differences in the temperatures across the cells can cause differences in the ageing rates, since the later are strongly influenced by temperature [21, 49] (Figures 5.23 and 5.24).
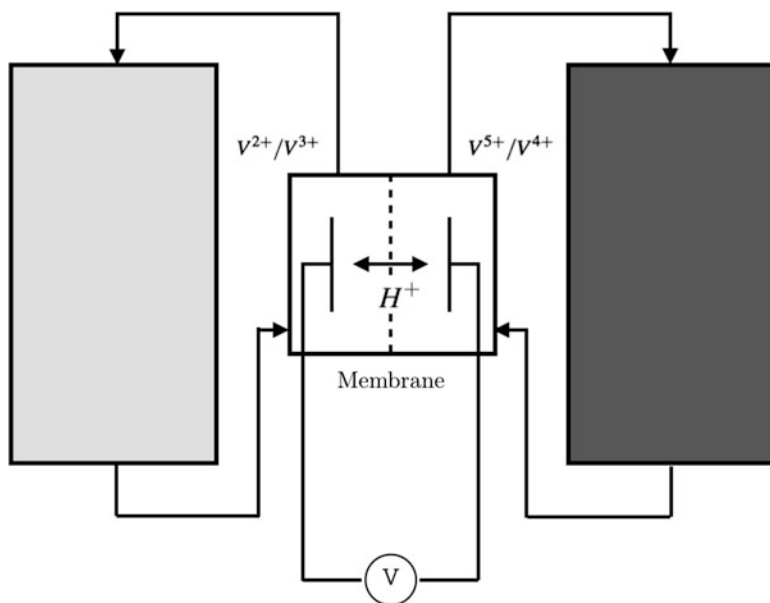
Fig. 5.23 Principal layout of a vanadium flow battery unit
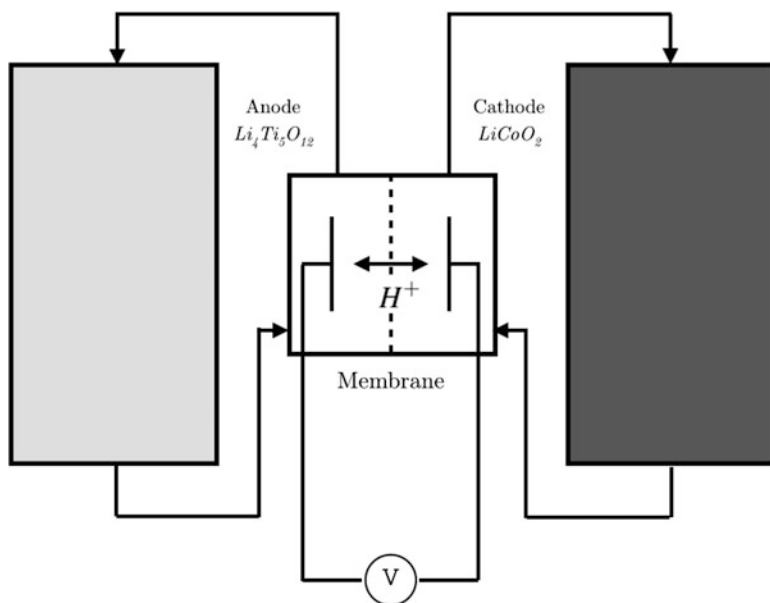
Fig. 5.24 Principal layout of Li-ion flow battery unit

5.2   Flow Battery Models

5.2.1   Chemistry of Flow Batteries

Oxidation and Reduction Reaction
The functionality of a battery is based on reduction and oxidation reactions or (redox reaction). Redox reaction is where electron transfer occurs from one species to another. A molecule is oxidized when it loses electrons and reduced when it gains electrons.

Reduction means that an oxidant takes electrons from another substance:

$$oxidant + e^- \rightarrow product \tag{5.26}$$

Oxidation means that a reductant transfers electrons to another substance:

$$reductant \rightarrow e^- + product \tag{5.27}$$
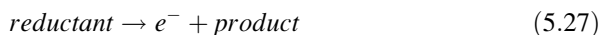
5.2.2   Molality and Molarity

The molality is the number of moles of a solute dissolved in one kilogram of solvent and the molarity (or molar concentration) is the number of moles of a solute dissolved in one liter of solution. The molality m_B is defined as:

$$m_B = \frac{n_B}{n_A * M_A} \qquad \left[mol\ kg^{-1}\right] \tag{5.28}$$

Where:

$$
\begin{aligned}
n_A &= \text{Number of mole of the solvent} & [-] \\
n_B &= \text{Number of moles of solute B} & [-] \\
M_A &= \text{Molar mass of A} & [\text{kg/mol}]
\end{aligned}
$$

The molar fraction x_B is defined as:

$$x_B = \frac{n_B}{n_B + n_a} \qquad\qquad - \tag{5.29}$$

The molarity c_B is defined as the ratio of the number of the mole n_B to the volume of the solution V:

$$c_B = \frac{n_B}{V} \qquad \left[mol\ l^{-1}\right] \tag{5.30}$$

5.2.3 Chemical Equilibrium

The chemical equilibrium describes the state where the reactants or products concentrations are balanced [30]:

$$aA + bB < - - - > cC + dD \tag{5.31}$$
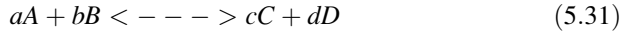
A and B are the reactants while C and D are the products. a, b, c, and d are stoichiometric factors introduced to maintain the composition of the reaction mixture. The chemical equilibrium is met when the reaction rates are equal. The reaction rate is a function of the activities a_i of the reacting substances raised to a power equal to the number of moles of each reacting substance. The equilibrium constant K is defined as:

$$K = \frac{a_C^c a_D^d}{a_A^a a_B^b} \qquad [-] \tag{5.32}$$

The activity a_i is the effective molar fraction given by:

$$a_i = Y_i x_i \qquad [-] \tag{5.33}$$

Here, Y_i is the activity coefficient used to determine the effect of ionic strength on the chemical reaction. In very dilute solutions the activity coefficient becomes close to one.

In dilute solutions, the activity a_i is defined as:

$$a_i = Y_i^c \frac{c_i}{c_o} \qquad [-] \tag{5.34}$$

Where:
$Y_i^c =$ activity coefficient of the species i in the molarity scale [–].
$C^o =$ Standard molarity (1 M $=$ mol/l)

5.2.4 Gibbs Free Energy and Nernst Equation

The cell potential can be defined as:

$$E_{cell} = \triangle \cdot V = E_{right} - E_{left} \qquad [V] \tag{5.35}$$

Here, E_{right} refers to the half-cell where reduction takes place and E_{left} to the half-cell where we get oxidation. The half-cell potentials are measured in relation to each other. The potential of different electrodes measured in relation to the hydrogen half-cell are presented in Table 5.1. The hydrogen half-cell potential is usually defined as zero [52]. Standard reduction potentials are given as E^o. The more

Table 5.1 Standard reduction potentials

Oxidant (e^- acceptor)	Reductant (e^- donor)	E^o[V]
Na^+	Na(s)	−2.71
Zn^{2+}	Zn(s)	−0.76
Fe^{2+}	Fe(s)	−0.44
Cd^{2+}	Cd(s)	−0.4
Pb^{2+}	Pb(s)	−0.126
$2H^+$	H2(g)	0.00
AgCl(s)	Ag(s) + Cl⁻(aq)	0.222
Hg_2Cl_2(s)	2Cl⁻(aq) + 2Hg(l)	0.268
Cu^{2+}	Cu(s)	0.337
Is(s)	2I⁻	0.535
Fe^{3+}	Fe^{2+}	0.771
Ag^+	Ag(s)	0.799
O_2(g) + $4H^+$	$2H_2O$(l)	1.23
Cl_2(g)	2Cl⁻	1.36

positive the half-cell potential, the greater the tendency of the reductant to donate electrons, and the smaller the tendency of the oxidant to accept electrons. When the potential difference between the reduction half-cell and the oxidation half-cell is positive the reaction will go to the right. This means that electrons will flow through the external circuit from left electrode to the right.

The standard free energy ($\triangle G^o$) determines if a process will take place under the conditions of constant temperature and pressure. The relation between free energy change and the potential difference are related as follows:

$$\triangle G^o = -nFE^o \qquad [J\ mol^{-1}] \qquad (5.36)$$

Here, n is the number of electrons and F is the Faraday constant. The value $\triangle G^o$ is a measure of the amount of work a system can do on the surroundings. The negative sign at the right side is due to a positive cell potential which means a negative free energy change. This gives a cell reaction spontaneously proceeding to the right. $\triangle G^o$ refers to a situation where all substances have the concentration of 1 mol. For other concentrations it can be rewritten as:

$$\triangle G = -nFE \qquad [J\ mol^{-1}] \qquad (5.37)$$

The Gibbs free energy $\triangle G$ is a sum of a constant term $\triangle G^o$, which represents the free energy change for a reaction when the activity of each product and reactant is the unity and a variable term that is a function of the temperature and the equilibrium constant K:

$$\triangle G = \triangle G^o + RT\ln K \qquad [J\ mol^{-1}] \qquad (5.38)$$

where R is the gas constant and T is the temperature. By combining Eqs. (5.11)–(5.13) we obtain

$$-nFE = -nFE^o + RT\ln K \qquad\qquad [J\ mol^{-1}] \qquad (5.39)$$

This can be rearranged into the well-known Nernst equation:

$$E = E^o - RT\frac{\ln K}{nF} \qquad\qquad [V] \qquad (5.40)$$

The Nernst equation shows that a half-cell potential will change by 59 mV per tenfold change in the concentration of a substance involved in a one-electron oxidation or reduction, for two-electron processes the change will be 28 mV per tenfold change in the concentration.

The activities a_i and the activity coefficients y_i cannot be measured directly. The formal redox potential $E^{o'}$ may then be used to give the measured value when experiments are performed at specified conditions. The formal redox potential then becomes:

$$E = E^{o'} - RT\ln\frac{c_C^c c_D^d}{c_A^a c_B^b}[V] \qquad (5.41)$$

The Nernst equation is accurate for solutions with a total ionic concentration below approximately 10^{-3} M. At higher concentrations, the Nernst equation values that are too high are obtained, as weak ion pairs are formed at electrode surfaces.

The most popular flow battery today is the vanadium flow battery because it utilizes only one active element, vanadium. It uses VSO_4 and $VOSO_4$ as a pair with $V^{2+} - V^{3+}$ at one electrode and $V^{4+} - V^{5+}$ at the other. Other types of flow batteries are, e.g., uranium redox battery, zinc and bromium redox battery, and polysulfide and bromium flow battery [28].

In 2011 Duduta et al. presented an idea about a new type of flow battery: semi-solid lithium rechargeable flow batteries. The battery was based on the principle of powdering the lithium-ion battery and dispersing the powder in an organic electrolyte. As a result, it combines the high energy density of lithium salts with the scalability of flow batteries resulting in higher energy density.

5.2.5 Vanadium Flow Batteries

Vanadium flow batteries [12, 58, 11, 40, 76] have been developed and tested for several decades and commercialized by several companies. They have been traditionally used for large scale installations such as grid storage units due to the technology's ability to store large amounts of energy. However, recent technological advancements have led to an increase in energy density and capacity, as a result, vanadium flow batteries today offer high round-trip efficiency, high depth of

discharge (DOD), long durability, and fast response time, thus making them viable for vehicle application [68].

A typical all vanadium system is comprised of two carbon/graphite electrodes (anode and cathode) and a semi-permeable ion exchange membrane separator that allows for the diffusion of hydrogen ions across a membrane while preventing the cross-diffusion of the electrolyte solutions from the two tanks [67]. The standard potential is 1.23 V. The capital cost for a VRB is approximately 400–700 $/kW (power package) and 100–150 $/kWh (electrolyte) [58].

There are two different electrolyte solutions in vanadium flow batteries. One is vanadium sulfate, with an oxidation state of V_2^+ and V_3^+ that is pumped through a cell with one of the two electrodes. In the other we have vanadium oxide sulfate, with V_4^+ or V_5^+ as the oxidation states. As V_2^+ is oxidized to V_3^+ on the negative side and V_5^+ reduced to V_4^+ on the positive side hydrogen ions are transferred through the membrane, transferring SO_4 to H_2SO_4 on one side of the membrane, and the opposite on the other side. In this way, since the battery utilizes four different redox states of vanadium, we can charge and discharge the electrolytes simply by reversing the flow of the electrolyte being pumped through the cell. The electrolyte solution has an indefinite life due to its reversibility and results in a battery with low replacement costs without waste disposal [57], which would be economically beneficial.

Thermodynamic data of vanadium ions at different valences is presented in Table 5.2.

The key issue for this type of batteries is it is not desirable for V and SO_4 to move through the membrane, but only H^+. An important challenge is to achieve this with a low cost membrane, otherwise it would increase the total cost of the battery. However, since the electrolyte only uses vanadium as the active element, and it can be recharge simply by inverting the process, any cross-diffusion between the solutions can be reversed, thus eliminating any energy loss to one discharge cycle, for as long as the total vanadium in the system remains constant.

The reactions in the flow battery of vanadium type could be written as:

$$VO_2^+ + 2H^+ + e^- \quad \rightarrow \quad VO_2^+ + H_2O \tag{5.42}$$

$$V^{2+} + VO_2^+ + 2H^+ \quad \rightarrow \quad VO^{2+} + V^{3+} + H_2O \tag{5.43}$$
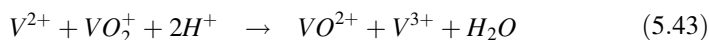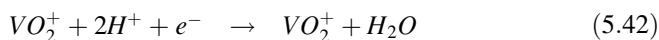
Table 5.2 Thermodynamic data for vanadium compounds at 298.15 K

Formula	State	$\triangle Hf^o$ [kJ/mol]	$\triangle Gf^o$ [kJ/mol]	Sf^o [J/mol K]
V^{2+}	aq	(−226)	−218	(−130)
V^{3+}	aq	(−259)	−251.3	(−230)
VO^{2+}	aq	−486.6	−446.4	−133.9
VO_2^+	aq	−649.8	−587	−42.3
H_2O	aq	−285.8	−237.2	69.9
H^+	aq	0	0	0

Values in parentheses were estimated [30]

V^{2+} is the charged state as well as $V^{5+}(VO_2^+)$, while V^{3+} and $V^{4+}(VO^{2+})$ are the discharged states.

An important issue is the cost associated with vanadium salts. Although vanadium exists in large amounts, for instance, in fly ash from coal fired boilers, and in minerals like shale oil, it still has a high cost due to relatively low production volumes. A kg of V_2O_5 powder typically costs about 15 EUR/kg, but its price could be as low as a third of this value if produced at large scale from abundant resources like fly ash [73] or high content ores (with high concentration % of vanadium). If this is achieved, the price for a complete flow battery could then be reduced to half of its current cost and make it as economically competitive as current Li-ion batteries. Larsson and Andersson [47] have demonstrated how the way the cell is mechanically built has a significant impact on the performance of the battery. The distance between electrode and membrane should be as small as possible. Aaron [1] found that by designing a cell stack where there was direct contact between the electrolyte, electrode, and membrane not only decreased the size of the battery but also increased the battery output and efficiency by reducing the charge transport distance.

Vanadium redox flow batteries (VRB) have been used in several commercial installations. At Huxley Hill Wind Farm, located in King Island, Tasmania in Australia, a 200 kW VRB battery was installed in 2003 to help balance 3 % of the total installed wind power capacity. Several installations have been built in China by Dalian Rongke Power that range from a few kW up to MW-scale [94]. The cost of these batteries is still high, compared to other battery technologies, especially since vanadium salts are still expensive, and polymer membranes are costly to manufacture. Extensive development work is attempting at developing less expensive and more selective membranes at Fraunhofer Institute [59], Dalian Institute of Chemical Physics and the Chinese Academy of Sciences [94]. While there is large potential for cost reductions in this area, the cost of vanadium salts still remains as the main problem.

Another limitation with vanadium salt batteries is the amount of salt that can be dissolved in the water. In comparison, in semi-solid lithium flow battery, the electrolyte stores the energy in small solid particles, thus increasing the energy density of the battery. It might be possible to run flow batteries with precipitated vanadium salts, to increase its energy density compared to the system when the salts are dissolved in a conventional way. Normally the molarity is 2 M, but with precipitated salts it is possible to increase the charge per volume unit. If the particles are made very small, (e.g., in the μm range), higher capacity per liter of electrolyte can be achieved, while keeping it aqueous enough to be pumped. This is of great interest for vehicle applications.

5.2.6 Semi-solid Lithium Flow Batteries

Proposed by Duduta et al. [27], this battery consists of a powdered lithium ion battery dispersed in an organic solvent that is also part of the electrolyte. This new

concept replaces the electrodes with the nano-sized constituent parts in the electrolyte, as a result, it creates a battery with ten times the charge storage density of a typical flow battery. This increase in energy density is possible because more active components can be added to the organic solvent, thus, effectively increasing the energy capacity by a factor of 20–30 times that of vanadium flow batteries [27].

Lithium ion batteries will have the following reaction at the positive electrode [34]:

$$LiCoO_2 \rightarrow Li_{1-x}CoO_2 + xLi^+xe^- \qquad (5.44)$$
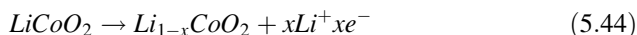
At the negative electrode the half reaction for graphite would be

$$xLi^+ + xe^- + xC_6 \rightarrow xLiC_6 \qquad (5.45)$$
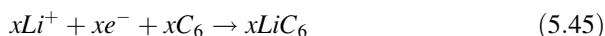
If we have $Li_4Ti_5O_{12}$ instead we can get:

$$Li_4Ti_5O_{12} + 3Li^+ + 3e^- \rightarrow Li_7Ti_5O_{12} \; E = 1.5 \; V \qquad (5.46)$$
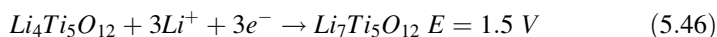
By using $Li_4Ti_5O_{12}$ some of the problems associated with the risk of fire by using graphite as an anode are reduced [91]. The compound, however, is an insulating material, and thus it would be necessary to make it into nano-sized particles to overcome this issue [48]. These characteristics ensure long life cycle and excellent cycle performance. The $Li_4Ti_5O_{12}$ inserts three lithium ions per formula unit, with a theoretical capacity of $175 \, mAh \, g^{-1}$, showing a flat voltage at 1.55 V versus a lithium electrode.

The overall reaction, however, has its limits. Overdischarge supersaturates lithium cobalt oxide, leading to the production of lithium oxide [18] described by the following irreversible reaction:

$$Li^+ + e^- + LiCoO_2 \rightarrow Li_2O + CoO \qquad (5.47)$$
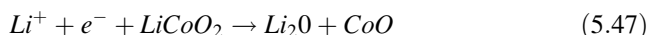
Overcharge up to 5.2 V leads to the synthesis of cobalt(IV) oxide [6].

$$LiCoO_2 \rightarrow Li^+ + CoO_2 + e^- \qquad (5.48)$$
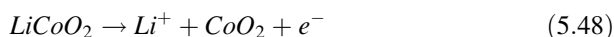
The lithium contains 11.6 kWh/kg at 3 V ($= 41.7$ MJ/kg). This can be compared to hydrocarbon fuels having similar energy content per kg.

The electrolyte in lithium-ion batteries, including flow batteries, contains salts, for instance, $LiPF_6$ or LiClO. The salt is dissolved in an organic solvent like ethylene carbonate, dimethyl carbonate, or diethyl carbonate. Li-ions pass a membrane and carrying positive ions, while the electrons are passing through the external conductor between the two electrodes and the load. The conductivity of the electrolyte is in the range of 10 mS/cm [88].

The main disadvantage, however, is that the organic solvent can decompose during the charging, especially at the negative electrode. A solid layer can be added

to provide with some isolation of the electrode, and help prevent this without significantly affecting the performance of the charging process. [8]

During the discharge process Li-ions pass from the negative to the positive electrode through the liquid and the membrane [50].

Tests have been done with different versions of electrolytes and different materials for the cathode and the anode. The cathode materials have been $LiCoO_2$ [51.2 M], $LiFePO_4$ [22.8 M], $LiNi_{0.5}Mn_{1.5}O_4$ [24.1 M], and $0.3Li_2MnO_3-0.7LiMO_2$ ($M = Mn, Co, Ni$) [39.2 M]. The anodes tested have been $Li_4Ti_5O_{12}$ [22.6 M], graphite [21.4 M] and Si [87 M]. The molar capacity is the number within brackets after each compound. In the tests, a solid concentration of up to 70 % has been tested, but 50 % seems more realistic. The molar capacity then should be 10–40 M, or 5–20 times higher than what is typical in a water solution (ca 2 M). The Li-ion approach can be used in a water system, but with an organic solvent it can be increased by a factor 1.5–3, and thus has advantages. The team at MIT has demonstrated a system with approximately 12 M concentration.

For a system with $LiCoO_2$ (20 vol%, 10.2 M) and 1.5 % Ketjen black as the cathode and $Li_4Ti_5O_{12}$ (10 vol%, 2.3 M) and 2 % Ketjen black as the anode with a non-aqueous electrolyte of dimethyl carbonate with 1 M $LiPF_6$ tests were run between 0.5 and 2.6 V with charging–discharging. The current collectors were copper or aluminum plates with a lithium reference electrode. A membrane with 0.1 μm nominal pore size was separating the two cell halves. The powder was grinded to a few μm particle diameter. The columbic efficiency was 73 % for the first cycle and 80 % for the second cycle. At 2.35 V average discharge voltage, the capacity for the system was 397 Wh/l (168 Wh/kg). For an $LiCoO_2$ graphite system at 3.8 V discharge voltage, the corresponding theoretical value should be 615 Wh/l (309 Wh/kg), showing a high potential compared to the 40 Wh/l (50 Wh/kg) for a 2 M aqueous redox system with 1.5 V discharge voltage.

Duduta et al. [27] believe a system with the capacity 300–500 Wh/l (specific energy 130–250 Wh/kg) could be reasonable for a large scale system. They have estimated a cost of $10–15/kg for active materials and $15/kg for non-aqueous electrolyte, which should give $40–80/kWh for the semi-solid suspension. It should then be possible to produce a complete system at the level $100–250/kWh for grid level storage and transportation applications.

From a manufacturing perspective, a particle suspension is more difficult to handle than a pure solution due to risk for sedimentation and clogging and therefore it is an important issue to be addressed.

5.2.7 Other Types of Flow Batteries

Polysulfide-Bromine Batteries

Polysulfide-bromine batteries (PSB) were developed in the early 1990s. The reaction during discharge at the positive electrode is given by [58]:

$$NaBr_3 + 2Na^+ + 2e^- \rightarrow 3NaBr \qquad (5.49)$$

and the reaction at the negative electrode is as described as follows:

$$2Na_2S_2 \rightarrow Na_2S_4 + 2Na^+ + 2e^- \qquad (5.50)$$
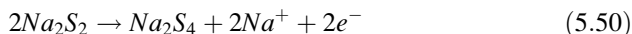
The reactions are reversed during charge. A cation-exchange membrane is used to separate the anolyte and catholyte. The membrane allows sodium ions to pass through. The open circuit voltage is 1.5 V in each cell. Cell stacks consist of bipolar electrode plates with insulating polymer frames in between. The frames also contain the flow channels for distributing the electrolyte into the cell compartments.

An advantage with flow batteries is that the temperature of the cell stack can easily be controlled by heating or cooling the liquid outside the stack. However, the additional energy required for this reduces the overall efficiency of the battery. Additionally, the pumping system also takes away part of the energy supplied. Finally, due to inefficiencies of the membranes, crystalline sodium sulfate is produced and has to be collected from the negative electrode frequently (e.g., every 2 weeks). The expected cycle life of a PSB is 15 years with a net efficiency of 75 %. The PBS battery is considered to be environmentally benign in general, however, toxic bromine vapor can be released if there is an internal rupture.

Zinc Bromine Batteries

Zinc bromine batteries (ZBB) are called hybrid batteries since one of the electrodes is participating in the reaction. The electrolyte consists of zinc bromide dissolved in water. During charging, zinc is plated onto the negative electrode. Bromine is simultaneously produced at the positive electrode forming a bromine complex that can sediment in the bottom of the positive electrolyte tank if no stirring is implemented. When the battery is discharged, zinc is dissolved to form zinc ions producing bromide ions at the positive electrode. The efficiency of the ZBB is around 60–75 %. The capacity is limited due to the zinc plated on the negative electrode.

Comparison of Different Flow Battery Systems

Other types of flow batteries systems having being developed, for example: vanadium-bromine, iron-chromium, zinc-cerium, uranium, neptunium, and soluble lead-acid redox flow batteries.

These have all been extensively studied, while some other types are more rare, like sodium or potassium sulfide-polysulfide in the anodic reaction and iodide-polyiodide or chloride-chlorine in the cathodic reaction [61].

Different type of redox batteries are compared in Table 5.3.

Most flow battery systems use cationic membranes and carbon or carbon composites as electrode material. For Li-ion batteries, a micro porous membrane can be used to reduce costs, and for the soluble lead-acid battery no membrane is needed at all. In a Li-ion battery, the electrode material is used as slurries, while the current is taken out by metal sheets made of copper or aluminum, shown as the electrode

Table 5.3 Comparison of different flow battery systems

System	Electrodes	eCell	Current	Efficiency [%]			Wh/l
		[V]	[A/m^2]	Volt	A	Energy	
Fe/Cr cation	Carbon	1.03	9	81.6	81.2	66.3	
Anionic	Membrane	0.77	64.5	73	99	72	
PSB	Carbon	1.54	600	75	90	67	
VRB	Graphite	1.70	800	73.2	98.2	71.9	40–50
Soluble lead acid	Carbon	1.78	100–600	82	85	65	
Li-ion	Cu or Al	2.35	80	80			400–600

material in the table. Iron-chromium batteries differ significantly from the rest of the group, since anionic membranes are used.

6 Battery Use in Transportation

6.1 Requirements For Transportation Applications

To use of batteries in transportation applications, they should fulfill several requirements, for instance, high power density, very high cycle life time ($> 200,000$ cycles), long lifetime, and safety. Great efforts have been undergoing from researchers and manufacturers all around the globe to develop better, lighter, and safer batteries to help the transition towards a fossil-free transportation sector.

6.2 Personal Vehicles

While electric personal vehicles have been around for over a century, their limited range and high cost when compared with internal combustion engines (ICE) made the latter the choice for most customers. However, the increase in oil price and a recent trend towards a more sustainable transportation system have stimulated car manufacturers to develop hybrid electric-gasoline and BEVs to satisfy the requirements of their customers. The most used battery for the latest category is the Li-ion one, given its high power-to-weight ratio, high DOD, and relatively long life time.

Regarding energy efficiency and environmental impact, electric vehicles offer numerous advantages. In comparison with ICE vehicles, an average mid-sized diesel passenger vehicle consumes 0.5–0.6 l/10 km (5–6 kWh/10 km) while its electric-equivalent vehicle would consume 1.5 kWh/10 km, a significant 75 % reduction. The main reason for this is because the overall energy efficiency conversion in a BEV can be as high as 80 % compared with the 25–30 % that ICEs can achieve. Most BEV use Li-ion batteries as the storage medium, however, even if flow batteries have a lower energy density, it would still be possible to use this

technology by compromising distance range. As a reference, with 210 l volume of electrolyte, a vanadium flow battery would contain 14 kWh, while the same size and weight in Li-ion battery could hold 72 kWh. The main advantage, however, is that in a flow battery the electrolyte can be refuelled faster in a similar scheme as conventional vehicles.

6.3 Trains

Train transportation is one of the most energy efficient means of transportation. According to Van der Spiegel [86], CO2 emission from trains are far less than of the cars and airplanes. The main reasons are the low running resistance and the regenerative brakes [62] which transmit the kinetic energy back to the electrical energy. Having electric trains replacing the diesel trains helps a lot regarding the cleaner transport. However, it is not possible to have the catenary system in all the tracks. According to Pagenkopf and Kaimer [65] 51 % of the train lines in Europe are equipped with overhead lines; this percentage is even less in other regions (Asia less than 35 %, Africa less than 16 %, and America less than 1 %). This is mainly due to the high installation and maintenance cost of the catenary system which makes installation of such systems not viable in tracks with low utilization. An example of these tracks are the branch lines. Branch lines are the routes connected to the main line that is not used as often as the main line. In these cases diesel trains are used instead of the electric trains. This will increase the travel time as the wagons need to be transferred to the diesel train from the electric train and it would demand a station at the intersection. Other infrastructure problems might also rise in places where installing the overhead line is not possible due to the limitations on the space available. An example of these cases are harbors in which installing an overhead line is not possible. In this case trucks are usually used instead.

The increasing price of the fuel and also the regulations regarding the emissions have caused the environmental problem with diesel trains to become the center of attention again. One way to address the problem is to increase the efficiency and reduce the emissions and fuel consumption of the diesel trains (see, for example, [53, 75, 92]). This will include both increasing the efficiency of the train units and also energy efficient train unit operation. There has been also studies on hybrid diesel trains with storage devices onboard (see, for example, [62, 4]). Another approach to reduce the environmental impact of the diesel trains is to completely replace them with a battery driven train.

Three types of energy storage devices are usually used for the railway application, i.e., batteries, flywheel, and double layered capacitors. Superconducting magnetic energy storage systems are also a new option which are still in experimental level [33].

Flywheels suitable for the application in the railway are huge in size which makes them not practical for onboard applications [29]. Moreover there are safety issues regarding installation of the flywheels on passenger trains [80]. Nevertheless,

they are great alternatives for stationary energy storage devices. Installing a fly-wheel as a stationary energy storage device on a track can reduce peak power while needing minimum maintenance and being tolerant to temperature. They can be charged either by regenerative brakes from the trains to avoid regeneration cancel-ation, or by grid in order to minimize the peak power from the grid [71]. The application of flywheels can be seen in New York City Subway and in Hong Kong [93].

Double layered capacitor, also known as supercapacitors or ultracapacitors, is another form of energy storage systems used for railway industry. They have relatively low energy density but, on the other hand, they can provide high power. Another disadvantage of the double layered capacitors is sensitivity to temperature; although they work consistent in low temperature, but their service life drops drastically with application in high temperatures [33]. They have been used both as stationary and onboard energy storage device for hybrid trains. The application can be seen in Germany, Spain, and Beijing [93]. There are also several application cases of supercapacitors as secondary energy source (see [78, 79, 3, 96, 80]).

Batteries have been used in train industry for more than a century for reducing the peak dc supply current [63]. Lithium ion batteries have been used on several substations in Japan as stationary energy storage systems to compensate voltage drop and absorbing regenerative energy (see [63, 83]). Nickel-metal hybrid batte-ries are also used in Japan for reducing energy consumption as stationary energy storage systems. Batteries have also been used onboard the trains. Li-ion batteries are used for hybrid catenary/battery driven trains and Ni-MH batteries are used for the hybrid trams [54]. There has also been studies on fuel cell hybrid trains in which the possibility of using Li-ion batteries and EDLCs are discussed [85].

Batteries have also been widely used in vehicle industry. Khaligh and Zhihao [41] studies the application of different battery types (i.e., lead-acid, nickel-metal hybrid (NiMH), lithium-ion, nickel-zinc (Ni-Zn), and nickel-cadmium (Ni-Cd)) for hybrid vehicles. Batteries can accommodate large amount of energy but, on the other hand, they cannot provide a large power at a short time [7], therefore to get the best performance out of the batteries they can be paired with ultracapacitors [56].

At the moment, there are battery driven trams and lightweight trains (e.g., PRIMOVE Project by Bombardier), however, the problem is more complex in the freight and long distance train; mostly because of the high power demand of such trains and the long travel times. Currently there are no fully battery driven trains in any railway system, however, there are hybrid electric trains introduced with batteries onboard. An example is the hybrid train developed by East Japan Railway Company that can run both on catenary-free and electrified lines [43]. IPEMU (Independent Powered Electric Multiple Unit) is also a project by Bombardier Transportations to design a hybrid electric train with batteries onboard the train. The idea is to charge the batteries from the catenary while driving on the main line and use them on the branch lines where no overhead line is available. Lithium (iron magnesium) phosphate is the battery used in this project.

Flow batteries are also going to be studied to be used for this purpose in the future as well. The use of the flow batteries can specially be of advantage here as the

energy and power component are separate in these types of batteries. Conventional batteries have to be installed under the train where there's a limitation regarding the space available, hence there will be limitation on the capacity of the batteries. This can be problematic in the long trips as the train consumes a large amount of power when accelerating (around 1000 kW peak power) and the batteries may not be able to provide enough power and energy capacity. Flow batteries, however, can overcome this problem as the cell stacks (power storage component) can be installed under the train near the propulsion system and the liquid tanks (energy storage component) can be installed, for instance, on the roof or in another wagon where there is more freedom regarding the size and space. Since the only thing that transfers from the tanks is the liquid, it would be safer compare to having batteries in another wagon and separate from the propulsion system. This is also beneficial for cooling the battery cells during the peak operation through cooling down the liquid.

Separation of the tanks and cell stacks can also be beneficial when it comes to the charging time. In the problem with the branch lines, the charging time is not of that importance as there is enough time to charge the batteries while the train is connected to the overhead line in the main track. In the longer catenary-free trips, however, the batteries need to be charged at certain stations. Short stopping time at the stations calls for a fast chargers and as a result there will be a need for facilities to provide the high peak power to charge the batteries as fast as possible; which may not be economically viable in some stations. A solution is suggested in [55] using a second battery at the station that will level the power load on the power system. Flow batteries can offer a more promising solution. Charged electrolyte tanks can be kept at the station and be swapped with the used liquid tanks. This would not put a high load on the power system, needs less financial investment, and at the same time reduces the charging time. Electrolytes can be charged at the station later while there's no train at the station.

Flow batteries can also be used on the conventional EMUs (Electric Multiple Units). As discussed earlier regenerative brake system is one of the reasons that made the train transportation energy efficient compare to other means of transportation. Using the regenerative brake the kinetic energy of the train is transmitted to the electrical energy which is used later on by the auxiliary systems or sent back to the overhead line. To get the best use of the regenerative brakes, however, the whole system including several trains should be studied which is big and complex optimization problem. This is because of the fact that ideally the energy sent back to the line will be used by another accelerating train at the same moment. If the energy restored using regenerative brakes is sent back to the line with no other train accelerating, the line voltage will increase momentarily. Therefore most of the energy shall go to waste. Xubin et al. [89] suggests a solution for this problem by optimizing the use of the regenerative brakes considering multiple trains in the system. However having a storage device on the train seems like a more promising solution. Although the energy can be sent to another accelerating train using the overhead lines, there will still be losses in the catenary system, while there will be less losses when transferring the energy and storing it in a storage device onboard

the train [38]. The energy stored on the onboard storage device can be later used by the train when accelerating instead of using the overhead line. Brenna et al. [14] suggests the use of the ultracapacitors for this purpose; flow batteries can be a better option as they can overcome the short term energy storage capability of capacitors.

Due to the environmental impacts of diesel propulsion systems, they are to be replaced with new options. Battery driven trains can be considered as the new generation of the trains and flow batteries can be a great option for the storage device as they mainly facilitate the integration of the electrified and non-electrified lines while having a low setup and maintenance cost. Nevertheless, a feasibility study should be done on the application of such batteries on trains as there are many aspects such as working temperature that should be studied thoroughly.

6.4 Heavy-Duty Equipment

In heavy-duty construction equipment, due to the large power consumption requirements and long duty-cycles, fossil fuels are still the preferred option for powering the engines. Some of these types of equipment include wheel loaders, bulldozers, and trucks.

Each one of the construction equipment units has a different consumption profile based on each individual working pattern. Wheel loaders, for instance, have very high peak power consumption for short periods of time, while in trucks, the energy consumption profile is flatter for longer periods of time.

A theoretical study performed on a wheel loader in 2014 at Mälardalens University in Sweden estimated the performance and characteristics of replacing the mechanical drive system of a 6-cylinder, 8 l in-line turbocharged diesel engine with a peak power of 200 kW by a VRB flow battery, and electrical motors directly attached on the unit's wheels.

In the original design, the diesel engine occupies most of the physical space required for powering the wheels, while the fuel tank is smaller, due to the large energy density in diesel. In the theoretical design for the VRB system, the size of the electric motors and the cells stack have a small impact on the overall size of the system, since they are directly incorporated in the wheels and the cell stack takes the space occupied by the diesel engine. The electrolyte tanks, however, had the largest impact on the vehicle's size and weight, by occupying an additional 2–3 m^3 with a theoretical weight over 3 tons (a 21 % weight increase on the 21 tons for a diesel-powered wheel loader).

The instant power for one cycle for different operations, in a wheel loader, are described in Fig. 5.25. The electrolyte volume needs to be enough to provide the required energy for several cycles, while the cells stack must be able to handle the peak power. The design parameters for a 200 kW VRB systems are listed in Table 5.4.
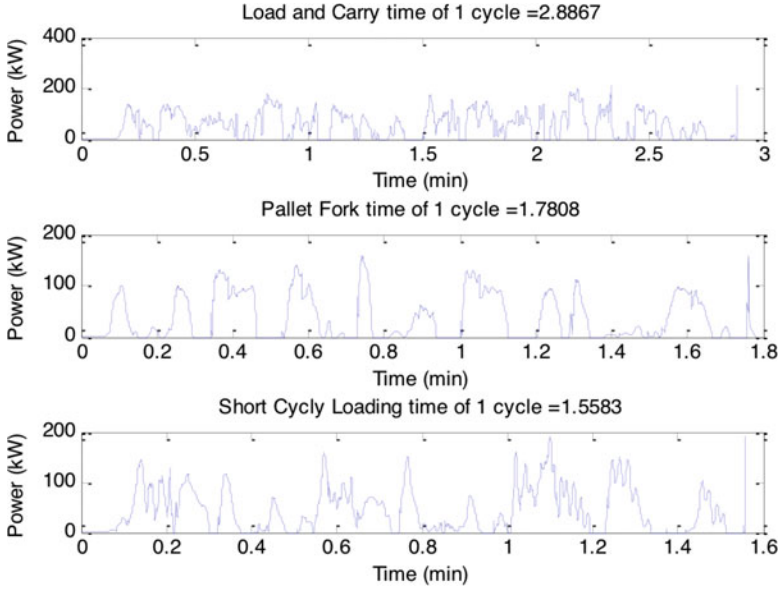
Fig. 5.25 Load requirements for 1 cycle through each application

Table 5.4 Design parameters for a 200 kW vanadium flow battery

Concentration of vanadium (M)	1.6
Concentration of H_2SO_4 (M)	5
Electrolyte density (kg/m^3)	1200
Cross sectional area of a cell (m^2)	1
Current density (mA/cm^2)	300
Power capacity (kW)	200
SoC limits	$0.05 <= SoC <= 0.95$

The state of charge (SoC) in a VRB is given by the concentrations of the vanadium species and varies from 0 (fully discharged) to 1 (fully charged) and it is calculated as follows:

$$SoC = (C_{V2+}/(C_{V2+} + C_{V3+})) = (C_{VO2+}/(C_{VO2+} + C_{VO2+})) \tag{5.51}$$

Due to the characteristics of the wheel loader, the total available volume was calculated to be 3.0 m^3 as shown in Fig. 5.25. Out of the total volume, 2.8 m^3 are dedicated to the battery itself; where 0.7 m^3 correspond to the cells pack and 2.1 m^3 are dedicated for two tanks with a total volume of 2.1 m^3 that store 148 kWh in the electrolyte of 1.6 M vanadium and 5 M H_2SO_4. The cells pack is built with 58 cells that provide a peak power of 200 kW. Additionally, the cells pack requires 2 end plates, 58 carbon felt electrodes, 58 membranes, 58 flow frames, and 57 bipolar

plates. The remaining $0.2\,m^2$ are used for the required 500 W pumps, piping, system controller, and heat exchanger.

With an installation capacity of 140 kWh, it was calculated that the battery could operate for approximately 45 min at the max power of 200 kW. However, as presented in Fig. 5.25, the load dictated by the wheel loader varies. By taking these three applications into consideration, it was calculated that the average running time of operation would be approximately 200 min. This makes the application unpractical for a standard VRB, however. If the electrolyte were to be replaced with a Li-ion flow battery, the running time could increase to 6 h, and thus it could be made possible to use under real practical conditions. The main problem would be the large initial cost for the system.

When analyzing the operation costs for the VRB-powered wheel loader, with a fuel cost of 1.5 EUR/l of diesel, the cost per kWh would be approximately 0.15 EUR/kWh while electricity cost (including taxes in Europe) would be 0.12 EUR/kWh. The main difference is that the conversion efficiency between the battery (for VRB) or tank (for diesel) to the wheels would be considerably higher in a fully electric wheel loader. Taking an average power consumption of 45 kWh/h, running the electric version of the construction equipment unit would cost approximately 5.4 EUR/h while its diesel-powered counterpart would cost up to 27 EUR/h. Looking at the results simulated in Sweden, for 3000 h work per year, the difference between both alternatives would reach up to 64,800 EUR/year in favor of the VRB wheel loader (Fig. 5.26).
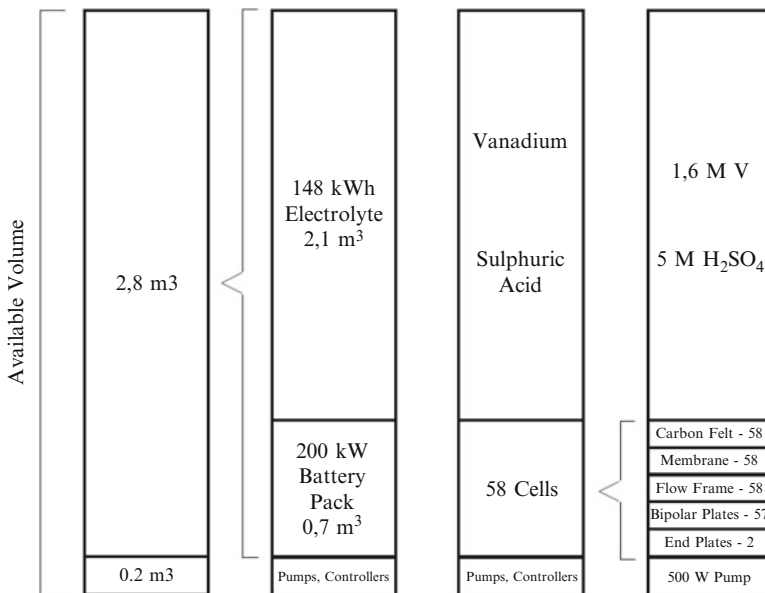
Fig. 5.26 System breakdown in reference to available volume

Additionally, a VRB-powered wheel loader would offer the additional possibilities of using locally produced electricity from solar panels or wind power turbines, for cleaner operations. Other options would include purchasing electricity for recharging the electrolyte tanks during night time at a reduced cost.

6.5 Challenges and Issues

Through the theoretical study [16], it has been shown that flow batteries can be designed to power heavy construction equipment and possibly trains. However, due to the inherently low energy density, the use of flow batteries remains to be only practical when space is not an issue, but chemical and physical limitations can be overcome to improve this for personal vehicle application.

In current VRBs the electrolyte concentration has an upper limit of less than 1.6 M solution of vanadium, leading to a low energy density of 10–50 [W h kg^{-1}], with a battery operating temperature of 10–40 °C. This is because at temperatures above this irreversible precipitation of V_2O_5 could form and damage the battery, therefore a heat exchanger would be necessary, [95]. It is, however, possible to increase the operating temperature range and increase the vanadium electrolyte concentration up to 3 M, which would result in a higher energy density. Other authors, [72] used precipitation inhibitors to stabilize a 3 M vanadium electrolyte solution, which would increase the energy density of VRBs by 60–90 %. The increase in energy storage would require less storage space and would increase the viability of flow battery implementation into the EV market.

Space can also be saved by improving the cell stack architecture. Using the correct electrodes and optimal membrane thickness can increase the power density by 23 % and 20 %, respectively [51]. Obtaining a higher voltage per cell would mean that fewer cells are needed and the extra space gained could be used for storing more energy.

6.6 System Aspects

For VRBs, the vanadium powder used to make the electrolyte poses minimal human safety concerns once mixed into the solution. However, its acidity level is comparable to the one in conventional lead-acid batteries and therefore, precautions have to be taken when handling the equipment, to avoid spillage. In the case of Li-ion batteries, an organic solvent would be preferable but given the high amount of solids, spillage should be avoided. For both types of flow batteries, all the liquids should be collected in vessels and discarded appropriately.

Recharging stations can be comprised of large VRBs using two sets of large electrolyte tanks; one with *charged* electrolyte to supply the incoming vehicles and one with *discharged* electrolyte to receive the electrolyte from them. A cell stack

connected to the grid can be used to recharge the used electrolyte and depending on the capacity of the storage tanks, this activity can be controlled in a way that low cost electricity is used for the recharging process (e.g., during night). Additionally, these recharging stations can be installed together with renewable energy power sources (e.g., solar or wind) for increase reduction in environmental impact. Additionally, to decrease the distribution costs, *charged* electrolyte can be transported with tankers to distribute it from a large supply station to smaller recharging stations closer to the vehicles that require the electrolyte.

Furthermore, these recharging stations can be placed in locations where their energy storage capacity can be used to balance power grid fluctuations (e.g., near large wind power farms) and thus use their electrolyte tanks connected to the cells stack, to supply energy back to the grid whenever instant power compensation is required. This can be done during times of high energy consumption when electricity cost is the highest and thus provide with an additional cost benefit from the VRB system.

7 Conclusions

Flow batteries offer great potential for transportation applications in heavy vehicles over conventional battery technologies, however, there are still several challenges to overcome, before the technology can be an economic and viable alternative. The presented results showed that it is technically feasible to electrify heavy vehicles using flow batteries, but it still remains to be impractical. One of the major drawbacks of the technology is the low energy density and the need for complex auxiliary systems, in order to allow these batteries to operate under the required conditions. In train transportation, low temperatures could freeze the electrolyte in the piping system and high temperatures can cause irreversible precipitation of V_2O_5 that could damage the battery. A heat exchanger would need to be added to the system to maintain the electrolyte's temperature within the desired operation range at the cost of efficiency reduction of the overall system.

Managing thermal behavior of high power Li-ion batteries during fast (dis) charge cycles is important for long cycle life and safe operation specifically in battery modules. The presented three-dimensional adaptive thermal models for single cells and battery module are capable to evaluate thermal behavior of cylindrical Li-ion batteries, under a variety of operating conditions. The experimental results for a 7.5 Ah $LiNi_{0.8}Co_{0.15}Al_{0.05}O_2$ (NCA Li-ion) batteries are used to validate the model. The geometric characteristics of the cells and module are taken into account. The voltage development under 6 C-rate discharge current is extrapolated from the experimental data. In addition, active cooling is coupled to the thermal model and simulated. Voltage, current, and temperature measurement during single cell cycling under controlled ambient temperature conditions and various discharge rates are used to determine the equilibrium voltage and consequently the overpotential. The results are used in calculating heat evolution in the

3D model. Simulations show that high temperature and the gradient occurs under 6 C-rate discharge when natural convection of air is applied. It was shown that forced cooling methods are only partially reducing the problem, effectively affecting only the surface temperature. Strong thermal gradients inside the packs and separate cells can lead to inhomogeneous ageing and must be taken into account in the pack design process.

References

1. Aaron DS, Liu Q (2012) Dramatic performance gains in vanadium redox flow batteries through modified cell architecture. J Power Sources 206:450–453
2. Abiko H, Hibino M, Kudo T (2003) J Power Sources 124:526
3. Aiguo X, Shaojun X, Yuan Y, Xiaobao L, Huafeng X, Jingjing F (2009) An ultra-capacitor based regenerating energy storage system for urban rail transit. In: Energy conversion congress and exposition, 2009. ECCE 2009. IEEE, New York, pp 1626–1631
4. Akli CR, Roboam X, Sareni B, Jeunesse A (2007) Energy management and sizing of a hybrid locomotive. In: 2007 European conference on power electronics and applications, 2007, pp 1–10
5 Al-Hallaj S, Selman JR (2002) J Power Sources 110:341
6. Amatucci GG (1996) CoO2, the end member of the lixcoo2 solid solution. J Electrochem Soc 143(3):1114–1110. doi:10.1149/1.1836594
7. Amjadi Z, Williamson SS (2009) Review of alternate energy storage systems for hybrid electric vehicles. In: 2009 I.E. electrical power & energy conference (EPEC), 2009, pp 1–7
8. Balbuena PB, Wang YX (eds) (2004) Lithium ion batteries: solid electrolyte interphase. Imperial College Press, London, ISBN 1860943624
9. Bergveld HJ, Kruijt WS, Notten PHL (1999) J Power Sources 77:143
10. Bergveld HJ, Kruijt WS, Notten PHL (2002) Battery management systems. Design by modelling. Philips research book series, vol 1. Kluwer, Boston
11. Bindner H, Ekman C, Gehrke O, Isleifsson F (2010) Characterization of a vanadium flow battery, Riso-R-1753, October 2010
12. Blanc C (2009) modeling of a vanadium redox flow battery electricity storage system, Thesis No. 4277, Ecole Polytechnique Federale De Lausanne
13. Botte GG, Subramanian VR, White RE (2000) Electrochim Acta 45:2595
14. Brenna M, Foiadelli F, Tironi E, Zaninelli D (2007) Ultracapacitors application for energy saving in subway transportation systems. In: International conference on clean electrical power, 2007. ICCEP '07, 2007, pp 69–73
15. Campestrini C, Horsche MF, Zilberman I, Heil T, Zimmermann T, Jossen A (2016) Validation and benchmark methods for battery management system functionalities: state of charge estimation algorithms. J Energy Storage 7:38–51. doi:10.1016/j.est.2016.05.007
16. Campillo J, Ghaviha N, Zimmerman N, Dahlquist E (2015) Flow batteries use potential in heavy vehicles. In: 2015 International conference on electrical systems for aircraft, railway, ship propulsion and road vehicles (ESARS), 3–5 March 2015, pp 1–6. doi:10.1109/ESARS.2015.7101496
17. Ceder G, Van der Ven A (1999) Electrochim Acta 45:131
18. Choi HC, Jung YM, Noda I, Kim SB (2003) A study of the mechanism of the electrochemical reaction of lithium with CoO by two-dimensional soft X-ray absorption spectroscopy (2D XAS), 2D Raman, and 2D heterospectral XAS? Raman correlation analysis. J Phys Chem B 107(24):5806. doi:10.1021/jp030438w

19. Danilov D, Ledovskikh A, Notten PHL (2011) Adaptive thermal modeling of rechargeable batteries for advanced automotive battery management systems. In: Proceedings of the international automotive congress, Eindhoven, p 50
20. Danilov D, Niessen RAH, Notten PHL (2011) J Electrochem Soc 158:A215
21. Danilov D, Lyedovskikh A, Notten PHL (2011) Voltage and temperature dynamic simulations for advanced battery management systems. In: Proceedings of the 7th International IEEE VPPC Conference, Chicago, USA, Sept 6–9
22. Dell R, Rand DAJ (2001) Understanding batteries. The Royal Society of Chemistry, London. doi:10.1039/9781847552228
23. Diorio N, Dobos A, Janzou S, Nelson A, Lundstrom B, Diorio N et al (2015) Technoeconomic modeling of battery energy storage in SAM
24. Doeff MM (2012) Encyclopedia of sustainability science and technology. doi:10.1007/978-1-4419-0851-3
25. Doyle M, Fuller TF, Newman J (1993) J Electrochem Soc 140:1526
26. Dreyer W, Guhlke C, Huth R (2011) Physica D 240:1008
27. Duduta M, Ho B, Wood VC, Limthongul P, Brunini VE, Carter WC, Chiang Y-M (2011) Semi solid lithium rechargeable flow battery. J Adv Energy Mater 1:511–516
28. Dumancic D (2011) Flow batteries status and potential. Master thesis work, Malardalen University Press
29. Eastham AR, Pringle DM, Austin PR (1982) An assessment of superconductive energy storage for Canadian freight railways. Can Electr Eng J 7:3–12
30. EPRI (2003) Comparison of storage technologies for distributed resource applications. EPRI, Palo Alto, CA, 2003.1007301
31. Fernandez RA, Cilleruelo FB, Martinez IV (2016) A new approach to battery powered electric vehicles: a hydrogen fuel-cell-based range extender system. Int J Hydrog Energy 41:4808–4819. doi:10.1016/j.ijhydene.2016.01.035
32. Fransson LML, Vaughey JT, Benedek R, Edstroom K, Thomas JO, Thackeray MM (2001) Electrochem Commun 3:317
33. Gelman V (2013) Energy storage that may be too good to be true: comparison between wayside storage and reversible thyristor controlled rectifiers for heavy rail. IEEE Veh Technol Mag 8:70–80
34. Gold Peak Industries Ltd. Lithium ion technical handbook (PDF) [Online 2003].
35. Hannan MA, Azidin FA, Mohamed A (2014) Hybrid electric vehicles and their challenges: a review. Renew Sust Energ Rev 29:135–150. doi:10.1016/j.rser.2013.08.097
36. Hardman S, Chandan A, Shiu E, Steinberger-Wilckens R (2016) Consumer attitudes to fuel cell vehicles post trial in the United Kingdom. Int J Hydrog Energy 41:6171–6179. doi:10.1016/j.ijhydene.2016.02.067
37. Hatchard TD, MacNeil DD, Basu A, Dahn JR (2001) J Electrochem Soc 148:A755
38. Hirose H, Yoshida K, Shibanuma K (2012) Development of catenary and storage battery hybrid train system. In: Electrical systems for aircraft, railway and ship propulsion (ESARS), 2012, pp 1–4
39. Iuni Y, Kobayashi Y, Watanabe Y, Watase Y, Kitamura Y (2007) Energy Convers Manag 48:2103
40. Jossen A, Sauer DU (2006) Advances in redox-flow batteries. In: First international renewable energy storage conference, Gelsenkirchen, Germany, October 2006
41. Khaligh A, Zhihao L (2010) Battery, ultracapacitor, fuel cell, and hybrid energy storage systems for electric, hybrid electric, fuel cell, and plug-in hybrid electric vehicles: state of the art. IEEE Trans Veh Technol 59:2806–2814
42. Kiehne HA (2003) Battery technology handbook. CRC Press, Boca Raton
43. Kono Y, Shiraki N, Yokoyama H, Furuta R (2014) Catenary and storage battery hybrid system for electric railcar series EV-E301. In: 2014 International power electronics conference (IPEC-Hiroshima 2014 - ECCE-ASIA), 2014, pp 2120–2125
44. Kruijt WS, Notten PHL, Bergveld HJ (1998) J Electrochem Soc 145:3764

45. Lantelme F, Mantoux A, Groult H, Lincot D (2006) Solid State Ionics 177:205
46. Larminie J, Lowry J (2003) Electric vehicle technology explained. Wiley, Chichester. doi:10.1002/0470090707
47. Larsson D, Andersson H (2012) Experimental evaluation of vanadium flow batteries. Malardalen University Press (in Swedish)
48. Lee BG, Yoon JR (2012) Preparation and characteristics of Li4Ti5O12 anode material for hybrid supercapacitor. J Electr Eng Technol 7(2):207–211. doi:10.5370/JEET.2012.7.2.207
49. Li D, Danilov D, Zhang Z, Chen H, Yang Y, Notten PHL (2015) J Electrochem Soc 162:A858
50. Linden D, Reddy TB (ed) (2002) Handbook of batteries, 3rd edn., Chap. 35 McGraw-Hill, New York. ISBN 0-07-135978-8
51. Liu QH, Grim GM, Papandrew AB, Turhan A, Zawodzinski TA, Mench MM (2012) High performance vanadium redox flow batteries with optimized electrode configuration and membrane selection. J Electrochem Soc 159(8):A1246–A1252. doi:10.1149/2.051208jes
52. Lower SK (2004) Electrochemistry: chemical reactions at an electrode, galvanic and electrolytic cells. Simon Fraser University
53. Lu S, Hillmansen S, Roberts C (2010) Power management strategy study for a multiple unit train. In: IET conference on railway traction systems (RTS 2010), 2010, pp 1–6
54. Masamichi O (2010) Onboard storage in Japanese electrified lines. In: 2010 14th International power electronics and motion control conference (EPE/PEMC), 2010, pp S7-9–S7-16
55. Masatsuki I (2010) Development of the battery charging system for the new hybrid train that combines feeder line and the storage battery. In: 2010 International power electronics conference (IPEC), 2010, pp 3128–3135
56. Miller JM (2008) Trends in vehicle energy storage systems: batteries and ultracapacitors to unite. In: Vehicle power and propulsion conference, 2008. VPPC '08. IEEE, New York, pp 1–9
57. NewSouth Innovations (n.d.) Vanadium redox battery [Online, 2012]. Available at: http://www.ceic.unsw.edu.au/centers/vrb/technology-services/vanadium-redox-flow-batteries.html
58. Nguyen T, Savinell RF (2010) Flow batteries. Electrochem Soc (Fall 2010)
59. Noack Jens (2009) Improved redox flow batteries for electric cars [Online, 2009]. Available at: http://www.fraunhofer.de/en/press/research-news/2009/10/improved-redox-flow-batteries-for-electric-cars.html
60. Notten PHL, Kruijt WS, Bergveld HJ (1998) J Electrochem Soc 145:3774
61. Goodenough JB, Abruna HD, Buchanan MV (2007) Basic research needs for electrical energy storage. Report of the basic energy sciences workshop on electrical energy storage, April 2–4, United States. doi:10.2172/935429
62. Ogasa M (2008) Energy saving and environmental measures in railway technologies: example with hybrid electric railway vehicles. IEEJ Trans Electr Electron Eng 3:15–20
63. Okui A, Hase S, Shigeeda H, Konishi T, Yoshi T (2010) Application of energy storage system for railway transportation in Japan. In: 2010 International power electronics conference (IPEC), 2010, pp 3117–3123
64. Onda K, Ohshima T, Nakayama M, Fukuda K, Araki T (2006) J Power Sources 15:535
65. Pagenkopf J, Kaimer S (2014) Potentials of alternative propulsion systems for railway vehicles 2014; a techno-economic evaluation. In: 2014 Ninth international conference on ecological vehicles and renewable energies (EVER), pp 1–8
66. Pals CR, Newman J (1995) J Electrochem Soc 142:3274
67. Parasuraman A, Lim TM (2013) Review of material research and development for vanadium redox flow battery applications. Electrochim Acta 101:27–40
68. Piergiorgio Alotto MG (2014) Redox flow batteries for the storage of renewable energy: a review. Renew Sust Energ Rev 29:325–335
69. Pop V, Bergveld HJ, Danilov D, Regtien PPL, Notten PHL (2008) BMS: accurate state-of-charge indication for battery-powered applications. Springer, New York
70. Raijmakers LHJ, Danilov DL, van Lammeren JPM, Lammers MJG, Notten PHL (2014) J Power Sources 247:539

71. Richardson MB (2002) Flywheel energy storage system for traction applications. In: International conference on power electronics, machines and drives, 2002 (Conf. Publ. No. 487), pp 275–279
72. Roe S, Menictas C, Skyllas-Kazacos M (2015) A high energy density vanadium redox flow battery with 3 M vanadium electrolyte. J Electrochem Soc 163(1):A5023–A5028. doi:10.1149/2.0041601jes
73. Rydh CJ (1999) Environmental assessment of vanadium redox and lead-acid batteries from stationary energy storage. J Power Sources 80:21–29
74. Shadman Rad M, Danilov D, Baghalha M, Kazemini M, Notten PHL (2013) Electrochim Acta 102:183–195
75. Shaofeng L, Hillmansen S, Roberts C (2011) A power-management strategy for multiple-unit railroad vehicles. In: IEEE transactions on vehicular technology, vol 60, pp 406–420
76. Skyllas-Kazacos M, Rychick M, Robins RG (1988) All-vanadium redox battery, US Patent no. 4,786,567, 22 Nov 1988
77. Song L, Evans JW (2000) J Electrochem Soc 147:2086
78. Steiner M, Scholten J (2004) Energy storage on board of DC fed railway vehicles PESC 2004 conference in Aachen, Germany. In: 2004 I.E. 35th annual power electronics specialists conference, 2004. PESC 04, vol 1, pp 666–671
79. Steiner M, Klohr M, Pagiela S (2007) Energy storage system with ultracaps on board of railway vehicles. In: 2007 European conference on power electronics and applications, Aalborg, pp. 1–10. doi:10.1109/EPE.2007.4417400
80. Steiner M, Klohr M, Pagiela S (2007) Energy storage system with ultracaps on board of railway vehicles. In: 2007 European conference on power electronics and applications, 2007, pp 1–10
81. Sulaiman N, Hannan MA, Mohamed A, Majlan EH, Wan Daud WR (2015) A review on energy management system for fuel cell hybrid electric vehicle: issues and challenges. Renew Sust Energ Rev 52:802–814. doi:10.1016/j.rser.2015.07.132
82. Sun X, Yang XQ, McBreen J, Gao Y, Yakovleva MV, Xing XK, Daroux ML (2001) J Power Sources 97:274
83. Teshima M, Takahashi H (2014) Lithium ion battery application in traction power supply system. In: 2014 International power electronics conference (IPEC-Hiroshima 2014 - ECCE-ASIA), 2014, pp 1068–1072
84. Thaler A, Watzenig D (2014) Automotive battery technology. Springer, Cham. doi:10.1007/978-3-319-02523-0
85. Tsukahara K, Kondo K (2013) A study on methods to design and select energy storage devices for fuel cell hybrid powered railway vehicles. In: IECON 2013 - 39th annual conference of the IEEE industrial electronics society, 2013, pp 4534–4539
86. Van der Spiegel B (2009) Railway energy measuring, managing and billing (April 2009). In: 6th International conference on the European energy market, 2009 (EEM 2009), 2009, pp 1–8
87. Wang Y, Zhang C, Chen Z, Xie J, Zhang X (2015) A novel active equalization method for lithium-ion batteries in electric vehicles. Appl Energy 145:36–42. doi:10.1016/j.apenergy.2015.01.127
88. Wenige R, Niemann M, Heider U, Jungnitz M, Hilarius V (1997) Liquid electrolyte systems for advanced lithium batteries. In: Proceedings of the Industrial Chemistry Symposium, Seoul, Korea, 1997
89. Xubin S, Hu C, Xiaowei H, Mengyang Z, Hairong D (2014) Regenerative braking energy utilization by multi train cooperation. In: 2014 I.E. 17th international conference on intelligent transportation systems (ITSC), 2014, pp 139–144
90. Yang XQ, Sun X, McBreen J (2000) Electrochem Commun 2:100
91. Yi T-F, Jiang L-J, Shu J, Yue C-B, Zhu R-S, Qiao H-B (2010) Recent development and application of Li4Ti5O12 as anode material of lithium ion battery. J Phys Chem Solid 71(9):1236–1242

92. Yong D, Yun B, Fang-ming Z, Bao-hua M (2011) Energy-efficient freight train operation guide system for diesel locomotives. In: 2011 I.E. international conference on service operations, logistics, and informatics (SOLI), pp 548–553
93. Yong J, Jianqiang L, Wei T, Shahidehpour M, Krishnamurthy M (2014) Energy harvesting for the electrification of railway stations: getting a charge from the regenerative braking of trains. A. Electrific Mag IEEE 2:39–48
94. Zhang HM (2010) Redox flow battery for energy storage. ECS Trans 28(22):1–5
95. Zimmerman N (2014) Vanadium redox flow battery: sizing of VRB in electrified heavy construction equipment. School of Business, Society and Engineering, Mälardalen University
96. Zongyu G, Jianjun F, YiNong Z, Di S, Lan J, Xiaoling Y (2014) Control strategy research of wayside supercapcitor energy storage system for urban rail transit. In: The 26th Chinese control and decision conference (2014 CCDC), pp 4786–4791

Part II
Overview of Applications

Chapter 6
Plug-In Electric Vehicles' Automated Charging Control: iZEUS Project

David Dallinger, Robert Kohrs, Michael Mierau, Simon Marwitz, and Julius Wesche

Abstract This chapter examines how plug-in electric vehicles can be managed to balance the fluctuation of renewable electricity sources. The evaluations of this chapter were object of the iZEUS Project "Intelligent Zero Emission Urban System" funded by the German Federal Minister for Economic Affairs and Energy. In this context, different control strategies are introduced and, in order to investigate indirect control via electricity tariffs, an electricity market analysis of a system with a high share of generation from renewable electricity sources has been conducted. The analysis uses driving data collected from battery electric and plug-in hybrid vehicles in a research project which means that real charging and driving behavior can be considered. The results show that it is difficult to implement smart charging based on economic arguments because the incentives from day-ahead electricity markets are relatively small. In addition, a novel, autonomous control approach is being discussed for plug-in electric vehicles. While measuring the voltage at the grid connection point, plug-in electric vehicles are able to fully independently generate operation schedules that can avoid load peaks and integrate fluctuating power outputs from distributed renewable generation sources. The results reveal that combining indirect, price-based control to consider the system level with autonomous voltage-based control to consider the situation in distribution grids is a very promising control approach that allows electric vehicles to benefit from sustainable renewable generation and avoids load peaks due to simultaneous charging.

D. Dallinger (✉) • S. Marwitz • J. Wesche
Fraunhofer Institute for Systems and Innovation Research, Breslauer Straße 48, Karlsruhe 76139, Germany
e-mail: dbdallinger@yahoo.de

R. Kohrs • M. Mierau
Fraunhofer Institute for Solar Energy Systems, Freiburg, Germany

6.1 Introduction

This section provides the background to the objective of studying the role of electric vehicles in a modern electricity system and introduces the research project in which large parts of this work have been conducted.

6.1.1 Background

Plug-in electric vehicles (PEVs) are a promising option to increase efficiency in the transport sector, provided that these vehicles are powered with electricity generated by renewable energy sources (RES). In theory, using RES to power vehicles is a win-win situation. PEVs are ideal RES consumers because of their high electricity-to-wheel efficiency compared to fuel cell vehicles or those based on liquefying RES. RES installations benefit from PEV demand that could boost RES expansion. In practice, this interaction is more complex because the most promising RES—photovoltaic and wind energy—are fluctuating sources. The value that needs to be considered when combining renewable generation and PEVs is not the amount of energy available (in kWh) but rather the amount of power available (in kW).

The far-reaching changes fluctuating generation will bring to modern electricity systems are illustrated in Fig. 6.1 which shows the fluctuating generation, the system load, and the resulting residual load for an example scenario reflecting a likely situation in Germany in 2030. The residual load fluctuation for these 3 weeks in summer is mainly caused by the high installed photovoltaic capacity. Compared to the system load, huge ramp rates can be observed and, for some hours, the generation from fluctuating sources even surpasses the system load demand (negative residual load).
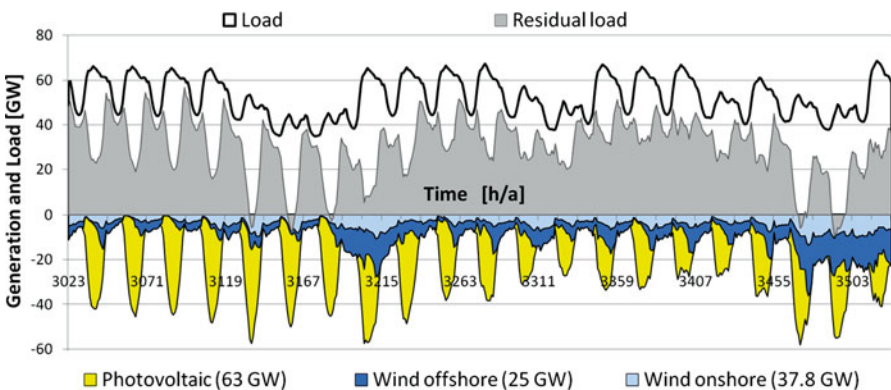
Fig. 6.1 Example of the possible residual load situation for 3 weeks in summer, Germany, 2030

PEVs are able to balance the increasing fluctuation of the residual load by providing flexible charging loads and vehicle-to-grid services (V2G). This makes it possible to integrate RES into the energy system. To achieve this win-win situation, it is necessary to develop flexible control strategies that are able to manage the rapid changes in electricity systems with high RES shares.

6.1.2 The iZEUS Project

The Project "Intelligent Zero Emission Urban System—iZEUS" was funded by the German Federal Minister for Economic Affairs and Energy. iZEUS is part of the funding program "Information and Communication Technologies for Electric Mobility II—Smart Car—Smart Grid—Smart Traffic." The project partners are ads-tec, Daimler, EnBW (coordinator), the Fraunhofer ISI and ISE, KIT, Opel, PTV, SAP, and TWT. Toyota and bridgingIT supported the project as associate partners. The main aim of the involved Fraunhofer institutes, the Fraunhofer Institute for Systems and Innovation Research ISI and the Fraunhofer Institute for Solar Energy Systems ISE, was to investigate to which extent controlled charging and discharging of PEVs can support the grid integration of fluctuating renewable generation. Large parts of the work presented here were conducted within the iZEUS Project.

6.1.3 Objective and Procedure

The objective of this study is to investigate different control strategies for PEVs. The main intention of the control strategies is to combine PEVs and fluctuating renewable generation. This requires more flexibility than other common control methods such as time-of-use pricing or load shifting to nighttime hours. The chapter is structured as follows. First, possible control methods are introduced and discussed (Sect. 6.2). Second, real PEV driving data from the iZEUS field trial are presented and analyzed because PEV drivers' behavior determines the potential to balance the system. The applied simulation methods and results are then presented and the main conclusions discussed.

6.2 Charging Control Methods

Different control methods are discussed to avoid load peaks due to charging PEVs and to make full use of their demand response potential for balancing the electricity system. Three main methods can be distinguished to control distributed generation units and flexible loads: direct control, indirect control, and autonomous distributed control. The three methods are described in the following section.

6.2.1 Direct Control

Direct control is a common method applied in conventional power systems consisting of large power plants and transmission grids. Power plants or large pumped-storage hydro plants are controlled to meet demand from a centralized objective. Exact operation schedules are defined by the utility and implemented by the controlled generation units. Where PEVs are concerned, this means that the operating schedule needs to be defined by a third party outside the vehicle (e.g., a system service provider or the utility). This implies the necessity to communicate to this third party specific information about the battery such as the state of charge (SOC), capacity, and battery health requirements as well as information about consumer preferences such as the electric range buffer, next expected trip, and willingness to participate in smart charging programs. The information from several PEVs is collected and a charging schedule is generated for each unit and returned to the vehicle. This method enables almost perfect control of PEVs while considering the operation of other PEVs and power plants.

To explain the possible disadvantages of direct control in the case of small units connected to distribution grids, it is necessary to look at the general changes taking place in the electricity system and the characteristics of distributed energy systems. Recently, the share of distributed generation units has risen sharply. In particular, massive price drops and subsidies for photovoltaic systems have boosted the shares of small-scale generation units. In contrast to conventional power plants, these units are often connected to the distribution network and not to the transmission grid. Further, generation fluctuates according to weather conditions as in the case of photovoltaic systems and wind turbines. The situation in conventional, load-based distribution grids is predictable with a very high degree of certainty. Adding distributed generation and flexible loads to the distribution grid makes the situation much more complex.

To realize direct control of PEVs that are connected to the distribution grid, it is necessary to have not only information on a system level (transmission grid/day-ahead market) but also information on the local situation (distribution grid). This information can be provided for a small closed system such as a smart home [1], but collecting all the information for larger areas with many loads and generation units requires a significantly greater effort. In the past, collecting such data was too expensive and also of limited interest because very few controllable devices were available in distribution grids. However, due to the progress made in developing advanced information and communication technologies, this topic is again becoming of interest within the topic of smart grids, but it is still unclear which applications are economically feasible.

With regard to the very limited information available on the distribution grid level and the small scale of PEVs, applying a direct control approach to PEVs will be more complex than, e.g., controlling a pumped-storage plant connected to the transmission grid. Further, the main purpose of PEVs is to provide mobility. This results in restrictions on the power storage availability and SOC reductions

(energy use for driving) that need to be communicated to an external control instance. The communication of vehicle-internal and consumer data is a big issue. The big vehicle manufacturers accept neither the communication of battery data nor charging schedules set by a third party. It is also doubtful whether consumers will agree to communicate their driving habits. The communication of sensitive data therefore represents a major obstacle to direct control of PEVs.

Disconnecting loads is a simplified direct control approach that does not necessarily require bidirectional communication. It is common to disconnect grid areas in case of significant breakdowns in order to stabilize the system. Disconnecting all PEVs could be a possible control approach to avoid the breakdown of a larger grid area.

6.2.2 Indirect Control

Indirect control is realized using incentives and is already being applied to control PEVs in California (Pacific Gas and [2]). Incentives can be provided as time-of-use (TOU) or other electricity tariff designs such as critical peak or dynamic tariffs. The tariff reflects the power system's status. In contrast to direct control methods, here, the consumer or a device programmed by the consumer can decide whether to react to the incentive or not. Hence, the operating schedule is set by a local controller within the vehicle, where information on the vehicle battery and the driver's preferences are available without the need for vehicle-external communication. For this reason, vehicle manufacturers' acceptance of indirect control is generally higher. The final control decision, however, remains in the hands of the drivers, which probably increases acceptance but also requires their active participation.

The main challenge associated with such indirect control is how to create the right kind of tariff. For successful control of PEVs, the tariff should reflect the situation on a system level as well as the local grid. The system level's status is represented by day-ahead or intraday electricity market prices. No information is available for the local situation. Tariffs that represent the specific situation of local grids are rare. In addition, any widespread simultaneous reaction to a tariff could also result in peaks if only one tariff is used to control many PEVs (for further information, please refer to [3, 4]). Therefore, one challenge from using indirect control is being able to predict PEVs' reaction to the control signal. The possibility of forecast errors reduces the reliability of indirect control compared to direct control, but the fact that it does not require bidirectional communication[1] (no communication of the vehicle to the backend system) is an advantage.

In the context of integrating fluctuating renewable generation, tariffs based on day-ahead or intraday markets are best able to reflect the supply of renewable

---

[1] If onboard metering is available, the vehicle could support the billing process and send information once a week or month (not real time).

generation units on a system level. Due to their very low marginal generation costs [5], a high share of fluctuating renewable generation results in a reduction of the electricity prices (due to the merit-order effect). Hence, the market mechanism of today's electricity markets already provides incentives to charge PEVs when the supply of renewable energy sources is high.

6.2.3 Autonomous Distributed Control

The main characteristic of autonomous control is the lack of an external control signal; vehicles only use internal sensors. In the case of smart charging, this is mainly realized by measuring the voltage and the frequency. Negative frequency and voltage deviations indicate the need for more power generation or less consumption. Vice versa, positive frequency and voltage derivations indicate the need for less power generation or more consumption. Hence, both frequency and voltage indicate the current status of the electricity system and can be used as control signals.

The concept of autonomous control is already widely realized. Big power plants adapt their generation to stabilize the frequency on a system level (primary control markets). The net frequency is the same for all nodes in the network and all grid levels (transmission grid and distribution grid). Consequently, frequency is an indicator for the entire network. A frequency-based control approach to PEVs was introduced by Yang et al. [6].

On the distributed grid level, generation units such as photovoltaic systems adapt their generation or disconnect at certain voltage or frequency levels. Furthermore, in many microgrids, the autonomous control of generation and storage units is a common approach. The voltage in distribution grids is sensitive to local changes in generation and load and is affected by the patterns of fluctuating generation units as well as local consumers. As a result, measuring grid voltage provides information about the local situation that can be used by PEVs to optimize their charging behavior in terms of integrating renewable generation and avoiding peaks caused by simultaneous charging.

6.2.4 Discussion on Charging Control Methods

It is not yet clear which control strategy will prevail for PEVs. In practice, it is likely that different control strategies will be combined to realize the control goals for different applications and operating conditions. The main advantages and disadvantages of the different control strategies have been summarized in Fig. 6.2.

The authors believe that the question "Who defines the charging schedule?" is crucial. Both vehicle manufacturers and utilities demand to control the vehicles' operation. Ultimately, we think that vehicle manufacturers or vehicle owners will

Strategy	Utility	OEM	Consumer	Advantages	Dis-advantages
Direct control	Defines the charging schedule	Provides vehicle and battery data	Provides information on the expected driving behavior	Perfect control	Acceptance of users and OEMs is questionable
Indirect control	Competitors	Provides control signal (Tariff)	Defines the charging schedule	Less communication effort	Load estimation, with the possibility of forecasted errors necessary
Autonomous	-	Grid monitoring	Defines the charging schedule	Simple charging infrastructure	Additional hardware to measure the voltage is needed

Fig. 6.2 Overview of control strategies (*OEM* original equipment manufacturer)

make the final decision about the charging schedule. This is because utilities cannot determine the vehicles' design or communication protocols. Even the charging infrastructure at the most important charging location—at PEV users' homes—cannot be directly influenced by the utilities. From a market perspective, it is also clear that the supply side and the demand side should be separated (unbundling). Hence, flexible loads act as competitors to utility-owned generation units. From this point of view, direct control by utilities or a third party can only be an option as the last resort to avoid a power blackout. In addition, the local generation of operating schedules implies that they are controlled in the vehicle or by another device owned by the consumer (e.g., a smartphone or computer). From a technical point of view, this means that charging infrastructure can be kept simple. Controllers, grid monitoring technology, and communication units could be directly implemented in the vehicles. For these reasons, in the iZEUS project, the Fraunhofer Institutes ISE and ISI focused on autonomous (considering the local situation) and indirect control (considering the system level) as the most promising options to intelligently connect PEVs to the grid.

6.3   Driving and Charging Behavior

The manner vehicle batteries are used is an important factor for PEVs' total costs of ownership as well as their ability to provide grid services. Many regular trips with a high share of electric driving increase the fuel savings compared to a conventional vehicle and help to recoup the higher investment costs of PEVs. From an energy management perspective, higher electricity use results in a higher amount of energy

available for load management. Large amounts of energy make load management more attractive but also reduce the degree of freedom, because longer charging times are required that reduce the period during which the vehicle can provide grid services. Hence, driving behavior is the major factor that determines the operation and possible profits of PEVs on energy markets. In the following section, the specific driving behavior of the vehicles involved in the iZEUS test fleet is analyzed.

6.3.1   iZEUS Test Fleet

The iZEUS test fleet consists of purely electric and plug-in hybrid vehicles. Overall, more than 60 vehicles were involved, provided by Daimler AG, Opel AG, and the Toyota Motor Corporation. The user incentive to participate in the research project was a reduced battery leasing rate and a navigation applet provided with a Tablet computer. In the following analysis, real driving data were used from 28 Daimler Smart Fortwo electric drive and 3 Toyota Prius PHVs. For both vehicle types, logging data are analyzed from the time period October 1st, 2013, to June 30th, 2014, using vehicle internal systems provided by the Toyota Motor Corporation and Daimler AG. The vehicle data are summarized in Table 6.1.

The Smart Fortwo is a purely electric two-seater with a usable battery capacity of 17.6 kWh. The electric range is about 119 km at a driving efficiency of 0.15 kWh per km. The Smart BEV's driving efficiency strongly depends on the usage of auxiliary equipment such as air conditioning and heating.[2] The maximum single trip range realized within the investigation period was 93 km. The smart vehicles were located in the areas surrounding Stuttgart and owned by companies and private users. Exact information on the charging infrastructure of individual users is not available.

Table 6.1 Overview of iZEUS vehicle fleet

Parameters	Smart for two electric drive	Toyota Prius PHEV[a]
Battery	17.6 kWh	5.2 kWh
Efficiency[b]	0.148 kWh/km	0.139 kWh/km
Number of vehicles	28	3
Electric range/longest trip	119 km/93 km	18 km/240 km
ϕ trip duration/rane	0:11/6.9 km	0:16/12.7 km
Test period	1 Oct–30 June	1 Oct–30 June

[a]Own calculation
[b]Pre-series vehicle

---

[2] Driving efficiency quantile = 9.9 kWh/100 km (alpha = 0.2) and quantile = 19.3 kWh/100 km (alpha = 0.9).

The Toyota Prius PHV is a pre-series, midsize vehicle based on the third Prius generation. The battery capacity is 5.2 kWh. The purely electric range is about 18 km and the efficiency is 0.14 kWh/km. The vehicles were lent for 6 weeks mainly to full-time employees from the Karlsruhe Institute of Technology as well as the Fraunhofer ISI and Fraunhofer ISE, who included administration and research workers. The Prius vehicles were located in the areas surrounding Karlsruhe and Freiburg. Charging infrastructure was available at the workplace. Exact information on the availability of charging infrastructure at employees' homes is not available. It is assumed that more than 50 % of the employees who used the vehicles were able to charge at home. Other public infrastructure provided by the utility EnBW AG was available [7].

6.3.2   Driving Data Evaluation

Data are evaluated separately for the Prius PHV and Smart Fortwo. This could provide some first indications of whether BEVs and PHEVs are used differently. Given the limited data available, the difference in vehicle type (mid sedan vs. small vehicle), as well as the different users and use cases, the evaluation can only indicate preliminary conclusions when comparing BEVs and PHEVs. Nevertheless, the data do reflect real PEV driving behavior and are therefore of high research interest.

The 28 Smart vehicles involved in the evaluation conducted 19,415 trips with an overall range of 134,715 km and an average trip range of 6.9 km. The average estimated yearly driving distance is 6286 km per year (minimum 1566 km/a; maximum 16,861 km/a). The 3 Prius PHVs realized 1090 trips with an overall range of 13,854 km. The average range per trip is 12.7 km and the average estimated yearly driving distance is 9554 km per year (minimum 8465 km/a; maximum 11,286 km/a). The average yearly driving distance in Germany is between 12,000 and 14,000 km per year.

The trip range is an indicator for how vehicles are used. The accumulated frequency of different trip classes is illustrated in Fig. 6.3 for both the Smart and
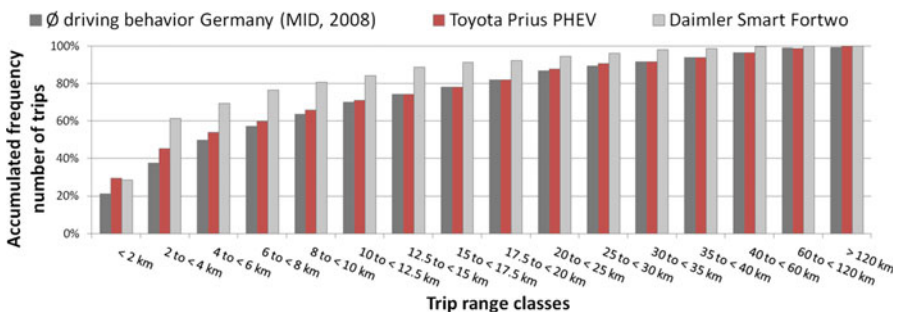
Fig. 6.3 Accumulated frequency of trip range in iZEUS versus German average
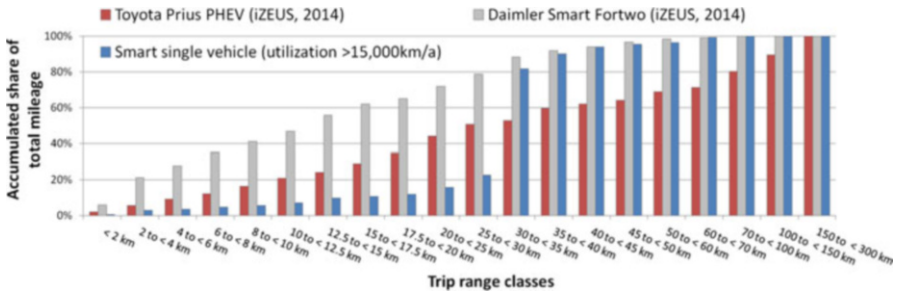
Fig. 6.4 Accumulated share of total mileage for different trip range classes

Prius vehicles in iZEUS, as is the German average taken from the survey Mobility in Germany (MID 2008). The German average and the Prius PHV driving behavior are similar for many trip classes. Only for trips shorter than 10 km do the Prius data have slightly higher frequencies than the German average. The reasons for this are unclear. It could be because of the specific user segment, the novelty of vehicles that results in short test drives, or a type of rebound effect. A reduction in the number of trips by bicycle or on foot in favor of trips using PEVs might be motivated due to participating in a research project, the environmental benefits of PEVs, or again simply the novelty of the vehicles.

There are a higher number of trips between 2 and 20 km observed for the Smart BEVs. This could be because of the vehicle's characteristics (small size, two-seater), the specific user segment, and/or the limited electric range of 119 km. Again, it is not possible to offer conclusive reasons for the differences in behavior.

Figure 6.4 illustrates the total mileage share of different trip range categories and clearly shows which trip classes contribute most to the total mileage driven by the vehicles. In case of the Smart vehicles, trips with a range below 30 km make up nearly 80 % of the total kilometers driven. These vehicles do not fully use their total potential electric driving range of 119 km. It is not clear whether the Daimler Smart users also had access to an additional vehicle and consequently only used the Smart to realize short trips. To further investigate this issue, Fig. 6.4 also includes the driving behavior of a single Smart BEV that has one of the highest utilizations in the fleet trial. For the single Smart BEV, the trip class 30 to <35 km contributes a high share to the total mileage. This is a strong indication for a regular/daily trip in this range class (e.g., to the workplace or to the workplace and home again). For the Prius PHV, trips below 30 km only represent about 50 % of the total mileage. About 20 % of the Prius' total mileage comes from trips longer than 100 km.

The relatively low utilization of the Smart vehicle battery is also demonstrated in Fig. 6.5. Figure 6.5 shows the SOC when starting[3] a trip and ending[4] a trip for the

---

[3] SOC-Start: Sorted in descending order.

[4] SOC-End: Sorted in ascending order.
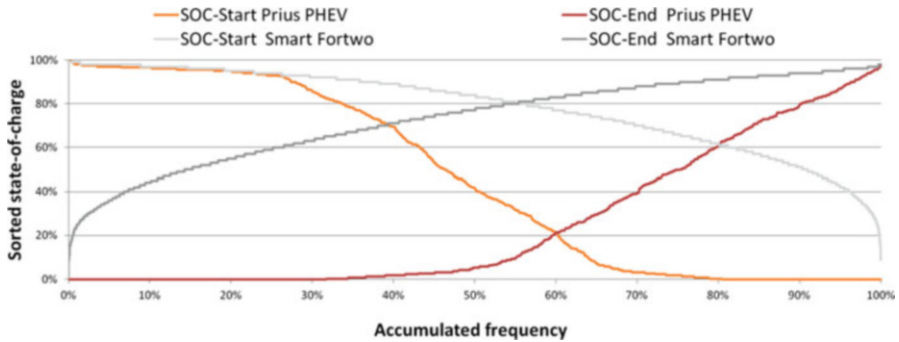
Fig. 6.5 State of charge before starting a trip and when ending a trip

Smart and Prius vehicles. For both vehicle types, the battery is fully charged (SOC > 95 %) before a trip in about 20 % of all cases. The Prius starts 30 % of trips with a fully discharged battery, whereas the Smart ends less than 10 % of trips with a battery discharged more than 40 %. In other words, 40 % of the Smart BEV's battery is not or only rarely used.

6.3.3 Charging Behavior

Charging and driving behavior are closely related. From an economic point of view, frequent charging results in fuel savings for PHEVs and a higher daily driving range for BEVs. Therefore, unlike conventional vehicles, regular daily charging is expected for PEVs. Here, especially the basis location of the vehicles (at home for private users and at the company/workplace in case of business/private users) plays an important role. In iZEUS, the charging location was not logged for all vehicles.

Furthermore, the availability of infrastructure is not entirely clear. For the Prius vehicles, infrastructure at the user's workplace was available in all cases and additional infrastructure at home in many cases.

Charging behavior is captured by changes in the SOC. The following analysis shows the charging results for the iZEUS fleet. Figure 6.6 illustrates the accumulated trip frequency and the driving range before charging. Hence, the figure indicates after which driving mileage the vehicles are plugged in for charging. For the Daimler Smart fleet again a much more restrictive use of the battery was found. In 80 % of all trips, the battery is charged after a range of less than 20 km. This frequent charging implies that only a low amount of energy (about 3 kWh for 20 km) is charged and therefore charging times are mostly shorter than 1 h.

Prius PHV users do not charge as frequently after short and medium mileages as the Smart users. One reason is the general tendency of Smart BEVs to make short trips. Further, it seems that Smart BEV users are very keen to avoid a restricted
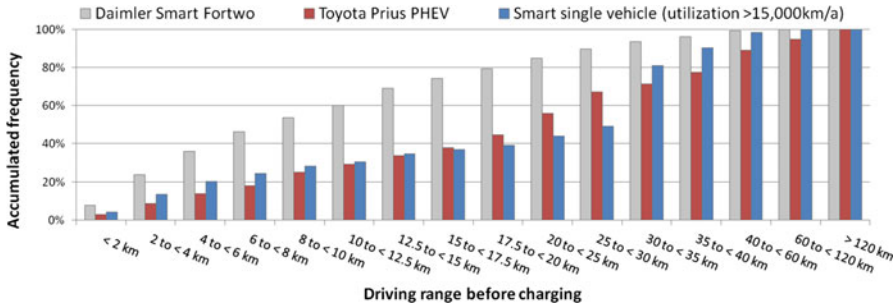
Fig. 6.6 Frequency of driving range before charging
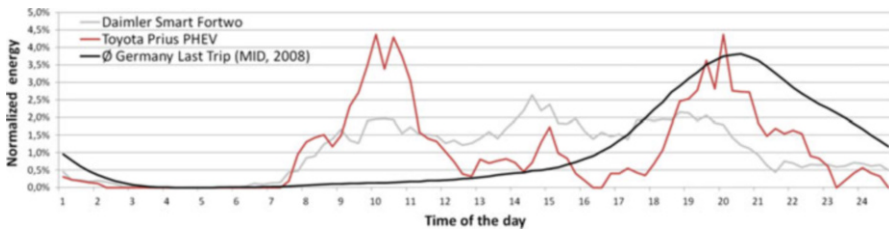
Fig. 6.7 Load curve for an average working day of different PEVs with 4 kW charging power

driving range due to a discharged battery. Reanalyzing the high utilization of the single Smart BEV (Smart single vehicle) for short trips shows that the behavior is similar to the Prius users. This user seems to be much more confident about the vehicle's electric range. The steep rise in frequency in the range class 30 to <35 km again indicates that the user makes a regular trip in this range class. Further, it seems that the user has the opportunity to charge after this trip.

The observed average charging behavior on weekdays is given in Fig. 6.7. Three different load curves are shown assuming a charging power of 4 kW per PEV. The German average is represented by the black line and simulated using average driving behavior based on a mobility survey [8] and a "last trip charging" strategy [9]. The last trip charging strategy assumes that users plug in their vehicles after the last trip of the day and charge until an SOC of 100 % is reached. The peak in the early evening is typical for last trip charging. The load curve of the Prius PHEVs' users shows two main peaks: the expected last trip charging load peak during the evening (after arriving at home) and a second load peak after arriving at work. The morning load peak after arriving at work is as high as the last trip charging load peak and could represent a second serious challenge to uncontrolled charging in case of a significant market diffusion of PEVs. Especially in the case of PEVs equipped with small batteries,[5] it is likely that PHEVs' users will increase their

---

[5] The preproduction Toyota Prius PHV used in iZEUS has an electric range of 14–18 km with a usable battery size of about 2.5 kWh.

electric driving share due to a second charge at work. This causes strong simultaneous charging behavior when employees arrive at the workplace. In the iZEUS fleet trial with Prius users, the work arrival peak is enhanced by the availability of infrastructure at work, the user group of mainly full-time employees, and the possibility to charge for free. Nevertheless, a work arrival peak is a likely future scenario that needs to be considered. The load curve of the Daimler Smart users does not show significant peaks and fluctuates only slightly from the morning hours to the early evening with a small peak at 3 o'clock in the afternoon. The Daimler Smart user group consists of private and business users. The flat load curve could be explained by business users charging during working hours as well as the high frequency of short trips that result in short charging times.

6.3.4   Discussion on Driving and Charging Behavior

Evaluating the real driving data collected in the iZEUS project allows the following conclusions to be drawn.

Representativeness of the data: It is not clear how representative the collected data are to describe the future driving behavior of PEVs. The Smart BEVs were purchased[6] by private and company fleet test participants. The relatively low average mileage indicates that most vehicles are not being used economically. Hence, other reasons seem to dominate the decision to buy during this early phase of BEVs' market diffusion. For companies and tech-savvy users, this might be their high-end technology image. The data are therefore probably only representative for early adopters of a new technology and not for future markets with higher volumes.

The Prius PHVs are lent to users with free charging at work and, as a result, only the additional operating costs are covered by the users. Consequently, each user stood to benefit from utilizing the Prius PHV instead of their normal vehicle. This fact and the evaluation results comparing the Toyota Prius data with average German driving data (see Fig. 6.3) are indicative for a usage similar to conventional vehicles. Whether this would also apply to the usage of self-owned PHEVs cannot be determined.

SOC utilization: The Daimler Smart's battery is utilized in a completely different way to that of the Toyota Prius. This is obviously due to the different battery size, but also to driver behavior. It seems that BEVs are charged more frequently to an SOC of 100 % and are only rarely discharged below 40 %. This provides very important information for the design of the usable battery capacity. For BEVs, the upper boundary of the usable SOC is more important. Here, a bigger buffer is necessary to reduce the calendar life aging that can result from fully charged batteries. At least for the behavior observed in the trials, deeper cycles that reduce

---

[6] The battery could be leased.

battery cycle life are not a big issue for the batteries of the participating BEVs. For the participating Toyota Prius PHVs, the SOC is fully charged and discharged in equal proportions (about 30 %) at the start of a trip (see Fig. 6.5). Here, both usable SOC boundaries seem to be equally important.

Range anxiety: It cannot be determined whether Smart BEVs' users are worried about the vehicle's limited range. Nevertheless, their frequent charging compared to the Toyota PHEVs with a similar availability of infrastructure indicates that a fully charged battery is of greater interest to BEVs' users. This could be because BEVs' users plan trips with higher accuracy to guarantee a charging opportunity at the point of arrival, or because they want to ensure as large a driving range as possible. The specific charging behavior could also affect the smart charging capabilities of BEVs. The differences in charging behavior between BEVs and PHEVs are not yet part of the scientific discussion, but are of great interest for further research.

Load curve shape: The shape of the load curve is important to quantify the effects of PEVs on the grid and whether additional power plant capacities are needed to meet PEVs' demand. The observed charging behavior is different to previous assumptions made about charging PEVs. The Smart BEVs' load curve rises between 8 and 9 o'clock in the morning and remains level during the day before falling between 8 and 9 o'clock in the evening. The shape is similar to instant charging behavior. The impact here is much smaller than for simulated German average last trip charging and the Prius PHVs' charging behavior. The Prius PHVs' load curve is characterized by the typical evening peak and a work arrival peak. This can be explained by the specific design of the fleet test and the availability of charging infrastructure. Nevertheless, these results are very important because they show how sensitive charging behavior can be and that it is necessary to consider uncertainties in the shape of the load curve.

6.4 Simulation of Charging Control

The following sections present the simulation methods and scenarios. Simulation method and scenario assumptions are the basis for the results presented in Sect. 6.5.

6.4.1 Methods

The PowerACE model and a grid simulation tool are used to model how PEVs affect the overall electricity system and local grids. PowerACE is an electricity market model that can be applied to investigate how fluctuating renewable electricity generation affects electricity spot market prices. The incentive-based indirect control strategy uses prices as control signals (see Sect. 6.4.1.1).

The grid tool is used to investigate autonomous distributed control. Because electricity spot market prices only represent the overall situation within the electricity system, an additional local control component becomes a possible control option. The basic idea is to monitor the situation in the local grid and to use this information to decide how to charge or discharge the PEVs' batteries. This method is introduced in Sect. 6.4.1.2. In practice and also in the PowerACE simulation environment, it is possible to combine both control strategies. In the following, the control strategies are discussed separately. The indirect control method focuses on the incentives for PEVs' users in a 2030 scenario. The section on autonomous charging focuses on the basic principle of autonomous control for PEVs.

6.4.1.1 Indirect Control

PowerACE is an electricity market simulation model that includes an agent-based indirect control mechanism for PEVs [9]. The modeled electricity prices represent the basis to control PEVs via dynamic pricing and are used to calculate the savings due to smart charging and V2G.

Electricity prices for a scenario with a high share of RES generation are calculated using the agent-based simulation model PowerACE [10]. This model provides a detailed representation of the German electricity sector and simulates the electricity spot market. Spot market prices are calculated on an hourly level for an entire year. The merit-order follows the marginal electricity generation costs of power plants, which are mainly comprised of fuel and CO_2 prices as well as start-up costs. For intermittent renewable energy generation, the variable costs are assumed to be zero. Hence, prices are low in hours with high renewable power supply or a low residual load. This merit-order effect [5, 11] of intermittent renewable energy generation in a uniform price auction is one possible reason for higher price spreads and price fluctuation in energy systems with a high share of renewable generation.

Vehicles are modeled as agents receiving a control signal that consists of a price forecast of the electricity auction [9]. A graph search optimization algorithm is used to find the charging spots with the lowest price [12]. The optimization time period is given by the driving behavior, which is taken from the Daimler Smart BEVs and Toyota PHEVs participating in the iZEUS project. In terms of charging strategies, two cases are distinguished. In the first case, real PEVs' charging behavior is used from the PEVs participating in the iZEUS project. In the second case, smart charging is applied based on the price signal provided by the PowerACE market simulation.

The introduced simulation model makes it possible to examine the possible savings and control incentives of PEVs. The method is used to investigate a 2030 scenario and captures the effects of fluctuating generation on electricity prices as well as the real driving behavior of PEVs' users collected during the iZEUS field test.

6.4.1.2 Autonomous Distributed Control

The principal idea behind autonomous control is to monitor the grid and use this information to manage charging and V2G operation. Especially in distribution grids with a high share of fluctuating renewable generation, local monitoring could be advantageous because it becomes more complex to predict the situation. Possible monitoring measurements are the frequency and the voltage at the PEVs' grid connection point. In the following, the voltage is used as an indicator because it represents the local grid situation to which the vehicle is connected.

Autonomous voltage-based control could be applied as a stand-alone control or to supplement other control methods. The stand-alone option allows grid-conform charging to be realized without any third-party intervention. Specific hardware or communication on the grid side is not required. A relatively simple autonomous control system implemented only in the PEVs undermines the argument of network operators that too many PEVs harm the grid. As an extension of already implemented charging control methods such as time of use (TOU) or other price-based indirect control methods, autonomous control can compensate possible disadvantages. The most obvious is to even out the simultaneous reaction of PEVs to time-of-use prices that is already being observed in California [4] and investigated using simulation approaches ([3]: 676).

The voltage in the grid is affected whenever one or several vehicles charge or discharge their batteries. Charging results in a drop of the voltage, whereas discharging causes the voltage to rise. This also applies to other consumers and distributed generation such as photovoltaic systems. Voltage in the low-voltage network should be kept in the range of plus/minus 3 % of the nominal voltage.

Possible options (O) to stabilize the grid using PEVs are given as follows:

O1: Reduce the active charging power. No reactive power is provided (cos φ = 1). The reduction of charging power results in a lower voltage drop due to charging but also causes a charging delay because of the reduced charging power. In many cases, especially for charging at home and work, increasing the charging time is not an issue for the consumers because the PEV standing time is more than sufficient to charge the vehicle even at reduced power.

O2: Provide V2G and feed power back into the grid. No reactive power is provided (cos φ = 1). The battery is discharged and the voltage in the grid is increased. V2G is not common in today's PEVs. Therefore, this option is less likely. Further V2G results in additional losses due to discharging the battery and to additional battery wearout. Hence, energy-based billing or other compensatory payments are needed to provide V2G.

O1.1: Providing inductive reactive charging power. Inductive power results in a voltage drop. Hence, inductive charging enhances the drop in voltage effect due to charging. The application of this charging strategy is therefore limited to situations with high distributed generation or overvoltage.

O1.2: Providing capacitive reactive charging power. Capacitive power results in a voltage rise. This charging strategy helps to reduce the voltage drop due to

charging. Hence, in a situation with too much demand in the grid, capacitive reactive charging enables a higher power to be used without violating the low-voltage boundary.

O2.1: Providing inductive reactive V2G power. Feeding power back causes a rise in voltage. Inductive V2G power reduces the rise in voltage. Hence, in situations with high supply from V2G and/or distributed generation, inductive reactive power enables more power to be fed back.

O2.2: Providing capacitive reactive V2G power. Capacitive V2G power enhances the voltage-increasing effect of feeding power into the grid. The application of this V2G strategy is therefore limited to situations with high demand and low voltage.

O3 and O4: Providing inductive (O3) or capacitive (O4) reactive power. Besides providing both real power and reactive power at the same time (O1.1, O1.2, O2.1, and O2.2) as well as only real power (O1 and O2), another possible strategy is to only provide reactive power (O3 and O4). If PEVs are connected to the grid, they can help to stabilize it by providing inductive reactive power, which reduces the voltage, or by providing capacitive reactive power, which raises the voltage. The effects are rather small but the strategy can be beneficial in some situations or specific grids. Further, providing reactive power is associated with losses due to the power electronics but does not result in battery wearout [13].

Grid simulation based on a nonlinear equation system and an iterative approach is used to examine the described autonomous control strategies. The grid simulation is done quarter hourly and based on the Gauss-Seidel method ([14]: 968).

The voltage level in each time step is calculated in a first grid simulation without PEVs. The resulting voltage values then form the basis for the autonomous control strategy. A second grid simulation includes the charging or V2G operation of the PEVs. The share of real and reactive power is adjusted according to a linear function of the voltage (see Fig. 6.8). To provide an example the function for actual capacitive reactive charging power is given in the following equation.[7] The actual capacitive reactive charging power (operation O1.2) share $Q_{\text{cap},y}$ is calculated according to (6.1):

$$Q_{\text{cap},y} = (1 - V_x) * \frac{Q_{\max}}{(1 - V_{\min})} \quad \text{For voltage } V_x > V_{\min} \text{ and } V_x < 1 [\text{p.u.}] \quad (6.1)$$

where V_x is the actual measured voltage, $Q_{\max}$ is the maximum reactive power that can be provided, and $V_{\min}$ is the lower voltage boundary. V is given in the per unit system (p.u.). For voltage values lower than $V_{\min}$, Q is constant and is set to $Q_{\max}$.

The results of the second grid simulation with adapted charging and discharging are used to quantify how autonomous charging can contribute to stabilizing the grid (see Sect. 6.5.4).

---

[7] For inductive charging and V2G cases, a simple adaptation of the equations is necessary.

Fig. 6.8 Reactive power
provided by PEVs based on
node voltage level
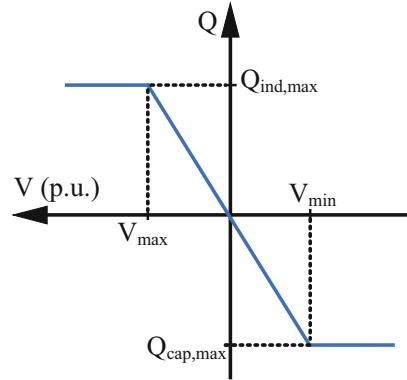
If the autonomous control strategy is used in combination with optimized price-based operating schedules (indirect control), it is necessary to compensate the energy used for the autonomous control services. For example, if capacitive reactive charging power is provided, it would be necessary to extend the charging period, because the real charging power is reduced by providing reactive power. In this case, additional charging time slots in the price-based optimization are needed to guarantee that the battery is fully charged within the charging schedule.

In the iZEUS project, an autonomous control system was realized using a three-phase voltage measurement chip and a smart charging controller. Upon receipt of the voltage measurement and a price signal provided according to ISO 15118, the controller calculates a specific charging or V2G operating strategy. Additionally, a 22 kW bidirectional four-quadrant onboard charger was developed that manages charging and V2G operation (see Sect. 6.5.2 and [15]). This demonstrates the feasibility of the autonomous control approach even if the currently available PEVs so far do not feature chargers with active power electronics.

6.4.2 Scenario

To analyze PEVs' control strategies, scenarios are defined for the electricity system (indirect control) and the grid simulation (autonomous control). The scenario[8] for the electricity system defines the input parameters of the PowerACE model. The PowerACE model is used to investigate the incentives for indirect control due to participation on the day-ahead spot market for electricity. Here, assumptions about fuel prices as well as the amount of generation from fluctuating renewable sources are very important because they affect the day-ahead spot market prices and PEVs' incentives. A simple grid is defined for the grid simulation. Further, a function is

---

[8] The scenario is the same as in [3].

introduced for the relation between voltage and the provided reactive power. Vehicle parameters for both simulations are taken from the iZEUS field trial.

6.4.2.1 Electricity System

In order to investigate the incentives for PEVs to integrate renewable energy generation into the grid, a scenario is defined based on surveys available in the literature. This scenario assumes very high generation shares from renewable energy sources (necessary to reach the German Government's CO_2 reduction target). The main scenario used here, which is called "GER 2030," refers to the "Lead Scenario 2010," which was part of a survey investigating high generation shares from renewable energy sources in Germany conducted on behalf of the German Federal Ministry for the Environment, Nature Conservation, and Nuclear Safety [16].

The installed capacity of fluctuating renewable generation is shown in Fig. 6.9. Values until 2012 represent real installations in Germany. The future assumptions are based on [16]. The total installed capacity from fluctuating generation in 2030 is 125.8 GW, which equals 162 % of the 77.8 GW peak load. The generation share of intermittent RES is 47.6 %, with 87 TWh, 95 TWh, and 57 TWh coming from wind onshore, wind offshore, and photovoltaics, respectively. Total electricity demand is 502.1 TWh per year. The hourly characteristics of RES generation and the load curve are taken from [17, 18] with 2008 as the reference year. Electricity imports and exports as well as storage technologies such as hydro-pumped storage are not taken into account because the focus is on how V2G can contribute to balancing RES-E.

The assumed power plant park includes power plants >10 MW from [19] that are still available in 2030. New installations are added that assume an optimal power plant mix to serve the residual load curve for the assumed load and RES-E scenario [3]. The installed capacities are 749 MW from oil power plants,
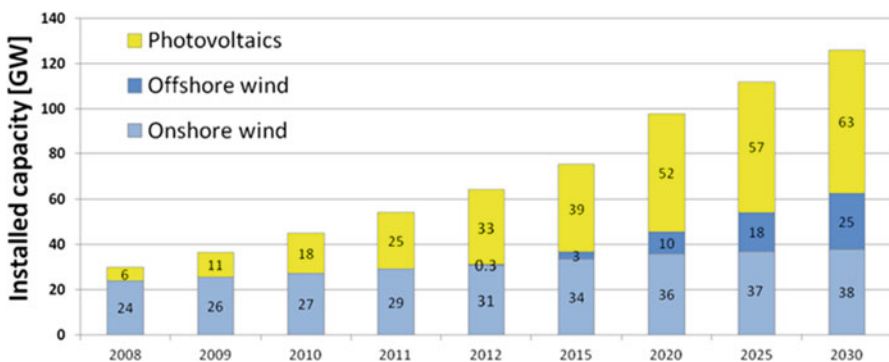
Fig. 6.9 Installed capacity of fluctuating generation in Germany. *Source*: [3, 16]
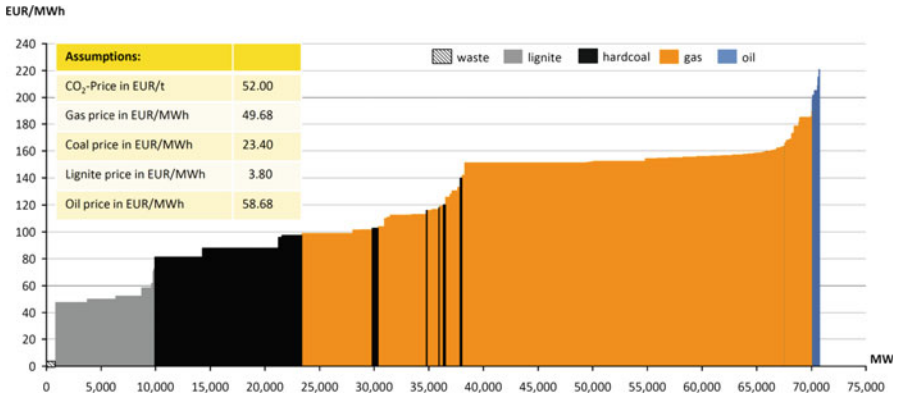
Fig. 6.10 Merit-order curve of the power plant park in Germany in 2030. Source: Own assumptions based on [19, 20]; CO_2 and fuel prices [16]; figure created by David Biere

32,461 MW from gas turbines, 13,942 MW from combined cycle gas turbines, 14,375 MW from coal power plants, 9119 MW from lignite power plants, and 820 MW from waste power plants. The assumed fuel prices and the resulting merit-order curve of the fossil power plant park are given in Fig. 6.10.

6.4.2.2 Grid Simulation

The local distribution grid is modeled as a single-branch 0.4 kV[9] network, which consists of two nodes. The cable which connects the nodes is between 150 m and 6 km long and of type NAYY-J 4×95.[10] The first node represents the slack bus, which is connected to the next higher voltage level. The second node is the grid connection point of one PEV and a household. A typical profile with a fixed real power factor of 0.95 and maximum power of 3 kVA is applied to the household. The PEV can charge or discharge with a maximum power of 4 kVA. The energy needed and the time of arrival at the grid equal the typical home arrival behavior observed in the iZEUS project. The minimum power factor (cos ϕ) is set to 0.5. Hence, the modeled car is capable of providing a maximum reactive power of 3.46 kVAr (Fig. 6.11).

---

[9] Line-to-line voltage: usual low voltage level in Germany.

[10] Details are available in [21].

Fig. 6.11 Low-voltage test
feeder (four nodes)
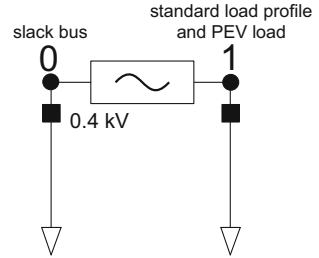
6.5   Results

The results section starts with a consumer survey of tariff designs to control PEVs
conducted during the iZEUS project. Next, the results of the energy system
analysis, prototype development, and grid impact analysis are presented.

6.5.1   Indirect Price-Based Control: A Consumer Survey

Technology acceptance is crucial for the dissemination of innovative technology.
Any technology like the electric vehicles' automated charging control will only be
successful in the market if the target group is willing to accept it. Technology
acceptance is usually high if a personally perceived benefit exists which is big
enough to justify any necessary efforts taken [22]. It does not matter whether the
benefit originates from the technology itself, or if it is artificially created (e.g.,
financial benefits through subsidies).

   To exploit the full potential of integrating energy from renewable sources into
the grid, electric vehicles' automated charging control obliges the owners of
electric cars to enter variable electricity supply tariff contracts. Currently, such
variable tariffs that offer smart and flexible charging opportunities for electric cars
to meet the fluctuating demand and supply patterns of the electricity grids are only
very rarely available in Germany. Thus, it is not surprising that, so far, no research
has been done concerning their general acceptance and preferred configuration.
Research of this topic is essential in order to learn about the acceptance of charging
tariffs in general and about the preferred configuration of specific features in order
to minimize the effort involved in introducing the respective tariffs, discover the
preferences of future users, and increase the acceptance of such tariffs.

   We therefore studied consumer preferences for systems (tariffs) of demand-side
management for electric vehicles by applying a scenario-based survey design. The
main part of the questionnaire consisted of five short texts, each describing a
possible scenario offering an electricity tariff for electric vehicles, which are
summarized here:

- *Manual* (*MC*): Charging is operated entirely manually, several rate periods, possible reward up to 150 Euro p.a. (depending on charging behavior).
- *Automated Charging* (*AC*): Automated charging control, mobility buffer of 40 km, origin of energy used is the standard German mix, reward 100 Euro p.a.
- *Automated Charging—Comfort* (*AC-COM*): Automated charging control, mobility buffer at 70 km, origin of energy used is the standard German mix, reward 85 Euro p.a.
- *Automated Charging—ECO* (*AC-ECO*): Automated charging control, mobility buffer at 40 km, origin of energy is solely renewable sources, reward 85 Euro p. a.
- *Automated Charging—V2G* (*AC-V2G*): Automated charging control including feedback when the supply of renewables is low, mobility buffer at 40 km, origin of energy used is the standard German mix, reward 130 Euro p.a.
- *No Tariff*: This alternative includes the option not to select a new tariff for charging the electric vehicle, but to charge it with the currently used standard home tariff.

The scenarios differed with regard to (a) whether charging management is operated automatically or manually, (b) whether a vehicle-to-grid option is included, (c) the minimum range guaranteed by the system (mobility buffer stated in kilometers), and (d) the generation sources of the electricity used. Additionally, each scenario provided explicit information about the sustainability, possible financial savings, and necessary efforts by the consumer to operate the system. The participating sample of 1027 individuals is representative for the German population with regard to socio-demographic criteria.

Analyzing the results (see Fig. 6.12) reveals that the automated vehicle-to-grid tariff is the most preferred option with almost 22.9 % of the total votes. This is followed by the manual charging tariff (MC) with 17.8 %, the automated charging version with eco touch (AC-ECO) with 14.1 %, the automated charging tariff in the comfort version (AC-COM) with 14.1 %, and the standard automated charging tariff (AC) with 12.6 %. Remarkably, almost 18 % of the test persons did not favor any of the tariffs, and chose the "No tariff" option.

Fig. 6.12 Consumer survey results
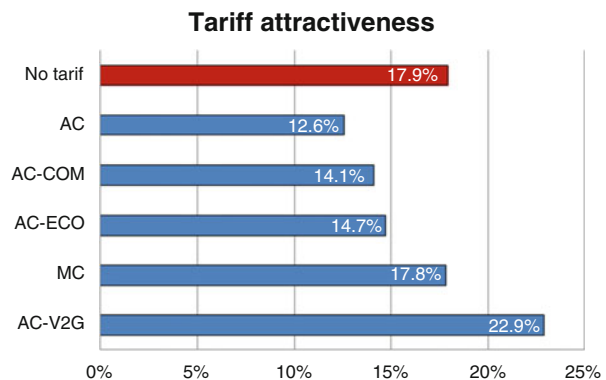
The main conclusion is that, despite varying preferences within the offered tariffs, more than 80 % of the persons interviewed are generally open-minded to one of the tariffs offered and are thus willing to contribute to demand-side management in the mobility sector. In addition, further analyses of the data showed that the indicated scenario preference is usually in line with the motives for their choice, e.g., sustainability or simplicity.

6.5.2 Energy System Analysis

The energy system analysis is based on work by Dallinger et al. [3] using travel survey driving data. The results presented here show possible smart charging and V2G revenues using real PEVs' driving data. The analysis is based on the energy system scenario introduced in Sect. 6.4. The simulation is conducted with the PowerACE model. Section 6.5.2.1 presents the results on smart charging only. Section 6.5.2.2 shows the results for smart charging and V2G.

6.5.2.1 Smart Charging Savings

In the following, the savings obtained due to controlled or smart charging are presented compared to uncontrolled charging for an electricity system scenario in 2030. The uncontrolled charging behavior is the same as the charging behavior observed during the iZEUS field trial. Controlled charging uses the same mobility behavior, but shifts the charging process during the observed parking time. The control signal is the electricity price simulated by the PowerACE model for a 2030 scenario. Hence, charging is realized at minimum electricity prices within the constraints of the observed parking times and energy demand for driving. The differences in yearly electricity costs between uncontrolled and controlled charging are given in Fig. 6.13.
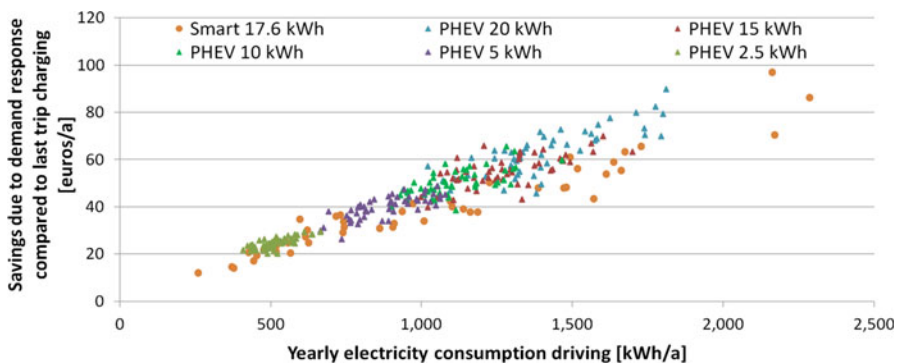
Fig. 6.13 Savings for controlled charging compared to uncontrolled charging

For the Toyota Prius PHVs, the observed driving behavior is randomly assigned to 50 simulated vehicles on a weekly basis. Further, the battery size in the simulation is varied between 2.5 and 20 kWh. For the Daimler Smart BEVs, the observed driving behavior is directly assigned to a simulated BEV.

The results show that the yearly electricity costs are mainly a linear function of the electricity demand. Savings are between 10 and 100 euros per year. In case of smart charging, a larger battery enables a longer grid management time and therefore the opportunity for additional savings. However, comparing Daimler Smart BEVs with a usable battery size of 17.6 kWh and Toyota Prius PHVs with a usable battery size of only 2.5 kWh indicates that bigger batteries do not result in additional savings (see Fig. 6.13 for electricity consumption between 400 and 700 kWh).

If the same driving behavior is assumed with a bigger battery, as simulated for the Toyota Prius PHVs, higher electric driving shares result in an increase of the yearly electricity demand and savings. For higher consumption values, a higher variability of the savings obtained is also observed (for example, see the three Smart BEVs with a demand over 2000 kWh/a). Here, due to the higher utilization of the vehicles (reduced parking times), the periods when vehicles are connected to the grid become more relevant. A high installed capacity of photovoltaic systems is assumed in the applied 2030 scenario. Due to the photovoltaic peaks, low prices during the day are more likely (see Fig. 6.1). The fluctuation of renewable generation deviates from the conventional picture of low prices during the night and higher prices during the day. Therefore, it becomes more important that PEVs are available during the day to realize savings due to low smart charging prices.

6.5.2.2 Vehicle-to-Grid Savings

Smart charging is extended by the ability to feed power back into the system in order to simulate vehicle-to-grid savings. The V2G efficiency is 94 % and battery aging is assumed according to [20].

The simulation results are given in Fig. 6.14. Savings compared to uncontrolled charging are between 50 and 300 euros per year. Savings follow a step function when
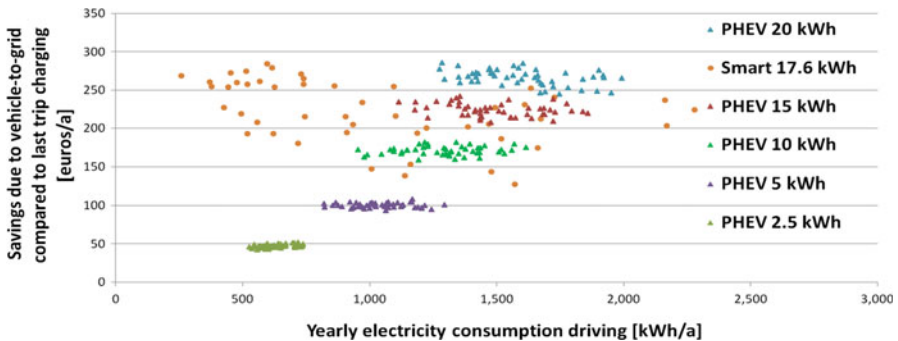
Fig. 6.14 Vehicle-to-grid savings compared to uncontrolled charging

simulating PHEVs applying the Toyota Prius driving behavior observed in the iZEUS project. Each simulated battery size results in a different magnitude of savings. Battery size strongly affects the possible savings for V2G in contrast to the results for load shifting. The results are not as clear for the simulation of the Daimler Smart BEVs. Here, BEVs with low utilization are able to reach the highest savings. Vehicles with higher yearly electricity consumption show slightly lower savings.

Overall, possible incentives from day-ahead electricity markets will not significantly reduce the PEV total costs of ownership. Savings are low even with a high share of fluctuating renewable generation that increases the market price spreads due to the merit-order effect. With respect to the conducted consumer survey on the acceptance of price-based control, smart charging still seems a promising way to realize an electricity system with a higher share of renewable generation.

6.5.3   Prototype Development and Demonstration

The control strategy of autonomous distributed control (see Sect. 6.4.1.2) was implemented in an onboard control device referred to as the grid controller. The prototype development was conducted by Fraunhofer ISE and demonstrates the feasibility of autonomous distributed control. Its block diagram is shown in Fig. 6.15.

A metering board was developed based on an Analog Devices ADE7758 metering chip. This enables the grid controller to measure the root mean square
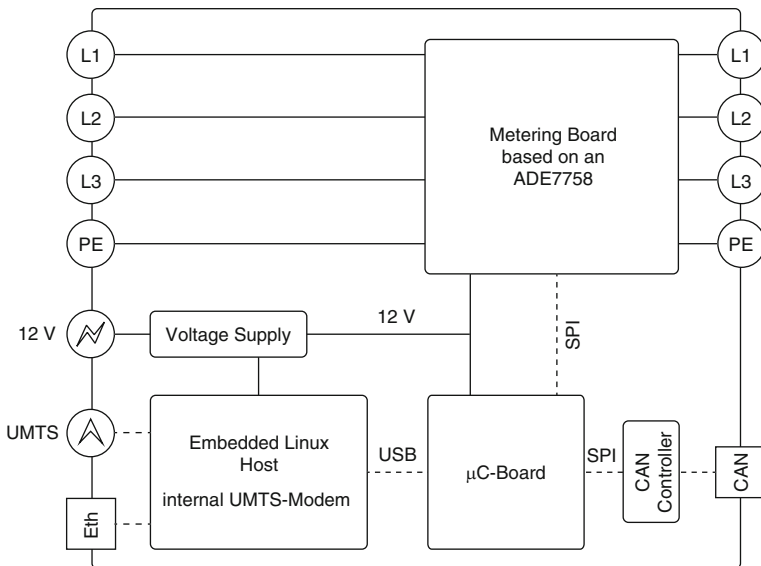
Fig. 6.15 Block diagram of the grid controller for integration in a PEV

(RMS) value of the voltage per phase, as described in Sect. 6.5.3.1. The μC board handles all tasks with hard real-time constraints such as the voltage controller and the onboard communication via the controller area network (CAN). An additional host controller running an OpenMUC[11]-based energy management system takes care of the intelligent charging strategies, representing the control level above the voltage controller itself. Both systems are described in Sect. 6.5.3.2. Ancillary components integrate the controller into the vehicle's system architecture as shown in Sect. 6.5.3.3.

In addition to the grid controller, a bidirectional, highly efficient 20 kW charger was developed at the Fraunhofer ISE, which is capable of adjusting the power factor upon request. Charger, grid controller, and additional vehicle control devices are interconnected via the onboard CAN bus. A similar setup was presented in [23].

6.5.3.1 Metering Board

The key component of the metering board is an Analog Devices ADE7758 IC. This three-phase electrical energy measurement IC provides all the signal processing required to perform active, reactive, and apparent energy measurement and RMS calculations. The metering board utilizes the acquisition of the three-phase voltage RMS values as input for the voltage controller. Other available metering values are the RMS values of the current, the maximum values of voltages and currents, and the present values of voltages and currents using the integrated waveform-sampling mode. The integrated temperature sensor allows monitoring the grid controller's status during operation. High accuracy of the metering system can be achieved using the IC's system calibration features for each phase, allowing RMS offset correction, phase calibration, and power calibration.

The metering board provides the circuitry for the current transducers, allowing measurements for a current range of ± 55 A with an accuracy of ± 0.25 %. Voltage sampling is done using a resistive voltage divider (1 MΩ:1 kΩ) providing a voltage range of ± 500 V with an accuracy of ± 0.5 %. Additional protection circuitry has been engineered in order to separate the power and the control circuits. Communication with the μC board as part of the control circuit is done via a serial interface.

6.5.3.2 Controller Architecture

The grid controller was developed to demonstrate the feasibility of the proposed autonomous reactive power control. Therefore, a specially designed component was developed. The final design would also integrate the different tasks into

---

[11] OpenMUC is an open-source energy monitoring and control software framework developed at Fraunhofer ISE. See www.openmuc.org.

existing components of the PEV, i.e., metering tasks into the charger, higher level communication, and control tasks into control devices.

The grid controller prototype comes with two control devices: a μC board based on an Atmel AT90USB646 and a piA-AM3505-embedded Linux system from the German electronics and software company pironex GmbH. This setup allows operating modes such as an intelligent upper-layer demand response algorithm, e.g., according to price signals, and the lower level voltage controller to stabilize the grid during charging.

The μC board handles the acquisition and processing of the meter data. It runs the real-time voltage controller, which is fed with the voltage RMS values and the reference charging power from the upper-layer charging algorithm. The EV-internal communication via CAN is also handled by the μC board, which effectively allows the embedded Linux system to only process the upper-layer control algorithms. Using an embedded Linux system enables control algorithms to be developed based on the OpenMUC software framework.

6.5.3.3   Automotive Integration

Various design decisions were made regarding the integration of the grid controller prototype into a PEV. Only components with an extended temperature range of -25 to $+85\ °C$ were used. The voltage supply circuitry was engineered to withstand various events where the supply may deviate from the 12 V voltage rating. The control algorithms of the embedded system realize a seamless integration into the charging process as defined in ISO/IEC 15118 by interacting with the respective in-vehicle control devices via CAN.

6.5.3.4   Demonstration

The grid controller prototype and 20 kW charger were included in a test bed as shown in Fig. 6.16. The grid was simulated by a three-phase AC source and subsequent feeder representation. The grid representation is controlled via COM.
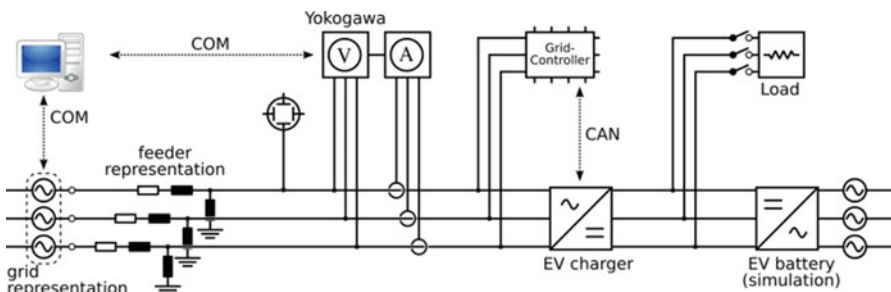
Fig. 6.16   Block diagram of the grid controller for integration in a PEV

The EV battery is simulated by a bidirectional three-phase converter and an optional resistive load. The grid controller requests a desired reactive and active current of the EV charger via CAN. The test bench is observed and documented using an oscilloscope and high-precision measurement equipment (Yokogawa). The feeder representation is adjustable to illustrate usual feeder characteristics via condensed elements. The tests with different feeder representations are still ongoing and therefore not included in this publication.

The following droops were measured to validate the controller at a charging power of 9 kW (3 kW per phase): The grid representation voltage was increased in 0.5 V steps and held for 10 s. The grid controller includes a PT1 characteristic with τ of 5 s to increase stability and hinder flicker production. Hence, a damped voltage signal is used to set the reactive power.

The biggest sources of uncertainty in the test bench are the grid representation, grid controller, and EV charger. Within the grid representation, the voltage deviation between three phases can be up to 2 V. Since the grid controller is not a high-precision measurement device like the Yokogawa, this leads to differences between CAN and Yokogawa due to deviations in the voltage measurement per phase of up to 1.2 V. Additionally, the PT1 characteristic leads to damped control signals. The deviation between the de facto reactive current provided by the EV charger and the desired values sent by the grid controller sums up to 0.2 A. Plotting the reactive power provided against the voltage eliminates the uncertainties due to the grid representation because each voltage level is reached at different times in the different phases. Figure 6.17 shows the reactive power provided against the current voltage from CAN. This reveals the uncertainties due to EV charger and grid representation leading to a small offset of the droop and deviations within the
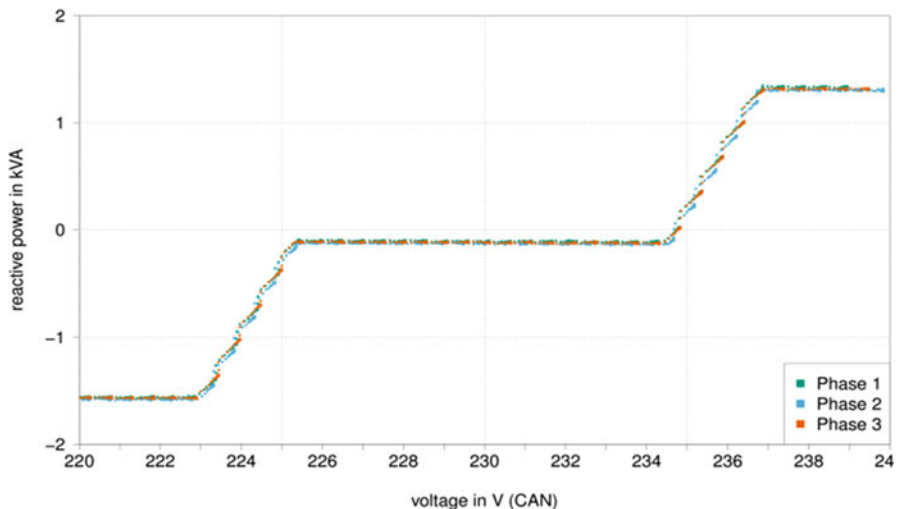
Fig. 6.17 Measured voltage droop at 9 kW charging with current voltage from CAN and reactive power measured by Yokogawa
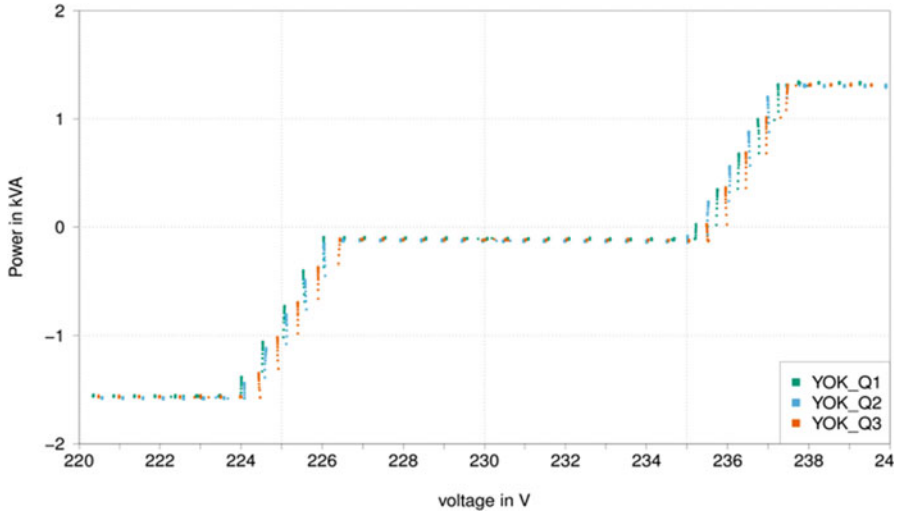
Fig. 6.18 Measured voltage drop at 9 kW charging with current voltage from and reactive power measured by Yokogawa

slopes. Due to the PT1 characteristics of the controller an almost continuous adoption of the reactive power is realized. This contradicts the reality of the stepwise voltage changes in the grid representation.

Figure 6.18 shows the reactive power provision against the voltage measured by Yokogawa. This additionally reveals the uncertainties in the measurements of the grid controller metering board. Grid representation uncertainties show in the slopes. Nevertheless, the desired droop is controlled with sufficient accuracy since the slopes are only applied to avoid discrete steps and therefore increase the stability of the control system, especially with multiple EVs. An interesting effect is the uncoupling of the droops per phase due to the comparatively cheap grid controller's limited accuracy in measuring the voltage. This effect adds additional stability to the system since multiple PEVs lead to less synchrony of the reactive power provision and therefore a limited uncoupling of the decentralized controllers.

6.5.4 Grid Impact Analysis

This chapter discusses the principal benefits of the autonomous control strategies introduced in Sect. 6.4.1.2. The following simulation results are based on the scenario assumptions introduced in Sect. 6.4.2.2. The simulated grid consists of two nodes connected with a cable that varies in length between 150 m and 6 km. A setup with long cables increases the sensitivity towards voltage deviations in the grid and therefore enables illustrating possible benefits of smart charging.
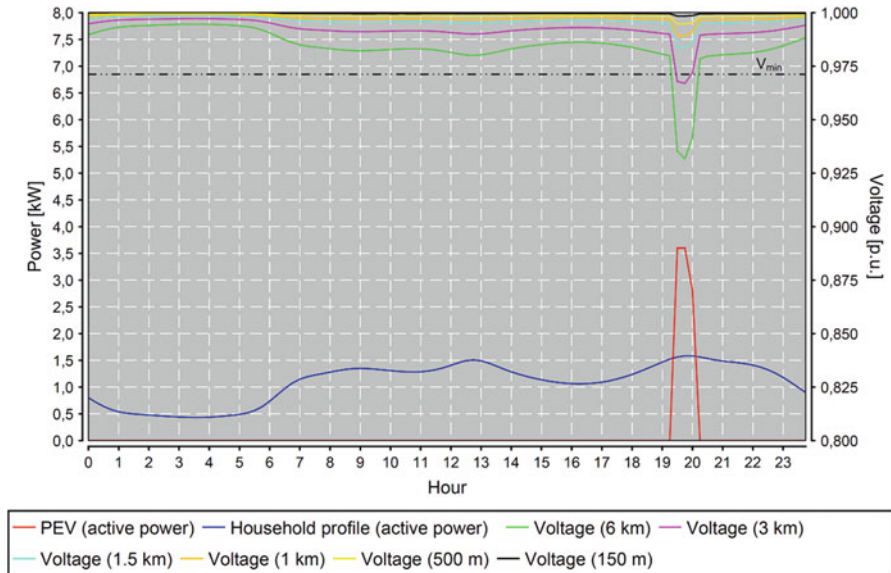
Fig. 6.19 Power and voltage profiles at node 1

In practice, most grids are less sensitive and consequently the smart charging benefits in terms of voltage control are smaller.

The voltage resulting from a grid simulation of one day is shown in Fig. 6.19. Voltage in the low-voltage network should be kept in the range of plus/minus 3 % of the nominal voltage ($V_{min} = 0.97$). Input parameters affecting voltage are the household load profile and the PEVs' charging profile. Even without PEV charging, the voltage drops close to the V_{min} boundary at noon and in the early evening for the 6 km cable. PEV charging at 6 pm with 3.6 kW power results in a massive voltage drop that violates V_{min} (6 and 3 km cable length). For cable lengths below 3 km, the voltage is less sensitive to charging.

The voltage drop for the 6 km cable can also be observed in Fig. 6.20 when P_{charge} is assumed to be 3.6 kW. Further, Fig. 6.20 shows all charging and V2G options of a PEV equipped with a four-quadrant 4 kW power inverter. To avoid violation of V_{min}, P_{charge} must be strongly reduced. A PEV equipped with a voltage-monitoring system that allows autonomous control is able to detect the available real power before violating V_{min}. In the example presented here, the power would have to be reduced from 3.6 kW to below 0.5 kW. This would delay the charging process. Hence, if instant charging is needed and V_{min} should not be violated, the charging strategy O_{12} is valuable. Here, the vehicle uses capacitive charging to lift the voltage while consuming a higher real power of 3.3 kW ($Q_y = 1.4$ kVAr and $S_y = 3.6$ kVA).

In the example presented, the PEV is able to strongly lift and reduce the voltage, thereby stabilizing the grid. Furthermore, providing reactive power in specific situations (when V_y is close to the voltage limits V_{min} and V_{max}) allows real charging
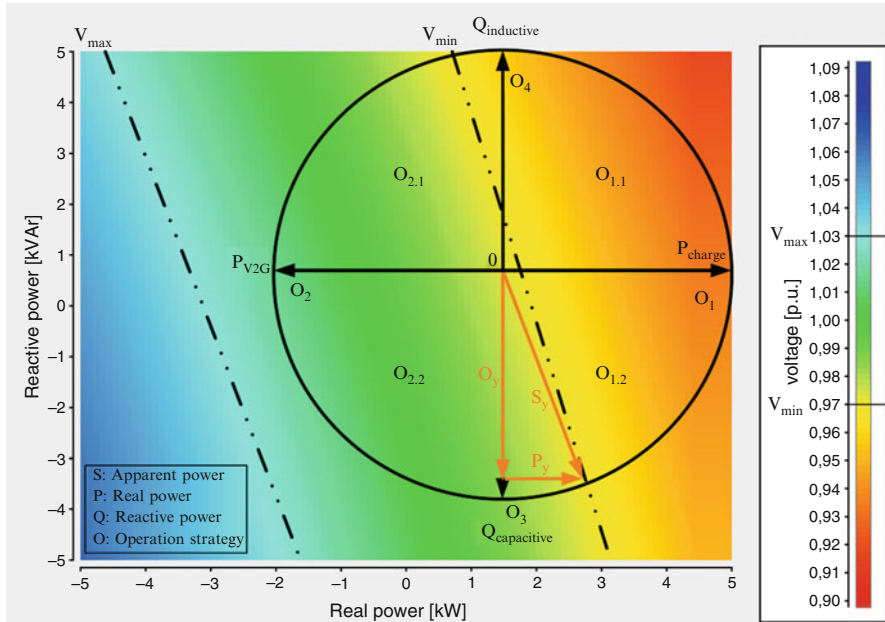
Fig. 6.20 V2G and charging control options for the PEV

or V2G power to be increased. In terms of renewable and especially distributed photovoltaic generation that lifts the voltage when available, the violation of V_{max} is an issue. Here, the PEV can reduce the voltage due to charging (O_1), charging while providing inductive reactive power ($O_{1.1}$), or if no real charging power is needed, just by providing inductive reactive power (O_4).

Even if the effects on voltage are lower in most grids, the presented results show that PEVs have a great potential to stabilize the grid and integrate fluctuating renewable generation. Autonomous control based on monitoring the voltage at the grid connection point will therefore be of great value in future smart grids. Further, it is possible to include PEVs in the existing infrastructure without complex charging control systems.

6.6 Conclusions

Using renewable energy generation to power electric vehicles makes it possible to decarbonize large parts of the passenger transport sector. Sustainable energy generation from renewable sources and electric vehicles' high efficiency in transforming this energy seem to be a match made in heaven. Nevertheless, the fluctuation of photovoltaic and wind generation is an issue that complicates the

interaction of renewable generation and plug-in electric vehicles because a control mechanism is required to match demand and supply.

Market-based electricity prices are able to reflect the supply of fluctuating renewable generation on a system level. Therefore, real-time prices are a promising option to control plug-in electric vehicles and support the grid integration of fluctuating generation. Electricity market simulation shows that smart charging and V2G revenues are only in a range between 10 and 300 euros per year. Nevertheless, consumers are open to using specific tariffs for smart charging of plug-in electric vehicles.

A general issue of controlling flexible demand and generation units connected to the distribution grid is that current electricity markets mainly reflect the overall system level. The local situation in low-voltage distribution grids is not mirrored by electricity prices and in many cases information on the local situation is missing. Plug-in electric vehicles that monitor the voltage at the grid connection point can collect this missing information and autonomously control their own charging behavior. The development of a bidirectional 20 kW charger with grid-monitoring function and the conducted simulations and tests show that autonomous voltage-based control is a very good strategy taking the distribution grid situation into account.

Both of the control strategies investigated, indirect price-based control and autonomous control, offer advantages for specific applications. Therefore, if a general control mechanism is needed for PEVs, combining both strategies seems to be a promising option to help balance electricity systems.

References

1. KIT: Karlsruhe Institute of Technology (2014) Energy smart home lab. http://www.izeus.kit.edu/57.php
2. Pacific Gas and Electric (2014) Electric vehicle time of the use tariff. http://www.sdge.com/clean-energy/ev-rates. Accessed 11 July 2014
3. Dallinger D, Gerda S, Wietschel M (2013) Integration of intermittent renewable power supply using grid-connected vehicles–a 2030 case study for California and Germany. Applied Energy 104:666–682
4. Schey S, Scoffield D, Smart J (2012) A first look at the impact of electric vehicle charging on the electric grid in the EV project. Paper presented at 26th Electric Vehicle Symposium (EVS-26), Los Angeles, 6–9 May 2012
5. Sensfuss F (2008) Assessment of the impact of renewable electricity generation on the German electricity sector. An agent-based simulation approach. Fortschritt-Berichte VDI. Reihe 16, Technik und Wirtschaft, x, 209, VDI Verlag, Düsseldorf

6. Yang H, Chung CY, Zhao J (2013) Application of plug-in electric vehicles to frequency regulation based on distributed signal acquisition via limited communication. IEEE Trans Power Syst 28(2):1017–1026

7. EnBW (2014) Die EnBW-Ladestationen. https://www.enbw.com/privatkunden/energie-und-zukunft/e-mobilitaet/ladestationen/index.html. Accessed 31 Mar 2014

8. MID: Mobility in Germany 2008 (2010) Project handling: Institute for Applied Social Science Research (infas) and the Institute of Transport Research of the German Aerospace Center (DLR) on behalf of the Federal Ministry of Transport, Building and Urban Affairs. http://www.mobilitaet-in-deutschland.de/mid2008-publikationen.html. Accessed 11 Jul 2016

9. Dallinger D, Wietschel M (2012) Grid integration of intermittent renewable energy sources using price-responsive plug-in electric vehicles. Renewable and Sustainable Energy Review 16(5):3370–3382

10. Sensfus F, Ragwitz M, Genoese M (2008) The merit-order effect: a detailed analysis of the price effect of renewable electricity generation on spot market prices in Germany. Energy Policy 36(8):3086–3094. doi:10.1016/j.enpol.2008.03.035

11. Nicolosi M, Fürsch M (2009) The impact of an increasing share of RES-E on the conventional power market—the example of Germany. ZfE Zeitschrift für Energiewirtschaft 03|2009. http://www.ewi.unikoeln.de/fileadmin/user_upload/Publikationen/Zeitschriften/2009/09_03_01_Nicolosi_Fuersch_Zfe.pdf

12. Dallinger D, Link J, Büttner M (2014) Smart grid agent: plug-in electric vehicle, sustainable energy. IEEE Transactions on Sustainable Energy 5(3):710–717

13. Ehsani M, Falahi M, Lotfifard S (2012) Vehicle to grid services: potential and applications. Energies 5(12):4076–4090

14. Schwab AJ (2009) Elektroenergiesysteme. Erzeugung, Transport, Übertragung und Verteilung elektrischer Energie, 2nd edn. Springer, Berlin

15. Dallmer-Zerbe K, Stillahn T, Erge T, Wille-Haussmann B, Wittwer C (2014) Analysis of the exploitation of EV fast charging to prevent extensive grid investments in suburban areas. Energy Technology 2(1):54–63

16. Nitsch J, Pregger T, Scholz Y, Naegler T, Sterner M, Gerhardt N, Von Oehsen A, Pape C, Saint-Drenan Y, Wenzel B (2010) Langfristszenarien und Strategien für den Ausbau der erneuerbaren Energien in Deutschland bei Berücksichtigung der Entwicklung in Europa und global. Deutsches Zentrum für Luft- und Raumfahrt, Fraunhofer Institut für Windenergie und Energiesystemtechnik, Ingenieurbüro für neue Energien, vol. BMU—FKZ0. http://www.erneuerbare-energien.de/inhalt/47034/40870/. Accessed 11 Nov 2013

17. EEX: European Energy Exchange (2011) Transparency in energy markets—Gesetzliche Veröffentlichungspflichten der Übertragungsnetzbetreiber. European Energy Exchange AG

18. ENTSO-E: European Network of Transmission System Operators for Electricity (2011) Hourly load values of all countries for a specific month. https://www.entsoe.eu/db-query/consumption/mhlv-all-countries-for-a-specific-month/. Accessed 11 July 2011

19. Platts (2010) World electric power plants database. http://www.platts.com/Products/worldelectricpowerplantsdatabase/Overview. Accessed 31 Mar 2012

20. Dallinger D (2013) Plug-in electric vehicles integrating fluctuating renewable electricity, vol 20. Kassel University Press GmbH, Kassel

21. Faber Kabel (2014) Starkstromkabel NAYY—J/O nach VDE 0276-603. Accessed 7 Aug 2014

22. Rogers EM (2010) Diffusion of innovations. Simon and Schuster, New York

23. Reichert S (2010) Considerations for highly efficient bidirectional battery chargers for e-mobility. In: Proceedings of the VDE Kongress 2010

Chapter 7
Experiences and Applications of Electric and Plug-In Hybrid Vehicles in Power System Networks

Cagil Ozansoy, Taha Selim Ustun, and Aladin Zayegh

Abstract Transportation electrification is inevitable driven by rising energy costs, climate and emission control requirements, and availability of petroleum supplies. Even a realistic 10 % electrification of transportation is expected to impact the electricity generation, transmission, and distribution capacities, and hence the world economy. In this chapter, the authors seek to enlighten the reader on electric vehicle usage around the world by discussing their applications, electric vehicle trials, and key learnings from these trials across three continents: America, Europe, and Australia. Special emphasis has been given to discussing the commuting trends across the three continents and how that effects the transition into the electrification of transportation. The chapter continues with an impact analysis of electric vehicles on car users, the power quality of grids, and finally carbon emissions. Finally, examples of charging infrastructure and worldwide vehicle-to-grid applications are reviewed. The chapter concludes with a discussion on the need for interoperable communication standards, as an enabling technology for the management of the transactions between the grid and electric vehicles.

C. Ozansoy (✉) • A. Zayegh
College of Engineering and Science, Victoria University, PO Box 14428, Melbourne, VIC 8001, Australia
e-mail: cagil.ozansoy@vu.edu.au; aladin.zayegh@vu.edu.au

T.S. Ustun
School of Electrical and Computer Engineering, Carnegie-Mellon University, Pittsburgh, PA, USA
e-mail: ustun@cmu.edu

7.1   Electric Vehicles in Smart Grids Around the World: Experiences and Applications in the USA, Europe, and Australia

The use of EVs in smart grids in the world is increasing and more and better charging stations are being retrofitted around major cities to enable EV users to charge their cars. The following subsections review the use of EVs around the world with a major focus given on the analysis of EV usage in Australia, Europe, the USA, and Canada. Commuting trends of people in these parts of the world are discussed followed by a discussion on earlier findings from various EV trials conducted in these parts of the world. The share of EVs across the worldwide markets is relatively small but surely on the rise. However, EVs are expected to start having a sizeable share in 15–20 years. Therefore, it is vital to acquire a comprehensive understanding of challenges facing EV users, charging infrastructure operators, and distribution grid operators. The following subsections present a worldwide analysis that will provide fruitful examination of EV usage around the world.

7.1.1   EV Potential and Applications of EVs in Australia

Section 7.1.1 reviews the potential for EVs in Australia. First, the commuting trends of Australians are investigated followed by an analysis of the EV market in Australia. Then, a comprehensive analysis of the EV trials conducted in various Australian states is presented. The findings demonstrate that although EVs do not currently represent a significant portion of the Australian market, they are expected to play a more dominant role in the many years to come.

7.1.1.1   Commuting Trends of Australians

In a recent article [1], Australians' love affair with cars has been investigated, and high car ownership and usage in Australia was elaborated linking the discussion to the very large potential market that exists for electric vehicles (EVs) in Australia. Australia is a very large continent, where widespread communities with insufficient public transport services live resulting in a very large car ownership ratio. The Australian population is growing and new suburbs are continuously being developed at the outer fringes of large cities resulting in large commuting distances to work or study.

Public transport is considered to be poor in Australia due to insufficient reach of public transportation services, high ticket costs, and safety concerns [1]. Therefore, driving is considered a necessity for Australians, and Australia has one of the lowest rates of public transport use when compared to other countries and a very high
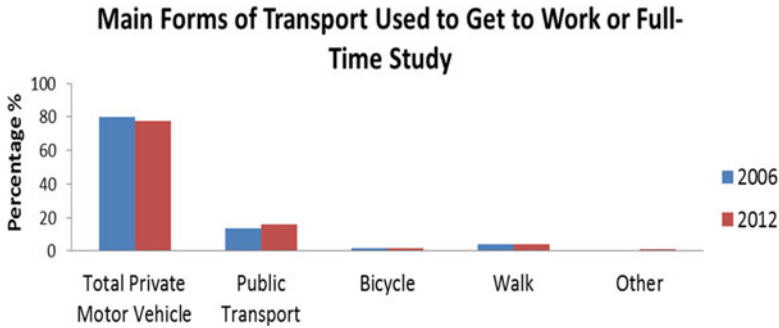
Fig. 7.1 Forms of transport used by Australians [4]

passenger vehicle ownership [1]. The total number of motor vehicles, including motor cycles, registered for the 2013 Motor Vehicle Census (MVC) was 17.2 million, which represents a 2.6 % increase from 2012 and a 12.3 % increase since 2008 [2].

In a recent article [3], the Australian Bureau of Statistics (ABS) has released new statistics to discuss the high vehicle ownership and use in Australia in comparison with the low public transport levels. Figure 7.1 demonstrates the main forms of transport used by Australians to get to work or full-time study. As shown in Fig. 7.1, only 16 % of Australians used public transport in 2012 to travel to work or full-time study [3]. The ABS article reports that the environmental impacts and exhaust emissions from passenger vehicles were amongst the least considered factors by Australians when purchasing a new passenger vehicle with 93 % of users not considering the issue despite the increased awareness on the adverse impacts of greenhouse gas emissions on the natural environment.

By fuel type, petrol (unleaded and leaded)-powered vehicles represent the biggest percentage (79.9 %) of the total vehicle fleet with 13.7 million petrol-powered registered vehicles in 2013. The proportion of hybrid and electric cars is not very well measured and reported since these fuel types are often not separately identified in the individual MVs of state and territories. As shown in Fig. 7.2, there is a clear increase in the number of other fuel vehicles between 2008 and 2013, which represent LPG, dual-fuel, and electric cars. However, the overall proportion of these fuel-powered cars within the market is very low compared to others.

7.1.1.2 Electric Vehicle Market in Australia

As discussed in the previous section, the share of the electric vehicles in the Australian market is almost nonexistent. A report produced by the Energy Supply Association of Australia (ESAA) reports that fewer than 500 EVs have been sold in Australia since 2011 when Mitsubishi i-MiEV was released [5]. Mitsubishi's i-MiEV, Nissan's LEAF, and Holden's Volt are the three leading EVs available in the Australian market, with Toyota's plug-in Prius and BMW's i3 in line for

(a) Relates to the type of fuel recorded by the motor vehicle registry.
(b) Other fuel types include LPG, dual fuel and electric.
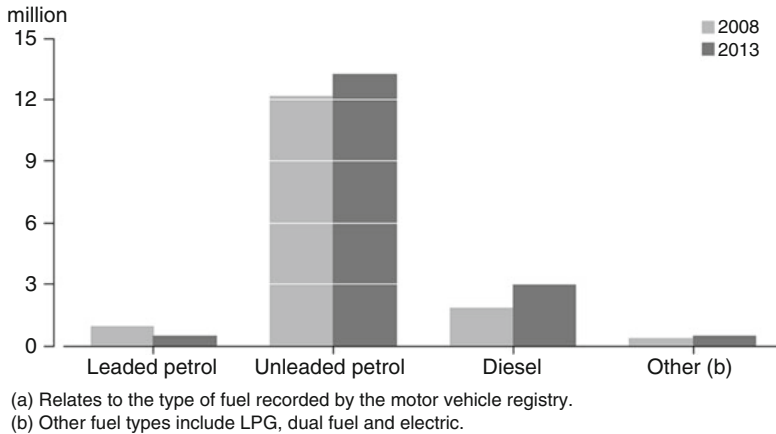
Fig. 7.2 Forms of transport used by Australians [2]

launch in Australia. An interesting statistics shows that the bulk of EV car pur-
chases in Australia were made by corporate companies rather than private motorists
[5]. The potential growth of the EV market in Australia has recently been forecasted
by a number of government and nongovernment agencies.

In 2011 and 2012, the consultancy firm AECOM carried out a range of studies
[6, 7], which predict a long-term transition from internal combustion vehicles (ICV)
to plug-in hybrid electric vehicles (PHEV) and electric vehicles [5–7]. The
AECOM report produced for the Australian Energy Market Commission [6] pro-
jects that around 20 % of the total new car sales will be EVs by 2020 and by 2030
that figure will rise to around 45 %. A Commonwealth Scientific and Industrial
Research Organisation (CSIRO) study [8] carried out in 2012 suggests that, by
2033, the market share of EVs within the total Victorian fleet will account for 12 %
on a base case and 48 % on a maximum uptake case scenarios. PHEVs on the other
hand are expected to comprise 21 % in the base case, and 51 % of the total Victorian
fleet in the maximum uptake case.

7.1.1.3 Trial of Electric and Plug-In Hybrid Vehicles in Australia

There have been many electric vehicle trials conducted throughout the world.
A number of trials have been conducted or are under way in Australia. The
following subsections present a review of the trials carried out in Western
Australia, Victoria, and Queensland. An analysis of the trials is provided from a
number of aspects including trial participants, organizations participating in the
trail, EV cars used during the trials, and finally the charging infrastructure. Some of
the key findings of the trials elaborated further in the following subsections include
the following:

- When EVs are used as part of company fleets, then most charging is likely to occur during early morning hours, which would help to lessen the concerns of electricity distribution utilities in regard to time of charging. This early morning charging could easily be offset by local solar PV generation, which would correlate with this demand in terms of time of the generation capacity.
- The need for providing customers more charging options and the need for managing peak demand during the likelihood of mass uptake and a network upgrade: The travel distance and battery capacity are amongst the most important factors that help to determine the electricity tariff that a customer should be on when it comes to recharging an EV.
- The importance of having a fully interoperable charging infrastructure to support seamless user roaming across the providers similar to banking services and mobile phone use.
- Although the running cost of an EV is low, the initial take-up costs including the cost of charging infrastructure and the car itself are potential holdups.

Western Australian Electric Vehicle Trial

Australia's first EV trial was run in Perth, Western Australia, with 11 locally converted Ford Focus vehicles and 23 fast-AC charging bays (Level 2) and completed at the end of 2012 [9, 10]. Determining the optimal number and locations of EV charging stations in the area was the goal of the trial, which also formed "part of a road mapping exercise for business and government" and assisted in the development of relevant standards and regulations [9].

According to [10] when the trial started in early 2010, there were no EVs available in Australia, and hence locally converted Ford Focus cars were used in the trial. During the conversion, each car was "equipped with a 23 kWh battery pack, a 27 kW DC motor, and a 1000 A motor controller" [10]. During the trial, they were used as fleet vehicles by the project partners with an objective to demonstrate their potential use in everyday driving. A single-charge driving range of 131 km was achieved, which is claimed to exceed 112 km driving range of the Mitsubishi i-MiEV [10].

The charging stations, based on the international charging norm IEC 62196, were installed around the Perth Central Business District (CBD) and they were capable of charging an EV in about 3.5 h from empty to full. Figure 7.3 shows the location of the charging stations installed around Perth CBD. Besides charging stations installed around Perth CBD, trial participants were also able to charge their EVs at their residences and business places using charging infrastructure installed at those locations. Some charging stations had high power outlets (32 A) and others lower power outlets (10 A or 15 A). The average charging time for an electric vehicle over the 6-month period reported in [9] was 2:06 h. On the higher powered sockets, the cars were charged in 1:26 h on average, and 2:32 h on the lower powered sockets.
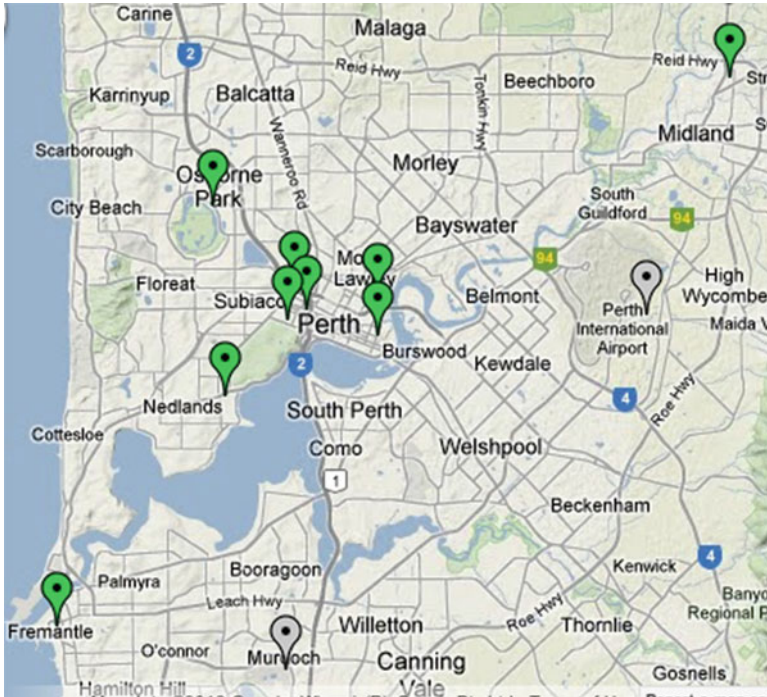
Fig. 7.3 Perth EV charging station network [9]

Another noteworthy statistics observed was the fact that after the vehicles were charged, they remained plugged in an extra 17:06 h, which signifies that only 12.9 % of the total parking time was spent on charging. The Conversation article [10] suggests that this was a direct outcome of charging stations being misused as free parking spots since both energy and parking were free for the duration of the trial. Applying standard fees for parking and power is suggested as a solution to change this behavior, which would otherwise block charging stations for other EV owners, who may have wanted to use them. The report written on the "Analysis of Western Australian Electric Vehicle and Charging Station Trials" also points out that, on average, EVs were not being driven for 97.84 % of the time or 23:29 h per day.

The charging infrastructure was capable of providing three-phase power, which charges three times faster and achieves a better grid balance [10]. The data recorded from the vehicles as well as the charging stations enabled researchers with a multitude of information on vehicle usage and charging patterns. When the EV was being charged at a charging location, then all charging stations would log customer IDs, start time, end time, and exact amount of electricity used for charging. If the EVs were charged at a user's residence or business place, then the system would factor in amount of electricity used during that non-charging

station event in the statistics data. This was done by approximating the amount of electricity used during those non-charging station (non-CBD charging) events from the battery level of the vehicles, distance traveled before charging, and recharging time at the station and the level of supplied power [9]. Hence, the integrity of data was maintained by taking into account the non-charging station events.

The total number of charging events over the 6-month period reported in [9] was 1203 with 186 home charges, 392 station charges, 548 business charges, and 77 in unknown locations. Therefore, only 32.58 % of the chargers were conducted at the CBD charging stations, which further highlight the need for and significance of correcting system data by taking into account non-CBD charging station charging. A very useful smartphone application was also developed that enabled the users with the ability to check the charge status of their EVs during the charging process [10].

Over a 6-month period, the cars were driven 17.56 km per day per car on average, less than the daily distance average (32 km) of a passenger vehicle in Western Australia. The usage corresponds to an estimated annual energy usage of 1.13 MWh. The maximum average daily kilometer was 48.53 km and the maximum EV distance in a single journey was 71 km, both of which are less than the maximum driving range of 131 km [9]. A concern with EVs is the short range they can travel without recharging. Yet, usage patterns in this trial show that cars were indeed underutilized and not used to their maximum range. This is indeed an important piece of knowledge demonstrating that, at least for city drivers, such a long full-charge driving range is not necessary. This is of course not taking into account the continuous recharging process that the user needs to go through similar to nuisance that would have been experienced if one had to fill up the petrol tank of his/her car every day or so.

Figure 7.4 shows the power drawn from the grid for car charging at various charging stations including home, business, and CBD station charging. As demonstrated, the business and CBD station charging peaks around 8 am until 10 am when EVs are driven from homes and parked to charge before being further driven.
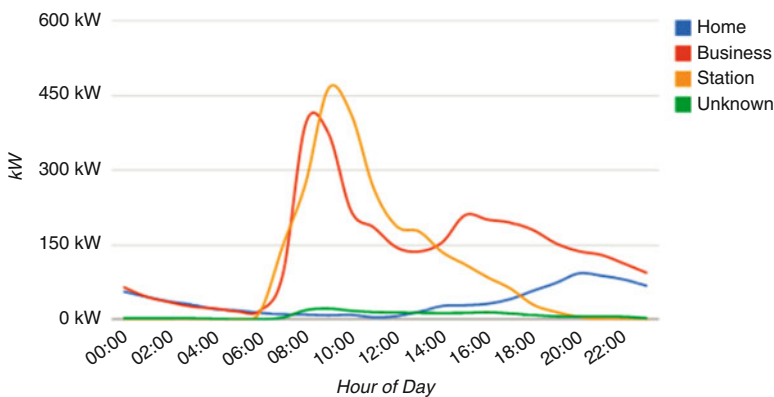
Fig. 7.4 Energy usage for charging over daytime [9]

Home charging peaks around 8 pm when cars are driven home and parked for slow charge. Home charging is a small component of the overall charging influenced by the restrictions of some participating organizations on their fleet vehicles such as not taking the vehicle home, and most EV drivers not being reimbursed for electricity usage in their homes.

The demand profile shown in Fig. 7.4 and the fact that most of the fleet charging was during the early morning hours would help to lessen the concerns of electricity distribution utilities in regard to EV charging magnifying the peak demand in the early evening hours. The research carried out suggests that this early morning charging could easily be offset by local solar PV generation, which would correlate with this demand in terms of time of the generation capacity. The results of this study are important, as according to [9], the initial EV market will be heavily biased towards the business fleet over the next half decade. The trial report does not report on any social investigations and the trial had purely focused on technical matters.

Ergon Energy's Queensland EV Trial

Ergon Energy's 18-month EV trial, which involved a fleet of five Mitsubishi i-MiEVs being driven by Townsville customers at Mt Low and Mysterton during separate 8-month periods, was completed in mid-2013. The objective of the trial was to determine the differences in location upon customer driving, charging behavior, and tariff preferences. The results of the trial will be used to shape Ergon Energy's strategy for managing the impact of large-scale uptake of EVs, which according to [11] "are expected to become cheaper in the next few years and reach a price point where sales will increase considerably" [11].

Figure 7.5 shows the locations where the trial was carried out. As expected, the EVs were driven a lot less by 138 km on average per week by the residents, who live in Mysterton, a predominantly residential suburb of Townsville. On the contrary, EVs were highly utilized by the Mt Low customers, who drove the cars 330 km on average per week [11]. As reported in [12], the driving range of the EV cars was about 90 km and it took about 7 h to fully charge the car [12]. The trial outcomes signify the need for providing customers more charging options and the need for managing peak demand during the likelihood of mass uptake and a network upgrade.

The trial has discovered that the travel distance and battery capacity are amongst the most important factors that help to determine the electricity tariff that a customer should be on when it comes to recharging an EV [11]. Metering.com [11] reports that "because of their location involving less driving, the Mysterton drivers were more likely to charge their EVs with the cheaper tariff, while the Mt Low drivers appeared less likely to because of its availability times and the distances to be driven." The trial has also shown that the further from the CBD, the greater will be the impact on the network due to the presence of customers, who will need to drive a lot further to access work, study, shops, and schools. The average cost of driving an EV per 100 km was determined to be AU $4.81, which is

Fig. 7.5 Ergon energy trial location in Queensland

quite economical when compared to the cost (AU$5.77) of driving a hybrid vehicle, and the cost (AU$7.69) of a small diesel car, and that (AU$11.54) of a small petrol car for an equivalent distance [11].

According to ABC [13], the observed peak charge time during the trial was around 10 pm, but recharging was observed to impact the Ergon network between 6 and 8 pm. An interesting assignment during the study simulated the recharging demand of 30 EVs using a battery system, which was connected to the Mt Low transformer. Another first was also achieved with the installation of a solar-powered EV charge station at Townsville Airport [12]. The cutting-edge technology, which used renewable energy generated from a 4 kW PV shade-membrane shelter covering six car parks, was an exciting new addition to Townsville's residential EV trial [12].

Victorian Department of Transport (DoT) Trial

The Victorian Government's Electric Vehicle Trial [14] is a $5 million project, which was first launched in October 2012 and will run until mid-2014, investigating the process, timelines, and barriers for transitioning to electric vehicle technologies. The Department of Transport, Planning and Local Infrastructure [14] is reporting EVs as a natural fit for Victorians, who mostly do short trips and drive on average 40 km per day. Low running costs of EVs and their innovative, less polluting nature are highlighted and the state of Victoria's strong presence in the EV sector, with businesses manufacturing hybrid and fully electric vehicles, is emphasized.

The "Victorian Electric Vehicle Trial Mid-Term" report reviews progress up to the halfway point in the trial with a discussion on experiences, results, and interpretations from the early stages of the EV market development in Australia. According to [15], the Victorian Electric Vehicle Trial has seen the collaboration of over 80 organizations including government bodies, electricity firms, charging infrastructure providers, vehicle manufacturers, and environmental groups, all wishing to contribute and have inputs in providing the foundations of an EV market "worth having." The objectives of the trial cover investigating technology as well as the social and environmental aspects, and the key goal is to ensure the safe and efficient rollout of EVs in Victoria considering the needs of Victorians and the impacts of EVs on the Victorian society and resources. The activities that have constituted the trail are [15]:

• *Household Vehicle and Fleet Vehicle Rollouts*

The interest in the trial was great. According to a Victorian state government report [16], total number of 2200 applicants completed the expression of interest to participate in the Victorian Electric Vehicle Trial. Figure 7.6 shows the distribution of applications in the Greater Melbourne area. Around 120 households were eventually given the opportunity to trial an EV for 3 months each. On the other
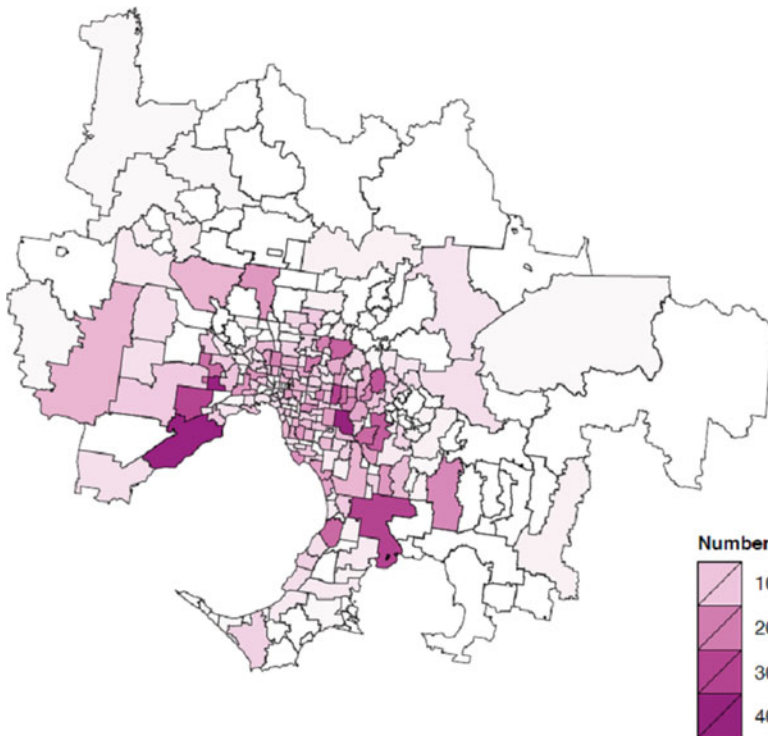
Fig. 7.6 Distribution of trial applicants in the greater Melbourne area

hand, around 40 fleet have been provided the opportunity to trial a range of EVs for up to 6 months at a time. A range of vehicles with diverse manufacturers and makes have taken part in the trial and significant differences were observed in the utilization rates of various vehicle makes. There were also EV make-based behavioral and attitudinal differences amongst the participants. Melbournians displayed liking towards the technology especially in terms of quiet, environmentally friendly, and low-cost operation with purchase price, size, and limited operating range being the criticized aspects.

The results of study indicate that the average running cost on renewable energy was $7–10 a week, far less than the cost of running an equivalent petrol vehicle. Results show that EVs are a viable transport option albeit the high purchase price, which stands as a major obstacle to take up the technology [15].

- *Charging Infrastructure Rollout*

This has so far included the installation of around 140 [15] charging outlets for household, fleet, and public use to establish the foundations of Victoria's EV charging network. A range of EV charging and infrastructure providers participated in the trial where "Level 2"-compliant charging outlets were primarily used. "Level 2" standard-compliant charging infrastructure is suitable for home/public use [1] and involves 240-V, 15 A charging, and charging system-EV interaction in accordance with the SAE J1772 technical specification. The charging infrastructure was specified and designed capable of providing up to 32 A in locations with sufficient electrical supply taking into account the fact that next-generation EVs are expected to draw up to 32 A.

The user feedback and network support provided by the trial charging infrastructure providers were quite diverse. For example, one network provider supplied users with the capability of remotely accessing the real-time information on charging status and charge management capability while others provided much reduced levels of support. Information on the location of charging stations was provided to users primarily through the trail website [14] that provided a Google Maps-based geographical information system.

There was full agreement amongst the charging infrastructure providers on the importance of achieving interoperability across different EV charging networks; however, this was not included as an objective in the trial time frame due to a large number of higher priority issues that had to be dealt with during that period. The importance of having a fully interoperable network is stressed throughout the report [15] to support seamless user roaming across the providers similar to banking services and mobile phone use. Collaboration between the charging service providers is recommended in [15] to progress towards a fully interoperable network that will provide a better customer experience. The need for a unique data key for individual users was identified by all parties as a low-cost option with potential future benefits. The department's "lookup" table and user identification codes, where charging infrastructure provider's own user identification details have been mapped to, are proposed as a suitable future framework for business-to-business or industry-wide interoperability.
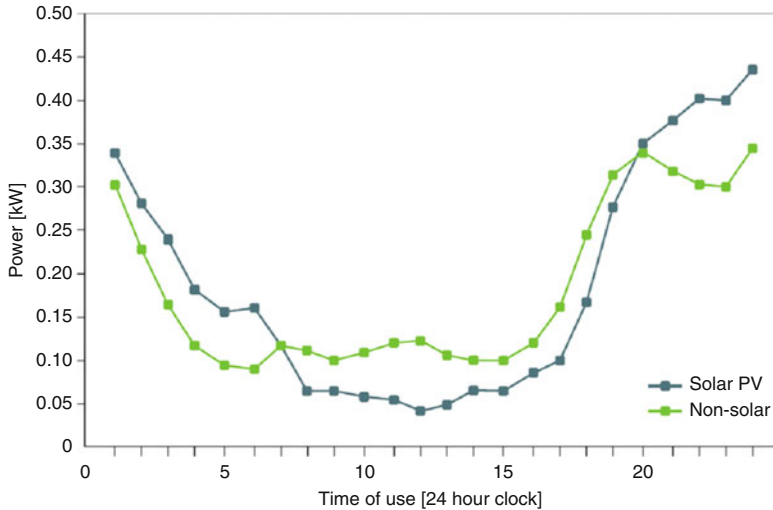
Fig. 7.7 EV charging demand profiles for solar and nonsolar trial participants [15]

The challenge of standardizing the charging requirements and specifications for different vehicle types including electric bikes, motorcycles, and passenger vehicles is identified as another obstacle in achieving a fully harmonized electric vehicle space. A standards development process for electric vehicles through Standards Australia is proposed as a means of addressing many of the standardization issues. The potential revenue impact of EV charging is also outlined as another concern in the EV space due to electricity not being subject to fuel excise. Increased use of EVs is expected to impact government revenues by contributing to a reduction in the fuel excise, which is the largest contributor to revenue raising in Australia [15].

The EV charging demand is reported to align with the general electricity household demand as shown in Fig. 7.7 [15]. As shown in Fig. 7.7, the charging demand starts to increase after 3 pm for both solar and nonsolar households implying that most trial participants started to charge their cars immediately after arriving at home.

An important observation made was in relation to the variation in the charging habits of trial participants with solar PV installations. This is clearly demonstrated in Fig. 7.7, which shows a continued rise beyond 8 pm in the power demand at houses where PV systems were installed. The likely cause of this is reported to be the time-of-use electricity tariff of PV households, which encourages PV household trial participants to defer their charging to off-peak periods in response to the financial incentives of doing so.

An electricity demand response and load control demonstration project was also undertaken as part of the overall trial by the participation of a small group of participants. These participants had their charging outlets bound to their residential smart meters upon installation and the project aimed to demonstrate the role Victoria's Advanced Metering Infrastructure could play in managing the EV

charging demand. A total number of 64 charge management events were issued to the charging outlets through the distribution network provider's infrastructure (Zigbee) as part of the project known as "grid-friendly" charging. These charge management events basically helped the electricity distributor to control the EV charging loads and were termed "peak charging" and "emergency charge management" events [15]. Such electricity distributor charging is considered as a tool that would assist the electricity distributor to preserve the reliability of the network and avoid network infrastructure investments that would lead to increases in electricity costs. A widespread acceptance of this charge management method was observed and participants overwhelmingly agreed to have their car charging managed in this way even in the absence of any financial benefits.

Majority of households who participated in the Victorian trial were satisfied that home charging alone was easy to use and understand, and met their needs, but more information about costs and energy use would have been desirable [15]. Participants also suggested that further information relating to the charge management of EVs such as time until complete charging would have been ideal. Victorian trial identified a number of issues and potential opportunities for home charging such as the expensive cost of the home-charging infrastructure, which is considered as a potential obstacle second to the start-up cost of purchasing an EV. Some of the other challenges are [15]:

- The likely increase in the cost of charging infrastructure with electricity supply upgrades, and shared parking arrangements
- The likely loss of the capital after house moves
- The wide varying specifications of charging outlets in response to specific needs of the user and his/her vehicle
- The potential voltage drop beyond the regulated voltage levels on distribution feeders with clustered EV take-up

Some of the potential suggested opportunities include [15]:

- Charging circuits to be designed and constructed as part of new construction and refurbishments
- Benefits of informing the public about the property value benefits of including charging circuits during the design and construction of new buildings
- The importance of proving guidance on the allocation, placement, and design of EV charging infrastructure
- Communicating the benefits of off-peak charging practices during the time-of-use electricity tariff periods
- The opportunity to use EVs as energy storage devices

7.1.2 EV Potential and Applications of EVs in Europe

The electric vehicles (EV) on the road have increased significantly in most European countries in the last 5 years [17]. Despite the good and reliable public transport in most West European countries, the move towards EV is mostly justified by economic, political, and environmental reasons. In Europe, the major incentive for the increase of EVs and the strong support and investment by the government are based on the following reasons:

- Reduce dependency on oil with cheaper fuel
- More silent operation through smart grid
- Reduce direct carbon emission CO2 (global warming)

The global warming is a major issue that has been widely discussed for many years. Faced with serious consequences, governments worldwide are enforcing plans for reducing carbon emission [17]. For example, by 2020 some network operators in the UK are planning to reduce carbon emissions by 45 % [18], while European Union (EU) countries are obliged to cut their emissions by 20 % [19]. The European Commission has put electric vehicles at the heart of its commitment to the long-term goal of reducing carbon emissions by 60 % within the transport sector by 2050.

Electric and alternative fuel vehicles have emerged as one of the key players in the quest to diversify road transport energy sources and thus potentially help the European Union achieve its CO_2 emission reduction targets. Accounting for more than 12 m jobs in the EU, the automotive industry is vital to the economy and, as such, developing innovative and alternative fuels will not only maintain competitiveness and create high-skilled employment opportunities, but also make the European economy more resource efficient [20].

7.1.2.1 Electric Vehicle Market in Europe

European EV market has increased due to government's strong support to resolve the upmentioned reasons. Figure 7.8 shows the sales of electrified vehicles in most of the European countries in 2013. Several governments have subsidized the high cost of EV compared to ICV. For example, France, responding to public concern about rising fuel prices and climate change, already backs the segment, offering drivers a rebate of 7000 Euros on the purchase of a battery-powered vehicle and 4000 Euros for a hybrid electric-gasoline model. The global market for electric cars in France is dominated by Renault SA, based in the Paris suburb of Boulogne-Billancourt, and Japanese partner Nissan Motor Co.

Germany is investing heavily to establish itself as the world leader in EV technology and steal a march on the likes of Japan, the USA, Korea, and China. The German Government announced that it would double its existing investment in the rollout of electric cars to two billion euros ($2.7 billion). Chancellor Angela
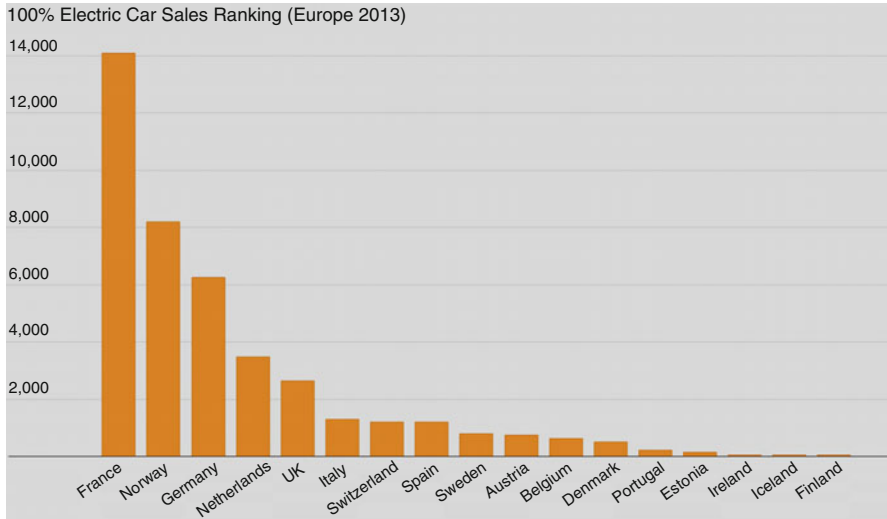
Fig. 7.8 Sale of EVs in Europe [21]

Merkel wants to have one million electric cars on German roads by 2020, and six million by 2030, with the likes of Mercedes-Benz, BMW, Audi, Porsche, and Volkswagen at the vanguard. A commission established by the German Government to spearhead the push to electric cars, the National Electric Mobility Platform, warns that the government instead needs to quadruple its investment if it wants to achieve its ambitious targets.

In Europe, specifically the impact of EV market is not limited to the transport sector, but more on the electricity sector. That has large effect on the electricity generation and on the grid load and stability. Also, it requires charging infrastructure and smart charging. Electricity grid, both transmission and distribution grids, varies considerably in terms of resilience to external pressure. Therefore the expected future electricity market of the EU has to consider the effect of the high increase in the EV on the road [21].

Across Europe, a greater variety of hybrid (HEV), plug-in hybrid (PHEV), and battery electric vehicle (BEV) models are being offered by manufacturers each month. Although government support is waning, the increasing availability of vehicle charging infrastructure that enables vehicles to charge at home, at the workplace, and in public places is facilitating market growth.

The top six European countries for BEVs on the road in 2020 will be Germany, France, Norway, the UK, the Netherlands, and Sweden, with this group representing more than 67 % of the total market, and each having a volume in excess of six figures. The situation is different for PHEVs, where only four countries are expected to exceed a volume of greater than 100,000 vehicles—Germany, France, Italy, and the UK—and these four represent 52 % of the total. By 2020, Pike Research forecasts that more than 1.8 million BEVs will be on Europe's roadways, along with 1.2 million PHEVs and 1.7 million HEVs [21].

GDP Per Capita Analysis,
CEE and Western Europe, 2007,2011,2017

Fig. 7.9 GDP per capita analysis in Europe [22]

A special study done by FROST & SULLIVAN on the forecast of EVs and charging infrastructure industries in Central and Eastern European countries [22] shows very interesting scenario as depicted in Fig. 7.9. The study shows that Central and Eastern Europe (CEE) as a region is expected to generate roughly 23 % of GDP of top four countries investing in the EV industry (the UK, Germany, France, Spain) by 2016. The development of the EV industry in CEE region is expected to grow by approximately 5.2 % annually in terms of GDP per capita during 2011–2017. EVs are not a priority at this time for CEE Government due to economic situation and the low purchasing power for the EV market.

7.1.3 EV Potential Applications of EVs in the USA and Canada

Similar to Australia, cities in the USA and Canada are widespread where people like having large houses with their own gardens. In addition to that, due to lack or inefficiency of public transport, people opt to use their own vehicles. In fact, results

Fig. 7.10 Comparison for
levels of public
transport [23]
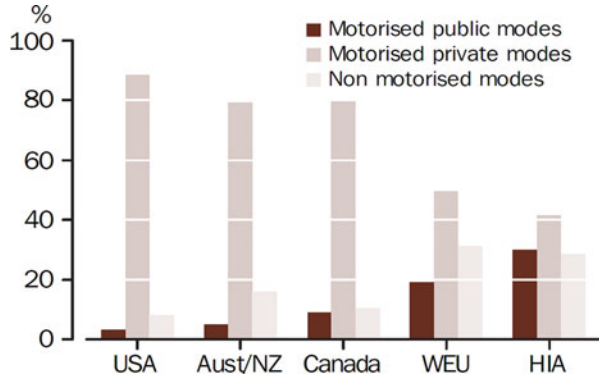
of a recent study demonstrate, as shown in Fig. 7.10, that the vehicle ownership/
usage behavior can be summed up in three categories:

1. Vast countries such as the USA, Australia, and Canada where private mode of
   motorized transport is very common
2. Western European Union (WEU) where a more decent share of public and
   non-motorized transportation can be seen
3. High-income Asian (HIA) cities, where private motorized transport is actually a
   less preferred mode of transportation

Daily work commute is significant in the US daily population change where
some counties experience 94.7 % and 111.4 % change increase (such as New York
County) while some lose 41.4 % of its population [24]. Although commuting
happens all around the country at significant levels, the share of public transporta-
tion is very small. The statistics in the USA indicate that Americans prefer private
vehicles for their daily commutes [25]. For instance, daily work commute means
distribution given in Fig. 7.11 which shows that 86.2 % of the US population uses
private automobile for this purpose [26].

It is notable to mention that share of public transportation and other means does
not show real change. It is observed that the mobility of the population is met by
private automobiles. The survey also documented the share of public transport in
50 largest metropolitan statistical areas. New York, New Jersey, and Long Island
regions lead the pack with a little more than 30 % public transportation use.
However, the figures drop dramatically after this. The next two regions only have
around 15 % while eight regions have 6 % public transport usage [27]. This low use
of public transport affects the quality and frequency of public transport vehicles
such as buses or trains. With less frequency, people tend to use their own vehicle
more and this loop results in poor service and low preference of public transporta-
tion. US-wide figures indicate that 79.9 % of the workers commuting drove alone
while only 10.1 % chose to car-pool [28]. This results in the highest motor vehicle
ownership per capita in the world: 828 motor vehicles per 1000 people [29].
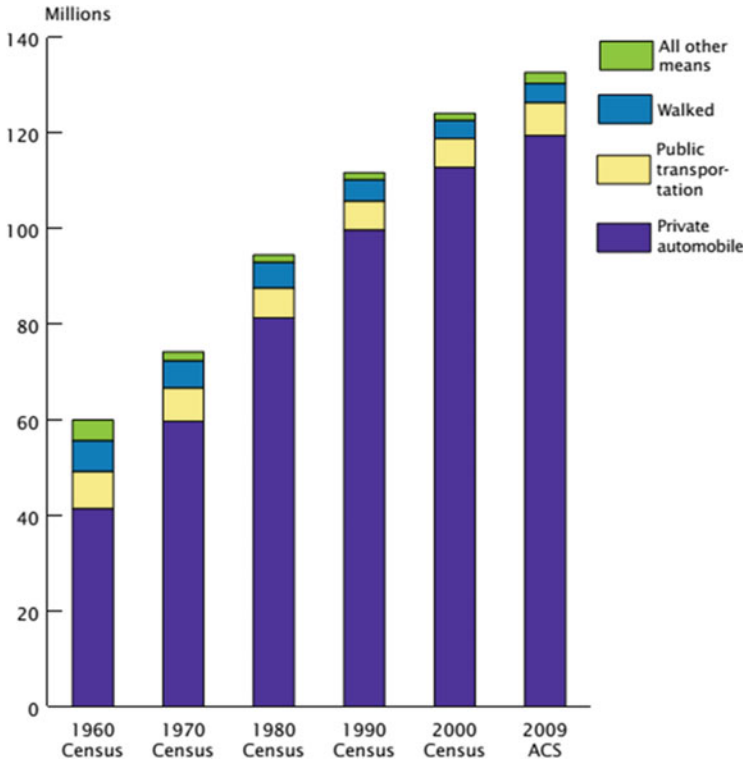
Fig. 7.11 Means of daily work commute in the USA [26]

As shown in Fig. 7.12, in 2011, only 9 % of American households did not have access to a vehicle while 34 % had one vehicle, 37 % had two, and 20 % had three or more vehicles. It is not a surprise that 70.2 % of total petroleum consumption in the USA is due to transportation and this corresponds to more than 1.7 billion annual metric tons of CO_2 [29].

Motor vehicle registrations from 1990 to 2009 show that the number of motor vehicles in the USA is increasing. Table 7.1 shows that overwhelming majority of them are privately owned and almost half of them are comprised of privately owned vehicles [30]. These figures do not include 7,883,000 motorcycle registrations in 2009.

Relevant to the discussion of electric vehicles and their adoption is the part of daily commute in the above given facts. On average, daily commutes account for approximately a quarter of the total daily travel in miles. Federal Highway Administration's (FHWA) National Household Travel Survey in 2009 shows that daily travel per person is 3.8 trips and 36.12 miles [31]. Figure 7.13 shows average annual trips and miles per household based on their purposes.

It is important to note that when miles and trips for a vehicle are investigated (red line with squares) it is observed that on average a trip for a car is slightly more than

Fig. 7.12 Motor vehicle ownership per household in the USA [29]
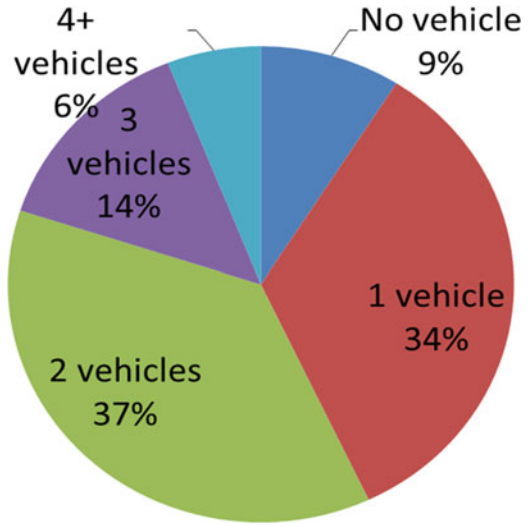
Table 7.1 State motor vehicle registration: 1990–2009

Type	1990	2009
All motor vehicles	**188,798,000**	**246,283,000**
Private and commercial	**185,541,000**	**242,058,000**
Public	**3,257,000**	**4,225,000**
Automobiles	133,700,000	134,880,000
Private and commercial	132,164,000	133,438,000
Public	1,536,000	1,442,000
Trucks	54,470,000	110,561,000
Private and commercial	53,101,000	108,269,000
Public	1,369,000	2,292,000
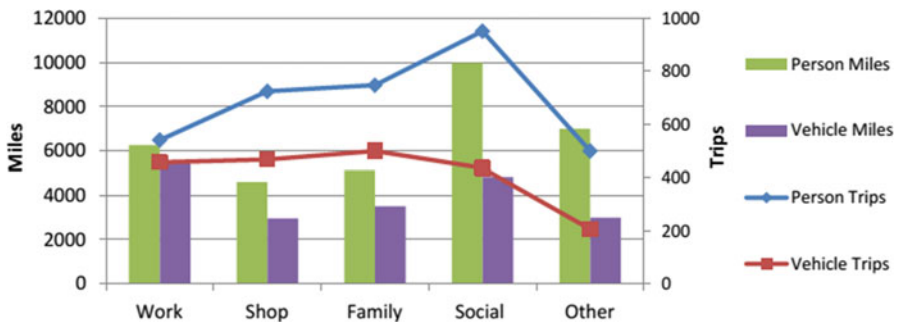
Fig. 7.13 Annual average trips and miles for a household [31]

Table 7.2 Urban/rural
vehicle travel [31]

	Trip length (miles)		Trip time (mins)	
Type	Urban	Rural	Urban	Rural
Work	11.11	15.36	22.36	24.34
Work related	15.53	20.99	26.66	29.41
Shopping	5.49	9.50	13.47	17.14
Family/personal	6.07	9.17	14.27	16.33
Other	10.98	16.06	20.16	25.13
Social	10.72	12.85	19.69	20.90
All	8.79	12.59	17.96	20.67

10 miles. Given the battery capacity and performance of current electric vehicles, it is safe to say that electric vehicles can meet the daily commute requirements in the USA. Table 7.2 shows the length of the trips with different purposes in urban and rural areas. Although rural areas have longer trips, especially for work-related trips, ranges of current electric vehicle are sufficiently long. This is crucial in capitalizing on vehicle usage and using it for electric vehicle migration.

In summary, motor vehicle ownership in the USA and the length of the trips show that there are a large number of vehicles in the USA. This high value of vehicle ownership can be utilized for electric vehicle migration, especially, due to the short range of trips in daily commutes. The car owners can cover the same distance with an electric car and help cut down on carbon emissions.

7.2 Impact Analysis of Electric Vehicles

This section presents the impacts of EVs on car users, grids and power quality, and finally carbon emissions. Considering the potential of EVs and increasing rate of migration to electrical networks, EVs are bound to make a strong impact at different levels. The relatively small driving range of EVs, small number of charging stations, and long charging times are some of the bottlenecks for users. As more and better charging stations are developed and put into operation, this is expected to become less worrying. Section 7.2.2 discusses the impacts of EVs on grids and power quality in electrical grids. A large uptake of EVs is expected to impact electrical networks at the distribution level. The increasing use of EVs is expected to make a positive impact on the environment when the charging power comes from renewables. Section 7.2.3 discusses the impacts of EVs on carbon emissions throughout the world.

7.2.1 Impacts on Car Users

It is true that EV uptake is estimated to be slow. Therefore, the impact would not be experienced abruptly. However, given the current trend towards EVs and the willingness to cut down dependence on petrol cars, it is safe to say that numbers

Table 7.3 Ranges of various electric vehicles

Manufacturer	Model	EV type	Electric range (km)	Battery size (kWh)
Toyota	Prius	PHEV	8	4
Buick		PHEV	16	8
Chevrolet	Volt	PHEV	64	16
Fisker	Karma	PHEV	80	22
Nissan	LEAF	EV	160	24
Toyota	RAV4 EV	EV	190	27
Cooper (BMW)	Mini E	EV	251	28
Tesla	Roadster	EV	354	53

and impacts of EVs will surge in the future. Today, the major difference between EVs and cars, which run on internal combustion engine, is the driving range. Due to constraints in battery technology, despite being more efficient, EVs have less range than regular cars. Table 7.3 shows ranges of different electric vehicles that are available in the market today.

PHEVs have ranges that are significantly small while pure EVs have ranges that are comparable or equivalent to ranges of conventional cars that run on petrol. Depending on the electric vehicle that is used, the car users might need to plan their routes and car usage more wisely. Especially, during the first years of migration to EVs, PHEVs would be more prevalent. They can run on both petrol and electricity and can go for long ranges. However, pure EVs with low ranges are likely to force users to be more aware of their usage. Statistics show that majority of daily car use is less than the range of electric vehicles. Therefore, this only becomes an issue when the owner decides to go for a long drive.

Another reason for this is the small number of charging stations during the first years of migration. Car owners have to make sure that they reach a charging station before their limited range expires. As the EV market grows and more charging stations appear, this challenge is expected to vanish on its own. Another aspect is the long charging hours and demand-side management applied by the grid operator. Car owners would be encouraged to, or at times obliged by the network operator, accept charging that is regulated by the grid. This may result in EV charging taking long periods. For a regular user this would have infinitesimal impact as the charging takes place at night and the owner would be fast asleep during that time. However, should there be an unexpected need for travel (an emergency case requiring long-range drive at night) the EV may not have sufficient charge. Again, this is a challenge that relates to the first years of migration as more and more EVs are deployed, better charging facilities and options will emerge, such as super-fast charging. Eventually, it is expected that even with a demand-side management program, EVs will have sufficient charge or can be super-charged in short periods. This would minimize the impact on the car users.

7.2.2 Impacts on Grids and Power Quality

The most trivial impact of EVs on grids is the increase in load. This is not as much as feared, though. Due to small number of EVs and the expected low pickup rate, impacts on grids are manageable and sometimes solved with regular upgrade and maintenance works. The power company "Southern California Edison" stated in its recent report that of almost 400 upgrades only 1 % was specifically required for EV power demand [32]. These upgrades are only required at distribution level, since the impact of EVs does not reach transmission and generation level yet [33]. Although grid operators are looking into ways of using batteries of EVs, V2G technology is not implemented commercially yet. There have been some pilot projects in by PG&E and Xcel Energy, both in the USA. These are projects of very small scales and their impact on the larger grid has not been investigated. The main idea was to verify the applicability of V2G technology. These pilot systems were successfully implemented and the applicability of the technology has been verified.

The impact on power quality is not a concern of EV charging since chargers have power electronics interfaces and the power quality is tightly controlled. In addition to regular battery charging, which has very high power factor, EVs may contribute to increasing power quality at the point of common coupling, if power electronics interface is utilized accordingly [34]. Figure 7.14 shows a sample neighborhood developed to investigate the impact of the electric vehicle charging and power injection to the grid. The results listed in [1] show that the impact of electric vehicles in the grid is only at the distribution level and no change is required at transmission and generation level. In addition, the upgrades that are required at distribution level can be made gradually as the electric vehicle migration progresses.
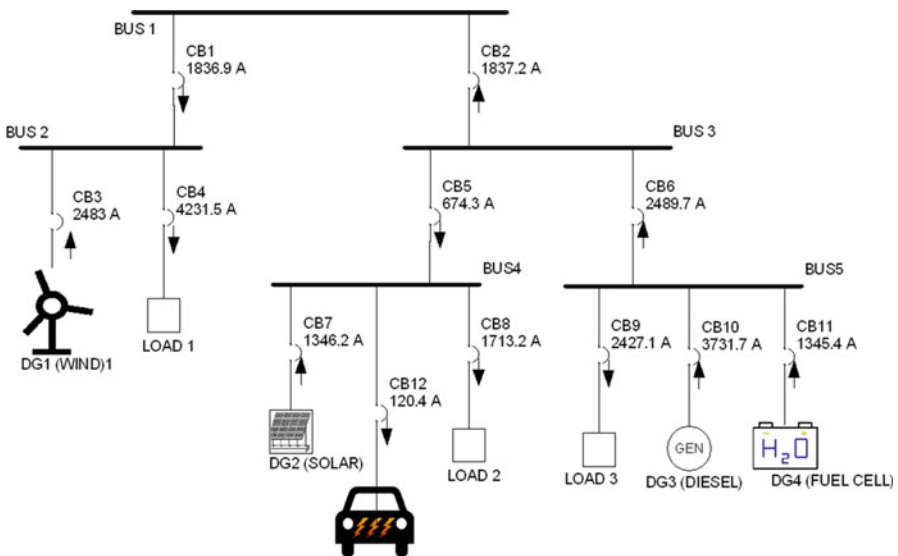
Fig. 7.14 Simulation model for EV impact studies

7.2.3 Impacts on Carbon Emissions

One of the most significant benefits of EVs to the broader community is certainly their positive impact on the environment and their potential to reduce the greenhouse gas emissions in the transport sector as well as the amount of imported fuels. Australia, for example, imports petroleum products from abroad and the transportation of these products is costing Australians and weakening the continent's economic performance and energy security. An increase in the share of EVs in the Australian transport market will not only lead to reduced fuel imports but also decrease the contribution of the emissions from the transport sector to the national emissions.

It is well known that when compared to petrol- or diesel-powered vehicles, the emissions from EVs are much lower and can further be offset if charging power is sourced from renewable energy sources such as solar, wind, tidal, or geothermal. Hence, the type of electricity (fossil, renewable, nuclear) used in the charging process dictates the overall environmental benefits of EVs [35].

Figure 7.15 presents a comparison of EV-related emissions in 20 of the world's leading countries after considering emissions associated with those related to electricity generation and vehicle manufacturing [36]. As demonstrated in Fig. 7.15, the carbon emissions associated with EVs in countries (such as India, South Africa, and even Australia) with coal-based generation are no different to

Fig. 7.15 Comparison of worldwide emission factors [36]

Electric Cars' Carbon Emissions: g CO$_2$e/km

Country	g CO$_2$e/km
India	370
South Africa	318
Australia	292
Indonesia	270
China	258
Turkey	204
Mexico	203
United States	202
United Kingdom	189
Germany	179
Japan	175
Italy	170
Russia	155
Spain	146
Canada	115
France	93
Brazil	89
Sweden	81
Iceland	70
Paraguay	70

Power Source
- Coal Based
- Fossil Heavy
- Broad Mix
- Fossil Light
- Low Carbon

Note: Results include emissions for vehicle manufacturing, direct grid emissions, indirect grid emissions and losses. Based on national averages for 2009.

Sources: DEFRA, GHG protocol, IEA, EPA, GREET, LCA literature

average petrol vehicles [36]. The rate of exhaust emissions from pure EVs propelled by electric motors is considered to be 0 g CO_2/km even though there are indirect emissions associated with EVs when they are plugged into the electricity grid [37]. The exhaust emission rate of plug-in hybrid vehicles is below 50 g CO_2/km [37]. According to a European Parliament study [35], the vehicle-to-grid and load management solutions could further make EVs part of an overall energy strategy allowing for the more efficient use of the fluctuating energy. In the European Union (EU), the number of new registrations of pure EVs has increased mostly driven by Germany and France.

In 2012, 700 new pure EVs were registered in EU whereas that number rose to 14,000 in 2012 [37]. In EU, GHG emissions in the road transportation sector are growing despite steady or even decreasing emissions in the other sectors [38]. Clearly, the focus of the EU should be on reducing the CO_2 emissions in the road transportation sector. A number of initiatives, such as the Green eMotion project [39], have already been initiated to achieve abatement in the road transport-related emissions. The "Green eMotion" project was launched as part of the European Green Cars Initiative (EGCI), and supports the target of reducing emissions by 60 % by 2050. One of the project initiatives focuses on the research and development of road transport solutions towards a more sustainable future.

In Australia, a significant portion of the overall emissions is because of GHG emissions from the transport sector. According to a recent report by CSIRO [40], the transport sector contributes to 16 % of the national GHG emissions and emissions from the road transport sector accounts for 87 % of these emissions. In Tasmania, the transport sector contributes to 24 % of the state's total emissions [41]. The same CSIRO [40] study identified EVs as one of the top three options in the abatement of GHG emissions. During the Western Australian EV trail [42], a survey conducted had shown that "zero tail-pipe emissions was considered the most desirable feature of EVs" by the trial participants [42]. Over the 20-year average Victorian lifetime, a renewable-energy-operated EV is expected to provide a reduction of over 50 % in terms of lifecycle carbon emissions [15].

Figure 7.16 shows the comparison of lifetime emissions from an EV when operated on renewable energy and on Victorian grid energy, which has a minor renewables component. Despite all these, the Victorian trial midterm report [15] argues that the projections indicate the break-even point in terms of zero net carbon emissions from EV operation to be some years away due to the small share of renewables in the overall generation mix. GHG emissions associated with the Victorian trial were equivalent to 79 tCO_{2e} at the midpoint mark but was accounted for and reconciled with renewable energy purchases. Few interesting arguments put forward in [15] include the following:

- In Victoria, the smart charging during off-peak periods is likely to be of higher intensity than demand charging during peak periods due to the characteristics of the Victorian electricity mix.
- Publicly accessible EV charging facilities are associated with electricity metering and billing complications demonstrating the need for renewable energy charging strategies.
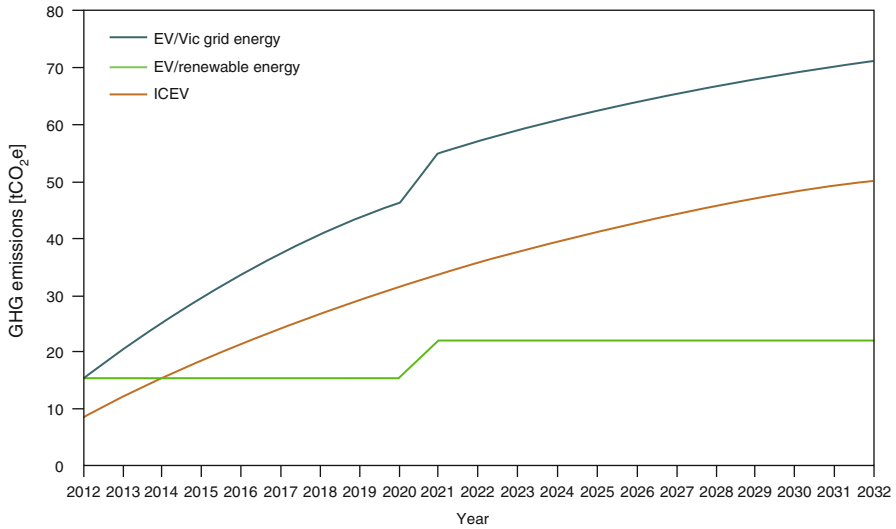
Fig. 7.16 Comparison of GHG emissions for EVs operated on renewable and nonrenewable energy types [15]

The USA is also taking ambitious targets for reducing its dependence on oil and GHG emissions by putting more EVs on the road [43]. This has been well supported by a number of federal and state policy initiatives to encourage the introduction and sales of EVs [43]. Throughout 45 % of America, electricity is generated with a larger share of cleaner energy sources implying that the global warming emissions of EVs in these regions are less than emissions from even the most efficient hybrids. In the remaining 55 %, where coal is still the main source of electricity, hybrids are considered less GHG emitters than EVs [44].

An important notion outlined in [44] suggests that an EV is likely to become less emission intensive over its lifetime as the share of renewables in the overall mix of electricity increases as older power plants are retired and cleaner electricity is generated. According to [44], "By 2020, global warming emissions intensity of electricity generation is expected to have improved in some regions of America by as much as 30 % over 2010."

7.3   Applications of Electric Vehicle Recharging/ Discharging

Widespread use of EVs requires expertise in different fields such as mechanics, power electronics, control, and battery technology and power systems. The latter two constitute the direct link between EVs and the electrical network that is present. The link under discussion is mainly one-way power flow from the network towards

the vehicle, i.e., recharge. Therefore, most of the charging apparatus/station applications focus on grid-to-vehicle power flow and try to enhance its performance.

Vehicle-to-grid (V2G) concept is the opposite of this idea where the charge present in batteries of electric vehicles is used to supply power to the electric grid, preferably for power support at peak times. This feature is still in development phase since it requires extensive data collection, e.g., state of charge (SOC) in batteries, pattern recognition, e.g., driving patterns of drivers, communication, coordination, and management, e.g., billing and payment. Accordingly, V2G technology is implemented in either pilot projects for further development or special applications (e.g., military).

In addition to vehicle-grid coordination, there are microscale applications such as electric vehicle discharge control, which focuses on the discharge amount of electric vehicle's battery. These applications aspire to enhance the discharge performance of the batteries and increase their time of use. These objectives hold key importance for electric vehicles as when they are achieved; longer battery life and longer travel ranges will facilitate mass migration to electric vehicles. In this section, several examples are given for electric vehicle chargers, vehicle-to-grid applications, as well as vehicle-battery implementations for enhanced performance. Furthermore, standard communication and interoperability aspects are discussed for coordination and management of infrastructure.

7.3.1 Electric Vehicle Chargers and Vehicle-to-Grid Technology

There are different EV charger applications in the market. Although these chargers have different topologies and vendors, the main classification used for them is the charging level used. As shown in Table 7.4, there are roughly three different charging levels.

Level 1 and Level 2a are directed towards residential use. The charge powers corresponding to these levels are not very high and can be provided with existing electrical infrastructure. However, the downside of having a small charge power is the long charging times since only "trickle charging" can be realized. Level 2b and, definitely, Level 3 require special arrangements in electrical infrastructure due to high power flow they require. While Level 2b, after required upgrade, can be realized for home use, Level 3 is specifically designed for "super charge" purposes.

Table 7.4 Electric vehicle charging levels

Charging set	Utility service	Usage	Charge power (kW)
Level 1	110 V, 15 A	Opportunity	1.4
Level 2a	220 V, 15 A	Home	3.3
Level 2b	220 V, 30 A	Home/public	6.6
Level 3	480 V, 167 A	Public/private	50–70

Fig. 7.17 Clipper Creek HCS-40 and Bosch Power Max Chargers [45, 46]
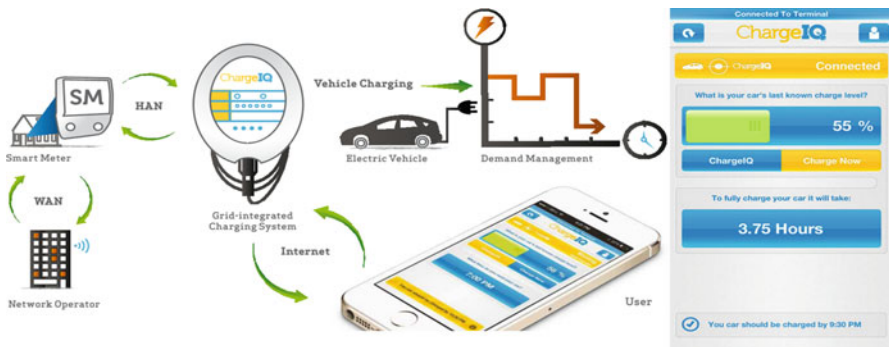
Fig. 7.18 ChargeIQ, smart charging solution [47]

Super charge is beneficial for fully charging the battery of an electric vehicle in a short period of time and for long-distance use, e.g., during a road trip. Therefore, Level 3 is expected to be used in large charging stations installed in intercity/ interstate highways. There are different chargers in the market such as Clipper Creek HCS-40 [45] and Bosch Power Max [46]. They can support Level 1 and Level 2 charging for residential purposes and vary in terms of quality, durability, and warranty (Fig. 7.18).

However, the real groundbreaking developments are being made in "smart charging" technology. Smart charge is the term coined for collaborative charging operation where different features of the electric vehicle and preferences of the

owner and grid operator are taken into account. An optimal solution is reached after meeting the demands of the owner and following the constraints of the grid operator. For instance, the vehicle owner may opt to choose "grid-friendly charging" where the charging will be managed by the grid and moved to off-peak hours. In return, the grid operator offers some incentives such as deductions in overall electricity bill. Needless to say, in order to realize "smart charging" a comprehensive communication and coordination system is required. Considering the entities involved in the process, it is required to synchronize smart meter, the electric vehicle (and charger), vehicle owner, and the grid operator. Accordingly, the charging operation is not a mere power transfer from grid to vehicle anymore; rather it is a large power management and optimization problem with several parameters.

This problem is solved with IT-based electric vehicle charging infrastructure that are connected to the electric grid. The owners, grid operator, as well as smart meter of the house have access to said charging infrastructure. The applications are based on available IT technology and the information exchange is performed over convenient communication lines (e.g., wired or wireless) in accordance with predetermined communication standards (see Sect. 7.3.4 for more discussion on standardization and interoperability). ChargeIQ, developed by an Australian company named DiUS, is a grid-friendly smart charging solution that comprises a charger and uses Zigbee standard for communication [47]. Figure 7.19 shows the
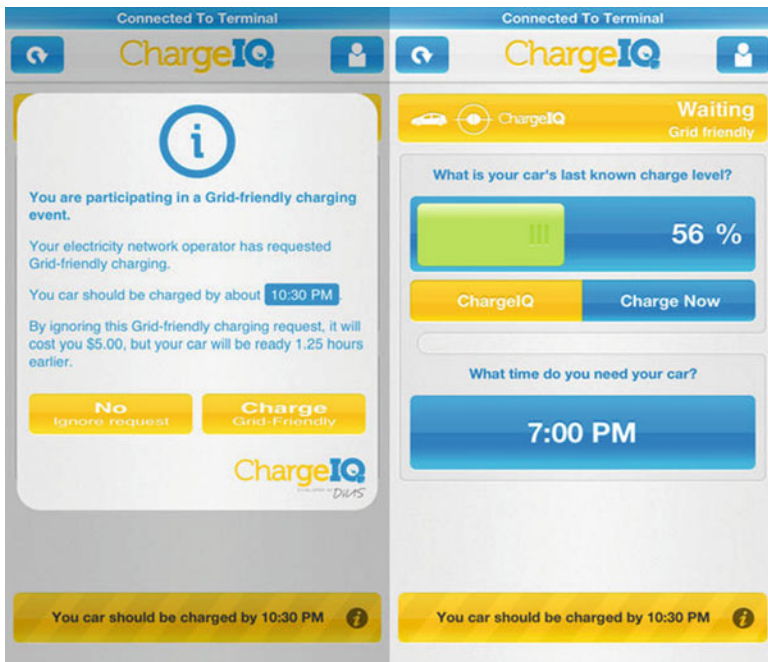
Fig. 7.19 Smart charging (demand-side management) in ChargeIQ [47]

working principle of ChargeIQ. Based on the figure, it is clear that the user (i.e., owner of the electric vehicle and the house) communicates with smart charger over Internet with the help of a smartphone. Smart charger is linked to smart meter over house area network (HAN), and reports any parameter change in the system as well as updates sent by the user. Smart meter is the interface between the charger and the network operator (i.e., grid operator). The coordination with the grid is performed over wide area network (WAN) for power dispatch and demand-side management.

As shown in Fig. 7.19, ChargeIQ smartphone application is very beneficial in following the SOC of the battery, the time required for full charge (3.75 h), and when the vehicle would be available (9:30 pm). This helps the owner manage his/her vehicle use and the charging times. It is observed that the system is operated in "Charge Now" option and vehicle is connected to the grid. Grid-friendly charging is the charging type when the owner agrees to give permission to the operator for managing charging times. In an effort to cut down the peak hour load, the grid operator would like to shift some load to off-peak hours. Considering that most people need their cars to/from the office, it is a fact that most cars sit idle at home in the evening. Therefore, some owners may not need their cars charged immediately. As long as the car is fully charged in the morning, the actual charging time is of no concern to them.

Figure 7.20 shows the implementation of this concept in ChargeIQ. A query screen is shown to the owner, asking whether he/she is willing to participate in grid-friendly charging. When agreed, ChargeIQ manages charging and power transfer is stopped during peak hours (Fig. 7.21).

This process increases the charge time, and awards the owner $5, but ensures that EV is fully charged at the specified time (i.e., 7:00 pm). Coordination of

Fig. 7.20 Charging locations in North America [48]
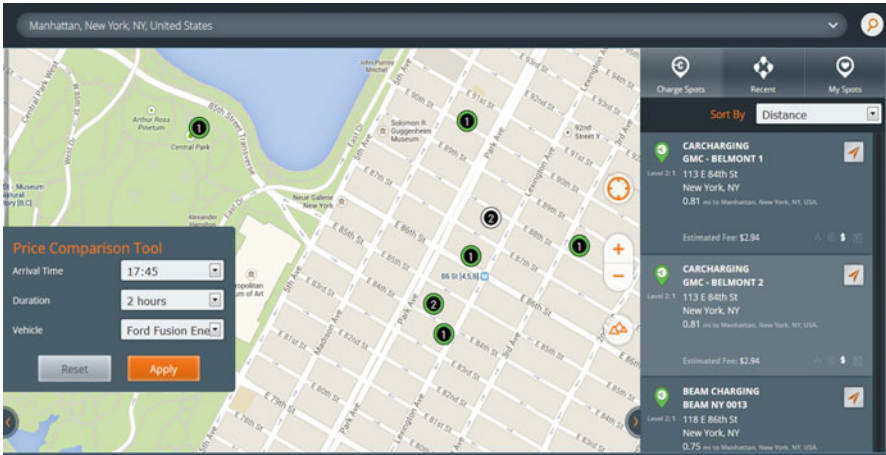
Fig. 7.21 Charging location details and price comparison [48]

Fig. 7.22 Charging stations on Paris roads [50]

charging stations is important that helps EV owners find available spots and charge their cars conveniently. Chargepoint [48] is an EV charging solution that lists nearby charging spots, their availabilities, costs, etc. This solution is Internet based and has a smartphone application. When a specific location is selected, say Manhattan, NY, as in Fig. 7.22, the application can be used to compare prices and get directions to a selected charging station. Furthermore, Chargepoint allows users to create their own account, save their preferences, and keep records of their recent charging stations. These applications are fast and enable for easy detection of available charging stations even in places that are unknown to the driver.

7.3.2 Vehicle-to-Grid Technology

Vehicle-to-grid (V2G) technology has been proposed to utilize batteries of electric vehicles as distributed storage devices and, thus, provide grid support. Considering the amount of the automobiles present in a neighborhood and assuming mass acceptance of electric vehicles, the amount of potential storage becomes significant [1]. Introduction of distributed generators and division of traditional large electric grid into several smaller sections, i.e., microgrids, changed the paradigm of power systems. Rather than large operation tolerances and bulk scheduling/dispatch, the new-age power systems require smaller windows and dynamic planning/dispatch is more preferred. V2G technology is a result of this urge to look for alternatives. Notwithstanding above, there are serious challenges that need to be addressed before V2G technology can be implemented commercially.

Continuous charge/discharge operation reduces the lifetime of the battery and it is not clear whether the owner or the grid operator shall bear the cost related with this technology. Although battery technology is always progressing, the prices are still very high and this makes V2G technology not profitable or worthwhile. Another challenge is the mobility and dynamic nature of electric vehicles. Unlike distributed storage devices that are deployed in power systems, electric vehicles come with many uncertainties. The availability of the vehicle, SOC, time period for which the vehicle will support V2G, and challenge to meet owner's charge requests (when the vehicle is required fully charged) can be counted as some of these uncertainties. It is true that the overall storage provided by the bulk amount of automobiles is very high. However, it is very difficult to know the exact number of vehicles, their exact places, and exact SOC. Accordingly, grid operators would abstain from highly relying on the storage provided by electric vehicles.

There are real-life implementations in military bases for improved power supply and there are good reasons for this. Due to their disciplined nature, military applications seem to be more suitable for V2G technology than other applications. Assessing the opportunity to use vehicles for better grid performance, the Air Force base in Los Angles [49] has replaced its entire vehicle fleet with electric vehicles. This has solid advantages for V2G technology:

- The vehicles will stay in the boundaries of the base most, if not all, of the time. The mobility of the vehicles is limited and this simplifies the problem.
- The range of travel has an expected upper bound. The vehicles used in the base will have an average distance traveled and will not fluctuate highly (as it would be in an ordinary neighborhood with people from all walks of life).
- These vehicles are entirely owned by the military and there is no ownership and V2G participation issues. As long as the base administration opts to implement V2G, every vehicle would participate in it.
- Unlike commercial applications, military applications tend to care more about reliability and durability more than the costs. Therefore, in a military application, high cost of vehicle batteries can be justified with independent and reliable power supply.

Table 7.5 Comparison between different implementation fields

	Commitment	Number of EVs	Baseline EV availability	Continuity
Military base	High	Less	Very High	Continuous
Stadium	Low	Moderate	High	Only during game hours
School/university	Low	Moderate	Moderate	Seasonal
Hospital	Low	Moderate	Moderate	Continuous
Neighborhood	Low	High	High	Continuous

The experience in military applications is valuable and sheds light to commercial applications. Network operators are looking into reducing uncertainties and increasing EV support in the grid. Some grids have introduced grid-support program for EV owners. Unlike grid-friendly charging, grid-support program not only moves charging to off-peak hours but also uses the charge stored in the batteries to perform peak shaving during peak hours. This is considered as a win-win situation as the grid operator decreases its peak load while the owner receives payment for V2G participation. In order to guarantee minimum participation, grid operators need to perform extensive surveying and estimate the base vehicle support for any given time.

Implementation in a residential neighborhood is easy since people mostly drive to/from school and work. Most stay home in the evening and their cars stay parked. There are other implementation opportunities as well. Large public places and their parking lots such as stadiums, hospitals, and universities can be utilized to reach minimum amount of support and reduce uncertainty. As shown in Table 7.5, a stadium or a hospital can be utilized as a V2G support hub. Supporters who came to watch a game give a hint about the amount of time they will spend in the premises. The grid operator will have more known parameters to perform scheduling.

Building on experiences acquired with these special implementations (military applications, pilot projects in selected neighborhoods, public places such as stadiums and hospitals) V2G technology can be implemented widely. Serious challenges such as battery lifetime costs should be addressed as well.

7.3.3 EV Charging Technology

EV charging can be divided into three categories: household connections, fast charging, and battery swap systems. A major obstacle in Europe especially in large cities is that most car owners do not own a garage but park their cars at the curb. This requires a multitude of capital-intensive public charging stations. Current charging stations are either free or at least highly subsidized by either electricity provider, car manufacturers, or local government [21]. There are three standards for EV power plugs. These are the American SAE, European International Electro-Technical Commission (IEC), and Japanese CHAdeMO standards. An international standard is still needed and is expected in 2017. There are strong hopes that

induction charging might become safe and user friendly by 2020. The development of plug-in vehicles in France is seen as a symbolic step towards more environmentally friendly transport to achieve national goals. The government has also announced an investment plan to support public infrastructure. An estimated one million public and private battery-charging stations will be built by 2015 under the plan. France is planning to deploy this infrastructure in all sectors of daily life, in particular for the following groups:

- Enterprises: Charging infrastructure will be installed for captive fleet of plug-in vehicles, such as corporate fleets.
- Public domain: Plug-in vehicles and charging infrastructure will also be deployed in public areas, such as roadways and public parking garages.
- Residential sector: Plug-in vehicles and charging infrastructure will be made available to individual users, with or without vehicle ownership [50].

France now counts about 6000 charging stations for electric vehicles and plans to increase that to 8000 points by the end of the year, as Montebourg said. Figure 7.23 shows a charging station in Paris. In the UK, there are already about 5725 public charging points and that number is growing fast, with both public and private investment. Figure 7.23 is the map of UK charging points and their types [51].

The government's Plugged-in Places scheme was launched to help kick-start this process. £30 million has been allocated to eight pilot regions that will see 8500 charging points installed over the coming years. The UK Government is setting official National Charge point Register to resolve the problem of multiple schemes of government and private companies installing charging points and different maps all competing to present charging point locations [51]. Three types of charging point are currently used in the UK [51]:

- "Slow" points use a standard 3 kW (13 A) supply (6–8 h for full charge).
- "Fast" points use single- or three-phase 7–22 kW (16–32 A) supply (3–4 h).
- "Rapid" points provide 40 kW+ AC or 50 kW+ DC supply (80 % charge in 30 min).

For most personal electric cars, it is expected that most charging will be performed at home, during (off-peak) nighttime hours when electricity is cheapest. Although a standard single-phase 13 A three-pin domestic socket is adequate to charge a car in 6–8 h, fleet cars can be charged in company special fast point or rapid point provided with special station arrangement [51].

7.3.4 Addressing the Interoperability Challenge

The Victorian trial discussed in Sect. 7.1.1.3.3 identified the need for having a fully interoperable charging infrastructure to support seamless user roaming across the providers similar to banking services and mobile phone use. Standardization and interoperability is one of the key challenges to be resolved to open the path to
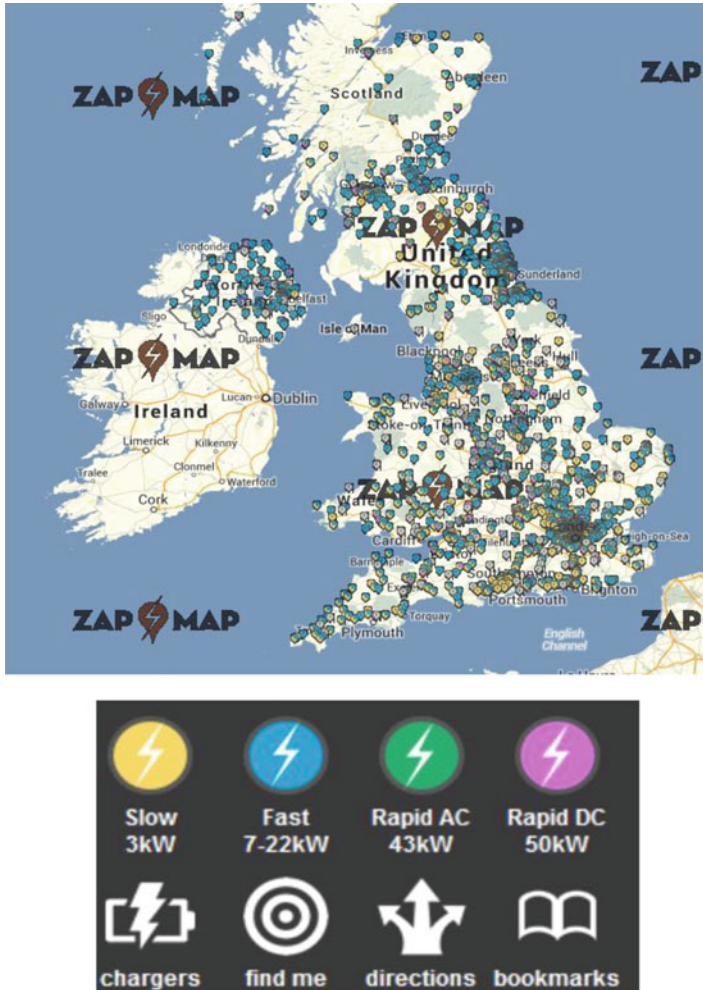
Fig. 7.23 Charging stations in the UK [51]

universal charging making it easier for customers to adopt EVs. The challenge is creating a platform where EVs could charge at any changing station and communicate with the utility grid operator enabling various functions such as billing, load management, and utility grid-managed charge management.

Work has long started to achieve such a fully interoperable EV charging system, not just in using standardizing smart charging hardware (the physical plug to connect to the car) but also in the area of two-way communication between the grid and the EV charging infrastructure. The Electric Vehicle-Smart Grid Interoperability Center opened in July 2013 aims to develop common standards and systems worldwide to ensure that EVs and charging stations could work together seamlessly with the grid. It is a joint venture between the U.S. Department of Energy (DOE) and the European Commission's (EC) Joint Research Centre (JRC) [52, 53].

7.3.5 Communicating Between EVs, Recharging Stations, and the Grid

International Electrotechnical Commission (IEC) has long been developing smart grid standards specifically covering aspects that relate to how smart grid components can effectively communicate and interact. IEC 65850 is an international standard originally developed for substation automation systems, which described the communication between devices in a substation and the related system requirements. It is an Ethernet-based standard that suggest wired exchange of protection, control, and measurement data within a substation automation system. However, it has been continuously expanded to cover other elements of future smart grids such as hydroelectric power plants, wind farms, distributed energy resources, and recently EVs. IEC 61850 defines standardized communication interfaces with object models [54–57] describing the data and processes within a system as well as communication methods in order to control and monitor the data and processes within a system and its subcomponents.

IEC 61850 was recently expanded to cover the abstract object modeling for distributed energy resources. The new subcomponent of the standard, IEC 61850-7-420 [58, 59], mainly covered object modeling of distributed energy resources such as photovoltaic and combined heat and power systems. A number of papers published in the literature argued for the need to extend IEC 61850-7-420 to cover EVs as well as suggested possible extensions to IEC 61850-7-420 for covering information models [60, 61] that apply to electric vehicles. Such extensions were not added to IEC 61850-7-420 but IEC is currently in the process of developing the IEC TR 61850-90-8 [62] as an addition to the standard set of documents to specially cover object models for electric mobility. Once complete, this communication standard will define the data within an EV system through abstract object modeling and the processes to be monitored and controlled, which will assist in the grid integration of EVs.

7.4 Conclusion

Rising energy costs, climate and emission control requirements, and expected decreases in the availability of petroleum supplies are driving the transition towards electrification of transportation. This chapter has sought to enlighten the reader on electric vehicle usage around the world by discussing their applications, electric vehicle trials, and key learnings from these trials across three continents: America, Europe, and Australia. Commuting trends and their impacts on the transition into the electrification of transportation have first been analyzed across these three continents. An impact analysis of electric vehicles on grids has also been presented including impacts on peak demand and power quality of the network. Examples of charging infrastructure and worldwide V2G applications have been reviewed.

References

1. Ustun TS, Zayegh A, Ozansoy C (2013) Electric vehicle potential in Australia: its impact on smartgrids. IEEE Ind Electron Mag 7:15–25
2. Australian Bureau of Statistics. Motor vehicle census 2013. [cited 2014 10 March]. http://www.ausstats.abs.gov.au. Accessed 31 Jan 2013
3. Australian Bureau of Statistics. Australian social trends: car nation 2013 [cited 2014 10 March]. http://www.abs.gov.au/AUSSTATS/
4. Australian Bureau of Statistics (2012) Waste management, transport and motor vehicle usage use survey
5. Energy Supply Association of Australia (2013) Sparking an electric vehicle debate in Australia. ESSA, Melbourne
6. AECOM (2012) Impact of electric vehicles and natural gas vehicles on the energy markets
7. AECOM (2011) Forecast updake and economic evaluation of electric vehicles in Victoria
8. CSIRO (2012) Spatial modelling of electric vehicle charging demand and impacts on peak household electrical load in Victoria. CSIRO, Australia
9. Speidel S, Jabeen F, Olaru D, Harries D, Bräunl T (2012) Analysis of western Australian electric vehicle and charging station trials. Aust Transp Res Forum 1:1–12
10. Bräunl T (2013) Trial complete: electric vehicles can work in Australia: The conversation. [cited 2014 22 May]. http://theconversation.com/trial-complete-electric-vehicles-can-work-in-australia-18843
11. Metering.com (2013) Ergon energy trial finds mass uptake of electric vehicles could impact its network. [cited 2014 23 May]. http://www.metering.com/ergon-energy-trial-finds-mass-uptake-of-electric-vehicles-could-impact-its-network/
12. Royal Flying Doctor Service Magazine (2012) Townsville welcomes state's first green electric vehicle charging station. http://www.flyingdoctor.org.au/IgnitionSuite/uploads/docs/Flying%20Doctor%20Queensland%20May%202012%20edition.pdf
13. ABC (2012) New charge point pops up as electric car trial continues. [cited 2014 23 May]. http://www.abc.net.au/local/stories/2012/06/14/3525454.htm
14. Electric vehicle trial: Department of transport, planning and local infrastructure. [cited 2014 15 May]. http://www.transport.vic.gov.au/projects/ev-trial
15. Department of Transport Planning and Local Infrastructure (2013) Creating a market: victorian electric vehicle trial mid-term report
16. State Govenment of Victoria (2010) The Victorian electric vehicle trial: results of 2012 applications. Department of Transport, Melbourne
17. IAE (2013) International energy agency and electric vehicles initiative of the clean energy ministerial, Paris, France
18. Infield HSaD (2009) The potential of domestic electric vehicle to contribute to grid technology. p 6
19. European Commission Energy (2011) European Country CO_2 emission by 2020
20. Joint Research Centre-European Commission (2011) Plugging the sustainability gap: boosting the european electric vehicle market
21. Van Essen H, Kampman B (2011) Impact of electric vehicles—summary report
22. Frost, Sullivan (2012) 360 Degree perspective of the Central and Eastern Europe electric vehicle industry
23. Kenworthy J (2003) A study of 84 global cities. Transport energy use and greenhouse gases in urban passenger transport systems
24. McKenzie B, Koerber W, Fields A, Benetsky M, Rapino M. Commuter-adjusted population estimates: ACS 2006–10. Washington, DC: Journey to Work and Migration Statistics Branch, U.S. Census Bureau.
25. U.S. Census Bureau. American community survey. 2008–2012
26. McKenzie B, Rapino M (2011) Commuting in the United States: 2009. American Community Survey Reports

27. U.S. Census Bureau (2009) American community survey
28. McKenzie B (2013) Out-of-state and long commutes: 2011. American Community Survey Reports
29. Administration Bureau of Transportation Statistics (2012) Transportation statistics annual report U.S.A.: U.S. Department of Transportation, Research and Innovative Technology
30. U.S. Census Bureau (2012) Statistical abstract of the United States: 2012
31. Federal Highway Administration (2009) National Household Travel Survey (NHTS)
32. Technica C. Southern California edison offers insight into impact of electric vehicles on grid 2013. http://cleantechnica.com/2013/08/13/southern-california-edison-offers-insight-into-impact-of-electric-vehicles-on-grid/
33. Rahman S (ed) (2011) How can we minimize electric vehicle's impact on the electric power distribution network. ISGT ASIA, Perth
34. Kesler M, Kisacikoglu M, Tolbert L (2014) Vehicle-to-grid reactive power operation using plug-in electric vehicle bidirectional off-board charger. IEEE Trans Ind Electron 61:6778–6784
35. Reiner DR, Cartalos DO, Evrigenis MA, Viljamaa MK (2010) Challenges for a European market for electric vehicles. European Parliament, Directorate General for Internal Policies, Policy Department, Brussels
36. Shrink That Footprint. Shades of green: electric cars' carbon emissions around the globe. http://shrinkthatfootprint.com/electric-car-emissions#3oboXAxlpQ8H48UF.99
37. European Environment Agency (2013) Monitoring CO2 emissions from new passenger cars in the EU: summary of data for 2012
38. ALPIQ (2010) Electric vehicle market penetration in Switzerland by 2020
39. Green eMotion [cited 2014 30 May 2014]. http://www.greenemotion-project.eu/home/index.php
40. CSIRO (2012) Greenhouse gas abatement potential of the Australian transport sector: Australian Low Carbon Transport Forum
41. Logic J (2014) Tasmanian electric vehicle demonstration concept investigation report. Energy Advisors
42. Terrence Mader, Thomas Bräunl (2012) Western Australian electric vehicle trial: final report
43. Department of Energy (2011) One Million electric vehicles by 2015. USA
44. Union of Concerned Scientists (2012) State of charge: electric vehicles' global warming emission and fuel-cost savings across the United States
45. ClipperCreek. http://www.clippercreek.com/store/product/hcs-40-30a-240v-charging-25-cord-3/
46. Bosch. Electric vehicle solutions. http://www.pluginnow.com/power-max
47. Percepscion. ChargeIQ. http://percepscion.com/chargeiq/
48. ChargePoint. http://www.chargepoint.com/
49. U.S. Department of Energy. Electric avenue, federal fleet success stories
50. IA-HEV (2013) France-charging infrastructure
51. Greencar V (2014) Next green car, electric car specialist, UK charging point
52. Stewart J (2013) Electric cars: a universal plug for all models? BBC. http://www.bbc.com/future/story/20130903-universal-plug-for-electric-cars
53. Argonne National Laboratory (2012) Electric vehicle-smart grid interoperability center. US Department of Energy. http://web.anl.gov/eesa/pdfs/success_stories/43_Smart_grid_mou_v2.pdf
54. International Electrotechnical Commission (IEC) TC 57 (2003) Communication networks and systems in substations—Part 1: Introduction and overview. IEC Standard IEC/TR 61850-1, 1st edn. Geneva
55. Ozansoy CR, Zayegh A, Kalam A (2007) The real-time publisher/subscriber communication model for distributed substation systems. IEEE Trans Power Delivery 22:1411–1423
56. Ozansoy CR, Zayegh A, Kalam A (2009) Object modeling of data and DataSets in the international standard IEC 61850. IEEE Trans Power Delivery 24:1140–1147

57. Ozansoy CR, Zayegh A, Kalam A (2009) The application-view model of the international standard IEC 61850. IEEE Trans Power Delivery 24:1132–1139
58. Ustun TS, Ozansoy C, Zayegh A (eds) (2011) Distributed Energy Resources (DER) object modeling with IEC 61850-7-420. Universities Power Engineering Conference (AUPEC), 2011 21st Australasian, 25–28 Sept 2011
59. Ustun TS, Ozansoy C, Zayegh A (eds) (2011) Extending IEC 61850-7-420 for distributed generators with fault current limiters. Innovative Smart Grid Technologies Asia (ISGT), 2011 I.E. PES, 13–16 Nov 2011
60. Schmutzler J, Wietfeld C, Andersen CA (eds) (2012) Distributed energy resource management for electric vehicles using IEC 61850 and ISO/IEC 15118. Vehicle Power and Propulsion Conference (VPPC), 2012 IEEE, 9–12 Oct 2012
61. Ustun TS, Ozansoy CR, Zayegh A (2013) Implementing vehicle-to-grid (V2G) technology with IEC 61850-7-420. IEEE Trans Smart Grid 4:1180–1187
62. International Electrotechnical Commission (IEC). Power systems management and associated information exchange [cited 2014 31 May]. http://www.iec.ch/dyn/www/f?p=103:30:0::::FSP_ORG_ID,FSP_LANG_ID:1273,25

Part III
Adoption and Market Diffusion

Chapter 8
Perceptions and Adoption of EVs for Private Use and Policy Lessons Learned

Iana Vassileva and Reinhard Madlener

Abstract Electric vehicles (EVs) are considered one of the most promising solutions to mitigate greenhouse gas (GHG) emissions produced in the transport sector. EVs have many potential advantages (e.g., in terms of avoided local and global pollutant emissions and noise reduction), but may also create new problems (e.g., in terms of stress on the electric distribution network or congested public transport lanes). The ultimate pollution emission benefit depends strongly on the fuel mix for electricity generation. Numerous governments at all levels worldwide have started to provide monetary and other incentives to render EVs more attractive for users, including research, development, and dissemination (RD&D) support, vehicle subsidies, provision of charging infrastructure, and privileged usage of bus lanes and dedicated parking lots. This chapter presents the different barriers explaining the slow market penetration of EVs so far, consumer perceptions and misconceptions, as well as lessons learned by policy makers and new empirical evidence and insights. Early adopter characteristics and selected examples where EV uptake has been particularly fast are also described. The conclusions show that subsidy and other incentive programs need to be carefully designed in scope, contents, and duration. In light of information deficiencies and misperceptions, information provision to potential EV adopters seems to be a no-regret policy option.

I. Vassileva
School of Business, Society and Engineering, Mälardalen University,
P.O. Box 883, Västerås SE-721 23, Sweden
e-mail: iana.vassileva@gmail.com

R. Madlener (✉)
Institute for Future Energy Consumer Needs and Behavior (FCN), School of Business
and Economics/E.ON Energy Research Center, RWTH Aachen University,
Mathieustrasse 10, Aachen 52074, Germany
e-mail: RMadlener@eonerc.rwth-aachen.de

8.1   Introduction

The transport sector is one of the largest greenhouse gas (GHG)-emitting sectors. In 2015, worldwide carbon dioxide (CO_2) emissions due to transportation amounted to about 25 % of the total carbon dioxide emissions, of which approximately 75 % was produced by cars and trucks. The transport sector was also responsible for nearly 30 % of the European Union's energy consumption [1, 2]. With this in mind, different initiatives and legislative measures have been introduced, with the intention to control and regulate the maximum global CO_2 emissions.

In the European Union (EU), where road transportation contributes to one-fifth of the total CO_2 emissions, the European Commission (EC) has set in the Climate and Energy Framework, which targets to raise the share of renewable energy sources to 27 % and to reduce GHG emissions by 40 % until 2030 [3]. Moreover, a white paper introducing the *Roadmap to a Single European Transport Area*, includes goals aiming at zero conventionally-fueled cars in cities until 2050, and a 50 % shift of medium-distance intercity journeys from road to rail and waterborne transport, which is expected to contribute to a 60 % cut in transport emissions by the middle of the century [4].

There are several regulations aimed at reducing emissions and promoting the electrification of road transport either directly or indirectly. An example is the EC Regulation No. 443/2009, setting the limit for CO_2 emissions for all new cars to 130 g CO_2/km, which is intended to be reduced to 95 g CO_2 from 2020 [5]. Some of the latest data presented by the EC shows that the average emission level of new cars sold in 2014 was 123.4 g of CO_2/km, which is significantly below the 2015 target of 130 g/km [1, 2].

In the case of the USA, the Environmental Protection Agency (EPA) has set different standards targeting GHG emission reduction and improvement of fuel economy. For cars produced between 2017 and 2025, the CO_2 emissions are expected to decrease from 131 g CO_2/km to 88.8 g CO_2/km, respectively. Although these reductions are expected to occur mainly through improvement of internal combustion engines, the electrification of roads and an increase in the use of EVs are also foreseen [6].

Since the global tendency indicates that private ownership of personal vehicles will continue to increase (especially in developing countries and in countries where car sharing and public transport are not considered as attractive alternatives), the promotion of EVs—in this chapter referring to battery electric vehicles, plug-in hybrid electric vehicles, and extended-range electric vehicles—plays an essential role in the efforts towards CO_2 emission mitigation and, more generally, sustainability in the transport sector.

It has been argued, however, that EVs are not completely environmentally friendly when viewed from a life cycle and total systems perspective, and that a successful reduction of CO_2 and other pollutant emissions associated to EVs is strongly dependent on the fuel mix of electricity generation [7–9] as well as the

distance driven [10]. Soret et al. [11] estimated the potential impacts of EVs on urban air quality in the Spanish cities of Madrid and Barcelona. The two cities suffered from exceeded annual and hourly limit values of atmospheric pollutant emissions, recording air quality problems on several occasions. The scenarios considered, assuming different EV penetration rates, showed that the most ambitious scenario of a 40 % penetration rate would cause reductions in the total nitrous oxide (NO_x) emissions of between 11 and 17 %, translating into air quality improvement of 8–16 % for the maximum hourly values. Additionally, the overnight charging of EVs showed no significant increases for any type of local air pollutant in the city. However, hourly maximum concentrations of ozone (O_3) increased due to the decrease of NO_x emissions.

When taking into consideration the overall impacts on airborne emissions, manufacturing, use, and recycling should all be included in the analysis. When examining the manufacturing processes, the chassis and body of both conventional and electric vehicles are quite similar. Still, EVs do not need fuel tanks, exhaust systems, and gearboxes. Moreover, the efficiency of internal combustion engines (ICEs) ranges between 28 and 30 %, while electric motors can reach up to 95 %. Based on some of the previously mentioned parameters, LCA studies have established that the environmental impacts of gasoline vehicles are significantly higher. However, by how much again depends to a large extent on the electricity mix and the vehicle mileage. Some researchers have found that, compared to the average ICE vehicle, electric cars are more environmentally benign, especially in countries with low GHG emissions [12].

Additionally, the users play an important role when it comes to saving energy that is consumed by EVs. Personal travel and driving behavior impact on EV performance, which affects the energy consumption associated with driving EVs [13]. Some of these factors are *technological* (fuel efficiency, brake energy recuperation, start/stop automatic, electronic devices), *social* (car-sharing initiatives, neighborhood/bandwagoning effects), *demographic* (age, gender), *economic* (income, fuel prices), and *environmental* (urbanization), among others [14]. As an example, drivers would need to adapt their driving style to regenerative breaking, or plan their trips according to the charging infrastructure availability, in order to maximize the distance traveled with one charge [15].

Apart from CO_2 emission reduction, compared to conventional vehicles, EVs have additional advantages that, among others, have been summarized in García-Villalobos et al. [16]. These include the reduction of energy dependence from oil-producing companies; overall reduction of air pollution, and consequently improving citizens' health, and EV's interaction with the grid, which can improve efficiency and reliability, depending on the charging strategy used [17–21].

The magnitudes of the above-mentioned advantages are very much dependent on the degree of EV uptake by the consumers (and of course other adopter categories as well, such as commercial vehicle fleet managers), and the way the EV users will be driving the vehicles. Due to the significant role of the consumer, this chapter puts the emphasis mainly on the adopter and user perspectives, as well as the impacts on the market penetration of EVs. This includes preferences and willingness to pay for

different alternative fuel vehicles (AEVs), AEV characteristics, and different cases where EVs have been successfully implemented. A good overview of the advances in consumer EV adoption research is provided in Rezvani et al. [22].

8.2 Preferences Regarding Alternative Fuel Vehicle Characteristics

Different types of alternative energy sources are used to mobilize vehicles (e.g., liquefied petroleum gas/LPG, compressed natural gas/CNG, ethanol, methanol, biodiesel, fuel cells, and electricity) and typically chosen based on cost and comfort considerations, existing infrastructure, as well as the countries' relevant environmental regulation and policy schemes (incl. specific R&D and technology promotion). Despite their mostly positive overall environmental balance relative to conventional fossil-fueled mobility, each of these alternative fuels (and related type of AFV) has also some disadvantages, e.g., in terms of infrastructure and storage challenges, high initial purchase cost/long payback period, low vehicle range, and long fuel-filling time or low density of fueling stations.

A recent comparative analysis study carried out by Ugurlu and Oztuna [23] provides insights regarding AFVs and comparing them with each other for distinguishing factors. The authors conclude that the most important factors for acceptance of AFVs include the initial purchase cost of the system, fuel costs, fueling station availability, fuel-filling duration, vehicle range, as well as performance and environmental impacts. Based on the authors' analysis and comparisons, LPG and CNG seemed to be the best options from an economic perspective, while EVs and fuel cell vehicles were considered the best option from an environmental point of view.

In order to evaluate the consumers' perceptions and individual preferences, based on a nationwide discrete choice experiment among potential car buyers in Germany, Hackbarth and Madlener [24] investigated the willingness to pay for a variety of AFV attribute improvements. The authors found that the willingness to pay for improvements of the different vehicle characteristics studied varied considerably across consumer goods. Interestingly, individuals who at first glance share many socio-demographic characteristics may nevertheless have very different preferences when it comes to AFVs. The authors find that, on average, AFVs are disliked, and that only in one of six classes of adopters identified battery electric vehicles are actually being favored over conventional fuel vehicles (but among several other types of AFVs). AFV "aficionados" are characterized by being younger, environmentally aware, and slightly less educated buyers of smaller (and cheaper) cars; they have high daily mileages and only moderate technical interest. Plug-in electric vehicles, in particular, also find enthusiasts among the older and technophile buyers of larger (and more expensive) cars. Moreover, vehicle attributes are found to need to meet some minimum requirements for

considering AFVs. Interestingly, certain improvements of vehicle attributes could increase the demand for AFVs cost-effectively, and consumers would accept markups for some of these attributes at a level that could enable their private sector provision and economical operation (e.g., fast-charging stations). Under present conditions, however, other attributes are found to need governmental support in order to compensate for an insufficient valuation (e.g., battery capacity).

In Hackbarth and Madlener [25], an earlier study of the same authors, they build on a rich body of literature on the demand for AFVs, but expand the earlier studies by additionally investigating plug-in hybrid EVs (PHEVs) as choice alternatives, as well as taking driving range, recharging time, and governmental incentives as additional vehicle attributes into account, in order to more realistically analyze consumer preferences regarding electric mobility. The seven vehicle types considered are described by purchase price, fuel cost, CO_2 emissions, driving range, fuel availability, refueling time, battery recharging time, and policy incentives. Driving range is found to have a positive impact on AFV adoption. As expected, it also affects the car-purchasing decision concerning BEVs more strongly, compared with the other fuel types. The almost doubled value of the coefficient is striking, indicating that car buyers indeed assign high values to an improvement of the limited driving ranges. The density of the filling station network also impacts vehicle choice positively: a widespread refueling infrastructure decreases the risk of being stranded with an empty tank or battery. Interestingly, refueling time of fuel-based vehicles does not seem to be a crucial factor, provided that it does not exceed the upper bound allowed of 10 min. The case is different for the battery recharging time, which is highly significant and negatively signed, indicating that a prolongation of the recharging process strongly decreases the utility of the respective vehicle. Confirming our assumption, the magnitude of this effect is dependent on the degree of electrification of the considered vehicles, which implies that the impact of a lacking fast-charging infrastructure on the choice of a battery EV is more severe than for a bi-fueled PHEV. Governmental incentives also affect vehicle choice positively, irrespective of whether they are monetary or of some other kind (free parking, bus lane usage, etc.). The car segment demanded affects the fuel type choice as well; for instance, consumers who indicated the purchase of a smaller vehicle were found to more likely choose a battery EV. The authors conclude that the choice probabilities of PHEVs could be increased with a manageable government purchase grant, while limited financial and nonmonetary government incentives appear unable to speed up the adoption of battery EVs. Finally, battery-leasing contracts are found to have almost no influence on vehicle alternatives, with battery EVs showing only small market share increases. An improvement of the driving range to 750 km for battery EVs is identified to have the same effect as a forceful joint action by the government and the private sector, although the latter policy intervention has a more pronounced effect on electric mobility overall, as it also boosts the demand for PHEVs and fuel cell EVs.

8.3   Penetration of Electric Vehicles and Policy Implications

8.3.1   Market Uptake

In general, results from market research suggest that EVs are not yet fully competitive and that the demand is still quite weak. Therefore, it is important to understand and identify the main driving forces explaining the consumers' decisions regarding the adoption and use of EVs.

The EVs' purchasing process follows the typical, well-defined steps for any purchase activity: starting with a *need or recognition,* followed by *information search*, *evaluation* of different alternatives, *purchase decision* and, finally, *post-purchase evaluation*.

The success of EV market penetration is considered dependent on several criteria analyzed in Zubaryeva et al. [26]. According to the *demography criteria*, early adopters have often higher incomes, which is why wealthier countries will typically adopt (at least capital-intensive) innovations earlier; also, individuals living in more densely populated urban areas might be more predisposed to purchasing EVs than those living in rural areas. The *environmental criteria* includes the daily and seasonal temperature variations, which affect the battery performance, and the "well-to-wheel" CO_2 emissions, which include those generated during the fuel/energy production and the use of fuel by the vehicle. Among the *economic criteria*, the fuel price is one of the most decisive for the EV market uptake: consumers are more willing to buy EVs when fuel prices are rising, especially in countries where battery charging is free. State incentives also help consumers to choose EVs over conventional vehicles. Regarding the *energy criteria*, which comprise the electricity mix and energy security, spare storage capacity of EVs can help to tackle the stability issues caused by the intermittent renewable energy sources on the electric grid. The *transport criteria* indicate that EV market penetration could be facilitated when targeting, at least initially, private households that are interested in having a second car (see also [27]). The commuting behavior of consumers also affects the choice of purchasing EVs; according to a survey, 60 % of drivers in Europe, despite driving less than 160 km a day, would not consider a driving range of less than 160 km as acceptable (Ernst & Young [28]).

Following the previously mentioned purchasing steps, Larson et al. [29] described the motivators and purchasing decisions gathered from consumers living in Manitoba, Canada. Regardless of the type of car, conventional or electric, the consumers stated that when purchasing their next car, the decision would be based mainly on reliability and secondly on handling in winter conditions, followed by the fuel efficiency, operating costs, and purchase/lease price, among others. The EV-specific characteristics that consumers considered as most important begin with the battery range meeting daily needs, followed by the ability to charge the battery at home; the total cost of the car, including purchase price and operating costs; the ability to charge the battery at work; the possibility to charge the battery quickly; the use of local-produced electricity as fuel; and, at last, subsidies and tax reductions.

In many countries, one of the main reasons for the slow EV uptake is the high purchase costs. Results presented by Hidrue et al. [30] show that the intention to pay for EVs is affected by the consumers' socio-demographic characteristics, their perceived lifestyle, and expectations regarding price development. Payback periods for EVs were found to vary between 6 and 8 years, which is longer if compared to conventional vehicles for which the period varies between three and five [31]. Moreover, the "resale anxiety" also discourages consumers from adopting EVs, due to the current immaturity of the markets and unknown resale values of EVs [32]. Based on their results, Lim et al. [33] suggest that allowing consumers to lease the EV batteries rather than buying them could reduce resale anxiety markedly and consequently lead to higher adoption levels, at least in the initial stages of market development.

A possible solution to the high initial costs is suggested based on a project carried out in Amsterdam (the Netherlands), where matching battery size to specific consumer needs is expected to significantly reduce initial purchasing costs: offering smaller batteries to users that typically drive short distances or that count on reliable charging infrastructure [34].

Other barriers holding car buyers back from deciding in favor of an electric car include limited range, high battery costs, accessibility to charging stations, long recharging times, low battery production volumes, and high costs of recharging infrastructure, among others [29]. With time, some of the initially considered negative EV characteristics have been contemplated by consumers as an advantage. For instance, results from a survey recently carried out in Germany suggest that the low levels of noise are regarded as something negative, mainly because of the safety issues and due to relevant feedback related to the engine noise typical for conventional vehicles. However, after driving EVs, drivers considered the quietness of the motor a positive experience [35].

In a recent study carried out by Accenture [36], in total seven factors have been identified as the main contributors to a long-term viable EV market growth. Currently, automotive original equipment manufacturers (OEMs) need to overcome challenges such as the need for different value chains and processes, the consumers' perceptions of practicality and functionality, and the potential advantages of EVs relative to possible disadvantages in terms of cost, cost savings, convenience, travel range, and low density or unavailability (e.g., at home or work) of charging infrastructure. The first of these seven factors is related to government regulations and subsidies targeting CO_2 emission reductions, or the tendency of cities towards increasing their sustainability and becoming "smart." Other factors include the integration of EVs within the product portfolios of OEMs; the collaboration within the e-Mobility value chain; provision of convenient charging infrastructure (with OEMs currently offering home-charging solutions with EV purchases); inclusion of innovative solutions to customers; and adjustment of their core operations and processes (e.g., services related to battery maintenance or replacement). The last approach for achieving a successful EV market adoption is the reduction of customer anxiety and the provision of consumers with what they expect from a positive e-Mobility experience.

As mentioned earlier, range anxiety—or the concern that EV batteries lose their power before reaching a destination or a charging station—is one of the main challenges preventing consumers from purchasing electric vehicles. In fact, recent research carried out by Achtnicht et al. [37], Krupa et al. [38], and Li et al. [39] indicates that the consumers' decision to purchase an electric vehicle is directly related to the availability of charging stations. Additional concerns include the types of chargers and their compatibility with the corresponding vehicle requirements.

Bonges III and Lusk [40] explored how new designs and placements of parking spaces and chargers could further improve the EV user's experience and attract the attention of potential EV users. As an example, a charger located in the corner of a parking lot may only be reached by one vehicle; a charger placed along the edge of a parking lot could reach two vehicles, and one in the middle of the rows could make it possible for four vehicles to be charged simultaneously. The authors additionally discussed possible solutions to free parking/charging spaces becoming overcrowded, or of lots being occupied even after the vehicle has been fully charged and the use of different kinds of permit/access cards (e.g., giving charging priority to BEVs over PHEVs or giving the permission to other EV drivers to unplug fully charged vehicles in order to plug in their own car). In conclusion, the authors draw the attention not only to the number of charging systems but also to their effectiveness, and to the need for regulation that allows unplugging charged EVs and eliminating the liability or activation of car alarms when the cars are unplugged by others than the owners of the vehicles.

In any case, studies evaluating driving behavior have demonstrated that the average distance before charging was way below the maximum range of the vehicles, in some cases 83 % of charge events occurred when the vehicle had more than half of its maximum allowable range remaining [41]. This information, if combined with the overall short daily driving distances, could help reducing range anxiety issues and change the consumers' negative perception about EV battery technology being insufficient for daily use.

Another opportunity to increase the market share of electric vehicles in countries where this type of transportation constitutes a sustainable option is to target multicar households. A comparative study recently carried out by Jakobsson et al. [27] shows that, from a technical and economic point of view, battery electric vehicles are considered as more suitable as second cars in multicar households, mainly due to their lower need for adaptation and the fact that the second car is typically used for short distances. Moreover, in a survey carried out by Vassileva and Campillo [42] results showed that in Sweden a remarkable 82 % of EV owners with more than one car in the household use their electric vehicle as their primary vehicle, which could be an indication of consumers gaining confidence and losing misconceptions.

In order to overcome market barriers and develop further adoption strategies, the characteristics of "early adopters" have been identified and analyzed in many countries. Curtin et al. [43] surveyed a representative for the US sample, to find out that the typical potential PHEV buyer is wealthy, with high pro-environmental

attitudes, who wants to demonstrate these to others by driving an environmentally friendly vehicle. Hidrue et al. [30] characterized early adopters to be young or middle aged, with a bachelor degree or higher; and, although income was not found to have any significant impact among US buyers, economic motives had a higher impact than environmental considerations. In contrast, results for Germany show that early adopters are typically middle-aged, full-time working male, with families who travel quite often since they live in areas outside the city [10]. Note that this is not in all respects in line with the above-described findings of Hackbarth and Madlener [24, 25] regarding individuals' preferences and early adopter characteristics, though. In a recent study in Sweden, based on results from 247 surveyed EV owners, early adopters have been characterized as male (81 %), between 40 and 45 years old, with high incomes and university degrees (77 %), and mostly being part of two- or four-member families [42].

Despite many studies showing that EV drivers typically live in large cities, there are also findings that suggest that EVs are more likely bought by drivers living in smaller cities, where, firstly, owning a car is more common and, secondly, having an EV is often more cost-effective [10]. This is also the case for early adopters in Sweden, where survey results indicate that the majority of private EV owners who registered their vehicles by March 2015 did not live in large cities [42].

In order to overcome the market uptake barriers and to encourage consumers to actually buy EVs, state and local governments in many countries have initiated incentive and subsidy programs, policies, and other initiatives. One example is the EVI (Electric Vehicle Initiative) that includes more than 15 governments from Africa, Asia, Europe, and North America, launched in 2010. By 2012, EVI accounted for 90 % of the world electric vehicle stock (led by the USA with 38 %, followed by Asia with 24 %). The initiative strives at encouraging the development of national deployment goals; leading a network of cities to share experiences and lessons learned; sharing information on public investment in research, development, and demonstration (RD&D) programs to ensure that gaps in vehicle technology development are well addressed; and engaging private-sector stakeholders [44].

Li et al. [45] report on lessons learned from business innovation and governmental regulation for promoting EVs in Shenzhen, China. They find, though focusing mainly on bus and taxi fleets, that the city has succeeded in fostering a distinct government-enterprise cooperation model, thus reducing financial pressure on the local government to promote the use of EVs, but also providing significant leeway to experiment with different innovative business models. Overall, they conclude that EV adoption can be further fostered by encouraging private investment in charging infrastructure by means of public-private partnerships and by standardizing EV technologies and production in order to break down local protectionism in the EV market.

Governments in Europe intend to promote EV sales by setting up adoption targets; for Europe as a whole, by 2020 the targets are set to eight to nine million EVs. The different European countries have set their own limits, e.g., the goals for France are two million vehicles; Germany, Spain, and the Netherlands are each
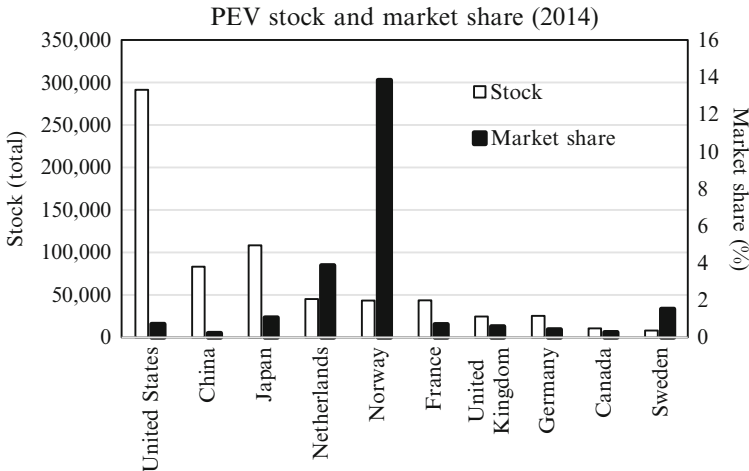
Fig 8.1 Stock and market share of EVs (battery electric vehicles and plug-in hybrid electric), compared to all vehicles, 2014 [47]

targeting one million; accompanied by incentive plans, one of the most generous is Norway, offering approximately €17,000 for the purchase of a new EV ([31]; see also [46]).

For 2014, the shares of EVs (battery electric and plug-in hybrid electric) in 11 different developed countries around the world are depicted in Fig. 8.1. The two by far highest shares of Norway and the Netherlands are striking.

Although the results suggest that financial incentives may not be the most cost-efficient method of reaching higher market uptake [48], some of the initiatives and subsidy programs have nevertheless effectively supported the rapid market uptake in many countries, some examples of which are described next.

8.3.2 Examples of Rapid EV Adoption and Lessons Learned

The USA, Japan, and Norway are considered to have one of the highest EV market penetration rates in absolute terms [49]. Their cases and lessons learned are presented in this section.

8.3.2.1 USA: California

In relation to the goal of the Obama Administration of reaching one million EVs on US roads by 2015, a federal tax credit of up to US$7500 has been established depending on the vehicle's battery capacity and for eligible EVs purchased in or after 2010 [50]. Additionally, the different states have implemented their own

incentive programs. California, one of the most pro-environmental states, started the Zero Emission Vehicle (ZEV) regulation, controlling both smog-causing pollutants and GHG emissions within the same package of standards. The ZEV regulation is expected to increase the use of this type of vehicle to 1.5 million ZEV cars by 2025 [51]. In February 2013, the Governor's Interagency Working Group on Zero Emission Vehicles published the so-called ZEV Action Plan, establishing milestones and strategies to overcome some of the current barriers. The ZEV Action Plan focuses on four distinct goals: (1) complete needed infrastructure and planning; (2) increase consumer awareness and demand; (3) transform the fleet; and (4) grow jobs and investment in the private sector. Regarding the "Consumer awareness and demand," the Action Plan stipulates an increased participation in consumer outreach campaigns, targeting awareness and information regarding the ZEVs' benefits and availability, as well as the continuation of strategies such as high-occupancy vehicle (HOV) lane access for ZEVs or different rebates and subsidies [52]. Regarding investments in infrastructure, in 2010 the State of California accounted for 80 % of the total charging stations installed in the USA overall [53].

The impact of efforts and strategies carried out in California over the previous decades is showing positive results when it comes to the acceptance and purchase of EVs. A survey, carried out at the end of 2011, shows that consumers with the highest interest in purchasing EVs were located in San Francisco, CA, followed by drivers living in other major Californian cities, such as Los Angeles and San Diego, ranking 5th and 7th, respectively [54].

Another study carried out for California showed that, by October 2013, there were more than 45,000 EVs purchased in the sunshine state. The results regarding the motivation behind purchasing EVs were analyzed for the three most frequently sold cars: Nissan Leaf, Chevrolet Volt, and Toyota Prius Plug-in-Hybrid. Owners of the Nissan Leaf listed "environment" (38 %) as the main motivational factor; "saving money" was chosen by 34 % of the owners of the Chevrolet Volt; in contrast, 57 % of the consumers driving a Toyota Prius PHEV selected the "HOV lane access" as their main motivational factor [55].

The early adopters were characterized as being young, with high incomes, purchasing EVs as an additional car; also, based on existing infrastructure investments and weather conditions, early adopters in the US market would primarily live in California [53].

However, on a national level, there are still EV market penetration barriers to overcome. With the aim of explaining the overall low EV market penetration rates in the USA, Krause et al. [56] examined the consumer perception of EVs from 21 cities, and found several important misconceptions regarding basic EV features. High maintenance cost of EVs in comparison to conventional vehicles, for instance, was one of the factors that most surveyed users believed in, overlooking for example the fact that EVs do not need oil changes, filter replacements, etc. Only 5.5 % of the respondents living in states offering purchase credits, as for instance California, where a US$5000 tax credit refund has been offered until 2012 (being reduced to US$2500 afterwards), are aware of these monetary incentives.

The results from this study show once again that consumers more likely to purchase EVs are young males, with high education and with pro-environmental beliefs.

As in other countries around the world, the USA still needs to overcome barriers, especially linked to consumers' low awareness, knowledge, and information availability that are preventing EV market update in large numbers.

8.3.2.2 Europe: Norway

Before turning to the country with currently the largest number of EVs per capita worldwide, Norway, we take a more European perspective. Aside from different legislations and regulations, the European Union has been promoting citizens' awareness and use of electric vehicles through several projects. One of them, the *Electric Vehicles for Urban Europe*, was a four-and-a-half-year project, where preferable options were suggested for cities to use EV technology in an optimal way. Three such options are the following: (1) the suggestion of promoting shared, instead of private, electric vehicles; (2) limit the duration of incentives and subsidies; and (3) recommendations for urban policy makers to develop frameworks that will suggest to consumers that the EVs are not just a temporary technology [57]. The idea of "shared EVs" (as one variant of car sharing) might be quite promising since it has been estimated that, in Europe, 50 % of the passenger cars belong to companies operating entire vehicle fleet, such as car rental agencies and corporations. The advantages making fleet organizations important to early adopters of EVs include, among others, (1) a frequent and intense usage; (2) centralized refueling stations; and (3) a better understanding of lifetime vehicle costs. The results of several studies investigating the reasons for organizations to prefer EVs suggest that using new technology, lower environmental impact, and attractive incentives play a decisive role in the selection process [31, 58].

EU support measures for EVs have been reviewed by Gass et al. [59], presenting also a case study on the impact of alternative policy instruments for promoting EV adoption in Austria based on total cost of ownership (TCO) calculations. The TCO calculations were based on technical and cost data obtained from a survey carried out among automobile manufacturers and importers in Austria, and accounted for expected cost reduction trends. The authors found that taxes (based on CO_2 or fuel efficiency) would have to be prohibitively high to render electric cars competitive against conventional ones, and that some up-front price support scheme seems favorable also in light of the higher weight assigned by consumers to up-front costs than to operating costs.

Norwegian support measures were compared and contrasted with those adopted in Austria by Figenbaum et al. [60]. In Austria, market stimulation for EVs is based on governmental support for so-called "Model Regions". In Norway, the incentives are at least threefold (direct, fiscal, and incentives providing relative advantages in order to rebalance certain drawbacks). The authors concluded that successful

market diffusion of EVs requires massive, expensive, and combined policies, and that central government backing, long-term commitment, and market-oriented incentives can help to reduce the perceived risks for market players on both the supply side (such as car importers) and the demand side (adopters). They also recommend that the lack of knowledge regarding EVs in the population at large needs to be tackled.

The local promotion of EVs in Italian cities has been described for two municipalities in the Marche region. The authors proposed guidelines for the local promotion of electric mobility, and pointed out the important role of the local utilities as operators of the distribution grid and important players to build up the public charging station infrastructure. In their study, the authors suggest that urban charging station infrastructure could be operated profitably without incentives, with payback periods of only 4–5 years in the most conservative scenario analyzed [61]. Norway has set to reduce CO_2 emissions by 16 Mt CO_2 eq. by 2020, which is 25 % lower than the reference period [62]. The country has the advantage of using hydropower as the main energy source, making the use of EVs a sustainable solution. As can be seen in Fig. 8.1, Norway is among the countries with the most rapid EV market penetration in Europe, both in absolute and relative terms: as of September 2015, there were 66, 276 (89.2 %) battery electric vehicles and 8006 (10.85 %) PHEVs registered [63]. In September, October, and November of 2013, EVs were the most often sold type of vehicle in Norway. In 2009, the country installed extensive charging infrastructure, which, combined with high financial incentives, allowed the country to be one of the top users of EVs [49, 60, 64]. Some of the most relevant incentives include exemptions on purchasing tax, toll road charges, taxes related to registration, and the yearly circulation tax; free parking and charging at publicly funded charging stations; and permission to use bus lanes; among others. The Norwegian Government also has plans to install fast-charging stations nearby highways in order to manage consumer concerns regarding battery-charging issues. Additionally, higher taxes on gasoline- and diesel-fueled vehicles are imposedon top of the 25 % value-added tax (VAT). All these incentives form part of the so-called Norwegian EV policy, which is an integral part of the Climate Agreement passed on by the Norwegian Parliament [46].

Holtsmark and Skonhof [46] and Aasness and Odeck [64] also analyzed the negative (and often unintended) effects of such incentives. Results showed that EVs in Norway were bought mainly as a second vehicle, used to replace short trips that otherwise would have been done by walking, cycling, or using public transportation, to some extent canceling out in this way the positive effects of EVs on GHG emissions. By providing free parking and allowing the use of bus lanes, EVs were used by drivers as a cost- and time-saving option for driving to Oslo, from two of the municipalities with highest ownership of EVs in the country, reducing toll revenues markedly and slowing down public transport on the dedicated lanes. The authors further found that marginal external costs of EVs in Norway are about the same as for conventional vehicles. The authors overall recommend that the approach adopted in Norway should not be copied in other countries without due consideration of the different situations and the (avoidable) adverse effects.

In fact, some of the arguments of the neighboring country, Sweden, for not providing strong political and incentive support are based on a similar dilemma: Should government investments focus on building EV charging stations, or is it better to concentrate on policy measures that would help shifting from private to public transportation [65]?

Regarding the user characteristics, EV drivers in Norway were found to have high income and higher education, and to be motivated by saving money and/or environmental topics. In fact, 41 % of consumers that bought an electric vehicle in Norway stated that "saving money" was one of their main reasons [31].

8.3.2.3   Asia: Japan

Japan's first EV incentive program began as early as in the 1990s, and has been one of several incentive programs that helped the country reach a leading position in EV sales in 2012, with a 28 % market share of global sales [46]. Indeed, for more than 10 years, Japan has been one of the leading countries in the development of EVs, accompanied by ambitious incentive programs for EV buyers, including subsidies covering half of the additional cost of an EV in comparison to a conventional vehicle [66]. The Japanese Ministry of Transport has supported several RD&D programs and has helped companies to promote the adoption and use of EVs. As an example, the ECO-Station project, which started in 1993, had the intention to build approximately 1000 charging stations (mainly fast-charging stations, combined with night energy storage systems). The early adoption programs induced the adoption of 655 EVs between 1977 and 1996.

Between 1990 and 1998, the Californian ZEV mandate mentioned above stimulated the Japanese federal government and manufacturers (mainly Toyota, Nissan, and Honda) to enter the EV development race during which the main focus was on batteries. As a result, the lithium battery project (LIBES) developed a Li-ion battery that was used, for instance, in the Nissan Hypermini [67]. In fact, US policy makers focused on the Nissan case for being the only manufacturer worldwide using more advanced lithium batteries [66].

Moreover, in Japan only nationally manufactured EVs were sold, providing evidence for the importance of national manufacturers' investments in EVs and their impact on market penetration [49].

In order to discover the characteristics of the early adopters in Japan, Radtke et al. [68] surveyed more than 1000 people that had purchased a new EV in the past two years. The EV drivers consider their cars as a perfect example of leading-edge technology; they invest time and money to keep up with the latest trends; they have high pro-environmental values; and women turned out to be the most excited persons regarding purchasing new models, mainly explained by their wish to be more "eco-friendly" and also by the fact that they generally dislike refueling their conventional cars with gasoline. The study identified a number of strong barriers preventing possible buyers from purchasing EVs: high prices (even after the

rebates), the low number of charging stations (especially in the areas where the respondents live), and the limited travel range.

Based on Japan's experience, the report suggests that there is a high need for education and information dissemination in order to match consumer needs and expectations regarding purchasing EVs.

8.4   Conclusions

This chapter evaluates the different aspects of electric vehicles, independently of their type and from a consumer perspective. Overall, EVs are considered to have a positive impact on the environment, especially regarding GHG emissions. However, despite countries around the world implementing subsidy and other incentive programs for increasing the market uptake of EVs, many consumers still consider such of vehicles as "work in progress," i.e., as not yet mature. Even though for many drivers EVs are a symbol of environmental friendliness, technological novelty, and pro-social values, several important barriers are found to slow down EV mass market development, including high vehicle and battery prices, low driving range, and insufficient and inconveniently placed charging stations. Governmental subsidy programs and their duration also need to be evaluated carefully, as in some cases they might become counterproductive in the battle towards reducing GHG emissions, e.g., where consumers buy EVs as an additional car and using it instead of walking or using public transportation, or where the electricity generation mix is still dominated by coal-fired power plants. Additionally, many consumers still have misconceptions about the EVs' capabilities, for instance regarding their driving range and lack of noise while driving. These mistaken beliefs or lack of information could be overcome by the introduction of new business models and marketing and education strategies that can be based on early adopter characteristics and used to attract new EV users.

References

1. EC (European Commission) (2015) Cutting energy use and carbon emissions in the transport sector conference, Brussels, 17 June 2015. https://ec.europa.eu/energy/en/news/cutting-energy-use-and-carbon-emissions-transport-sector-conference. Accessed 3 Mar 2016
2. EC (European Commission) (2015) CO_2 emissions from new cars and vans continue to decrease. http://ec.europa.eu/clima/news/articles/news_2015112601_en.htm. Accessed 3 Mar 2016
3. EC (European Commission) (2014) 2030 Climate and energy framework. http://ec.europa.eu/clima/policies/strategies/2030/index_en.htm. Accessed 3 Mar 2016
4. EC (European Commission) (2011) White paper: roadmap to a single European transport area—towards a competitive and resource efficient transport system. http://eur-lex.europa.eu/legal-content/EN/TXT/?uri=CELEX:52011DC0144. Accessed 3 Mar 2016

5. EC (European Commission) (2009) Official Journal of the European Union. Regulation (EC) No 443/2009 of the European Parliament and of the Council of 23 April 2009. http://eur-lex.europa.eu/legal-content/EN/ALL/?uri=CELEX:32009R0443. Accessed 14 Oct 2014
6. US EPA (United Stated Environmental Protection Agency) (2012) EPA and NHTSA set standards to reduce greenhouse gases and improve fuel economy for model years 2017–2025 cars and light trucks. Office of Transportation and Air Quality; EPA-420-F-12-051, Washington D.C.
7. Ajanovic A (2014) Promoting environmentally benign electric vehicles. Energy Procedia 57:807–816
8. IEA (International Energy Agency) (2009) Transport, energy and CO_2. http://www.iea.org/publications/freepublications/publication/transport2009.pdf. Accessed 12 Oct 2014
9. Mazur C, Madlener R (2010) Impact of plug-in hybrid electric vehicles and charging regimes on power generation costs and emissions in Germany. FCN Working Paper No. 20/2010. Institute for Future Energy Consumer Needs and Behavior, RWTH Aachen University
10. Plötz P, Schneider U, Globisch J, Dütschke E (2014) Who will buy electric vehicles? Identifying early adopters in Germany. Transp Res A 67:96–109
11. Soret A, Guevara M, Baldasano JM (2014) The potential impacts of electric vehicles on air quality in the urban areas of Barcelona and Madrid (Spain). Atmos Environ 99:51–63
12. Querini F, Dagostino S, Morel S, Rousseaux P (2012) Greenhouse gas emission of electric vehicles associated with wind and photovoltaic electricity. Energy Procedia 20:391–401
13. Galvin R (2016) Rebound effects from speed and acceleration in electric and internal combustion engine cars: an empirical and conceptual investigation. Appl Energy 172:207–216
14. Annual Energy Outlook 2014 with projections to 2040 (2014) U.S. Energy Information Administration (EIA). www.eia.gov/forecasts/aeo/pdf/0383(2014).pdf
15. Faria R, Moura P, Delgado J, de Almeida AT (2012) A sustainability assessment of electric vehicles as a personal mobility system. Energy Convers Manag 61:19–30
16. García-Villalobos J, Zamora I, San Martín IJ, Asensio JF, Aperribay V (2014) Plug-in electric vehicles in electric distribution networks: a review of smart grid charging approaches. Renew Sustain Energy Rev 38:717–731
17. Habib S, Kamran M, Rashid U (2015) Impact analysis of vehicle-to-grid technology and charging strategies of electric vehicles on distribution networks—a review. J Power Sources 277:205–214
18. Shabban MF, Eajal AA, El-Saadany EF (2015) Coordinated charging of plug-in hybrid electric vehicles in smart hybrid AC/DC distribution systems. Renew Energy 82:92–99
19. US DoE (US Department of Energy) (2014) Evaluating electric vehicle charging impacts and customer charging behaviors—experiences from six smart grid investment grant projects. Smart Grid Investment Grant Program, Washington D.C. http://energy.gov/oe/downloads/evaluating-electric-vehicle-charging-impacts-and-customer-charging-behaviors Accessed 12 Sep 2016
20. Luo Y, Zhu T, Wan S, Zhang S, Li K (2016) Optimal charging scheduling for large-scale EV (electric vehicle) deployment based on the interaction of the smart-grid and intelligent-transport systems. Energy 97:359–368
21. Ramachandran B, Geng A (2015) Smart coordination approach for power management and loss minimization in distribution networks with PEV penetration based on real time pricing. In: Rajakaruna S et al. (eds) Chapter 2: Plug-in electric vehicles in smart grids, power systems. doi:10.1007/978-981-287-302-6_2
22. Rezvani Z, Jansson J, Bodin J (2015) Advances in consumer electric vehicle adoption research: a review and research agenda. Transp Res D 34:122–136
23. Ugurlu A, Oztuna SA (2015) Comparative analysis study of alternative energy sources for automobiles. Int J Hydrog Energy 40:11178–11188. doi:10.1016/j.ijhydene.2015.02.115
24. Hackbarth A, Madlener R (2016) Willingness-to-pay for alternative fuel vehicle characteristics: a stated choice study for Germany. Transp Res A 85:89–111
25. Hackbarth A, Madlener R (2013) Consumer preferences for alternative fuel vehicles: a discrete choice analysis. Transp Res D 25:5–17

26. Zubaryeva A, Thiel C, Barbone E, Mercier A (2012) Assessing factors for the identification of potential lead markets for electrified vehicles in Europe: expert opinion elicitation. Tech Forcasting Soc Chang 79:1622–1637

27. Jakobsson N, Gnann T, Plötz P, Sprei F, Karlsson S (2016) Are multi-car households better suited for battery electric vehicles?—driving patterns and economics in Sweden and Germany. Transp Res C 65:1–15

28. Ernst & Young (2010) Gauging interest for plug-in hybrid and electric vehicles in the US. http://www.ey.com/Publication/vwLUAssets/EY-gauging_interest_for_plug-in_hybrid_and_electric_vehicles_in_select_markets/$FILE/EY-Gauging_interest_for_plug-in_hybrid_and_electric_vehicles_in_select_markets.pdf. Accessed 9 Oct 2014

29. Larson PD, Viáfara J, Parsons RV, Elias A (2014) Consumer attitudes about electric cars: pricing analysis and policy implications. Transp Res A 69:299–314

30. Hidrue MK, Parsons GR, Kempton W, Gardner MP (2011) Willingness to pay for electric vehicles and their attributes. Resour Energy Econ 33:686–705

31. Evolution. Electric vehicles in Europe: gearing up for new phase? Amsterdam Roundtable Foundation and McKinsey & Company, The Netherlands (2014) http://www.mckinsey.com/~/media/McKinsey%20Offices/Netherlands/Latest%20thinking/PDFs/Electric-Vehicle-Report-EN_AS%20FINAL.ashx. Accessed 14 Oct 2014

32. Haddadian G, Khodayar ME, Shahidehpour M (2015) Accelerating the global adoption of electric vehicles: barriers and drivers. Electr J 28:53–68

33. Lim MK, Mak H-Y, Rong Y (2014) Toward mass adoption of electric vehicles: impact of the range and resale anxieties. Manuf Serv Oper Manag 17:101–119

34. EV City Casebook (2014) 50 big ideas. Shaping the future of electric mobility. Urban Foresight Limited, Newcastle upon Tyne

35. Bühler F, Cocron P, Neumann I, Franke T, Krems JF (2014) Is EV experience related to EV acceptance? Results from a German field study. Transp Res F 25:34–49

36. Accenture (2014) The electric vehicle challenge. Electric vehicle growth in an evolving market dependent on seven success factors. https://www.accenture.com/se-en/~/media/Accenture/Conversion-Assets/DotCom/Documents/Global/PDF/Industries_15/Accenture-Electric-Vehicle-Challenge.pdf. Accessed 24 Feb 2016

37. Achtnicht M, Bühler G, Hermeling C (2012) The impact of fuel availability on demand for alternative-fuel vehicles. Transp Res Part D: Transp Environ 17(3):262–269

38. Krupa JS, Rizzo DM, Eppstein MJ, Brad Lanute D, Gaalema DE, Lakkaraju K, Warrender CE (2014) Analysis of a consumer survey on plug-in hybrid electric vehicles. Transp Res A 64:14–31. doi:10.1016/j.tra.2014.02.019

39. Li S, Tong L, Xing J, Zhou Y (2015) The market for electric vehicles: indirect network effects and policy design. Available at SSRN: http://ssrn.com/abstract=2515037 or http://dx.doi.org/10.2139/ssrn.2515037 http://papers.ssrn.com/sol3/papers.cfm?abstract_ id=2515037

40. Bonges HA III, Lusk AC (2016) Addressing electric vehicle (EV) sales and range anxiety through parking layout, policy and regulation. Transp Res A 83:63–73

41. Speidel S, Bräunl T (2014) Driving and charging patterns of electric vehicles for energy usage. Renew Sustain Energy Rev 40:97–110

42. Vassileva I, Campillo J. Adoption barriers for electric vehicles: experiences from early adopters in Sweden. Energy (forthcoming)

43. Curtin R, Shrago Y, Mikkelsen J (2009) Plug-in hybrid electric vehicles. University of Michigan. www.ns.umich.edu/Releases/2009/Oct09/PHEV_Curtin.pdf. Accessed 12 Oct 2014

44. IEA (International Energy Agency) (2013) Global EV outlook. IEA, April 2013. http://www.iea.org/publications/globalevoutlook_2013.pdf. Accessed 12 Oct 2014

45. Li Y, Zhan C, de Jong M, Luskzo Z (2016) Business innovation and government regulation for the promotion of electric vehicle use: lessons from Shenzhen, China. Journal of Cleaner Production, Vol.134, Part A, 15 October 2016, Pages 371-383(in press). doi:10.1016/j.jclepro.2015.10.013

46. Holtsmark B, Skonhoft A (2014) The Norwegian support and subsidy policy of electric cars. Should it be adopted by other countries? Environ Sci Pol 42:160–168

47. IEA (International Energy Agency) (2015) Global EV outlook. IEA/OECD, Paris. http://www.iea.org/evi/Global-EV-Outlook-2015-Update_1page.pdf. Accessed 2 Mar 2016

48. Committee on Climate Change (2013) Pathways to high penetration of electric vehicles. Final report for the Committee on Climate Change. http://www.theccc.org.uk/wp-content/uploads/2013/12/CCC-EV-pathways_FINAL-REPORT_17-12-13-Final.pdf. Accessed 16 Oct 2014

49. Sierzchula W, Bakker S, Maat K, van Wee B (2014) The influence of financial incentives and other socio-economic factors on electric vehicle adoption. Energy Policy 68:183–194

50. US DoE (US Department of Energy), Office of Energy Efficiency & Renewable Energy/Alternative Fuels Data Center Qualified plug-in electric drive motor vehicle tax credit. Washington D.C. http://www.afdc.energy.gov/laws/409. Accessed 12 Oct 2014

51. Zhou Y, Wang M, Hao H, Johnson L, Wang H, Hao H (2014) Plug-in electric vehicle market penetration and incentives: a global review. Mitig Adapt Strateg Glob Change 20(5):777. doi:10.1007/s11027-014-9611-2

52. OPR (Office of Planning and Research of the Governor of California) (2013) 2013 ZEV Action Plan. A roadmap toward 1.5 million zero-emission vehicles on California roadways by 2025. Governor's Interagency Working Group on Zero-emission Vehicles. Governor Edmund G. Brown Jr. https://www.opr.ca.gov/docs/Governor's_Office_ZEV_Action_Plan_(02-13).pdf. 1st Ed., February. Accessed 24 Feb 2016

53. Deloitte (2010) Gaining traction. A customer view of electric vehicle mass adoption in the U.S. automotive market. http://www.deloitte.com.br/publicacoes/2007/MFG.Gaining_Traction_customer_view_of_electric_vehicle_mass_adoption.pdf. Accessed 19 Oct 2014

54. Carley S, Krause MR, Lane WB, Graham DJ (2013) Intent to purchase a plug-in electric vehicle: a survey of early impressions in large US cities. Transp Res D 18:39–45

55. Center for Sustainable Energy (2014) What drives California's plug-in electric vehicle owners? California plug-in electric vehicle driver survey results. http://energycenter.org/clean-vehicle-rebate-project/vehicle-owner-survey/feb-2014-survey. Accessed 19 Oct 2014

56. Krause MR, Carley RS, Lane WB, Graham JD (2013) Perception and reality: public knowledge of plug-in electric vehicles in 21 U.S. Cities. Energy Policy 63:433–440

57. EVUE (Electric vehicles for urban Europe) (2010) European Commission, FP7-funded project. http://urbact.eu/sites/default/files/import/Projects/EVUE/outputs_media/2010-05-21_Final_EVUE_Baseline_study.pdf. Accessed 24 Feb 2016

58. Sierzchula W (2014) Factors influencing fleet manager adoption of electric vehicles. Transp Res D 31:126–134

59. Gass V, Schmidt J, Schmid E (2014) Analysis of alternative policy instruments to promote electric vehicles in Austria. Renew Energy 61:96–101

60. Figenbaum E, Fearnley N, Pfaffenbichler P, Hjorthol R, Kolbenstvedt M, Jellinek R, Emmerling B, Bonnema GM, Ramjerdi F, Vågane L, Iversen LM (2015) Increasing the competitiveness of e-vehicles in Europe. Eur Transp Res Rev 7:28

61. Comodi G, Caresana F, Salvi D, Pelagalli L, Lorenzetti M (2016) Local promotion of electric mobility in cities: guidelines and real application case in Italy. Energy 95:494–503

62. Singh B, Strømman HA (2013) Environmental assessment of electrification of road transport in Norway: scenarios and impacts. Transp Res D 25:106–111

63. Green car ("Grønn bil") (2016) http://www.gronnbil.no/statistikk/. Accessed 3 Mar 2016

64. Aasness MA, Odeck J (2015) The increase of electric vehicle usage in Norway—incentives and adverse effects. Eur Transp Res Rev 7:34

65. Nykvist B, Nilsson M (2014) The EV paradox—a multilevel study of why Stockholm is not a leader in electric vehicles. Environ Innov Soc Tran 14:26–44. doi:10.1016/j.eist.20114.06.003

66. Pohl H, Yarime M (2012) Integrating innovation system and management concepts: the development of electric and hybrid electric vehicles in Japan. Tech Forcasting Soc Chang 79:1431–1446

67. Åhman M (2006) Government policy and the development of electric vehicles in Japan. Energy Policy 34:433–443

68. Radtke P, Krieger A, Kirov S, Maekawa A, Kato A, Yamakawa N, Henderson D (2012) Profiling Japan's early EV adopters. McKinsey & Company report

Index